

**FLOW HYDRAULICS, BEDFORMS AND MACROTURBULENCE
OF SQUAMISH RIVER ESTUARY,
BRITISH COLUMBIA**

by

C. Scott Babakaiff

B.Sc. University of British Columbia 1991

THESIS SUBMITTED IN PARTIAL FULFILLMENT OF
THE REQUIREMENTS FOR THE DEGREE OF
MASTER OF SCIENCE
in the Department
of
Geography

©C. Scott Babakaiff

Simon Fraser University

December 1993

All rights reserved. This work may not be
reproduced in whole or in part, by photocopy
or other means, without permission of the author.

APPROVAL

Name: Scott Curtis Babakaiff

Degree: Master of Science

Title of Thesis: Flow Hydraulics, Bedforms And Macroturbulence Of
Squamish River Estuary, British Columbia

Examining Committee:

Chair: A.C.B. Roberts, Associate Professor

~~E.J. Yiekin, Professor
Senior Supervisor~~

L. Lesack
Assistant Professor

Mr. K. Røød, Hydrologist
Northwest Hydraulics

Dr. M.A. Church, Professor
Department of Geography
University of British Columbia
External Examiner

Date Approved: December 6, 1993

PARTIAL COPYRIGHT LICENSE

I hereby grant to Simon Fraser University the right to lend my thesis, project or extended essay (the title of which is shown below) to users of the Simon Fraser University Library, and to make partial or single copies only for such users or in response to a request from the library of any other university, or other educational institution, on its own behalf or for one of its users. I further agree that permission for multiple copying of this work for scholarly purposes may be granted by me or the Dean of Graduate Studies. It is understood that copying or publication of this work for financial gain shall not be allowed without my written permission.

Title of Thesis/Project/Extended Essay

Flow Hydraulics, Bedforms And Macroturbulence Of Squamish River Estuary.

British Columbia

Author:

(signature)

Scott Curtis Babakaiff

(name)

JAN 5 / 94

(date)

Abstract

Recent studies emphasize that a better understanding of relations between sediment transport, riverine/estuarine flows and macroturbulence will improve predictions of flow resistance and sediment transport. Macroturbulent features (e.g. boils) have been related to specific bedform or hydraulic conditions which are found in Squamish River estuary. Study aims included: 1) establishing predictive models for bedform parameters based on hydraulic and tidal variables and 2) relating boil characteristics (e.g. period, sediment entrainment) to hydraulic, tidal and bedform conditions.

Predictive models for mean bedform-height (h) and wavelength (w) explained up to 75% of the variance in h and w . Outliers tend to occur on days of tidal-height maximas or minimas in the fortnightly tidal cycle. Bedform h is more sensitive to flow variations than w , and this sensitivity is inversely related to water depth.

Observations of boil production, morphology, intensity and duration indicate that there are two types of boils in the estuary. Boil-production mechanisms could not be determined, but scaling parameters for both types are suggested. As $h > 0.5-0.6\text{m}$, the relation with w becomes strongly linear, and Type 1 boil intensity and sediment entrainment also increase sharply. This may suggest that bedforms become three-dimensional as scour holes form on the lee side. Sediment entrainment within Type 1 boils is also noted to be dependent on water depth. Type 1 boil period (t) also decreases rapidly as relative roughness (RR) increases, becoming asymptotic at $t = 1-10\text{s}$ as $RR > 0.2$.

Time series of streamwise current-speed display patterns also noted in simultaneous video footage of Type 2 boil eruptions at the water surface. Correlation of the time series suggests that boil period is not governed by speed, but there may be a feedback relation such that intense boil activity within the water column increases flow resistance, diminishing current speed and affecting boil production.

Dedication

To my father,
for all the inspiration and encouragement
I've ever needed.

Quotation

"That's the whole problem with science.
You've got a bunch of empiricists trying to
describe things of unimaginable wonder."

Calvin
June 21, 1992

Acknowledgements

Thanks to my senior supervisor, Dr. Ted Hickin, for providing the initial suggestions for my research, and for offering appropriate blends of criticism and encouragement during preparation of this thesis. The generosity volunteered (guidance, equipment, windshields, etc.) is also much appreciated.

Thanks to the members of my supervisory committee, Dr. Lance Lesack and Mr. Ken Rood, for wading through initial drafts of my thesis, supplying equipment and research/revision advice. Special thanks to the external examiner, Dr. Michael Church, for the careful inspection of my thesis, and subsequent revision suggestions.

The statistics advice of Dr. Dan Moore and technical assistance of Ray Squirrell and Gary Hayward is acknowledged. Acquisition of archival data and staff gauges from the Water Survey of Canada was made possible by Lynn Campo, Mark Crowley, Rocky Layne, Grant McGillvary and Joe Stewart. Equipment was also provided in Squamish by John Hinton. The useful hints (disguised as verbal assaults) passed on by the ancient mariners loitering at the Squamish docks must also be noted.

Much credit for the quality and quantity of data collected must go to my field assistant, Colin Wooldridge. Even while enduring the 3:30 A.M. awakening during Spring Tides, Colin still displayed creative methods of estimating the current speed and temperature of Squamish River (remember, a tree branch cannot always support the weight of a rain-soaked assistant). Assistance in the field was also ably provided by Walt Babakaiff and Rhea Watt.

The spiritual support necessary for my self-preservation was given by my family, friends and fellow graduate students. However, particular recognition goes to Jonathan Gibson and Jan Thompson for enduring my obsessions with tuna, popcorn and Elvis Presley Christmas albums. The Thursday-night Cariboo Trails Social Group also proved to be helpful. Not to be forgotten is a push in the right direction given many years ago by Mr. Keith Benjamin.

Finally, gratitude must be expressed to my chum, Rhea Watt, for her humor, warmth, encouragement and friendly abuse.

Personal and research funding was supplied by an NSERC grant given to Dr. Ted Hickin, and a graduate fellowship.

TABLE OF CONTENTS

	<u>Page</u>
Approval Page	ii
Abstract	iii
Dedication	iv
Quotation	v
Acknowledgments	vi
Table of Contents	vii
List of Tables	x
List of Figures	xi
CHAPTER 1- INTRODUCTION	
1.1- Introduction	1
1.2- Literature review	2
1.3- Study objectives	8
1.4- Field site	11
CHAPTER 2- METHODOLOGY	
2.1- Current speed and water-surface slope	
2.1.1- Field techniques	14
2.1.2- Data manipulation and regression analyses	21
2.2- Mean bedform parameters and water depth	
2.2.1- Field techniques	29
2.2.2- Transect analysis	30
2.3- Boil parameters	
2.3.1- Data collection	36
2.3.2- Data manipulation	41
CHAPTER 3- QUALITATIVE DESCRIPTIONS OF BOILS	
3.1- Introduction	44
3.2- Type 1 Boils	46
3.3- Type 2 Boils	56
3.4- Discussion	65
CHAPTER 4- CURRENT SPEED AND WATER-SURFACE SLOPE	
4.1- Introduction	69
4.2- Current Speed	
4.2.1- Surface current-speed regressions	73
4.2.2- Current-speed at 0.7d	
4.2.2.1- Regression analysis	76
4.2.2.2- Minimum durations of current-speed measures at 0.7d	78
4.2.2.3- Graphical inspection of time series	82
4.3- Water-surface slope	
4.3.1- Inspection of data	87
4.3.2- Comparison of slope and speed	91
4.4- Discussion	
4.4.1- Current-speed model results	94
4.4.2- Tidal-wave asymmetry	97
4.4.3- Current-speed time series	100
4.4.4- Implications	103

	<u>Page</u>
CHAPTER 5- BEDFORM ANALYSIS	
5.1- Introduction	105
5.2- Results	
5.2.1- Results of regression analysis	
5.2.1.1- Data inspection	109
5.2.1.2- Mean depth regressions	116
5.2.1.3- Mean bedform-wavelength and height regressions	117
5.2.1.4- Reliability tests	122
5.2.1.5- Alternative combinations of independent variables	123
5.2.2- Variability of results	
5.2.2.1- Influence of vegetation and direction of travel	125
5.2.2.2- Lag effects	130
5.3- Discussion	
5.3.1- Multiple regression models	137
5.3.2- Variability of results	140
CHAPTER 6- ANALYSIS OF BOIL PARAMETERS	
6.1- Introduction	143
6.2- Analysis of Type 1 boils	
6.2.1- Relations between bedforms and Type 1 boil intensity	
6.2.1.1- Graphical differentiation based on field observations	148
6.2.1.2- Graphical differentiation based on sonar inspection	152
6.2.2- Type 1 Boil parameters	
6.2.2.1- Boil presence, morphology and intensity	155
6.2.2.2- Mean boil-period	164
6.2.2.3- Secondary upwellings within Type 1 boils	170
6.2.2.4- Type 1 boil size and persistence	170
6.3- Analysis of Type 2 boils	
6.3.1- Relations between bedforms and Type 2 boil intensity	172
6.3.2- Type 2 Boil parameters	
6.3.2.1- Boil presence and intensity	172
6.3.2.2- Boil size and morphology	176
6.3.3- Type 2 Boil-period time series	
6.3.3.1- Frequency distributions	179
6.3.3.2- Mean boil-period	183
6.3.3.3- Reliability of digitization technique	185
6.3.3.4- Graphical inspection of boil-period time series	185
6.3.4- Comparison of Speed and Type 2 boil-period time series	
6.3.4.1- Graphical correlation	187
6.3.4.2- Quantitative correlation	190
6.4- Discussion	
6.4.1- Quantitative analyses of boil parameters	193
6.4.2- Comparison of speed and Type 2 boil-period time series	198
6.4.3- Postulated boil-production mechanisms	203
CHAPTER 7- CONCLUSIONS	
7.1- Summary of findings	210
7.2- Discussion and suggestions for future work	215

	<u>Page</u>
APPENDIX 1- REGRESSION TABLES AND TEXT APPENDICES	
1.1- Regression analysis tables	219
1.2- Symbols for variables and abbreviations	231
1.3- Data collection summary	232
APPENDIX 2- DATA APPENDICES	
2.1- Water- surface slope data	234
2.2- Surface current-speed data	241
2.3- Current-speed at 0.7d data	248
2.4- Bedform data	250
REFERENCES	268

LIST OF TABLES

<u>Table</u>	<u>Page</u>
3.1- Contrast of Type 1 and Type 2 boils	67
4.4- Time necessary for $U_{0.7d}$ to be within $\pm 5\%$ of 9 minute mean	79
5.9- Analysis of seasonal-scale lag in bedform-wavelength	133
5.10- Analysis of bedform lag induced by fortnightly-scale tides	134
5.11- Analysis of bedform lag induced by diurnal-scale tides	136
6.1- Chi-squared tests of Type 1 boil-period frequency distributions	166
6.2- Applicability of Strouhal's Law to Type 1 boils	168
6.3- Chi-squared tests of Type 2 boil-period frequency distributions	181
6.4- Calculated length scales based on Strouhal's Law	184
 APPENDIX 1.1:	
4.1- Regression tables- surface-speed on ebb tide	220
4.2- Regression tables- surface-speed on flood tide	221
4.3- Regression tables- 9 minute mean speed at 0.7d	222
5.1- Regression tables- Mean water-depth on ebb tide	223
5.2- Regression tables- Mean water-depth on flood tide	224
5.3- Residual analysis	225
5.4- Regression tables: mean bedform-wavelength	226
5.5- Regression tables: mean bedform-height	227
5.6- Regression tables: Log (mean bedform-height)	228
5.7- Outlier times and dates	229
5.8- Regression tables: Log (mean bedform-wavelength)	230

LIST OF FIGURES

<u>Figure</u>	<u>Page</u>
1.1- Study area	12
2.1- Current-speed and slope measurement sites	17
2.2- Sonar transects and study reaches	31
2.3- Bedform parameters and water depth from graphical output of sonar transect	35
2.4- Videocamera mounted in tree at R/B U/S station	38
2.5- Surficial macroturbulence videotaping sites	40
2.6- Oblique angle photography of boils at L/B	42
3.1- R/B site at HHT during maximum Spring Tide	45
Streamwise sediment-laden bands in lower estuary	45
3.2- Location of Type 1 and Type 2 boils	47
3.3- Patterns of boil lanes downstream of mid-channel bar	48
3.4- Secondary upwellings on u/s side of Coleman/Jackson structure	50
'Cauliflower' boil structure	50
3.5- 'Roller' boil structure aligned parallel to flow	51
Roller structure with straight long axis	51
3.6- Roller structure with curved long axis	52
3.7- Evolution of boil structures: Coleman/Jackson and roller (with horns)	53
3.8- Vortices formed on ends of roller structure	54
Secondary upwelling formed upstream of roller	54
3.9- Poorly-defined and short-lived secondary upwellings	55
3.10- Several orders of linear patterns of vortices in a boil	57
Downwelling on downstream side of boil	57
3.11- Roller structure within a Type 2 boil	59
Sucessive Type 2 boils oriented perpendicular to each other	59
3.12- Time series of Type 2 boil evolution displaying effect of upwellings on overall boil shape	60
3.13- Evolution of Type 2 boils- elongation, diffusion and segmentation	61
3.14- Time series of Type 2-boil diffusion	62
3.15- Time series of Type 2-boil segmentation	63
3.16- Time series of Type 2-boil elongation	64
4.1- Current speed vs. independent variables	74
4.2- RTI vs. minutes required for $U_{0.7d}$ to be within 5% of 9 min. mean	81
- TI vs drop/rise or $U_{0.7d}$ differentiated by rates of change in stage or Q	81
4.3- Moving average and binomial filters applied to speed time series: June 22 800	84
4.4- Moving average and binomial filters applied to speed time series: June 27 620	85
4.5- Filtered current-speed time series	86
4.6- Water-surface slope vs. independent variables	90
4.7- Water-surface slope and current speed vs. T	92
4.8- Surface current-speed vs. T	93
4.9- Water-surface slope vs. current speed differentiated by ebb and flood tide	95

<u>Figure</u>	<u>Page</u>
5.1- Mean bedform-parameters vs. T	110
5.2- Mean bedform-parameters vs. Q and D	111
5.3- Mean water-depth vs. D and T	113
5.4- Mean bedform-parameters or d vs. standard deviations of the means	114
5.5- Log (bedform parameters) vs. independent variables	119
5.6- Log (bedform wavelength) vs. D	120
Mean bedform-parameters vs. values predicted from full-regression models	120
5.7- Mean bedform-parameters vs. values predicted from split-sample models	124
5.8- Alternative combinations of variables for scaling relations	126
5.9- Comparisons of Reach 1 vs.6 and 2 vs.7(Water depth and bedform height)	128
5.10- Comparisons of Reach 1 vs.6 and 2 vs.7(Bedform wavelength)	129
Bedform height vs.LTH differentiated by time in fortnightly tidal cycle	129
5.11- Max.daily drop and estuary discharge-Squamish R.estuary: May-Sept.1992	132
6.1- Boil intensity as function of bedform wavelength and height (Reach 7 and 3)	149
6.2- Reach 2 boil intensity as function of bedform wavelength and height or depth	150
6.3- Boil intensity as function of bedform wavelength and depth (Reach 3 and 7)	151
6.4- Boil intensity as function of bedform height and depth (Reach 2 and 7)	153
6.5- Reach 3 boil intensity as function of bedform height and depth	154
6.6- Sediment entrained in boils as a function of bedform wavelength and height	156
6.7- Sediment entrained in boils as a function of bedform wavelength and depth	157
6.8- Sediment entrained in boils as a function of bedform height and depth	158
6.9- Mean bedform-parameters vs. T (differentiated by boil intensity)	160
6.10- Boil morphology as a function of mean water-depth and bedform height	162
6.11- Boil morphology as a function of mean bedform-wavelength and height	163
6.12- Filtered boil-period time series	165
Boil period vs. relative roughness	165
6.13- Sonar record of scour hole in lower estuary	169
6.14- Reach 4 boil intensity as function of bedform height and wavelength or depth	173
6.15- Boil intensity as a function of water-surface slope and T	175
6.16- Boil intensity as a function of surface current-speed and T	177
6.17- Type 2 boil with strongest downwelling on R/B D/S side	178
6.18- Boil-period histograms	182
6.19- Filtered boil-period time series	186
6.20- 6.23 Comparative plots of filtered boil-period and current-speed time series	
6.20- June 22 0759-0814; June 26 0950-1001	188
6.21- June 18 1456-1510; June 22 0651-0706	189
6.22- June 27 0618-0633; June 23 0638-0653	191
6.23- June 18 1355-1410; June 23 0800-0815	192
6.24- Photos of bedforms exposed on intertidal area	206

CHAPTER 1- INTRODUCTION

1.1- INTRODUCTION

Rivers and estuaries are characterized by two kinds of unsteadiness: turbulent and macroturbulent. Turbulence involves continuous, small-scale random motions throughout the flow which are isotropic and well described by normal Gaussian statistics.

Macroturbulence, however, involves large-scale intermittent and distinctly non-random anisotropic perturbations to the flow. Turbulence has been of scientific interest for centuries, but macroturbulence has been largely ignored in fluid dynamics. Ironically, macroturbulent phenomena may be integral to sediment transport and flow resistance in rivers and estuaries, but very little research has been attempted to date, and most of our knowledge is based on a limited number of studies.

Matthes (1947) proposed a classification of macroturbulence which included rhythmic and cyclic surges (e.g. velocity pulsations), continuous rotary motions (e.g. eddies) and discontinuous/ intermittent vortex action (e.g. boils). He further noted that although all forms of macroturbulence represent expenditures of energy in overcoming channel roughness, the process creating boils at the surface is the "most powerful form of energy at work on stream beds". Macroturbulent phenomena may be interrelated, but boils will be the main focus of study in this thesis.

In rivers, boils are quasi-circular features which erupt at the water surface as an upwelling of fluid (often entraining sediment much coarser than the surrounding quiescent flow).

This term is not exclusive to structures found in natural flows; early flume studies referred to quasi-permanent bulges in the water surface related to local flow acceleration, as boils (Znamenskaya, 1963; Simons and Richardson, 1966).

The paucity of boil studies may be related to the apparent intermittent and/or random appearance of boils in rivers. Fortunately, if a significant tidal flux is superimposed on the river flow, boil production is concentrated at certain stages in the tidal cycle (Rood and Hickin, 1989; Kostachuk et al.,1991). Thus, observational difficulties may be considerably reduced.

Although the deficiency in field studies has prevented elucidation of processes related to macroturbulence generation, insight may be gained by examining generation of similar features from flume studies. Yalin (1977) postulated that the generation of microscale turbulent fluctuations may be related to irregularities in boundary geometry. He proposes that these irregularities are then magnified by sediment transport associated with the turbulent fluctuations in a feedback-type relation. In recent decades, researchers have attempted to relate macroturbulent features found in natural flows to microscale turbulent features.

These comparisons suggest that even if microturbulent and macroturbulent features are generated by similar processes, the complexities of natural flows (e.g. bedforms, tidal and discharge fluctuations) may conceal relations with physical or flow parameters. A brief history of these results illustrates the components which must be investigated to study macroturbulence in an estuarine environment.

1.2- LITERATURE REVIEW

Since the mid-1960s, flume studies involving various flow visualization and hot-wire anemometry techniques have been conducted in order to describe the flow structure near the boundary layer (e.g. Offen and Kline, 1975; Sumer and Deigaard,1981). It was finally

concluded that there is a 'complex quasi-ordered flow structure which consists of a deterministic sequence of fluid motions occurring randomly in time and space, but with a mean recurrence period that is fairly constant when scaled by the outer flow variables' (Allen, 1985). This sequence came to be known as the burst cycle. Bursting is quantitatively defined as some deviation of instantaneous fluctuating speed components from the time-averaged value. The required magnitude of the deviation to qualify as a burst, however, is not presently agreed upon.

Rao et al.(1971) found that the average period between these turbulent bursts = $d/U = 3$ to 7 (where d = depth of the boundary layer, U = free stream velocity), but Grass (1971) surmised that bed roughness may alter the scaling equation. Laufer and Badri Narayanan (1971) found that shear stress reductions occurred intermittently in the boundary layer with frequencies that scaled similarly to the Rao et al. data. They suggested that these reductions in shear stress correspond to some stage in the bursting cycle, but confirmation of this hypothesis in higher Reynolds number (Re) flows (natural flows) was still lacking.

Previous research in tidal currents employing velocity meters to measure Reynolds stresses near the bed found that a high proportion of the stress was contributed by short-period fluctuations (Bowden, 1962; Bowden and Howe, 1963). Subsequent studies at high Reynolds numbers by Gordon (1974, 1975a) confirmed the scaling equation of Laufer and Badri Narayanan (1971). The research also seemed to confirm the lab findings of Kline et al. (1967) regarding burst sensitivity to longitudinal pressure gradients. The frequency and intensity of bursting events were reduced during accelerating current speeds and increased with decelerating current speeds. Thus, if the intermittent fluctuations of shear stresses are linked with the bursting cycle, there should be enhanced sediment entrainment at the bed during decelerating current speeds. This hysteresis in tidal flows may be explained by the time required for the turbulent kinetic energy (TKE) to dissipate.

Since the dissipation of TKE takes time, maximum TKE will be lagged some time after maximum current speed. This lag also increases with distance from the bed. There may also be a hysteresis produced in suspended-sediment concentration, again increasing with distance from the bed (Thorn, 1975). These effects have not been found in all studies (e.g. Bowden and Ferguson, 1980), and the complication of bedform lags may make it difficult to isolate the cause of the hysteresis with certainty. Kostaschuk et al. (1989a) further note that there may be complexities related to the salt-wedge intrusion on a semi-diurnal scale, and to the progressive removal of fines from the bed on a seasonal scale.

The postulation of Jackson (1976) that boil production is related to stages in the bursting cycle is known as the burst-boil conjecture. The primary evidence is the similarity of the scaling of boil periodicity at a river surface to that of bursting in flumes. Results perceived to be consistent with the burst-boil conjecture have been found by many workers (e.g. Nakagawa and Nezu, 1977; Sumer and Deigaard, 1981), and Allen (1985) claims that the motion within a boil is 'as if a horseshoe eddy reached the surface'. Whether or not the surface expression known as boils are a result (exclusively, or partially) of bursts in the boundary layer, however, is debatable (Allen, 1985; Rood and Hickin, 1989; Kostaschuk et al., 1991). McLean and Smith (1979) concluded that there seem to be a variety of mechanisms that trigger intermittent turbulent events which display consistent scaling. Kostaschuk and Church (1993) suggest that the Strouhal Law ($tU/d = 2\pi$) adequately describes the periodicities of boil events (t), and that boil-production mechanisms include Kelvin-Helmholtz and wake-flow instabilities. The former are represented by interfaces between water masses of differing speeds (or densities) which tend to roll into spirals; the latter relates to flow separation downstream of obstacles such as bedforms.

As the flow near the bed rises over the stoss side of a bedform, it will accelerate and subsequently decelerate as it descends over the crest onto the lee side. The adverse pressure gradient established on the lee side often results in flow separation (Raudkivi, 1966), setting up a rotational eddy in the lee. The extent of this separation zone downstream of the bedform crest is not known for certain. Proposals include $6h$ (Raudkivi, 1963), $4.3h$ (Engel and Lau, 1980), $4.1h$ (Engel, 1981) and $1/3w$ (Karaham and Peterson, 1980) (where h =bedform height and w = wavelength). These flume-generated results may have limited application in natural flows where bedforms may display a variety of shapes and orientations. For example, if the crest of the bedform is oblique to the flow, a helical vortex may be created as the lee eddy (Znamenskaya, 1963; Dyer, 1986).

The notion that boils are produced by the intermittent ejection of eddies from the lee of dunes has been pondered by researchers for many decades. Znamenskaya (1963) found that when values of dune steepness (h/w) are between 0.04 and 0.1, the eddy created in the lee of the dune is periodically ejected, and moves up the pressure slope of the next downstream dune, rising towards the surface. Lapointe (1992) questions the postulated ejection of these separation features towards the surface, but recent work by Best and Bennett (1993) indicates that there may be a significant upward ejection of fluid from along the bedform shear layer. Research of this phenomena has been minimal, but similar ideas have been discussed in laboratory studies of mixing-layer vortices shed in association with flow separation.

Flow visualization research in flumes ($Re = 10^4 - 10^5$) suggests that two scales of vortices are shed from flow separation zones (Hillier and Cherry, 1981; Ota et al., 1981; Kiya and Sasaki, 1983). There is an oscillation of the shear layer near the separation zone (known as 'flapping') which is similar to the process described by Znamenskaya (1963). There is

also shedding of weaker 'mixing-layer vortices', perhaps stretching into corkscrew patterns (Jimenez, 1983). The mixing-layer vortices are shed with a frequency of $0.6-0.7 U/L$ (where L = downstream length of separation zone), while the flapping sheds larger vortices with a frequency of less than $0.2 U/L$ (Kiya and Sasaki, 1983). This latter frequency is similar to that of the Strouhal Law, and Itakura and Kishi (1980) found that the vortex-shedding frequency follows a Strouhal scaling (with dune height replacing d). Proposed explanations of this flapping include entrainment and subsequent ejection of fluid from the interior of the recirculation zone (Mendoza, 1988), or the build-up and subsequent 'release' of vorticity within the separation bubble (Kiya and Sasaki, 1983). Allen (1985) concluded that these vortices may be the cause of the boils described by Jackson (1976). Recent flow-visualization studies suggest that the proposed interaction between outer and inner-flow structures may indeed exist.

Best (1992) summarizes the flume-based fluid dynamics findings of the last decade, noting that multiple hairpin-shaped vortices may generate multiple-burst events. The subsequent interaction and coalescence is postulated to generate larger structures such as those noted by Falco (1977). In fact, Nychas et al. (1973) and Praturi and Brodkey (1978) concluded that burst events were directly dependent on the passage overhead of transverse Helmholtz vortices. Levi (1983) relates the bursting at the boundary to a travelling wave with $L=2\pi d$ moving with velocity (u). This travelling wave then induces turbulent events at a variety of scales with a period described by the Strouhal Law ($=2\pi d/u$). The interaction of this wave with bedforms has been speculated by some researchers (e.g. Kostaschuk and Church, 1993), and it is evident that some relation between the mean flow, turbulent events and bedforms must exist.

Leeder (1983) concluded that the interaction between turbulent flow, sediment transport and bedforms is a feedback system. He notes that there is a lack of data on the effects of

bedforms on flow structures, and on the association between structures of various flow depths at high Reynolds numbers. Similar to the hypothesis of Yalin (1977), Lapointe (1989) concludes that, if there is a feedback relation, bursting must be seen as a link between turbulent flow and the deformable boundary. This finding was echoed by Best (1992). Naden (1987) notes, however, that it is this link between turbulence and bedforms which is the least understood.

Fielding (1993) claims that studies such as Kostaschuk and Church (1993) address the pressing research issue of the nature of turbulent flow and its role in sediment transport. Lapointe (1989) notes that data regarding the frequency and intensity of turbulent events as a function of bedform geometry, flow parameters and flow separation are needed. The complexities of undertaking such studies have been noted by several workers (e.g. Williams et al., 1989; Lapointe, 1989), and although these complexities may be reduced by studying boils in an estuarine (rather than a fluvial environment), tidal control may also obscure the relations between hydraulics, bedforms and macroturbulence.

Variability in discharge and tidal effects over short temporal and spatial scales may produce complex lags or spatial heterogeneities in physical processes. McDowell and O'Connor (1977) suggest establishing empirical relations between relevant variables at a variety of sites. Hubbell et al. (1971) found that hydrodynamic conditions in Columbia River estuary were so extreme that no consistent relations between variables (including current velocity, salinity and suspended sediment concentration) existed. Examination of these relations on seasonal, fortnightly and semi-diurnal scales, however, accounted for much of the unexplained variability (Gelfenbaum, 1983).

It seems likely that estuarine macroturbulence may also exhibit variability over such temporal scales. It is postulated that consideration of wide ranges in hydraulic, tidal and

bedform parameters will be most appropriate for elucidating scaling parameters for macroturbulent features. An example of a high-energy sand-bed river with significant tidal effects superimposed on large fluctuations in discharge is Squamish River estuary.

1.3- STUDY OBJECTIVES

There has been much research completed on various components of the hydraulics of Squamish River, but several studies are worth careful consideration. Rood and Hickin (1989) examined the role that boils have in suspending and transporting sediment, and contemplated the relation between the boils and bedforms in Squamish estuary. Previously, Hickin (1978), Rood (1980) and Hickin (1989) inspected patterns in sediment transport and current speed of Squamish River. The results of these four studies suggest that hydraulic parameters, bedforms and macroturbulence may be inter-related in Squamish estuary. A broad empirical approach is taken in this thesis so that many processes potentially related to boil activity may be considered. The main objective of this thesis is to quantitatively relate properties of the macroturbulence noted at the surface to bedform and hydraulic parameters in Squamish River estuary. This objective is addressed by studying each element of the hydraulics-bedforms-macroturbulence inter-relation as independent components. The results of these analyses are then integrated to resolve the main objective. The thesis objectives are explicitly stated in this chapter, investigated in Chapters 3-6, and specifically addressed in the evaluation of the enterprise presented in the Chapter 7. The first step is to examine boil characteristics in Squamish estuary. Recent studies (e.g. Kostaschuk and Church, 1993) suggest that attempts to scale boil parameters with hydraulic measures may be affected by multiple boil-production mechanisms. In fact, there may be more than one surface expression of boil activity (e.g. Coleman, 1969; Rood and Hickin, 1989). Rather than simply inspecting boil frequency, boil morphology and

evolution were observed throughout the research period, allowing for a qualitative inquiry in Chapter 3:

1) Is there evidence of more than one type of boil in Squamish River estuary?

The quantitative analysis then begins with examination of the basic hydraulic parameters in the estuary such as current speed, water-surface slope and water depth. Variability in these parameters are then related to postulated causative independent variables such as river discharge and tidal variations on semi-diurnal and fortnightly scales. In order to have simultaneous measures of both the hydraulic variables and boil parameters, it was envisioned that rating-curve relations could be established so that the hydraulic parameters need not be monitored over the full study duration:

2) Can current speed, water-surface slope and water depth at various sites in the estuary be reliably predicted based on multivariate regressions?

This question is addressed in Chapters 4 and 5. This analysis must also include consideration of the fluctuations in current speed of Squamish River (e.g. Rood, 1980).

Similarly, the dependence of bedform wavelength and height on several independent variables is examined, but such an analysis may be complicated by temporal lags in bedform changes behind hydraulic and tidal forces. Therefore, bedform parameters will be obtained from sonar transects of the estuary, and Chapter 5 will inspect two distinct

questions:

3) Can bedform height and wavelength in various reaches in the estuary be reliably predicted based on multivariate regressions? and,

4) Can the lags in bedform height and wavelength behind fluctuations in hydraulic and tidal conditions over a variety of temporal scales be identified?

If the proposed interdependence among bedforms, turbulent phenomena and hydraulic parameters indeed exists, a quantitative analysis of boil properties may suggest boil production mechanisms. Ultimately, prediction of hydraulic and bedform parameters based on such observable water-surface boil properties as sediment entrainment and periodicity may be possible. These observations may be useful for efficiently estimating some component of flow resistance or sediment transport. The general question that Chapter 6 explores is:

5) Can properties of the macroturbulence noted at the surface be quantitatively related to bedform and hydraulic parameters in Squamish River estuary?

The value of this exploratory research does not rely on definitive answers to such questions. This thesis might be likened to an expanded pilot study since the vast potential for research in this field has only recently been recognized. From a river engineering standpoint, the need for a more complete understanding of sediment transport and flow resistance cannot be denied, and this may only be attained through an approach integrated with study of macroturbulence.

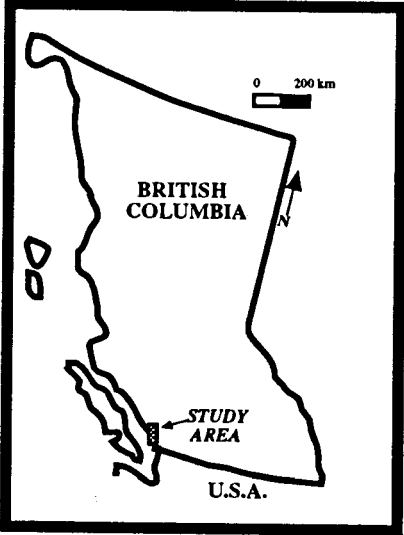
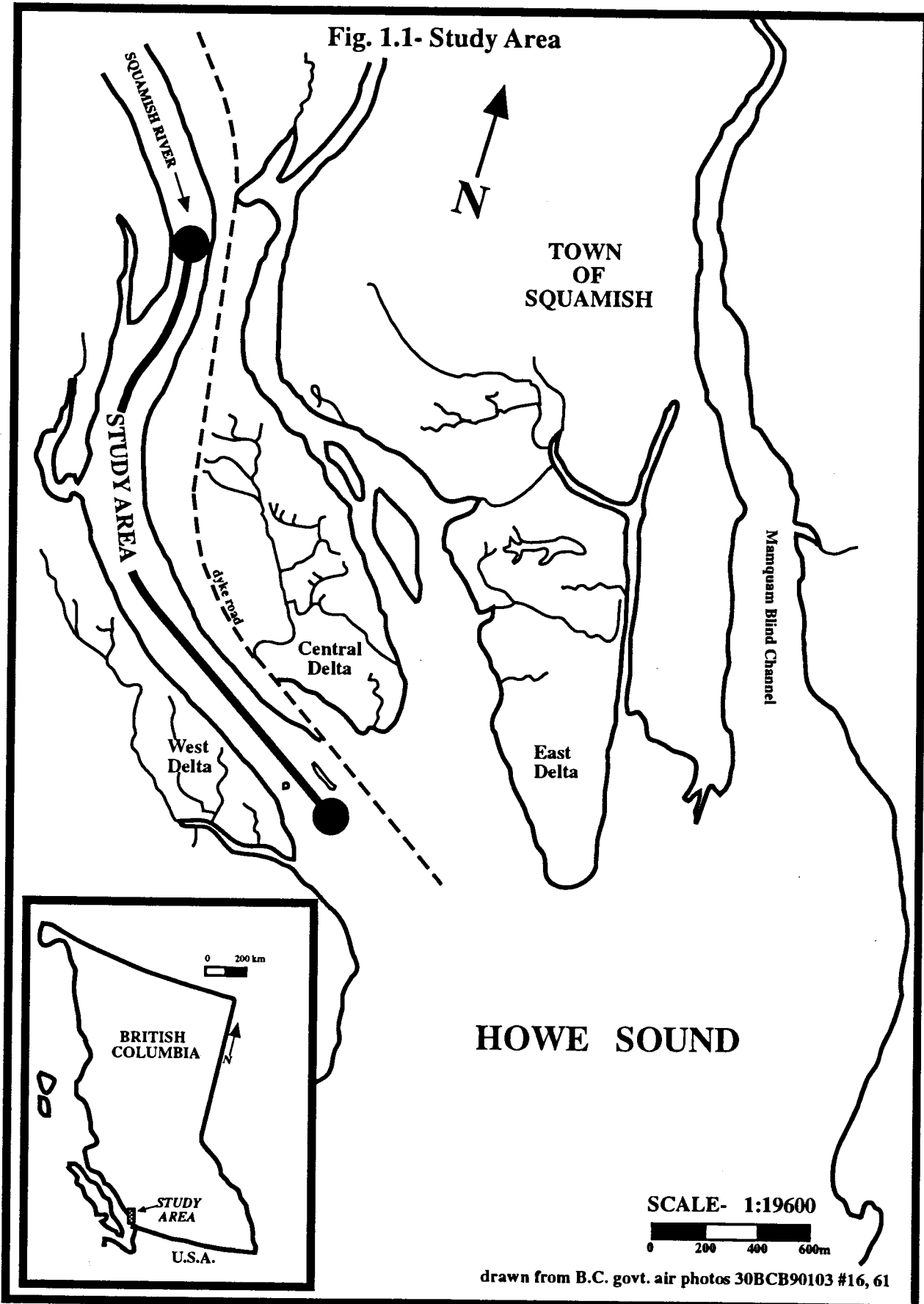
1.4- FIELD SITE

Squamish River drains into the fjord of Howe Sound approximately 40 km north of Vancouver, British Columbia (Fig. 1.1). The drainage basin covers an area of 3600 km², much of which is mountainous and glaciated terrain. The region has a modified-marine climate, with cool, wet winters and warm, dry summers. Heavy precipitation in the fall and winter is related to orographic forcing, with the steep valley sides funnelling storms up Howe Sound. These storms produce short-period flood events, but they may have extreme magnitudes if the precipitation induces snowmelt at higher altitudes. These fall and winter flash floods are superimposed on a seasonal pattern of runoff characterized by a late spring-early summer freshet.

Over the >70 year discharge record on Squamish River at Brackendale (WSC station 08GA022), the mean annual discharge has been 250 m³/s, with maximum annual floods exceeding this value by an order of magnitude. This value is typically about 70% of the discharge received by the estuary since there are also contributions from Mamquam and Cheakamus Rivers, and Monument Creek. Recent years have been wetter than the historical record, with mean annual discharges exceeding the long-term mean seven times in the last decade.

On clear warm days during the summer, strong thermal heating combined with the funneling effect of Howe Sound produces strong land-sea breeze circulations. The light northerly winds which prevail from midnight until about 9 A.M. shift to southerlies as the land mass warms more quickly than the water mass. As early afternoon approaches, the wind strengthens and may produce steep, violent waves in the estuary. The winds then peak in late afternoon and diminish quickly after sunset. These winds and waves have

Fig. 1.1- Study Area



SCALE- 1:19600
0 200 400 600m

drawn from B.C. govt. air photos 30BCB90103 #16, 61

been known to amplify and/or advance high tides in the area, but they only occur on about 50% of the days between May and August (Hoos and Vold, 1975).

Tidal regime in Squamish River estuary is of the mixed type, with two highs and two lows diurnally. However, the tidal heights are not equal: there is a 'higher high tide' (HHT) and a 'lower high tide' (LHT), and similarly for the low tides (HLT and LLT). Variations in tides, winds and river discharge also produce fluctuations in water salinity in the estuary. When discharges are low in the winter, tidal effects may be noted just downstream of the junction with the Mamquam River, and saline waters may also extend several kilometers upstream of the mouth. As discharge increases during the freshet, tidal effects are barely notable at WSC station 08GA053 (7 km upstream of the mouth) and the salt wedge may not extend past the river mouth. The lower five kilometers of Squamish River estuary where the tidal effects on hydraulic parameters will be most pronounced constitutes the study reach (Fig 1.1). The research methodology is described in Chapter 2.

CHAPTER 2- METHODOLOGY

2.1- CURRENT SPEED AND WATER SURFACE SLOPE

2.1.1- Field Techniques

Measurement of water-surface slope and current speed at various sites along Squamish River estuary required choices of appropriate instrumentation and techniques in a high-energy, debris-laden channel. Logs transported by the river provided a constant threat to instrumentation, and extremely windy conditions often prevented stabilization of the research vessel for data collection. The sites chosen for collection of slope and speed data also demanded consideration of macroturbulence and bedform data requirements (Note: Appendix 1.3 is a list of all data collection on a daily basis). Measurements of bedform parameters and surface current speed were made throughout the research period (May- August, 1992). Water-surface slope data were collected in June, as were simultaneous time-series measures of boil period and current speed at $(0.7 \times \text{water depth})$ from the surface. Attempts to photograph and quantify boil parameters were made in July and August.

Time-efficient measurement of water-surface slope between two stations requires the depth of water at each to be known either by utilizing automated instruments (stage recorders or pressure transducers with data loggers) or staff gauges. It was felt that the benefits of automation were outweighed by the potential problems with installation, tampering and malfunction. In addition, a continuous record (stage recorder) would require time-consuming digitization, and the cost of transducers and data loggers was not justified. Therefore, stage was recorded at the boundaries using a set of Water Survey of Canada staff gauges (graduated to 0.01m).

The major difficulty in selecting sites for staff gauge installation was that the area of the river associated with the primary feature of research (intense boil activity) is the thalweg. To allow for videotaping of the boils, the choices for study reaches were limited to regions where the thalweg impinged on the bank. In the estuary, these regions have steep and unstable banks up to 4m in height. This dictated the use of single staff gauges (5m length) at each station, rather than using a combination of shorter staff gauges at increasing elevation above the bed. The difficulty associated with using such long staff gauges makes the criteria of Forrester (1983) for gauge installation even more relevant; he listed several, including:

- presence of a firm stream bed, with strong lateral supports;
- sufficiently deep water so the gauge is not stranded at low tide;
- accessibility of the gauge by launch and foot;
- protection of the gauge from waves, current, and other damage.

In my study area, the first two criteria could rarely both be met. The ideal sites were where large (up to 1m diameter) logs incorporated into the bank jutted out into the river. These logs did not move with the tide, and gauges were secured to them with stabilizing cross beams and rebar driven into the bed or the log.

Forrester's concern with gauge protection was a serious consideration due to the size (and frequency) of logs transported by Squamish River. No preventative measures could be utilized, and damage from floating debris forced the removal of the gauges at both sites earlier than planned.

Initial surveys indicated that a study reach length of at least 125-150m was required if water-surface elevation differences over the tidal cycle could be measured with the gauges. Since the sites of slope measurement corresponded to the thalweg impingement

on the bank, there may have been super-elevation of the water surface. An attempt was made to keep the study reaches approximately 150m long, but the length was ultimately dictated by the availability of adequate sites for gauge location (the sites chosen are shown in Fig.2.1).

The duration of slope measurement at a site was based on two considerations: tides and temporal constraints. The fortnightly period of the Spring-neap tidal cycle defines a minimal study period. Since data collection could only be performed at one site over the day, this required 4 weeks of measurements. If the time required for inspection, installation and subsequent removal of staff gauges is included, this constitutes a significant proportion of the total field season. Slope was to be measured for two weeks at the left bank (L/B) (June 2-15) and the right bank (R/B) (June 16-29), but damage to gauge supports shortened these periods by 2 days in each case.

After June, one staff gauge was moved back to a position on the L/B, approximately 500m downstream of its previous location. The staff gauges were then used to indicate stage as required in other components of the study. Near the end of the field season (August 22-26) the L/B staff gauge was moved back to its previous position on the R/B, and slope was measured for 5 additional days. This was done because it was evident that discharge was considerably lower in August than it had been in June. Unfortunately, lateral erosion at the L/B had removed the previously utilized log supports, and the staff gauges could not be reinstalled there.

A measure of current-speed within the thalweg at the two study sites (and at sites chosen later in the field season) could not be reasonably obtained from the bank. Each measurement station is shown in Fig.2.1; the location of current speed measurements was typically dictated by other data-collection requirements. Dinehart (1992) warns of the

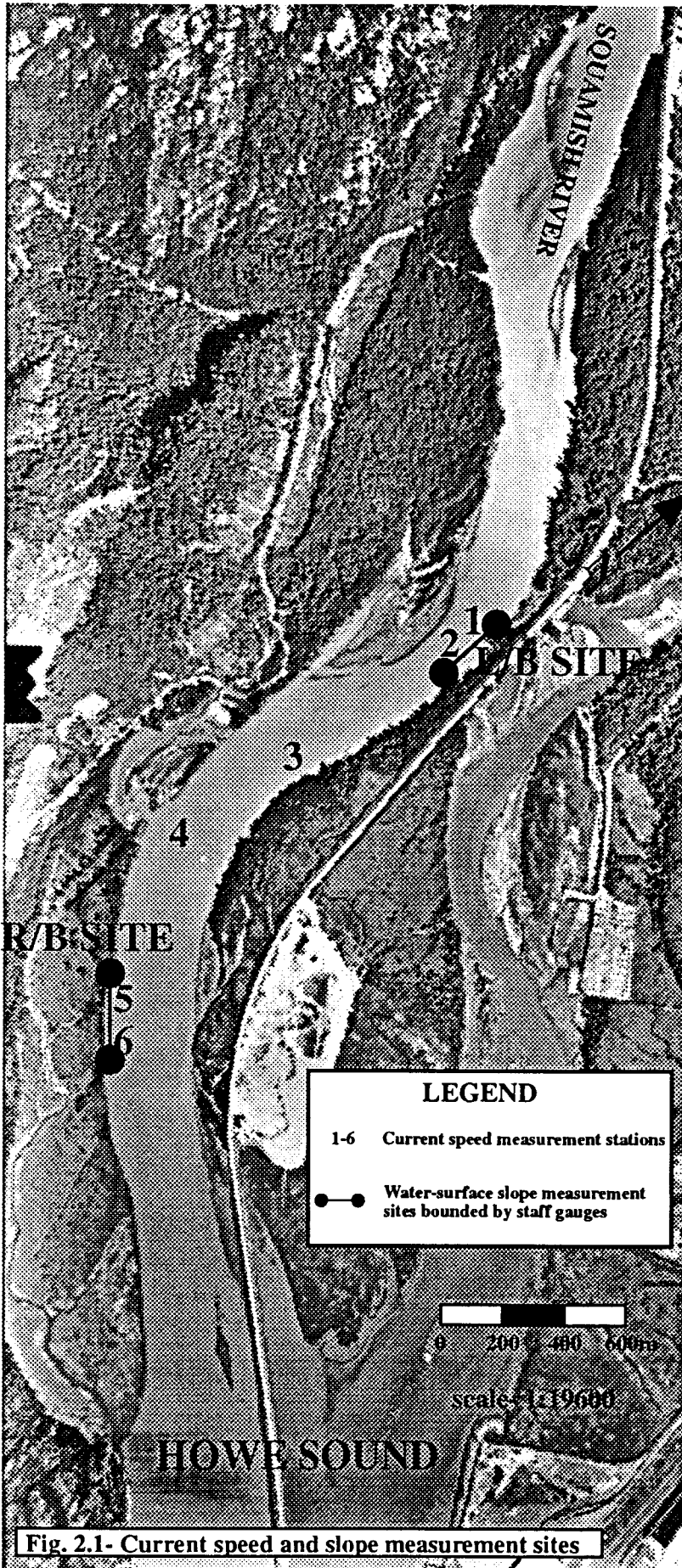


Fig. 2.1- Current speed and slope measurement sites

difficulty in acquiring streamflow data in debris-laden channels, and indeed there were challenges in measuring current speed from the research vessel on Squamish estuary.

An NBA Controls DNC 3 current meter equipped with a 37 kg weight was used to obtain the current speed. Downstream displacement of the meter during data collection was only apparent once current speed exceeded 2 m/s. A greater concern was the stabilization of the vessel itself. The bed of the river near the field sites incorporates large trees and logs, most of which seem extremely stable. Anchors could not be used for stabilization because they were very difficult to retrieve once snagged on the subsurface trees. Instead, a tree in the thalweg at each measurement site which reached the surface at low tide had a buoy attached to it. This was utilized to keep the bow stationary in the flow. There was some bow movement associated with tying off in this manner, but no more than using an anchor, and it was an order of magnitude less than the lateral movement in flow.

Attempts were made to minimize the lateral movement by using a series of 15 kg weights tied to the stern and dropped to the river bed. This technique worked well as long as the lines were kept taut as the tide rose or fell. However, if conditions were particularly windy, the hull acted as a sail, and it was impossible to maintain position to better than about 5m. If this occurred, the measurements were disregarded. Data were also fouled and disregarded if river debris became tangled in the propellor of the current meter. This was not difficult to recognize when the propellor was visible (ie. near-surface speed measurements), but if the measurements were taken at depth, this was not always so.

The speed at the surface was taken as the average reading over a 30 second interval (Usfc). Then, the current speed was measured at (0.7* total depth) (U0.7d), with depth

measured using a Lowrance X-16 echo sounder. Quite unexpectedly, the speed at this level fluctuated extremely, often with an apparent periodicity. Thus, the speed was sampled at a frequency of 5 seconds with a duration of 10 minutes (greater than the presumed limit of stationarity). The robust sampling frequency was chosen not only for the ease of digitization, but because the meter has an internal averaging interval of 3 seconds. A similar technique was utilized by Jackson (1975).

Collection of the speed data was often hampered by windy conditions and/or waves. If there was sudden lateral movement due to bursts of wind, the fouled data simply was disregarded, but continuous wind and waves often resulted in data collection being abandoned. Even when wind and waves were not present, high-frequency fluctuations in surface speed resulted in a subjective decision. When attempting to visually integrate the readings (to obtain a median value) over a 30-60 second interval, the range in a reasonable value could be as high as 0.5 m/s. Typically, higher speeds resulted in greater possible ranges of median values. The estimated range for each median was noted, and the average was 7%, but will be taken as +/- 10%. For example, when a surface speed of 2.2 m/s was reported, a reasonable (median) value could be between 2.0 and 2.4 m/s. The range of speeds noted during this period was much greater, but the extreme values had limited duration (ie. jumps on the needle). The value of 10% (rather than 7%) was used so that any measurement error associated with the current meter itself (ex. 0.025 m/s or half the smallest division on the recording meter) would be negligible. This will not tend to underestimate the error for the lower speeds since their median ranges were typically <<10%.

For the speed readings at 0.7d, it is difficult to attribute an error value. There is often a strong, lower-frequency (order of 100 seconds) oscillation with high frequencies superimposed on the record. The amplitudes of these long fluctuations are not constant,

nor are they present in every record. With over 100 instantaneous speed readings taken over the 10 minute time-series, it would seem a reasonable assumption that the high frequency fluctuations will average out to zero.

To test for stationarity of the mean through the 10 minute time series, a non-parametric approach known as the Runs Test was utilized. It was recommended by Bendat and Piersol (1969) and has been employed in other studies of turbulence (Rood, 1980; Soulsby, 1980). To give an adequate number of elements for the test to be applied, the 600 second records were divided into 30 segments of 20 seconds, and the sample mean was determined for each segment. The tests were repeated using the group-median values (e.g. Rood, 1980), but the results were similar to those performed with the mean values.

All time series were visually inspected, and classified as either stationary or non-stationary. Sixteen records were judged to be non-stationary and thirteen were confirmed as being non-stationary at the 95% confidence level. The test is not strictly valid if there are any dominant periodicities in the time series which are longer than the averaging time (20 seconds), but fortuitously, only two of these thirteen records had such periodicities. These records were included in the data set for subsequent analysis, but they were noted as being potential outliers. The same treatment was given to the three records that appeared non-stationary, but were found stationary by the Runs Test. Those records that were found to be non-stationary from both the visual inspection and the Runs Test were removed from the data set used in regression analyses.

Those records which appeared stationary were also tested, and 43% were found to be non-stationary. Of course, decreasing the length of record will increase the probability of the mean remaining stationary. If the record length is decreased to nine minutes, the

number of records found to be non-stationary drops to 25%. However, a further decrease to eight minutes yields a minimal drop in the number of non-stationary records to 23%, as does a decrease to 7 minutes (22%). From a visual inspection of these records, it is found that almost all have dominant periodicities longer than 20 seconds, thus violating the assumptions of the Runs test. It is therefore concluded that restricting all remaining time series in the data set to a duration of nine minutes will remove any non-stationarity of the mean due to rapid changes in stage. As a final note, the 13 records that were removed from the data set due to non-stationarity (visual and test results) were re-tested with nine minute records, and all were still found to be non-stationary.

Significant drops in current-speed at depths cannot be definitely interpreted as data fouling, since they were occasionally noted on the surface when there was no debris present. Data collection at depth was interrupted only when velocities dropped and remained low for at least 45 seconds. At this point, the current meter was raised to the surface, and typically the propellor was obstructed with debris.

To describe and analyze turbulence in natural flows, McQuivey (1973a) recommends using variables which are physically significant and based on readily collected data. The variables recommended include the turbulence intensity (TI) and relative turbulence intensity (RTI). These are respectively the standard deviation and the coefficient of variation of the fluctuating component of current speed.

2.1.2- Data manipulation and regression analyses

Multiple regression analyses are used in this thesis to predict bedform and hydraulic parameters. A least-squares fit has been employed even though certain assumptions are violated. These include the presence of collinearity effects (Marquardt and Snee, 1975)

and of measurement errors associated with the independent variables (Jones, 1979). The effects of collinearity are accounted for, and the problem of errors in X is insignificant provided that the variance in X is (much) less than the variance in Y, or if the measurement errors are not large compared to the random errors (Chatterjee and Hadi, 1988). For much of the data in this thesis, the measurement errors in X are unknown, but we can assume that they are present, and that they are relatively insignificant.

The computerized statistical package chosen to perform the regression was SYSTAT 5.0 for the Macintosh. The stepwise procedural choices within SYSTAT include the possibilities discussed by Chatterjee and Price: forward selection, backward elimination, and an interactive option for either. The backward procedure is generally recommended over the forward for several reasons. First, because the model with the full variable set can be examined (Chatterjee and Price, 1991), but more importantly, backward elimination is more robust with respect to multicollinearity (Mantel, 1970) and forward selection has a greater tendency to overfit the model (McNeil et al., 1974). Even better, with the interactive option the model can be studied at each step, and the decision of variable entry/removal is left up to the researcher. This allows inspection of a variety of potential models which may be based not only on F or p values, but on the avoidance of collinearity between variables.

The tables that will define the model chosen for any particular regression will include both the traditional parameters presented in a regression analysis, and a few measures selected to highlight potentially useful factors. These tables are referenced within the text of the thesis, but are collected within Appendix 1.1. The descriptors that are typically displayed include: sample size(n), the regression equation (including the independent variable(s) chosen and the coefficient(s)), the squared multiple correlation coefficient(R^2), the squared multiple correlation coefficient adjusted with respect to the

degrees of freedom (Adj. R^2), the standard error of the estimate (s.e.e.) and the F ratio (F) based on the analysis of variance of the fitted regression line.

For each variable chosen within any regression, the tolerance values (Tol.) and the standardized/beta coefficients (b) are also included in the tables. For each regression equation, the coefficient of variation and the estimated significance level of R^2 were found. **Tolerance** is a measure of the multicollinearity that each variable has with other variables in the model. So, $\text{Tol.}(X_1) = 1 - R^2$ (between X_1 and the remaining X variables in the equation). This means that the smaller the value of Tol., the greater the intercorrelation of the independent variables. Kleinbaum et al. (1988) recommend that variables with tolerance values less than 0.10 should not be allowed in the final model selected. **Standardized coefficients** allow a comparison of the relative standardized strengths of the effect that each independent variable has on the dependent variable (Sokol and Rohlf, 1981). This is not equivalent to the partial correlation coefficient unless there is no multicollinearity present (Younger, 1979), therefore they do not reflect the absolute importance of the independent variables, but they may be utilized as an approximation. The **Coefficient of Variation** is used to test if the variation in the model as measured by the standard error of the estimate is 'excessive' (Younger, 1979). This, of course, is necessarily judgemental based on the purpose of the model and the nature of the study. Lastly, the **estimated significance level of R^2** is based on tables presented by Wilkinson (1979). This value is useful because the typical t and F-distributions are biased in most subset selections (Pope and Webster, 1972).

Typically, natural polynomials (e.g. X^2) or interaction terms (e.g. X_1X_2) are also recommended for inclusion in the analysis. This quest for a better explanation of residual variance irrespective of its relevance was not attempted in this study.

Suggested guidelines regarding sample size build from the assumption of positive error degrees of freedom ($n-k-1 > 0$, where k = the number of independent variables in the model). Kleinbaum et al. (1988) recommend that $n > 5-10k$, and this recommendation was met whenever possible in this thesis.

The residuals of each point are used to first test the assumptions of least-squares linear regression and then to detect outliers. To test the assumptions, one may employ a variety of graphical analyses offered by SYSTAT. To test for *normally-distributed errors*, a bell-shaped histogram was used as an indicator of normality. By plotting the residuals versus the predicted values of the dependent variable, one may check if the errors have a *constant variance* ('homoscedasticity'). When the residuals are scaled by their estimated standard error (known as standardized residuals) they should lie within a band less than 2-3 units above or below $y=0$. If the errors are assumed to be *independent*, there should be no discernable patterns visible in the plot. Lastly, if the population is assumed to be described by the *same linear model*, a parameter known as Cook's distance (C_d) is plotted versus the estimated values of Y , and there should be a random scattering of points, with no values of $C_d > 1.0$ (Chatterjee and Price, 1991). Points which break any of these assumptions may be tentatively classified as outliers, but the leverage and Cook's distance will also be inspected.

A point identified as an outlier was not simply discarded; it was examined carefully for accuracy (transcription error), relevancy (importance in the data set) and special significance (abnormal conditions). As well, this information may be useful for further investigation.

A model is defined as *reliable* if it predicts well for subsequent samples from the population, but R^2 values or F statistics can be highly biased. The reason for this bias is

that when utilizing a subset selection procedure (say, choosing k predictors from a maximum number of m), the exact F distributions are unknown, except when $k=m$ or $k=1$ (Wilkinson, 1979). As explained by Kleinbaum et al.(1988), F values will be overestimated unless the null hypothesis of no significant overall multiple regression is true. As a result, statisticians have attempted to create tables for assessing the significance of R^2 .

Wilkinson (1979) created a set of tables for determining the significance of the R^2 values determined from stepwise selection at confidence levels of 95 and 99%. These results will be included in the summary tables for each regression model. However, there is an assumption inherent in these values which is not met by my model selection criterion: these tables assume that k is chosen before the model is determined. Although these tables may not be strictly applicable, the values will be noted. Wilkinson (1979) stated that the effects of a non-fixed k on the tables needs to be further researched, but there have been no subsequent studies.

The technique used to examine the reliability of models in this thesis is a cross-validation based on split samples (e.g. Snee, 1977). It is often employed since it can be performed on a single set of data, assuming that it is large enough to do so. The technique to be used is that outlined by Kleinbaum et al. (1988). The procedure is to randomly split the data, fit a regression model to the first split, obtain an R^2 value (predicted vs. actual values), and then utilize the model fit from the first split to predict values in the second split again obtaining an R^2 value. The difference between the two R^2 values is then defined as the 'shrinkage on cross-validation'. There are no strict values regarding the reliability of a model based on the shrinkage, but the authors recommend that if shrinkage is greater than 0.9, the fitted model is presumably unreliable, and if it is less than 0.1, it is presumably reliable. Hocking (1983) has found that in cases

where the shrinkage value is great, it is typically due one of two effects: either particularly influential points have been isolated in the split, or a collinearity has been created.

As stated by Weisberg (1983), 'statistical techniques should be used as aids to understand a problem, and not as substitutes for independent thought'. Results of (regression) analyses are not accepted as dogma, and comparisons with appropriate theoretical knowledge are made when possible. Younger (1979) warns that it is rare in a regression analysis that one finds significant predictors with small standard errors which are both theoretically and practically appealing. She further recommends that the final choice of model should be made by the researcher and not the statistician. It is this balance between statistical significance and scientific importance which was aimed at.

The independent variables used in the regressions in this thesis were obtained from either the Canadian Hydrographic Service (CHS) Tide Tables or Water Survey of Canada (WSC). All data manipulation was subsequently performed within an Excel or Lotus spreadsheet program. Four independent variables were employed, including a measure of the fluvial discharge supplied to the estuary, and three tidally-related variables.

The discharge data used (supplied by the WSC) is the calculated hourly instantaneous discharge of Squamish River estuary. It is taken as the sum of the hourly instantaneous discharges from the three major fluvial systems supplying water to the estuary. The Squamish, Cheakamus and Mamquam rivers have WSC stations (08GA022, 08GA043, and 08GA075, respectively) in reaches just upstream of the confluences. The sum of these stations expresses the vast majority of the estuary discharge, but there is a weakness in using a sum of stations. As well as the propagation of uncertainties in these measurements, the automated stage recorders are known to malfunction occasionally.

Even if only one of the stations is inoperative for a short while, there will be a gap in the data. Fortunately, the records are complete for almost the entire field research period. The hourly measurements of estuary discharge were then interpolated at any time of measurement of the dependent variable, provided that there was not a gap in either hour bounding that measurement.

The tidal data were extracted from the tide tables for Pt. Atkinson, the reference port for Squamish. The adjustments made to the tidal heights and times at low and high tides (as suggested by the CHS and confirmed in Buckley (1976)) were relatively minor (on the order of a few centimeters and minutes). The three variables chosen to describe the tidal effects detail distinct features thought to influence the hydraulic and bedform parameters in the estuary.

All data reported in this thesis were collected either on the ebb tide from HHT to LLT or the following flood tide from LLT to LHT. The other tides produced minimal variation in depth and current speed, and typically occurred at inconvenient sample times (ie. between 2000 and 0400). The variation in the tidal heights (and rates of rise and fall) over the fortnightly cycle depends on the lunar perigee and apogee, producing Spring and Neap tides respectively. Thus, it was decided that a temporal variable explaining the proximity to high or low tide be included as an independent variable. As well, quantifying the effect of the Spring-neap tidal cycle requires a measure of the absolute drop or rise, and the rate of tidal drop or rise. These tidal variables are reported as **Time(T), Drop(D) or Rise(R), and Low Tide Height (LTH)**, respectively. These variables are calculated from the information in the tide tables by:

$$T = \frac{\text{time interval between } t \text{ and HHT}}{\text{time interval between HHT and LLT}}$$

$$D = (T)(\text{Tidal height @HHT} - \text{Tidal height @LLT})$$

$$R = (T-1)(\text{Tidal height @LHT} - \text{Tidal height @LLT})$$

$$LTH = \text{Tidal height @LLT}$$

(note: Appendix 1.2 is a summary of all abbreviations and symbols used in the thesis)

Note that LTH is a measure which is strongly correlated with the average rate of drop or rise over the diurnal half-cycle. For the purpose of multivariate analysis these variables should be independent, but note that there may be some correlation between them (e.g. T and D). There is no correlation between the tidal and discharge variables since the Pt. Atkinson CHS station is not influenced by river discharge, and similarly, the WSC stations are upstream of any tidal influence (Hickin, 1989). The effect of the systematic change in stage due to the tidal wave cannot be quantitatively ascertained with the staff gauges. The stage measured to the nearest centimeter does not change within one hour of low tide, an interval likely much longer than the propagation time of the tidal wave through the study area.

Since high tides are amplified or advanced by local winds, subsequent effects on these tidal parameters could include:

- 1) an increase in R (and D on subsequent ebb);
- 2) a decrease in T on the flood tide (and an increase on the subsequent ebb);
- 3) an increase in LTH on the subsequent ebb tide.

The regressions performed in this thesis are differentiated by ebb and flood tides in order to fit a linear least-squares regression. There is a slight deviation from linearity in

the tidal variables near the times of high and low tide, but it is minimal (Buckley, 1976), and deemed insignificant within the accuracy of the tide tables.

The most complex regression models considered include the estuary discharge and all three tidal variables. The model selection utilizes an approximate F-to-remove value of 4.0. This value was chosen a priori because it was felt that it would include an adequate number of explanatory variables without compromising model reliability. A subsequent analysis of the data indicated that almost 95% of the partial F values were either less than 2.5 or greater than 6.0. Thus, the model selection procedure is relatively insensitive to this precise cutoff.

2.2- MEAN BEDFORM PARAMETERS AND WATER DEPTH

2.2.1- Field Techniques

The bedform parameters along the thalweg of Squamish River estuary were investigated because the high-speed filament was associated with the most intense macroturbulence. The study region was divided into several reaches, and the mean-reach values of water-depth, bedform-height and wavelength were obtained from graphic-output sonar. Results are dependent on both data collection (e.g. transect path and speed, reach identification and differentiation) and digitization (e.g. definition and measurement of bedform parameters). Observations of boil intensity in the thalweg were also made during collection of bedform data.

Bedform profiles were obtained along a 2km path length utilizing a graphic output Lowrance X-16 depth-recording sonar. The path was chosen to follow the thalweg at low tide, but there is a divergence at approximately mid-path due to trees incorporated into the bed. Each profile of the path-length is known as a 'transect', with over 600 such

transects run during the field season. Most were run in pairs, first upstream, then downstream, with the downstream path following a slightly different route in places (Fig. 2.2). Presumably the upstream transects yield more reliable information since a slower and more uniform speed can be maintained while still following the survey route.

The transect was divided into twelve 'reaches', which are segments between two objects on the shore chosen to break the transects into straight lengths of approximately homogeneous average velocity, width and depth. During the traverse, when the shore marker intersected a sighting bar on the survey boat, the profile was marked. The length of each reach was measured on the shore (and verified on air photos), so that the actual length of features identified on the profiles could be determined. If a bedform straddled the boundary between reaches, the distances were extrapolated, and the bedform was included in the reach containing its crest. Although sinuous-crested bedforms with similar spatially-averaged lengths and heights may display considerable lateral variation when viewed in streamwise cross-section (e.g. Gabel, 1993), it is assumed that such error will be averaged out in the analysis.

2.2.2- Transect Analysis

Digitization of graphical data is a time-consuming process, and not all reaches from every transect could be analyzed. Even once all reaches fouled by waves or other navigational difficulties (e.g. wind) were removed, over 95% remained. Therefore, only five reaches were digitized from the upstream-moving transects, and two of those five from the downstream-moving transects (Fig. 2.2). The reaches selected to be analyzed were those in which the widest range of surficial-macroturbulence characteristics and intensity could be recognized (thus elucidating bedform control). Also included were those which had speed (reaches 2,4,5,7) and slope (reaches 1,5,6) measurements taken for

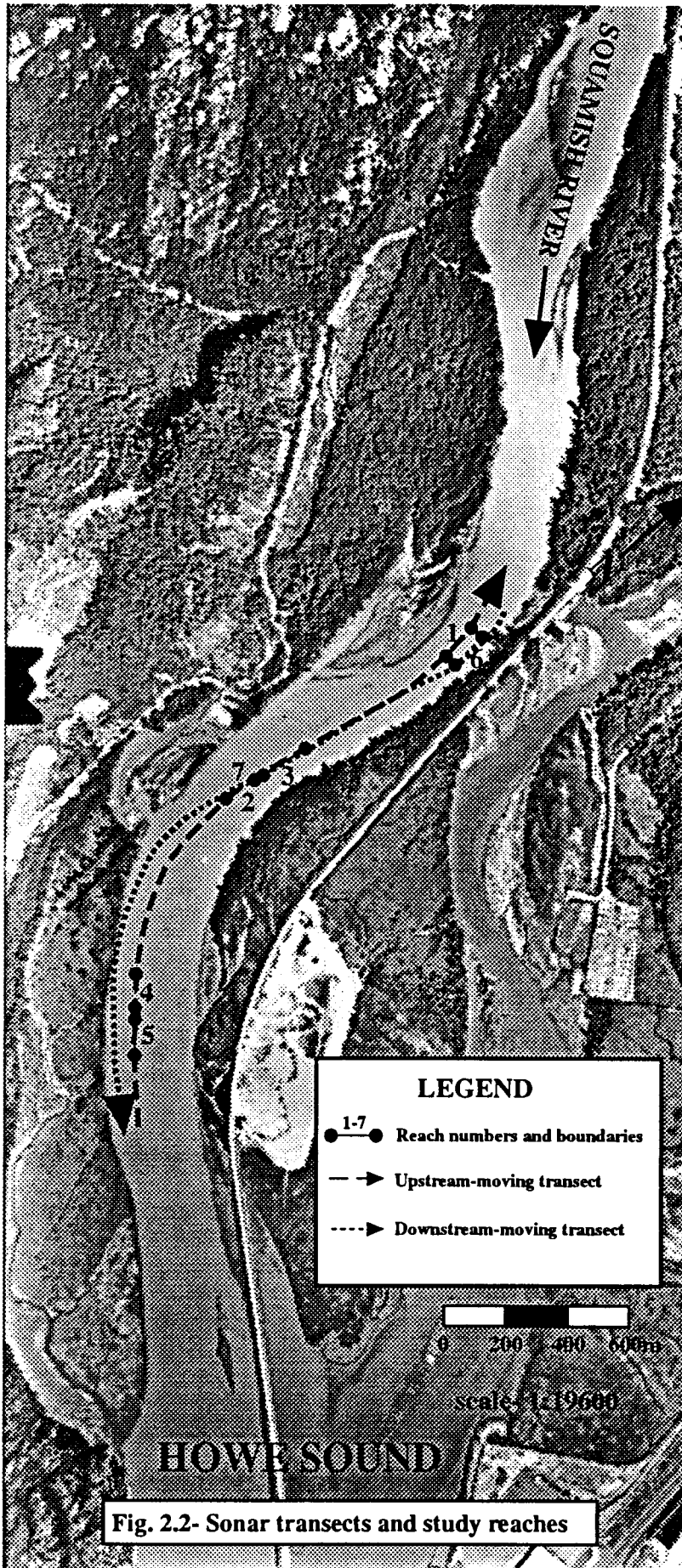


Fig. 2.2- Sonar transects and study reaches

at least part of the research period. Also, reaches were selected so that upstream and downstream comparisons could be made (reaches 1 versus 6, and 2 versus 7). Note, however, that reach 1 is just streamward of reach 6 (details in section 5.2.2.1). Of the approximately 600 transects run, 100 were selected for each of the 7 reaches. These were chosen to cover the full range of tidal and fluvial conditions encountered.

To ensure that the transects to be digitized included the full range of flow conditions, the independent variables used in the regression analyses are interpolated for each transect, and Q, D, and T were differentiated into classes to create a 3-dimensional matrix. T was divided into 7 classes (0-0.25, 0.26-0.5...1.26-1.50, and >1.51), while 4 classes were used for Q (<425, 425-525, 525-625, >625 m³/s) and D (<1, 1-2, 2-3 and >3m). For Q and D, the transects to be digitized were chosen such that approximately 25% fell into each class. For T, 8% fell into the extreme classes, while the middle 5 classes had approximately 16% of the transects each. An attempt was made to fill each cell in the matrix, but several remained empty. Some were for logical reasons (e.g. T 0-0.25 and D>1m cannot occur), and other because the prescribed conditions were rare (e.g. Q= 525-625 m³/s).

In order to determine individual bedform properties from a continuous profile, a bedform must be operationally defined. This definition is necessarily somewhat subjective depending on the scale of the features along the profile, but this is acceptable as long as consistency within the analysis is maintained. A portion of the digitization was contracted out and a 20% subset of those transects were double-checked to ensure repeatability. Although measurements of individual bedforms frequently differed slightly, the reach-mean values of height, wavelength and depth differed by more than 5% in less than 10% of the cases, and never differed by more than 10%. Predictably, these cases were limited to those reaches with few bedforms (typically, less than 8).

As noted by Robert and Richards (1988), the varied choice of measurement technique of bedform height and wavelength, and the arbitrary elimination of small-scale heights and wavelengths prevents comparison of empirical results. In this study, bedforms measuring less than 0.05 cm on the graphical output could not be digitized. Secondary bedforms on the stoss side of larger features also presented difficulties in digitization. It still remains unclear whether superimposed dunes are related to dune lag or are an equilibrium dune condition (Gabel, 1993). Although uncommon, their occurrence on profiles was noted ('notes' column of Appendix 2.4), and the treatment was consistent. If the height of the secondary features exceeded 20% of the height of the 'parent' bedform, or if the secondary features were better defined than the parent feature, each secondary feature was digitized as a separate bedform.

Similarly, there is not a commonly accepted technique for measuring the morphometric parameters of bedforms. Wavelength may be measured as crest-to-crest (e.g. Korchokha, 1968; Allen, 1969; Engel and Lam Lau, 1980), trough-to-trough (Kachel and Sternberg, 1970; Yalin, 1977; Karahan and Peterson, 1980; Richards, 1982; Dinehart, 1992) or both (Allen, 1985). Bedform height may be measured as the difference between the crest and preceding trough (Kachel and Sternberg, 1970; Karahan and Peterson, 1980; Richards, 1982), following trough (Korchokha, 1968; Yalin, 1977; Allen, 1969, 1985) or unspecified (Jackson, 1975; Kostaschuk et al., 1989b). Even the depth of water over bedforms is measured inconsistently among studies: depth from water surface to dune crest (Znamenskaya, 1968; Jackson, 1975; Karahan and Peterson, 1980) or to one-half dune height (Yalin, 1977; Jackson, 1977; Allen, 1985).

Presumably, these inconsistencies can be attributed to the bedforms often being symmetrical (and two-dimensional), thus it being irrelevant whether height is measured on the up or downstream side. The importance of the wavelength measures depend upon

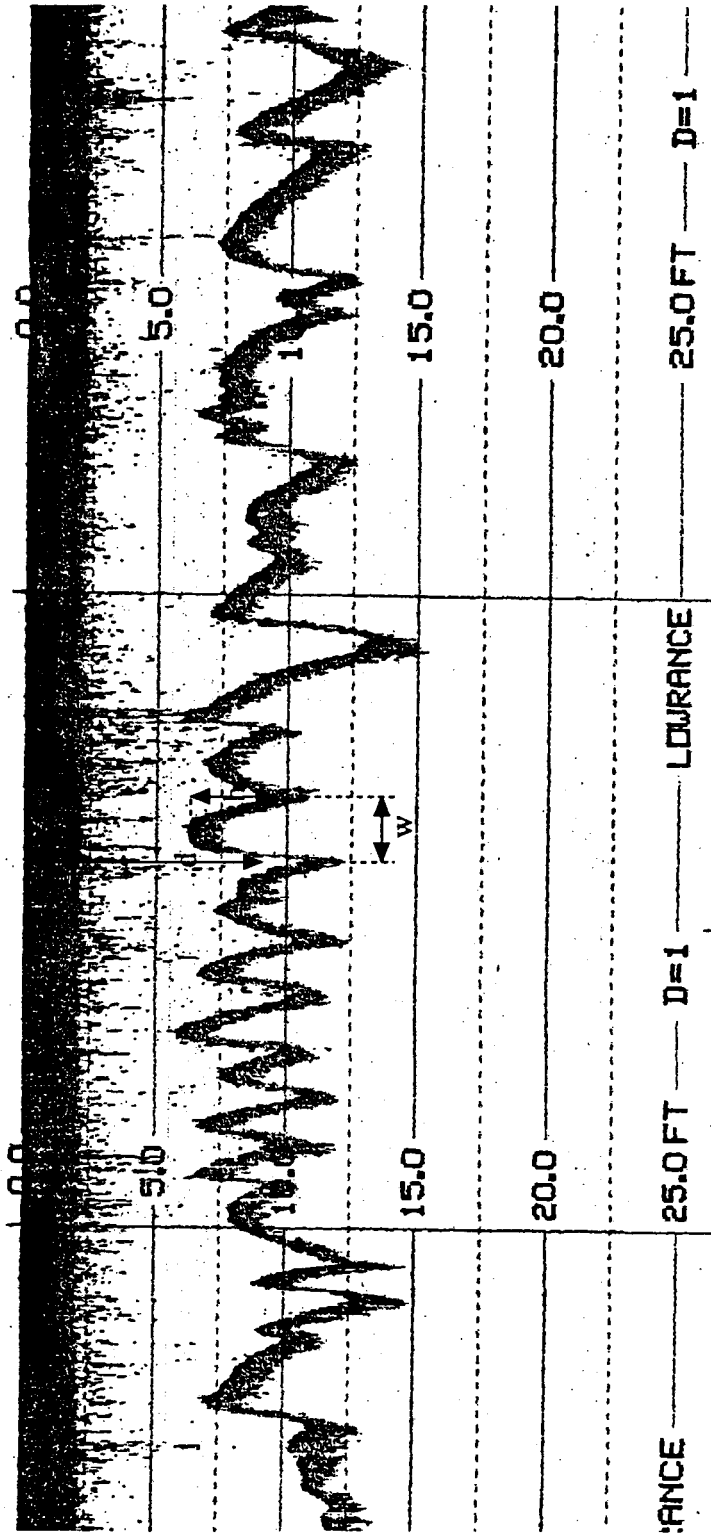
whether individual bedforms are the study focus or if means of several bedforms are examined. In my analysis, reach-means of wavelength (w), height (h) and depth (d) are used (Jackson, 1975; Allen, 1985), and the results are relatively insensitive to the measurement technique.

The bedforms in the study area are asymmetrical (ebb-tidal asymmetry), and bedform height is measured on the upstream side. This presumes that in the unidirectional flows, it is the displacement of the streamlines on the upstream side that controls the macroturbulence. Wavelength is measured as the trough-to-trough distance, and depth is measured as the distance from the water surface to one half the bedform height on the downstream side (Fig.2.3). The standard deviation of the d , w and h was also calculated.

Once h , w and d were obtained from digitization, multiple regressions were fitted to the data for each of the seven reaches. The independent variables used are those outlined in section 2.1: interpolated values (at the time of the start of the transect) of Q , D , T , and LTH . An important difference is that on the flood tide, R is not utilized independently. It is assumed that the bedforms will be most strongly controlled by the tidal drop since the velocity asymmetry is so strong (e.g. Dalrymple et al., 1978). As well, there may be a lag in the bedform-response such that the effects of the flood tide are not indicated by the bedforms well in excess of $T = 1.00$. These assumptions are examined, and the regressions are repeated using the 'absolute drop' ($= \text{Drop}_{T=1.0} - \text{Rise}$). Again, the regressions are differentiated by ebb and flood tide in order to fit a linear least-squares fit, and the most complex models considered include all four variables, and utilize the F-to-remove value of 4.0.

Transformations are attempted if deemed necessary, and the policy of not mixing transformations is upheld. Although mixed transformations have been justified by

Fig. 2.3- Measurement of bedform parameters and water depth from graphical output of sonar transects



researchers as improving predictive ability of models (e.g. Kostaschuk and Atwood, 1989), my agenda of model simplicity and reliability (based on the exploratory nature of the research) will remain.

Qualitative measures of macroturbulence during the transects are utilized in the analyses of this chapter. At the time the transect was run, observations regarding the structure and intensity of the boils were made according to the following outline (note: a further differentiation based on morphology will be introduced in Chapter 6):

Level 1- strong 'eruption', sediment and organics entrained, audible

Level 2- weak 'eruption', sediment and organics entrained

Level 3- strong 'upwelling', organics entrained

Level 4- weak 'upwelling', bit of organics

Level 5- gleans; very weak upwellings, no organics

Level 6- calm, placid surface

In addition, from the graphic output, it was noted if sediment was entrained from the bed, whether or not it reached the surface, if there were secondary bedforms, and if there were trees on the bed.

2.3- BOIL PARAMETERS

2.3.1- Data collection

Collection of simultaneous current-speed and boil-period time series required filming the boil activity for later digitization. There are numerous difficulties associated with obtaining video records of macroturbulent phenomena, most notably the lighting and weather requirements. Subsequent digitization of video requires reliable definition and timing of inter-boil periods. Accurate correlation of the boil-period and current-speed time series depends on precise timing of data collection.

The details regarding the collection of the current-speed data are reported in section 2.1.1. Attempts were made to film the water-surface macrotubulence from the research vessel, but during strong currents the boat was an unsuitable platform. Also, since measurement of the current-speed required the attention of both crew members, filming from the boat and current speed measurement could not be performed simultaneously. This meant that the camera had to be located onshore, and that current-speed (and water-surface slope) measures were taken in direct proximity.

The film sites chosen had to meet several requirements. These included the presence of persistent boil generation, a film platform which would be stable (in high winds) and elevated (for a high-oblique view), and ambient light that would be adequate over a wide range of conditions. Built structures were tested, but trees near the river bank provided superior height and stability, and permitted inconspicuous instrumentation. The number of potential sites was limited to where the thalweg impinged on the bank, and it was decided to have two sites on each bank. One for boil *generation* and the other where the structures were noted to *advect* past.

The video camera was fixed to the tree-mounted platform and left to run continuously (Fig.2.4). There were intermittent battery changes and camera adjustments over the daily filming duration of approximately four hours (governed by battery life). Initial observations indicated that filming two hours before and after LLT would produce results best suited to digitization. However, as the research continued, adjustments in this schedule were made for lighting conditions, and the Spring-neap tidal cycle.

Filming was problematic in rainy and foggy conditions, resulting in poor-quality video. In addition, under clear skies, the quality of video was influenced by the time of LLT. At

the R/B, if the L/LT was before 0900 filtering was ideal, but after that time, bright reflections on the water surface obscured the pattern of the boils. At the L/LT, the water was less bright, and after 1200, created dark shadows on the water surface. Clear, sunny weather also affected streamflow video footage at the R/B. Not only was the direct sunlight too bright, but the ambient winds typically created ripples or waves on the water surface, thus obscuring the boils. Filming was performed in conjunction with current-speed data collection at the L/LT from June 2-15, and at the R/B from June 16-30 (Fig. 2.5). As research progressed, the techniques were improved, thus the data collected



Fig. 2.4- Videocamera mounted in a tree at the R/B U/S station

the R/B, if the LLT was before 0800 filming was ideal, but after that time, bright reflections on the water surface obscured the pattern of the boils. At the L/B, the thick vegetation reduced brightness, and after 1200, created dark shadows on the water surface. Clear, sunny weather also affected afternoon video footage at the R/B. Not only was the direct sunlight too bright, but the anabatic winds typically created ripples or waves on the water surface, thus obscuring the boils. Filming was performed in conjunction with current-speed data collection at the L/B from June 2-15, and at the R/B from June 16-30 (Fig.2.5). As research progressed, the techniques were improved, thus the data collected at the R/B was of a much higher quality later in the program. It became evident that bright but overcast skies in the early morning (0500-0900) were the ideal filming conditions. Unfortunately, soon after this realization, the video quality began to degenerate, apparently due to increasingly misaligned video heads in the camera.

During most current-speed and water-surface slope measurements, a qualitative estimate of the maximum intensity of boil activity (based on the rating scale introduced in section 2.2) was made. During sonar measurement of the bedform properties, the dominant morphology of the macroturbulent features arriving at the surface within each reach was noted. Reliable estimates of boil size require adequate scaling of dimensions and consistent definitions of boil boundaries. Quantification of boil expansion rates would demand time series of the boil-size estimates. Photographic data are subject to the same difficulties as the video data.

Low-level time-series photos of the water surface taken in July and August, 1992 are used to quantitatively estimate boil size and expansion rates. The location and size of the boils determined which of two photographic techniques were employed. If the production site was not reasonably close to the river bank, the photos were taken while anchored in the flow using a remote-activated camera affixed to an extendable pole.

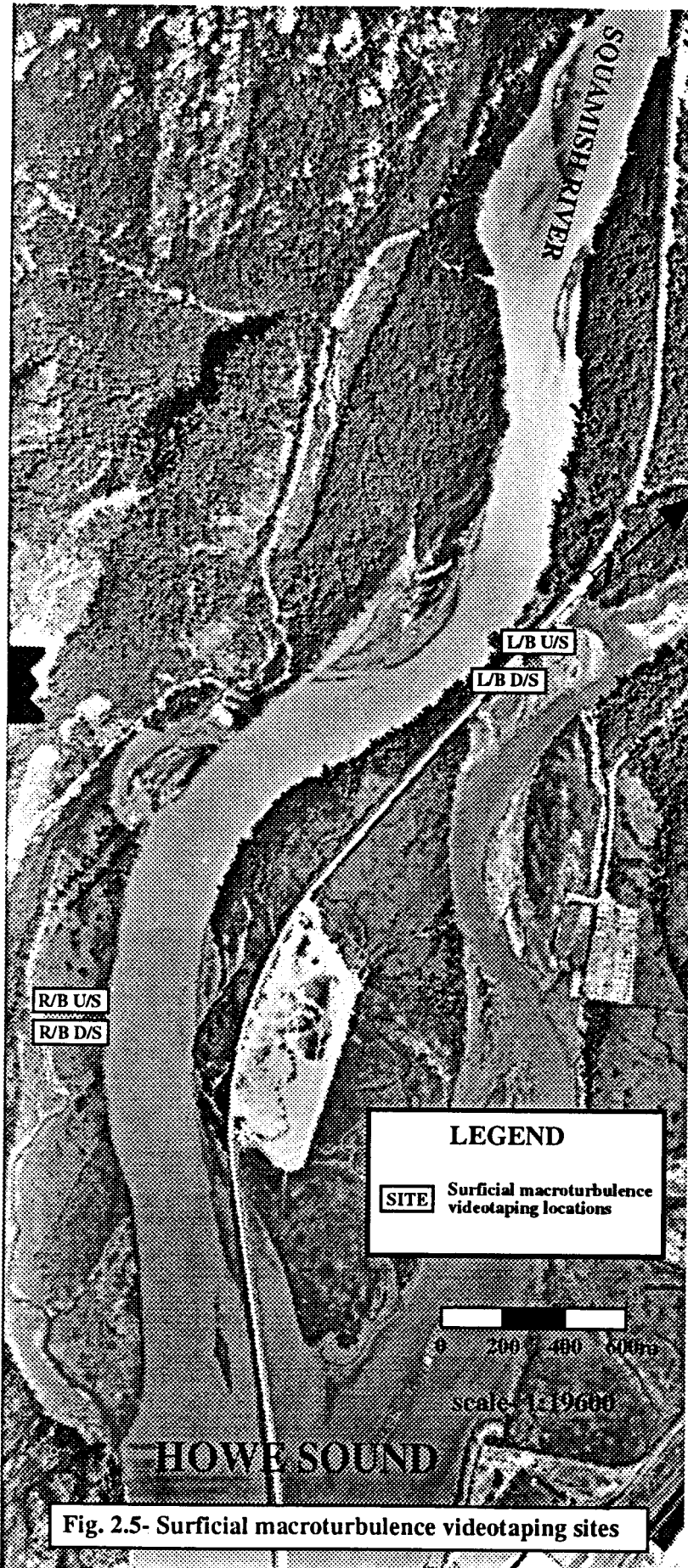


Fig. 2.5- Surficial macroturbulence videotaping sites

Scale was determined from items of known size placed in the photo domain at the river surface. If the production site was near the river bank and the boils were too large to employ the pole-photography technique, oblique-angle photos were taken from sites near the bank, approximately 5-8m above the river surface (dependent on stage) (Fig.2.6).

The camera used was a Pentax Zoom 90 with a 35-90mm zoom lens. During photography of the boil structures, video footage was also obtained. Unfortunately, the video quality was poor due to degenerative vibrational problems with the video heads. The photos were taken at a period of no less than 1.6 seconds, which is the refractory period of the camera. The exact period could be determined from the audio portion of the video footage because the photographer indicated verbally when a photo was taken. The duration of the photographic time series was 3-7 photos, depending on boil activity and lighting conditions.

2.3.2- Data manipulation

As noted previously, not all video records of the surface macroturbulence could be digitized. Over 100 hours of video were collected, but more than half were discarded due to poor differentiation of structures as a result of poor lighting or weather conditions. There was also a relatively narrow range of boil *intensity* that could be digitized. Bounding conditions had either such intense activity that structures could not be attributed to a single generation site, or such weak activity that the upwellings could not be recognized reliably. The surface current-speeds associated with these intensities indicate that for digitization to be possible (under ideal lighting and weather conditions) speed must not exceed 2.0 m/s for the R/B U/S site, and 1.2- 1.4 m/s for the other sites. Ultimately, just over 25% of the collected video record was digitizable.



Fig. 2.6- Boil photographic technique at L/B

The analysis began with identification of the most distinct upwelling site for each time series. The choice was obvious for the production sites, but more difficult for the advection sites where there were upwellings with a variety of origins. As a boil broke the surface at that site, the time was recorded. A 'macro' program was written in Microsoft Excel 3.0 which, by pressing a key sequence, automatically recorded the time based on the computer's internal stopwatch (to the nearest second) in a spreadsheet. This allowed the time of each boil eruption to be saved without stopping the video record. Then, the spreadsheet was used to calculate the period between each boil appearance. Rather than digitizing all video footage possible, only film taken in conjunction with the current-speed time series was digitized. The internal stopwatch of the video camera was used to display the actual time during filming, and the current-speed measurements were carefully synchronized. As footage allowed, video digitization for each time series lasted 15 minutes, typically bounding the current-speed time series by approximately 2.5 minutes before and after. Then, over this 15-minute span, the mean boil-period was calculated. It was not possible to obtain a reliable measure of the boil duration from the video record. Sonar was used to obtain the depth measurements utilized in Chapter 6 at the site of the current-speed measurement, which may be several metres downstream of the video site.

As outlined in Chapter 4, simultaneous boil period and current-speed time series could not be obtained at current-speed measurement sites #3 and 4. A measure of the surface current-speed was taken, and the fathometer was left to run continuously for several minutes to get depth and bedform height estimates. Other boil-period time series were obtained by timing the period between boils with a stopwatch. Observations of boil qualities within the estuary are summarized in Chapter 3.

CHAPTER 3- QUALITATIVE DESCRIPTIONS OF BOILS

3.1- INTRODUCTION

Scientific observations of the macroturbulence displayed at the surface of rivers, estuaries and tidal channels have been made for over one half-century. However, there have been few systematic studies, and specific terms for observed features have not been unequivocally used in the literature. Jackson (1976) concluded that features described in previous studies termed 'structural eddy formations' (Korchokha, 1968) or 'Type III(1) macroturbulence phenomena' (Matthes, 1947) are analagous to the boils described by Coleman (1969). Coleman (1969) and Jackson (1976) present diagrams of a macroturbulent structure with a point-source upwelling. It assumes a circular shape as water flows away from the center towards a sharp boundary marked by vortices, or a distinct decrease in suspended sediment. The structure then grows radially, flattening as its energy diminishes, and dissipates within one minute. This is known henceforth as the 'Coleman/Jackson model'.

Throughout the observational area, the boils are strongly influenced by tidal conditions. The current is non-reversing, and near HHT (particularly during Spring tides), current speeds greatly slacken and the river surface becomes mirror-like (Fig.3.1a). As the water level drops during the ebb tide, the increase in current speed is attributable to both the increasing water-surface slope and the decrease in the cross-sectional area as bars become progressively exposed.

Field observations of boils often suggest a common morphology and evolution, but Rood and Hickin (1989) noted that the structures in Squamish River estuary may be complex. Therefore, the initial weeks of the field season were spent observing the boil

a)



b)

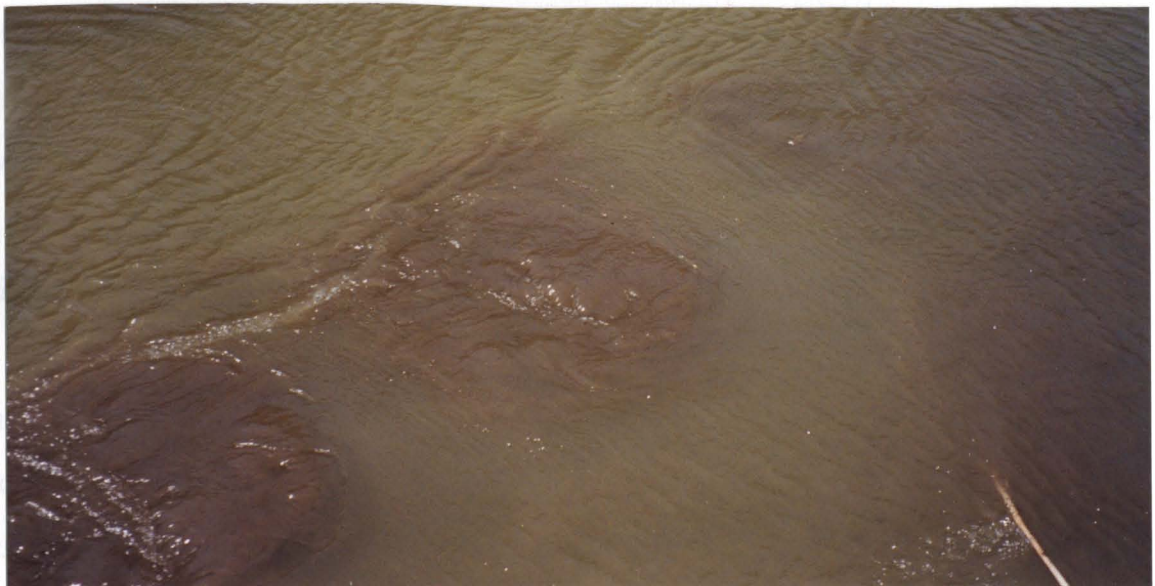


Fig. 3.1- a) R/B site at HHT during maximum Spring tide
 b) Streamwise sediment-laden bands in lower estuary
 (flow is towards lower left corner of photo; note rope
 (diameter=3cm) for scale)

structures over the semi-diurnal tidal cycle from HHT to LLT to LHT at sites from the river mouth to a distance 5km upstream. It was evident that there were two distinct types of boils confined to specific regions within the estuary (Fig.3.2).

3.2- TYPE 1 BOILS

Approaching LLT in the lower estuary, the water surface often exhibits streamwise parallel bands of alternating smooth and rough patterns. As the depth decreases, these bands become differentiated by the sediment and organics entrained by macroturbulent features (Fig.3.1b). These lanes of boil activity become most strongly developed in the late ebb, particularly during Spring tides. The bands only maintain a parallel structure over a short distance before the mid-channel bar disrupts the pattern. On the ebb tide, the lanes of boil production become tied to areas of flow separation on the bar head. The lanes increase both in number and width 1-1.5 hours before LLT (Fig.3.3). As LLT approaches, the bands begin to decrease in width, but they increase in number near the L/B while they diminish near the R/B. This trend continues to the flood tide, and then all bands dissipate a few hours after LLT. This description is based on observations on days with tidal drops exceeding 3.0m.

Within these bands, sites of repeated boil production were noted, but the duration rarely exceeded 5 minutes and never exceeded 10 minutes. Once a production site stopped, another site was typically created within a 10m radius. The structures observed in the lower estuary frequently followed the Coleman/Jackson model, but there were also periods when features did not compare to their model.

Structures with a single point-source upwelling, and downwelling which encircles the structure as it expands and advects downstream are often observed in the lower estuary.

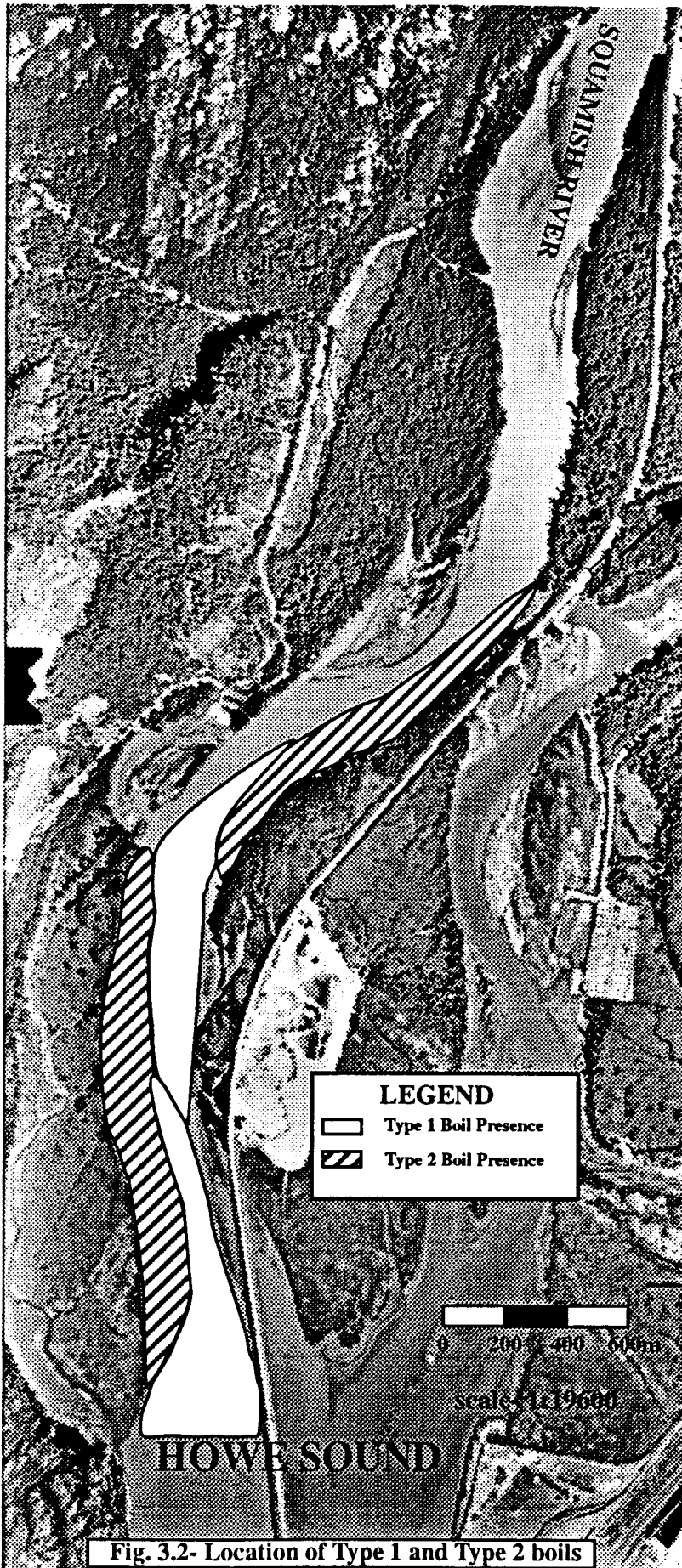


Fig. 3.2- Location of Type 1 and Type 2 boils

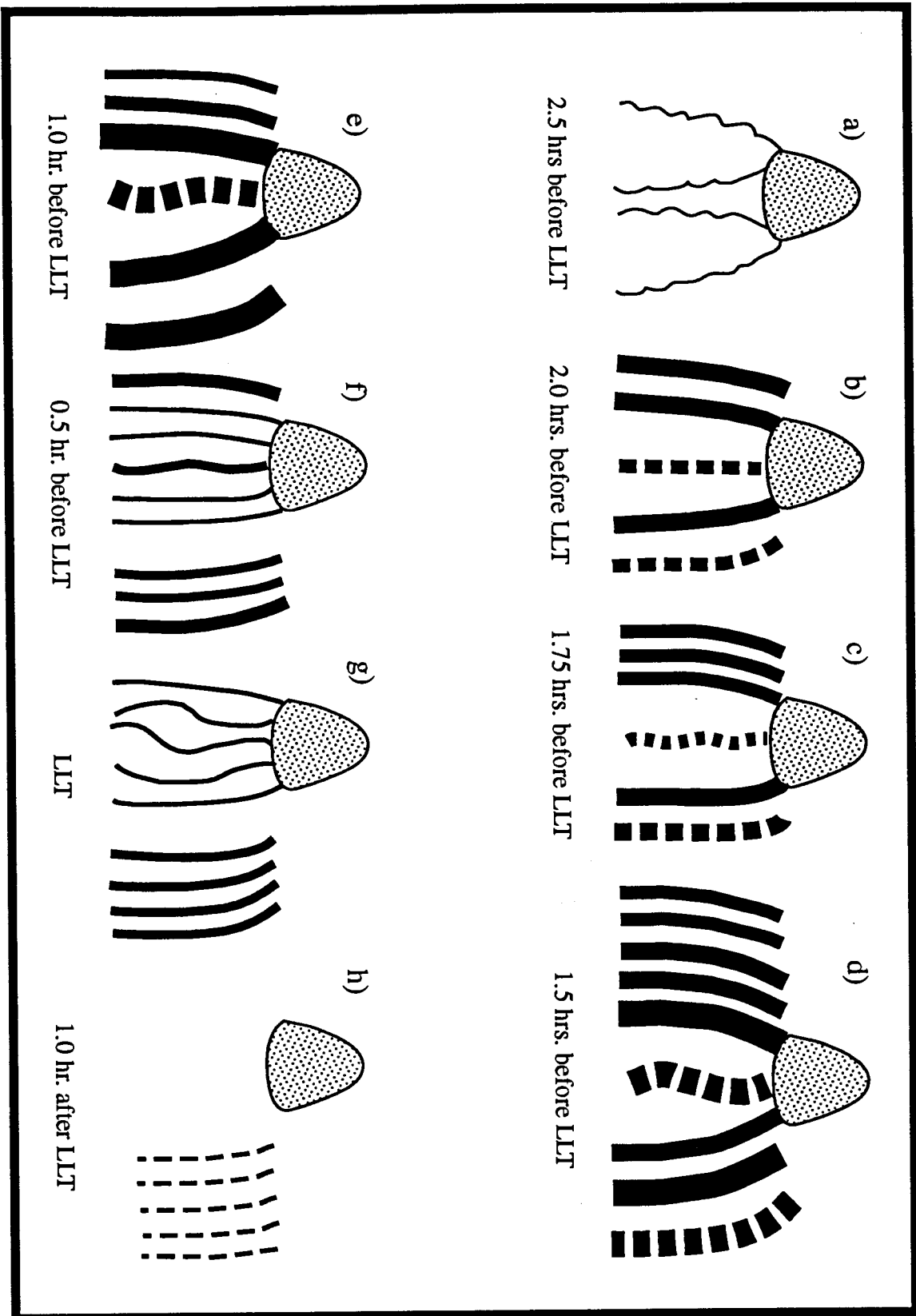
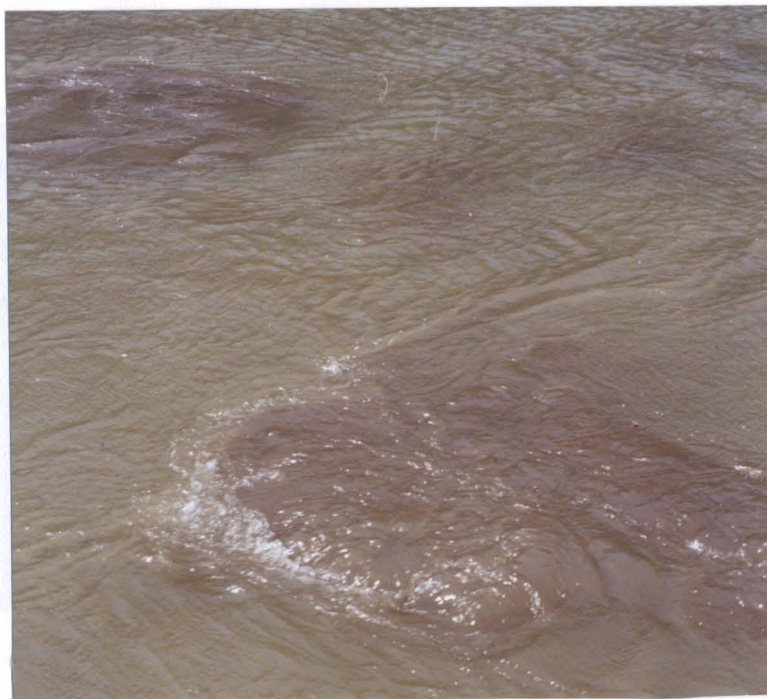


Fig. 3.3- Patterns of boil lanes downstream of mid-channel bar (surrounding LLT during a Spring tide)

This is similar to the Coleman/Jackson model, but secondary features could also be present on the upstream side (Fig.3.4a). As LLT approached, two distinct structures not fitting the Coleman/Jackson model were observed in the lower estuary. During Spring tides, some boils erupting at the surface did not display one or two point sources, but had tens of small point-sources of upwelling, each entraining much sediment and organics. These violently erupting boils do not have specific preferential downwelling regions, and the edges are poorly defined. In plan view, the chaotic pattern of upwellings creates a structure appearing similar to a head of cauliflower (Fig.3.4b). These boils are defined as having a 'cauliflower' morphology.

Upwelling was also noted to occur along a linear source, with rotation along a horizontal axis, and preferential downwelling along a linear front. This downwelling was frequently oriented normal to the flow on the downstream side of the upwelling, but could also be aligned parallel with the flow (Fig.3.5a). These boils have been termed 'rollers'. The ends of the roller could either be straight (Fig.3.5b) or curved (Fig.3.6), and this seems to determine how the structure will evolve. After the initial upwelling, there is a distinct cycle of events leading to dissipation. As illustrated in Fig.3.7, the ends begin to curl towards the center of the feature as it spreads and rains out sediment. As the structure thins, the ends loop strongly, and often form strong vortices on one side or both (Fig.3.8a). If the axes were initially straight, the structure would then simply dissipate. However, if they were curved, a secondary feature often upwells either just between the vortices, or on the upstream side of the structure (Fig.3.8b). These secondary features may spawn several additional smaller features, but all are poorly defined and short-lived (Fig.3.9). Although the secondary features provide another input of energy, there are no additional upwellings beyond 5-8 seconds after the original boil broke the surface, and the structure dissipates as it is advected downstream. It can be identified as an oval patch

a)



b)



Fig. 3.4- a) Secondary upwellings on u/s side of Coleman/Jackson structure (boil is approx. 1m wide (normal to flow))
b) Cauliflower boil structure (3cm diameter rope)
flow is towards left side of photos for both a) and b)

a)



b)

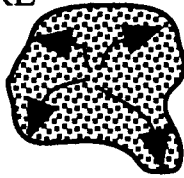


Fig. 3.5- a) 'Roller' boil structure aligned parallel to flow (flow is towards lower left corner of photo; long axis of each roller is approx. 1.3m)
b) Roller structure with straight long axis (flow is towards bottom of photo; 3 cm diameter rope for scale)

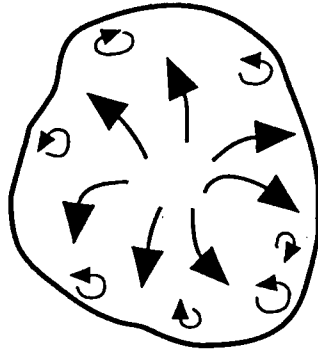


Fig. 3.6- Roller structure with curved long axis (flow is towards lower left corner of photo; 3cm diameter rope for scale)

a) eruption (t)



b) t + (1 to 5s)

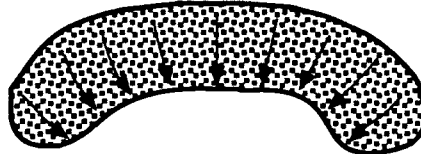


ROLLER STRUCTURE WITH HORNS

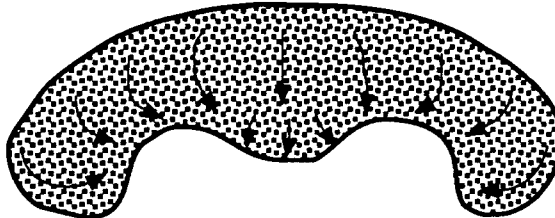
a) eruption (t)



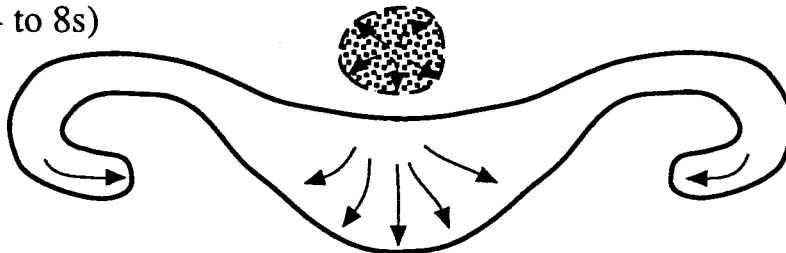
b) t + (1 to 2s)



c) t + (2 to 4s)



d) t + (4 to 8s)




 = greater suspended sediment content than surrounding flow (visually)

Fig. 3.7- Evolution of boil structures: a) Coleman/Jackson and b) roller (with horns)

a)



b)

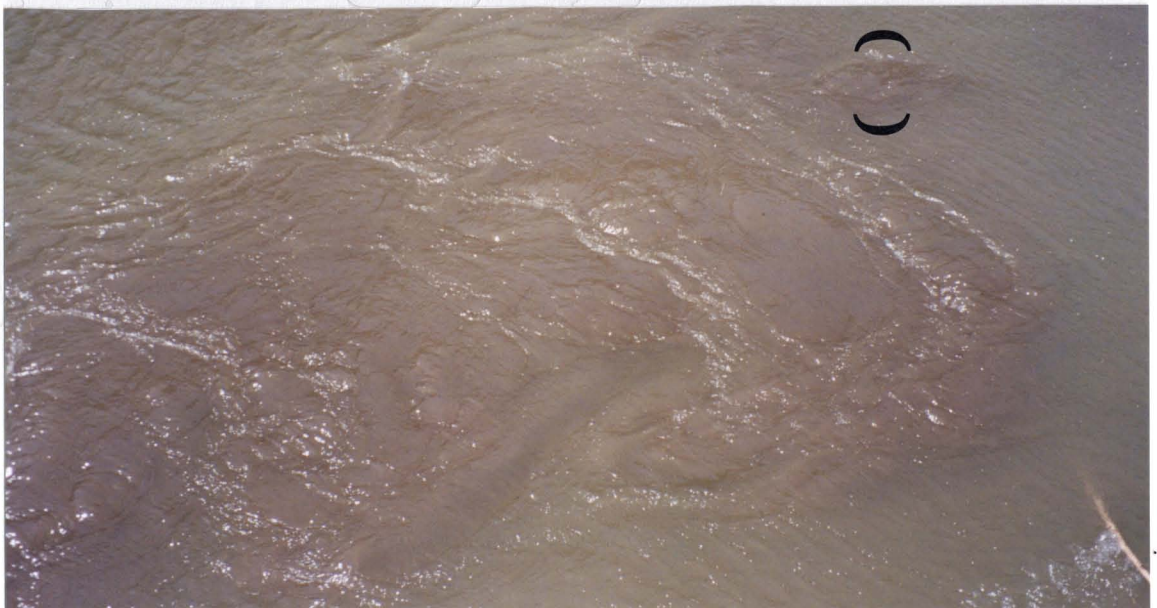


Fig. 3.8- a) Vortices formed on ends of roller structure (flow is towards bottom of photo; structure is approx. 2m wide)
b) Secondary upwelling formed upstream of roller (flow is towards lower left corner of photo; 3cm rope diameter)



Fig. 3.9- Poorly defined and short-lived secondary upwellings
(flow is towards bottom of photo; structure is
approx. 0.8m wide)

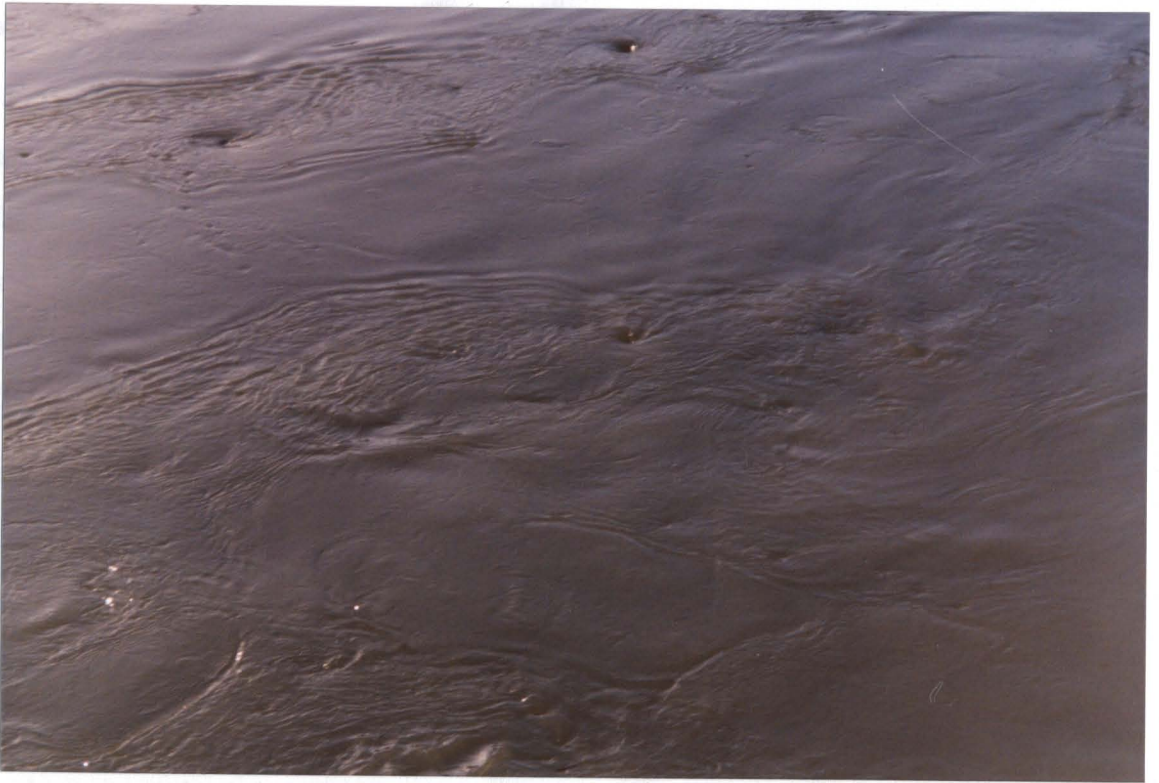
of smooth water for tens of metres downstream, occasionally up to several hundred metres downstream.

Further upstream, the observed morphology, evolution and production sites of the boils were quite different from those in the lower estuary. The exception is where the thalweg crosses from the L/B to the R/B (ie. sites 2, 3 and 7 in Fig.2.2). Although the production sites seem to occur randomly rather than in lanes, the duration (less than 5 minutes) is similar to the lower estuary site. All three structures described above are noted at sites 2, 3 and 7 with intensities similar to those in the lower estuary. The most extensive boil activity in the middle and upper estuary occurs where the thalweg impinges on the banks.

3.3- TYPE 2 BOILS

Wherever the thalweg moves along the outside bank in the estuary, there are numerous slump blocks and undercut trees in the channel which produce turbulent wakes. There were also several sites along both banks that were the production sites for a more persistent form of macroturbulence. The intermittent upwelling of fluid produced a structure that would grow in surface area and stretch downstream as the upwelling continued. After detaching, the patch of smooth water moved downstream, acquiring a rotation in accordance with the lateral velocity gradient. Over several hundred metres downstream of the production site, the boil also underwent continual change- stretching, expanding and contracting as numerous upwellings continually rejuvenated it. The contribution of many individual upwellings produced an agglomeration that typically had a surface area of 10-20 m², but occasionally exceeded 60 m². The upwellings within the boil agglomeration are frequently bounded by foam, vortices, or areas of downwelling, but precise delineation of the boundaries required ideal lighting conditions (Fig.3.10a,

a)



b)

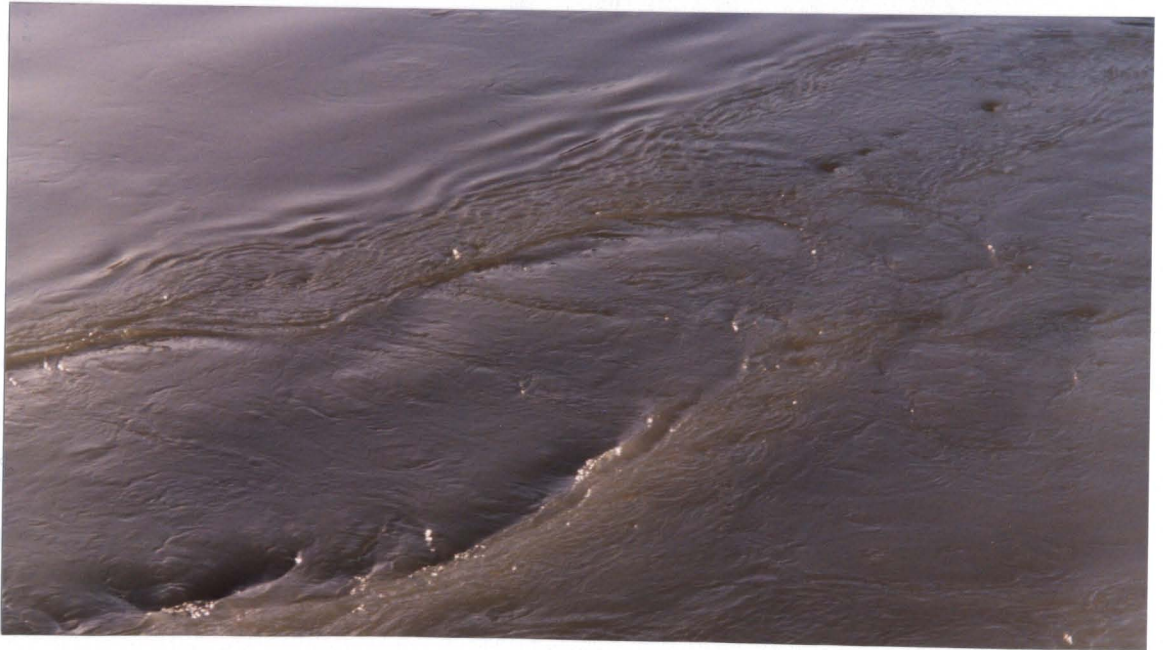


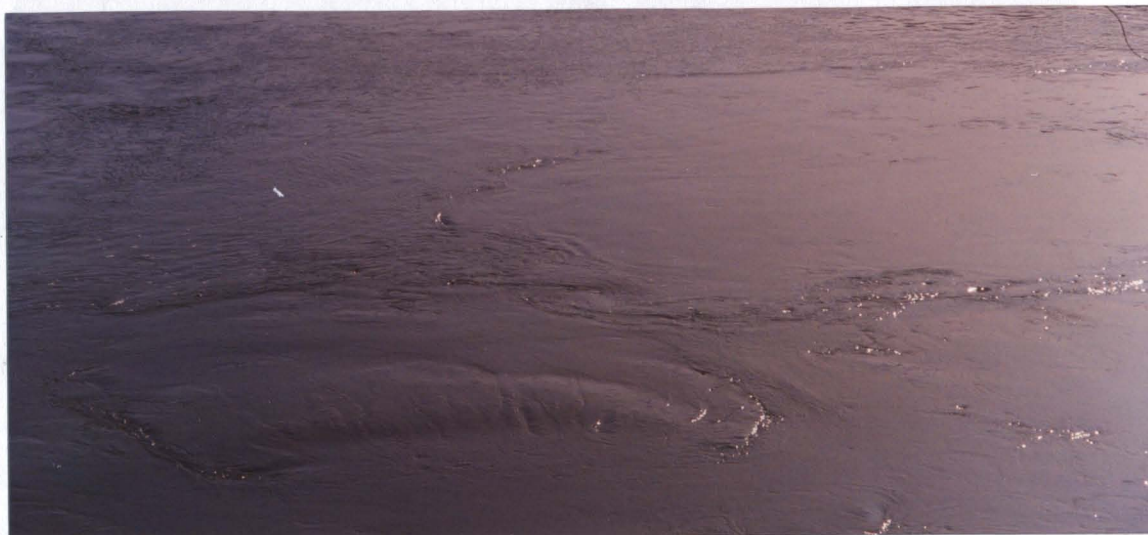
Fig. 3.10- a) Several orders of linear patterns of vortices in a boil
 b) Downwelling on downstream side of boil
 for both photos, flow is towards upper right corner;
 largest vortices have approx. 20cm diameters

3.10b). As the boils advected past, the upwelling sites appeared random, but with the passage of several boil structures, it was apparent that they remained persistent over at least several tens of minutes. As the structure passed, the frequency and strength of the upwellings at any particular site seemed to increase. The shape of the upwellings (not the agglomeration) either followed the Coleman/Jackson model, or appeared as rollers (Fig.3.11a). In plan view, the agglomerations typically appeared as ovals stretched downstream, but the shape is governed by the position and strength of the upwellings. This is displayed in the time series photos of Fig.3.12a-d. Even successive boils may be oriented in different directions (Fig.3.11b). In fact, the upwellings within the agglomeration displayed wide ranges of intensity, expansion rate, duration, size and orientation over short temporal scales. All these factors produce the seemingly random evolution of the agglomeration as it is advected. Just as there are identifiable production sites and transportation/advection regions for these structures, within 200-300m, they typically lose their vigor.

Although some boil agglomerations managed to persist for several minutes and travel in excess of 500m downstream of their production site, most became enveloped into the surrounding flow in one of three ways. The structure either 'elongates', 'segments' or simply 'diffuses' (Fig.3.13). The patterns noted were not mutually exclusive for any particular structure, and operationally are subjective. Sets of time series (period approximately 2 seconds) display examples of diffusion (Fig.3.14a-d), segmentation (Fig.3.15a-d) and elongation (Fig.3.16a-d). Just downstream of where these agglomerations seem to lose their energy is typically another production site, and the cycle of production, transportation, and destruction, is repeated.

Qualitatively, it seems that the morphology, evolution and production sites of the boils noted in the lower estuary and at sites 2, 3 and 7 are quite different from the boil

a)



b)



Fig. 3.11- a) Roller structure upwelling within a Type 2 boil (structure is approx. 3m wide)
b) Successive Type 2 boils oriented perpendicular to each other (structure is approx. 1.5m wide)
for both photos, flow is towards bottom of photo

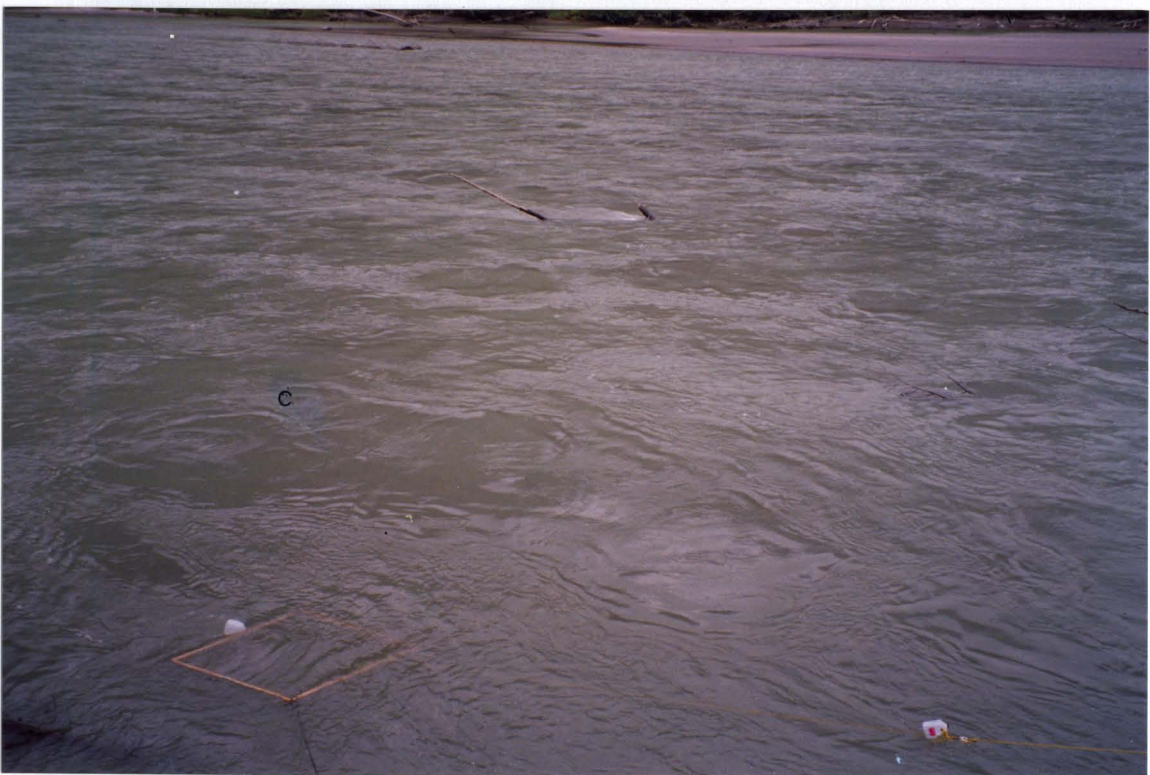


Fig. 3.12 a-d) Time series of Type 2 boil evolution displaying effect of upwellings on overall boil shape (grid size =2x2m, period between photos =2s)



b



d

Fig. 2. Evolution of Type 2 in ...

- a) stable ...
- b) diffuse ...
- c) segmented ...

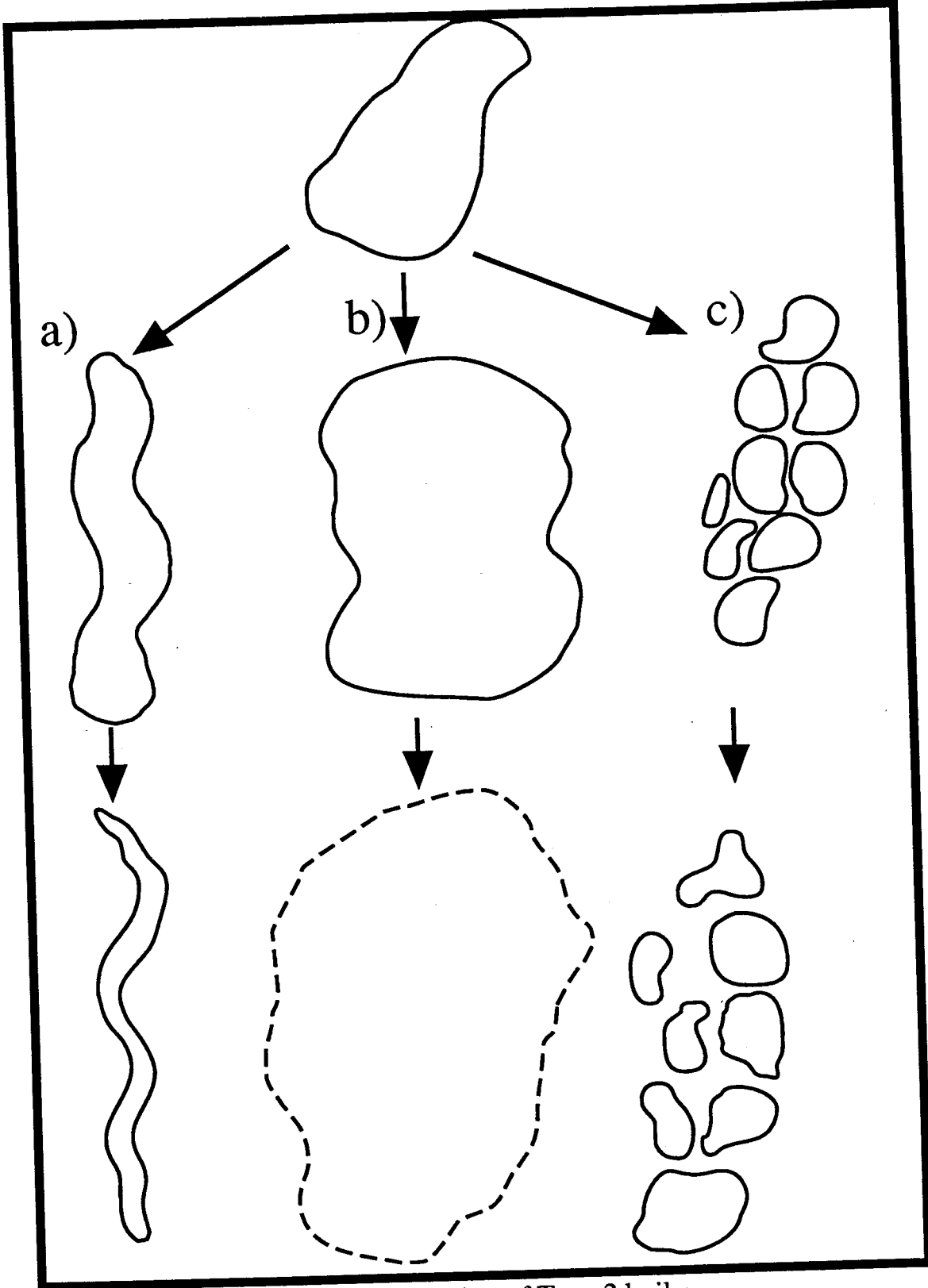


Fig. 3.13- Evolution of Type 2 boils:
a) elongation
b) diffusion
c) segmentation



Fig. 3.14 a-d)- Time series of Type 2 boil diffusion
(distance between markers= 8.7m)



Fig. 3.13 a-d) Top series of Type 2 bed segmentations
(distance between buoys = 8.7m)

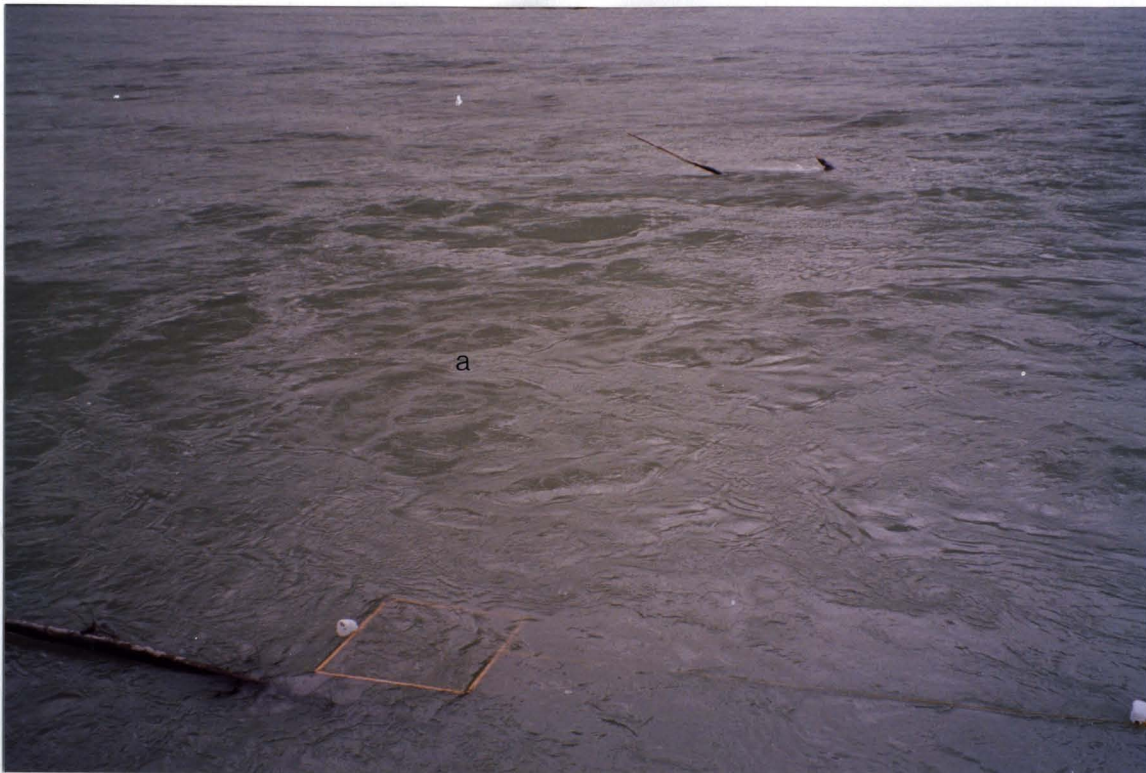


Fig. 3.15 a-d)- Time series of Type 2 boil segmentation
(distance between markers =8.7m)



Fig. 2.16 a-d) Time series at Port 2, boat mooring



Fig. 3.16 a-d)- Time series of Type 2 boil elongation



the bedforms, rather than to the shifting of secondary crests. The secondary crests
production was observed by several researchers (e.g., and 1944; Coonton, 1969) prior to

agglomerations found along the L/B and R/B. The boils hereafter will be referred to as Type 1 and 2 respectively. In Chapter 6, a quantitative analysis of the intensity, period, morphology and evolution of the structures with respect to a variety of hydraulic and bedform conditions serves to define and contrast the boil types more conclusively.

3.4- DISCUSSION

Downstream of the R/B D/S staff gauge site, boil production typically is isolated to streamwise linear bands whose width and lateral spacing fluctuate with hydraulic and tidal conditions. The lateral variability in band width and number may be related to gradients in current speed and/or direction. The production sites within these bands shed boils for durations rarely exceeding five minutes and never exceeding ten minutes. Boil activity was noted to be intermittent and somewhat periodic. Coleman (1969) related streamwise parallel bands of boil activity to longitudinal scours which may be a product of secondary circulation cells. Fukuoka and Fukushima (1980) attributed the bands of boil production to secondary circulation cells/cylinders, and noted that they have a transverse spacing equal to twice the depth. This finding was also noted by Gulliver and Halverson (1987), but they warn that the boundaries of such circulation cells will frequently shift in the streamwise and transverse directions. These secondary currents have been related to shear flow instability, but findings to date are inconclusive (Allen, 1987).

Due to the vast amounts of sediment entrained in the boils of the lower estuary, it seems more likely that the limited duration of the production sites is related to local changes in the bedforms, rather than to the shifting of secondary cells. The stationarity of boil production sites observed by several researchers (e.g. Lane, 1944; Coleman, 1969) may in

fact be related to steady bedform parameters. Presumably, this rarely occurred in Squamish River estuary while sediment-laden boils were produced.

The surface morphology and evolution of the boils within these bands frequently followed the Coleman/Jackson model, however two distinct structures were noted which had characteristics that did not fit their model. The 'cauliflower' structures have tens of small point-source upwellings within each boil, but there are no distinct sites of downwelling, and a poorly defined boundary is typical. 'Rollers' have linear-sources of upwelling and downwelling, and rotate along a horizontal or near-horizontal axis. The rollers are frequently noted to evolve into a 'horn' shape rather than simply dissipate, and the presence of secondary upwellings was attributed to curvature at the ends of roller axes. Secondary upwellings, inevitably weaker and more poorly defined than the original upwelling, are also associated with the Coleman/Jackson model and the 'cauliflower' structure. This suggests that there is some additional or more general causative mechanism; Korchokha (1968) related paired structures to bedform shape.

Upstream of the R/B D/S site, the lanes of boil production are rarely noted; instead, boil activity is most strongly associated with the thalweg. Where the thalweg crosses from left bank to right bank, the structures observed are similar to those in the lower estuary. Where the thalweg moves alongside the concave bank, the boil qualities (presence, production sites, morphology, intensity, size and evolution) are unlike those of the lower estuary. These macroturbulent structures were termed 'Type 2' boils, while those of the lower estuary and thalweg crossing were called 'Type 1' boils. A qualitative comparison is offered in Table 3.1.

Previous studies have suggested that there may be more than one means of boil production (e.g. Rood and Hickin, 1989; Lapointe, 1989; Kostaschuk and Church, 1993),

	TYPE 1 BOILS	TYPE 2 BOILS
PRODUCTION SITE-	variable and lasts <10 minutes; noted where thalweg crosses banks and in lower estuary	fixed; along concave-bank; originates at obstructions
UPWELLING-	intermittent and periodic	varies between intermittent and quasi-continuous
EVOLUTION-	energy strongest at initial upwelling; structure then spreads, with max. size occurring 3-6s after. Structure then diffuses and it rarely visible after 20s. There is a definite life cycle dependent on type.	undergoes initial increase in sfc. area; then displays continual change-stretching, expanding and contracting as upwellings continually rejuvenate it
MATERIAL UPWELLED-	typically organics; often sediment	rarely sediment; sometimes organics
SHAPES-	morphology may be related to depth and bedforms. They appear as rollers, circular or cauliflower structures; the first two may evolve into horns.	ovals stretched according to lateral shear and upwelling intensity and location. It eventually diffuses, stretches or segments
ROTATION-	inevitably rotates along a horizontal or near-horizontal axis	whole structure rotates on a vertical axis in accordance with lateral shear, but individual upwellings within may rotate along along a horizontal axis
UPWELLING DURATION-	initial upwelling lasts 1-3 seconds; there may also be secondary upwellings within next 5 secs. but the structure is rarely visible >1 min.	initial upwelling lasts 1-4 seconds, but the structure seems to induce upwellings as it is advected d/s such that it may survive for several mins.
STRONG PRODUCTION SITES-	seemingly random; perhaps controlled by local bedform R.R. or steepness	thalweg; only 3-5 dominant production sites per bank
BOIL SIZE-	typically 2 x 3m, up to 4 x 7m	typically 2 x 7m, up to 4 x 15m
U/S LIMIT-	approx. W.S.C. station 08GA053; perhaps related to grain size	unknown; definitely u/s of Mamquam River junction

Table 3.1- Contrast of Type 1 and Type 2 boils

and Coleman (1969) suggested that there may be more than one 'type' of boil. Although Coleman's Type B boil may simply be a gigantic vortex, his postulation that certain hydraulic regimes and bedform structures will produce specific patterns in boil activity is noteworthy. Inspection of the variability in hydraulic and bedform parameters in the estuary follows in Chapters 4 and 5, respectively.

CHAPTER 4- CURRENT SPEED AND WATER-SURFACE SLOPE

4.1- INTRODUCTION

Macroturbulence in rivers and estuaries typically has been related to mean hydraulic characteristics, fluctuating components of current-speed, or to bedform parameters. The intensity of macroturbulence also has been related to the bed shear. In natural channels with bedforms, the shear stress at the bed consists of bedload/grain roughness and form drag components. The former may be approximated by employing the Law of the Wall to velocity profiles, but velocity may be difficult to obtain reliably during unsteady flows. Proposed derivations of form drag often include a measure of bedform geometry such as steepness or relative roughness (e.g. Fredsoe, 1982; Wiberg and Smith, 1989). However, some models assume that for a given bed shear stress, the proportion of total drag contributed by bedform drag will be similar under any conditions (e.g. Engelund and Fredsoe, 1982). Field studies to test such models have been limited due to the difficulty of collecting reliable data.

Shear velocity estimates require accurate measures of velocity at a number of points above the bed. The precise location of the measures above the bed with respect to bedforms must also be known. This information could not be obtained in my study area due to high suspended-sediment concentrations, and large, dynamic bedforms. Instead, water-surface slope, current speed and water depth were considered as scaling variables.

As transitional regions between fluvial and tidal dominance, estuaries often display great variability in depth, water-surface slope and speed over short temporal and spatial scales. Therefore, the study area includes several data-collection sites, located to reflect the wide

range of tides and discharges. An additional complexity is the well-documented fluctuation in current-speed of Squamish River.

It has long been recognized that current speed in rivers may display large fluctuations on a variety of temporal scales. A component of the bedforms-mean flow-turbulence relations which has received minimal consideration in the literature is the variability in current-speed at a time scale on the order of minutes. Study of this phenomena, rather than simple recognition of its existence has been sparse, particularly in recent decades. In fact, a commonly acknowledged term for the variability does not exist. Rood (1980) noted that these fluctuations have been called pulsations (Matthes, 1947; Dement'ev, 1962), eddy structures (Nowell and Church, 1971), velocity fluctuations (Dement'ev, 1962; Savini and Bodhaine, 1971; Müller, 1982) and low-frequency turbulence (Lyapin and Chebotarev, 1976). They have also been called long-period oscillations of current speed (Jackson, 1977; Lapointe, 1989). Many of these terms suggest causative mechanisms; in this thesis, they will simply be known as 'fluctuations' in current-speed.

Early observations were mostly descriptive and primarily concerned with the influence of these fluctuations on estimations of discharge. Some studies, however, included tentative proposals regarding causative mechanisms. Dement'ev (1962) summarizes the early Russian work, which began in the 1870's. General conclusions include the consensus that pulsation amplitude increases towards the bed and banks, while between-river comparisons revealed an increase in the fluctuations with increasing current velocity and channel roughness. These findings were debated for several decades, with some researchers claiming that the minimal pulsation actually occurs at some depths due to the effects of wind and waves. Dement'ev (1962) ultimately concludes that characteristics of the measured fluctuations are irregular in magnitude and frequency over short space and time scales. A similar finding was noted by Matthes (1947).

Several causative mechanisms have been nominated, but none has been verified. Some Russian studies indicated that the fluctuations in the current-speed may follow changes in the water-level. Matthes (1947) postulated that fluctuations in both current-speed and stage occur as flowing water attempts to maintain equilibrium as the discharge and sediment load varies; subsequent observers have suggested similar hypotheses. Fluctuations in current-speed have been linked to variability of discharge (both temporally and spatially) by Dement'ev (1962), Morisawa (1985) and Chang (1988), and to variability in bedload or bedforms by Korchokha (1968), Jackson (1977) and Lapointe (1989).

Another proposed cause of current-speed fluctuations is that they may be linked to eddies or vortices which are either transported downstream (Jackson, 1977; Lapointe, 1989) or oscillate temporally or spatially (Müller, 1982; Gulliver and Halverson, 1987; Lapointe, 1992). Postulated energy sources for such eddies include lateral gradients in velocity or shear stress, but the survival of eddies far downstream from their generating sources has been questioned (Nowell and Church, 1971; Lapointe, 1989). Nowell and Church (1971) suggest that the fluctuations may simply be resonance effects from flow patterns imported from upstream.

The mean period of current-speed fluctuation within the transverse, unlike the magnitude, appears to be a constant for a given channel, and has been related to channel dimensions such as width or depth (e.g. Dement'ev, 1962). The techniques for determining such a mean period, however, have been questioned (Rood, 1980). This problem of analysis is exacerbated by non-stationarities in the flow which may be induced by tidal factors in estuaries (e.g. West and Oduyemi, 1989).

Tidal forcings in estuarine reaches produce periodic fluctuations in speed, depth and slope. This tidal control may produce wide ranges in the three variables over short temporal scales. Although tidal flux allows for efficient investigation, tidal wave propagation can produce complex sequences of changes in the variables of interest. Most estuaries will produce a combination of standing and progressive tidal wave properties, but this varies both within and between estuaries as a function of tidal regime (Knight, 1977).

If estuary depths are shallow, there will be frictional effects of the bed on tidal wave propagation. These effects will be more strongly displayed on the ebb tide, thus flood wave propagation will be more rapid. Explanations for this phenomenon are vague, but include a more rapidly decreasing relative roughness on the flood tide (Knight, 1977), or the crest of the tidal wave travelling upstream faster than the trough (Glen, 1979). In addition to this duration asymmetry there may also be differences between the maximum velocities of the ebb and flood tide, or temporal differences between stage maxima/minima and velocity maxima/minima. These were respectively called velocity and time asymmetry by Hines (1975). Quantifying the effect of the tidal wave on the hydraulic parameters in the study region is complex due to superimposition of short-period variations in discharge (Hoos and Vold, 1975).

Calculations of mean depth within the study reaches were obtained from the sonar transects which are analyzed in Chapter 5. This chapter investigates only the variation of slope and speed. Measurement of these variables in conjunction with other data collection was relatively time-consuming. Thus, predictive rating curve relations (based on multiple stepwise regressions) are attempted. Knight (1977) concluded that current speed was dependent on depth, slope, boundary roughness and exposure. Each of these variables, is in turn dependent on tidal factors and discharge.

4.2- CURRENT SPEED

4.2.1- Surface current-speed regressions

Plots of U_{sfc} versus the independent variables at each station indicate that all relations are essentially linear. Besides the flattening of the relation near high and low tides, there were two interesting features that may affect the assumptions of the regression analyses:

- 1) On the ebb tide, the variability in U_{sfc} generally increases towards LLT (especially $T > 0.75$). On the flood tide, the variability in U_{sfc} generally decreases from LLT to LHT (Fig.4.1a-d).
- 2) At station 2, there is a tendency for variability to increase as discharge declines.

The statistical importance of these features in the regression analyses are assessed when residuals are inspected. The speed-T plots become curvilinear near the turning of the tides, but this is masked by the high variability in U_{sfc} at LLT.

When data for all 6 stations are pooled, the regression models on both tides have single explanatory variables, and the models fit the data poorly (Tables 4.1 and 4.2 in Appendix 1.1). D is the only variable in the ebb tide model, and T is the only variable in the flood tide model. For both, the R^2 values are not excessively low, but this is perhaps inflated by the large sample size. For both data sets, outlier removal does not alter the variables chosen in the models, and the improvements in R^2 and s.e.e. are very similar.

Differentiating the data by stations reveals a pattern of dependence of the key independent variables in each model on proximity to the estuary mouth. On both tides, there is a general 50% decrease in the coefficient of variation due to the differentiation. With the ebb-tide models, as the sample size increases, so does the R^2 value. Sample

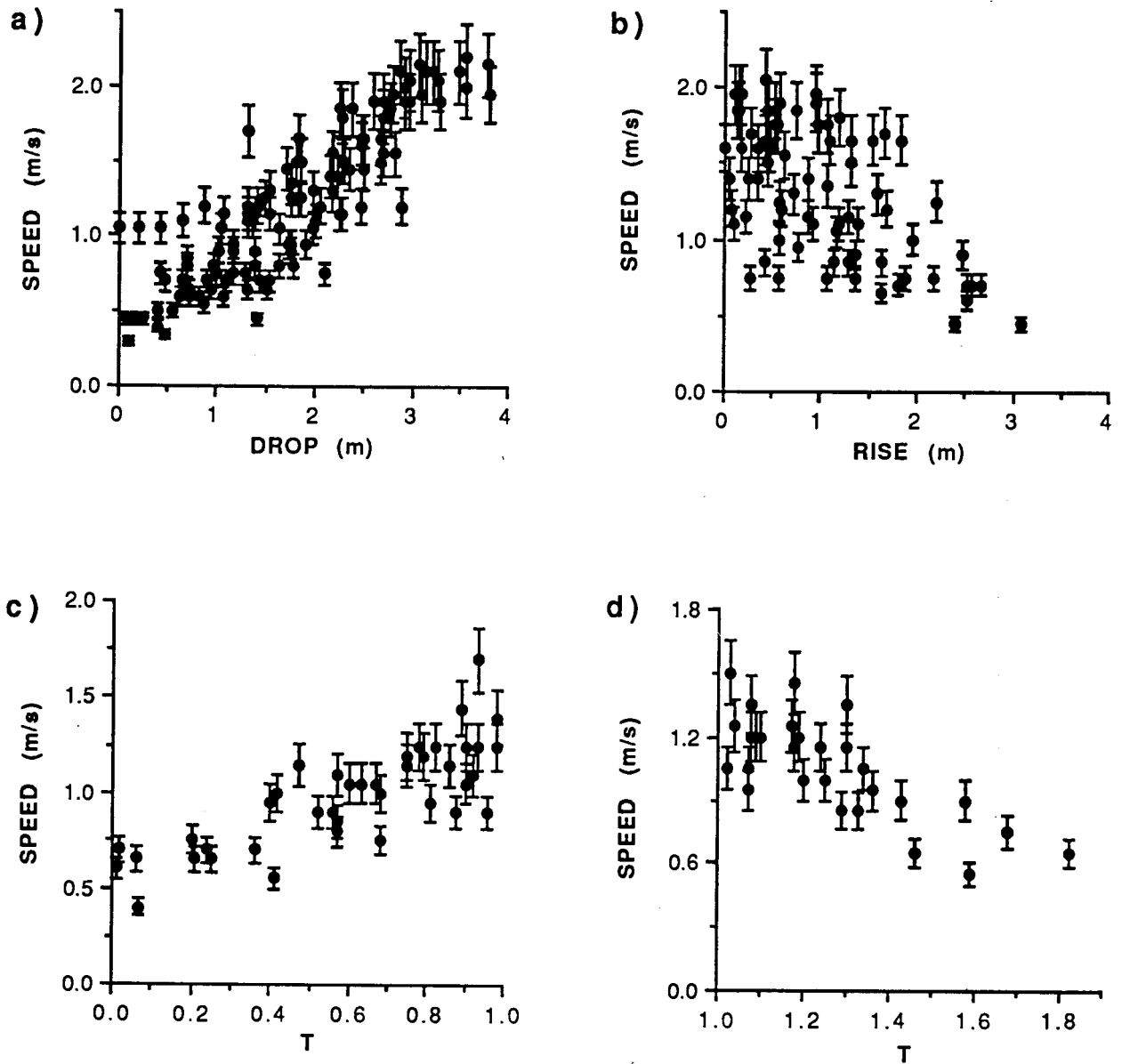


Fig. 4.1- a) Station 5 sfc. current-speed on ebb tide vs. drop
 b) Station 5 sfc. current-speed on flood tide vs. rise
 c) Station 3 sfc. current-speed on ebb tide vs. T
 d) Station 3 sfc. current-speed on flood tide vs. T

size influences the summary statistics and the reliability of the models is questionable. Thus, rather than discussing each station in turn, only the trends in the data are identified here.

Generally, the importance of estuary discharge in the models (as expressed by the beta coefficients) diminishes with proximity to the mouth, until it is insignificant in the model of the downstream-most station. D dominates the models of the two R/B stations, while T is present only in the two stations associated with the thalweg crossing from the L/B to the R/B. Note that the LTH is only important for station 5, but that there is collinearity between LTH and D (not enough, however, to disqualify either from the model). This is also true for the flood-tide model. Finally, for the upstream-most station, there is a negative correlation between Q and speed (this will be addressed in section 4.4). Only the models with $n > 30$ had any points judged to be outliers. Their removal does not influence the choice of variables included in the model, although there is a considerable improvement in the multiple correlation coefficient for station 4.

On the flood tide, the sample size influence on the R^2 is less apparent than on the ebb tide. The sample sizes are considerably smaller for the flood-tide data, but the R^2 values are larger on the flood tide for each station except station 5. Station 1 could not be included in the analysis due to small sample size ($n=4$). Irrespective of these smaller samples, several trends identified in the ebb-tide data may also be recognized on the flood tide.

The beta coefficient of T generally declines as proximity to the estuary mouth decreases. Note also that T is included in the model of every station except #5, and the LTH is important for both 5 and 3. The beta coefficient for Q remains essentially constant for the three upstream-most stations. Also, the division of the study reach into 3 regions (based

on the independent variable explaining the most variation in the dependent variable) is not as evident on the flood tide.

Comparing ebb and flood models for individual stations, station 4 includes the same explanatory variables, with similar beta coefficients. The models for stations 3 and 5 retain the variable with the highest beta coefficient. For stations 2 and 6, T replaces Q and D respectively, as the most important variable. Finally, the effect of outlier removal for the flood tide is similar to that for the ebb tide.

Utilizing the split-sample test of Kleinbaum et al. (1989) to test reliability, two of the four surface speed models had shrinkage < 0.10 (one of them negative) and two models were deemed unreliable. The effect of the small samples is also indicated by examining the assumptions of regression analysis based on the model residuals.

4.2.2- Current speed at 0.7d

4.2.2.1- Regression analysis

When $U_{0.7d}$ is plotted against all independent variables (for each station), the linear relations are again apparent. The regression models for $U_{0.7d}$ reveal several interesting similarities and differences to the surface-speed models. When the stations are pooled, both the ebb and flood tide models have low R^2 values, high standard errors, and T as the most important variable. Again, these pooled models are not as useful as models differentiated by station.

The speed records at 0.7d were only taken at four stations, and there are small sample sizes for each station. Although the values of the coefficients in each model are unreliable, the trends in the data may be useful. For both the ebb and flood tide, models

from the L/B have significantly better fits than the R/B stations (Table 4.3 in App.1.1). Among the R/B models, there is a better fit on the flood tide, while at the L/B, the ebb-tide models fit better.

Generally, the variables in the models for both speed measures are similar, but the fit is better with the U0.7d models. At station 2, Q is the most important variable for both tides based on the U0.7d models. This was also true of the surface-speed model for the ebb tide, but on the flood tide, T dominated. T was also included in the ebb model. Wilkinson's test indicates that the relations are significant at the 99% level.

For station 5, the models of U0.7d have D or R as the only variable in the models of both tides. The surface-speed models also have D or R as the most important variables, even with the large difference in sample size. Wilkinson's test indicates that the relationship is significant at the 99% level on the flood tide, but less than 95% on the ebb tide. This problem with sample size prohibits the use of the Kleinbaum et al. (1989) test for reliability in any of the models of speed at depth.

For station 6, T was the only variable in the models of both tides for the U0.7d. This was also true of the Usfc model for the ebb tide. On the flood tide, however, D was the only variable in the model. For both measures of speed, the model fit was better on the flood tide than the ebb. Wilkinson's test indicated that on both tides the relationship was significant only at the 95% level.

For four of the five stations where surface-speed models were obtained, and for all of the U0.7d models, a normal distribution of residuals may not be present. Several measures may be employed to rectify this, but it was not attempted since it is evident that the reliability of a predictive model with these small sample sizes is not satisfactory.

Data sets of current-speed at two levels in the flow have produced similar models of explanatory variables at the three sites where comparison was possible.

4.2.2.2- Minimum durations of current-speed measures at 0.7d

The regression analysis in section 4.2.2.1 was based on a nine minute mean of the current speed at 0.7d. The nine-minute duration was determined to be the maximum length of the time series which could be considered as stationary (section 2.1). However, an approximation of the nine-minute mean may be possible from shorter averaging times. This minimum duration of current speed measurement could also be related to the magnitude of the fluctuations in the speed time series (e.g. TI or RTI).

Historically, the primary concern with current-speed fluctuations has been the effect on discharge estimates (based on a mean current-speed, employing continuity). Although discharge estimates of Squamish River made by the WSC are based on stage-Q relations, stage may fluctuate on scales similar to those of current speed. Therefore, an estimate of the minimum duration of current-speed measurement required to obtain a time-averaged approximation of the nine minute mean throughout the estuary may be a useful finding. To accomplish this, the technique of Savini and Bodhaine (1971) was employed. The current-speed time series was filtered with a 30-second running mean, and the resulting largest and smallest values in the time series were noted. If both values were not within 5% of the nine minute mean, the procedure was repeated with a 1-minute running mean through the original data. This process was repeated with the filter length increasing by 30 seconds each attempt until both values were within 5% of the 9 minute mean.

There is not a recurring minimum measurement time in the estuary, nor even similar values over tidal cycles at a single site (Table 4.4). These values (both grouped and

DATE-TIME	MINS. NEEDED L/B U/S	DATE-TIME	MINS. NEEDED L/B D/S	DATE-TIME	MINS. NEEDED R/B U/S	DATE-TIME	MINS. NEEDED R/B D/S
03-0857	6	04-1109	5.5	18-1149	4	19-1104	3.5
03-0959	5.5	04-1228	5	18-1258	5.5	19-1225	3.5
03-1131	6	04-1438	5.5	18-1357	6	19-1519	6.5
03-1231	7	04-1557	6	18-1459	4.5	19-1635	5
03-1333	6.5	04-1653	5.5	18-1604	6	19-1752	6.5
03-1437	7	06-1310	5	18-1649	5	21-1059	5.5
03-1517	5	06-1420	6.5	20-1115	5.5	21-1207	5.5
05-1208	5.5	06-1509	4.5	20-1223	5	21-1301	6.5
05-1312	3.5	06-1622	4.5	20-1343	4	21-1415	2.5
05-1428	4.5	06-1712	3.5	20-1429	4	21-1520	4
05-1538	4	06-1815	7	20-1536	3.5	21-1634	4.5
05-1639	6.5	08-0811	5	20-1628	5	21-1748	6.5
05-1743	4.5	08-0933	6	20-1745	7.5	23-0540	5
07-1325	5.5	11-0823	4.5	22-0540	4	23-0641	6
07-1445	4	11-0926	4.5	22-0653	4	23-0802	3.5
07-1537	4	11-1015	6.5	22-0800	7	23-0904	5.5
07-1644	4	11-1120	8	22-0940	5.5	23-1040	6.5
07-1729	6.5	11-1326	5.5	22-1049	7	23-1202	5.5
10-0815	8			22-1203	6.5	27-0620	5.5
10-0854	>8			22-1304	4.5	27-0710	5.5
10-1004	7			24-0557	5.5	27-0819	3
10-1100	4.5			24-0710	5	27-0948	6
10-1204	>8			24-1009	4	27-1148	3.5
10-1304	8			24-1224	6	27-1330	6
10-1417	7			24-1323	7	27-1438	8
12-0850	8					28-0820	5.5
12-1115	6.5					28-1040	7
12-1212	7.5					28-1222	4.5
12-1338	7.5					28-1335	4
14-0954	7.5					30-0712	6.5
14-1125	7.5					30-0819	6.5
14-1236	6					30-0915	4
14-1330	6.5					30-1023	7.5
						30-1202	5.5

NOTE: All data were collected in June, 1992

Table 4.4- Time necessary for U0.7d to be within +/- 5% of 9-minute mean

differentiated by site) bear no graphically notable relations to U_{sc} , $U_{0.7d}$, depth, Q or T . The expected relation between the time required and the RTI was displayed best at the R/B D/S site, but also noted at the R/B U/S and L/B D/S sites (Fig.4.2a). Similar findings were found for the TI. These relations are not useful for a priori approximation of the required measurement time.

In order to elucidate the mechanisms controlling the magnitude of variation in $U_{0.7d}$, the plots of TI versus $U_{0.7d}$ at each station were examined and then differentiated by a variety of proposed factors. These factors included stage, discharge, and tidal regime. The plots of TI vs. $U_{0.7d}$ for the L/B display poor correlation, with low R^2 values (0.001 and 0.277 for u/s and d/s respectively). The R/B sites display positive linear relations (R^2 values = 0.587 and 0.371 for u/s and d/s respectively), and an asymptotic relation at the R/B U/S site. There was no tendency for TI to be greater during either tide at any of the four sites. Physical reasoning suggests that TI will be greater (relative to $U_{0.7d}$) when there are large changes in discharge (or stage(s)) as opposed to small ones. Plots of TI vs. $U_{0.7d}$ which have been differentiated by rates of change of discharge or stage should therefore display a diagonal separate.

The calculated ds/dt values were based on the change in stage measured at the staff gauges nearest each respective site over the hour bounding the speed measurement. When the TI vs. $U_{0.7d}$ plots are differentiated by a limit of $ds/dt = 0.18$ m/hr (chosen to approximately half the data), the expected diagonal separate is not noted. Instead, for three of the four sites, a vertical separate is found (e.g. Fig.4.2b). This is because the times of data collection concentrated near low tide. As a result, large ds/dt values are at mid-tide when current speeds will be generally lower than at LT (when ds/dt will be small). The other site (R/B U/S) displayed a diagonal separate but the opposite trend of

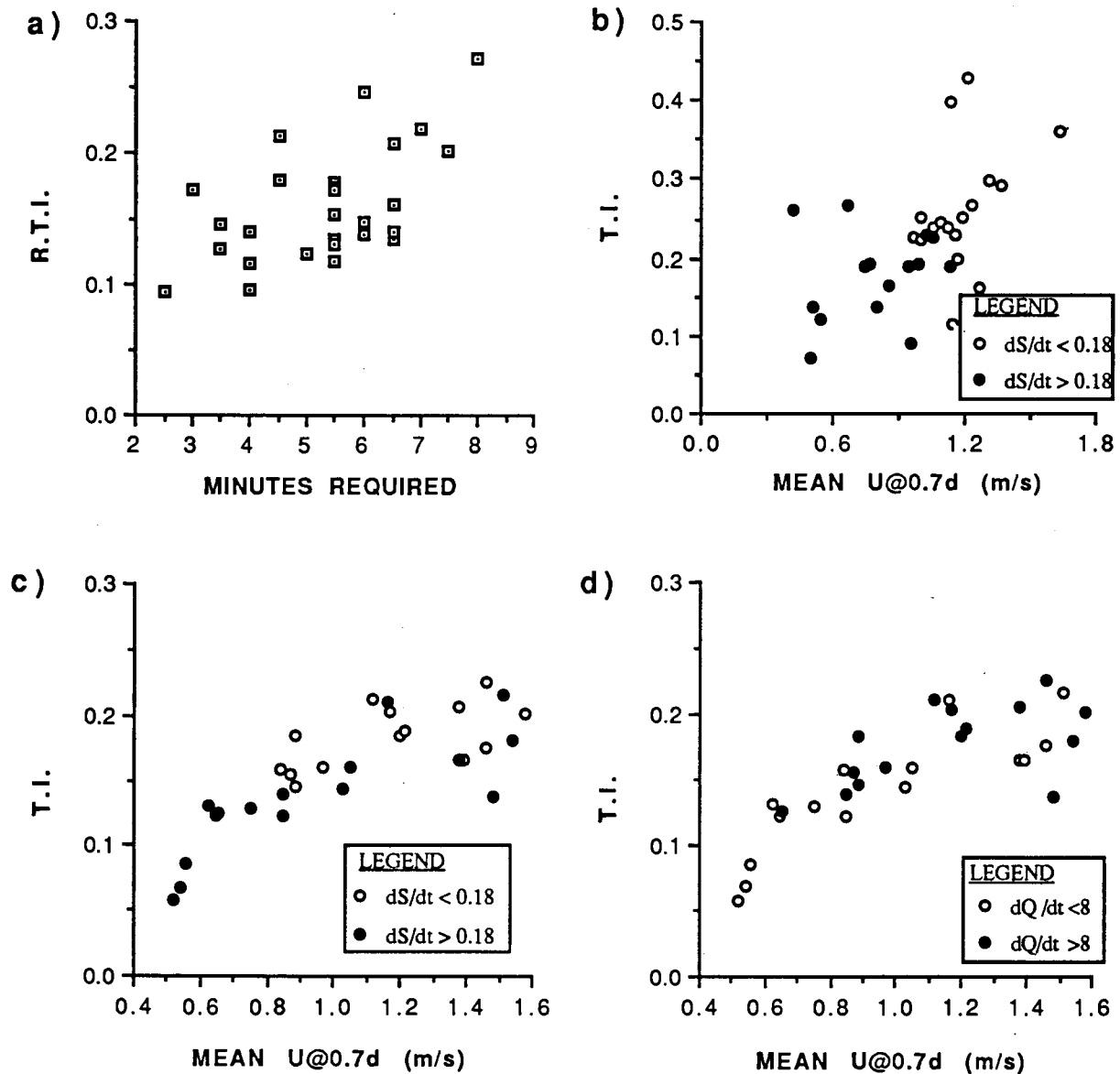


Fig. 4.2- a) Relative turbulence intensity at R/B D/S site vs. required time for mean current-speed at 0.7d to be within 5% of the 9-minute mean
 Turbulence intensity vs. mean speed at 0.7d -differentiated by the rate of change in stage at:
 b) L/B D/S site
 c) R/B U/S site
 -differentiated by the rate of change of discharge in the hour preceding data collection at:
 d) R/B U/S site

what was expected. It appears that a higher ds/dt produced a lower TI (Fig.4.2c). This pattern remains an enigma.

The effect of dQ/dt was examined by determining the change in estuary discharge in the hour preceding and that during current-speed data collection. The differentiation limit was again chosen to halve the data. For the L/B sites, there were random patterns for both the hours preceding and during data collection. However, both R/B sites may display the expected pattern of dQ/dt relative to TI and $U0.7d$, more notably in the hour preceding data collection (e.g. Fig.4.2d).

4.2.2.3- Graphical inspection of time series

Previous research shows that the patterns and periodicities displayed by current-speed time series often vary over cycles ranging from several seconds up to the length of the record (see section 4.1). Attempts to quantitatively relate temporally-averaged turbulence characteristics to basic hydraulic parameters in section 4.2.2.2 were not informative. If the deviations from the mean current speed can be related to changes in stage or discharge, it suggests that these fluctuations would occur on temporal scales shorter than those examined in section 4.2.2.2. Since such data were not collected, the search for causative mechanisms was abandoned and the current-speed time series plots were simply examined for notable patterns and periodicities.

Over one-hundred current-speed time series were collected, most displaying considerable deviations from the nine-minute mean value. These deviations frequently appeared as random variations about the mean although in many instances, there were apparent periodic fluctuations or repetitive patterns. A distinct pattern recognizable in the time series is a slow, unsteady increase in current speed followed by a rapid, steady

decrease. Rapid increases followed by slow unsteady decreases were also noted, but far less frequently. The patterns were often apparent, but fluctuations with periods of 10-20 seconds occasionally hid them. To aid visual recognition, a filtering function was applied to the time series.

Geophysical data are commonly filtered, with the equally-weighted moving average (ie. 'running mean') being the most simple and popular function. Howarth and Rogers (1992) note, however, that these filters often introduce both phase shifts and periodicities at certain frequencies, and 'polarity reversals' (where peaks in the filtered series correspond with troughs in the unfiltered series). Examples of such problems are illustrated by filtering the current-speed time series of June 22 (0800-0812) with a 7-term running mean (Fig.4.3a). Howarth and Rogers (1992) recommend that these problems may be avoided by building filters with the weights proportional to the binomial coefficients. Such filters follow the original time series closely, but also smooth out short-term fluctuations, as displayed by the application of a 7-term binomial filter (Fig.4.3b). A second example of the influence of these two filters is displayed in Fig.4.4a,b. For inspection, all time series were filtered with a 7-term binomial filter. The choice of filter length was subjective, but not influential on results since there were typically only subtle differences between the output of filter lengths between three and fifteen terms. This is attributable to the rapid expansion of the binomial coefficients.

There were several time series which displayed high frequency fluctuations ranging from tens of seconds (Fig.4.5a) to several minutes (Fig.4.5b). These fluctuations were often superimposed on longer-scale oscillations which exceeded 50% of the record length (Fig.4.5c). The noted tendency for current speed to accelerate unsteadily up to some maximum speed and then rapidly decrease was noted in many time series (e.g. Fig.4.5d (minutes 8-12)). These patterns will be studied in greater detail in Chapter 6.

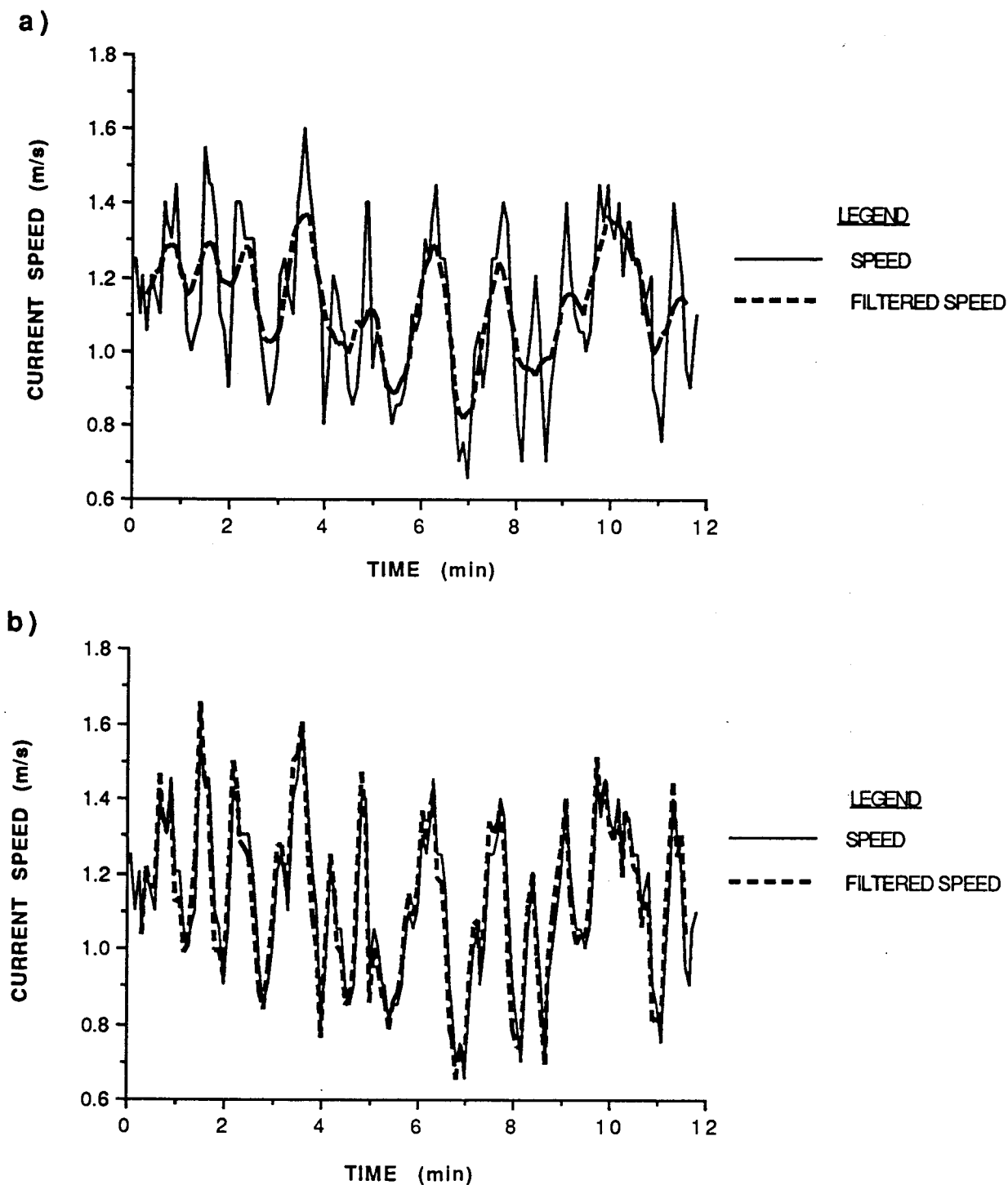


Fig. 4.3- Filter application to the speed time series of June 22 0800-0812:

- 7-term moving average
- 7-term binomial filter

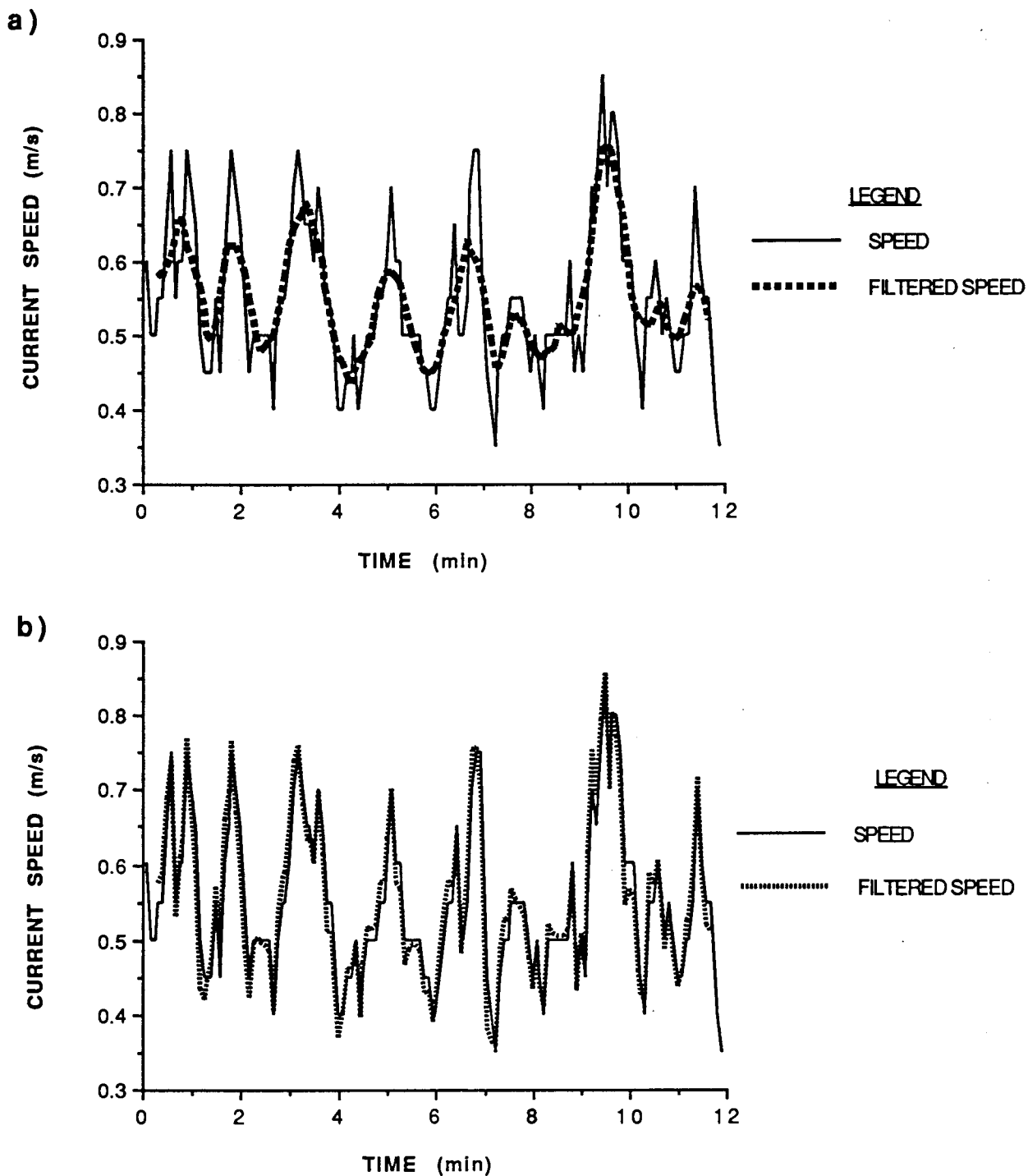


Fig. 4.4- Filter application to the speed time series of June 27 0620-0632:

- 7-term moving average
- 7-term binomial filter

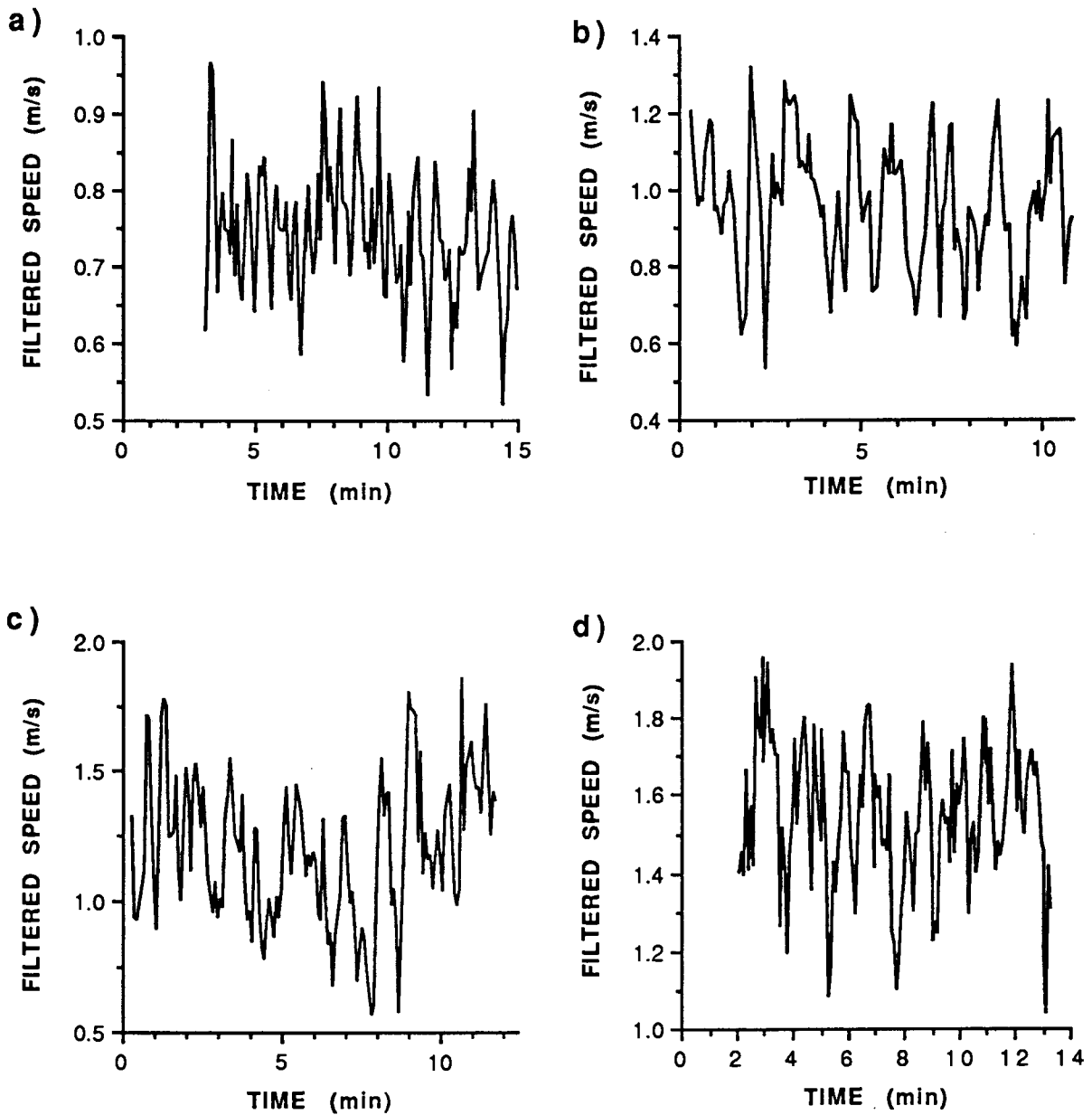


Fig. 4.5- Filtered current-speed time series:

- a) June 7 1535-1550
- b) June 22 1304-1315
- c) June 3 1231-1243
- d) June 24 0557-0612

4.3- WATER-SURFACE SLOPE

4.3.1- Inspection of data

From an initial examination of slope versus all independent variables, there are approximate straight-line relations for all combinations at each site, except for 3 cases. All occur on the flood tide, with the plot flattening out at the extremes (<1.15 and >1.55) corresponding to LLT and HHT.

It is also evident from this inspection that there is quite a scatter of points around even the strongest trends. In determining the slope of the water-surface in such a dynamic environment, the potential for errors to creep into the analysis certainly exists. Knight (1977) notes that even in straight reaches, errors in determining water-surface slope from surveys can be as high as 10%. Certain types of errors (e.g. systematic and illegitimate) are difficult to quantify, but their influence may be speculated upon. Systematic errors were kept to a minimum by careful surveying and staff-gauge installation (e.g. level gauges). Illegitimate errors were also minimized by not only double-checking gauge readings, but by utilizing a check built into the data collection procedure. By determining the difference between the staff-gauge readings at the time of measurement, any values which seemed odd could be re-examined. The effect of the random errors in reading the staff gauges and stadia rod during surveys can be quantitatively analyzed.

Since the staff-gauge heights were not installed relative to any datum (nor to each other), the difference in stage read between the gauges (DS) was compared to the difference in water-surface elevation between the gauges as measured from surveys (DE). These values were obtained on several days at high and low tide, since these are the times when water-surface slope is relatively stable. The values were compared graphically,

producing a linear relation such that $DE = DS + C$, where C = a correction factor. The error in C (dC) may be taken as the standard error of the regression, which was 0.0071. The error analysis is relatively sensitive to this value (ie. if dC increases by 100%, the total error in slope increases by 50%), thus to be conservative (in case this value is an underestimate), dC is taken as 0.01.

A simpler technique (and with less error) would have been to 'tie-in' the staff gauges by relating one to a relative zero mark on the other using a level. Unfortunately, this was not realized until the staff gauges had been removed. Instead, the distance between the staff gauges was measured with a level and stadia rod (DX), as was the difference in water-surface elevation between the staff gauges (DE). Then, slope (m) is DE/DX . The error in reading the staff gauges (dS) is assumed to be one-half the smallest division (0.005), as is the error in reading the stadia rod (upper(U) and lower(L) crosshairs on the level).

Subscripts refer to upstream(1) and downstream(2) staff gauges/stadia rod readings. The error analysis follows:

$$\begin{aligned} d(DX) &= 10[(dU_1 + dL_1) + (dU_2 + dL_2)] \\ &= 10(0.005m + 0.005m + 0.005m + 0.005m) \\ &= 0.2m \end{aligned}$$

Since $DS = S_1 - S_2$

$$DE = S_1 - S_2 + C$$

therefore $d(DE) = d(S_1 - S_2 + C)$
 $= dS_1 + dS_2 + dC$

Since $m = DE/DX$

$$\begin{aligned}
 \text{therefore } dm &= m \left[\frac{\delta(\Delta E)}{\Delta E} + \frac{\delta(\Delta X)}{\Delta X} \right] \\
 &= m \left[\frac{\delta S_1 + \delta S_2 + \delta C}{\Delta E} + \frac{\delta(\Delta X)}{\Delta X} \right] \\
 &= m \left[\frac{0.005 + 0.005 + 0.01}{\Delta E} + \frac{.2}{\Delta X} \right] \\
 &= m \left[\frac{0.2(\Delta E) + 0.02(\Delta X)}{\Delta E \Delta X} \right]
 \end{aligned}$$

Based on the range of slopes measured in the estuary and the distances between the staff gauges, the errors are roughly constant. For the L/B, they are between 1.027E-04 and 1.036E-04, and for the R/B, they are between 1.277E-04 and 1.290E-04. For the purpose of graphing, the error bars were taken as the upper limit for each site, but the difference is indistinguishable in the graphs to follow. Examples of the error bars are shown on plots at each site on both tides (Fig.4.6 a-d). The influence of the error is greatest when the slope is smallest, a fortunate correspondence for predicting boil activity which diminishes as high tide (and low water-surface slope) is approached (Rood and Hickin, 1989).

Multiple stepwise linear regression was to be employed for predicting water-surface slope. However, graphical analyses of the water-surface slope over diurnal tidal cycles indicated that there were intermittent minima or maxima which were not associated with variability in discharge or tidal parameters. These readings were noted in the field and double-checked, so they cannot be attributed to measurement error. Examples in my data set include June 4(1200-1346), June 6 (1333), June 17(1406), June 25 (0848), August 23(0955) and Aug 25(0751-0923).

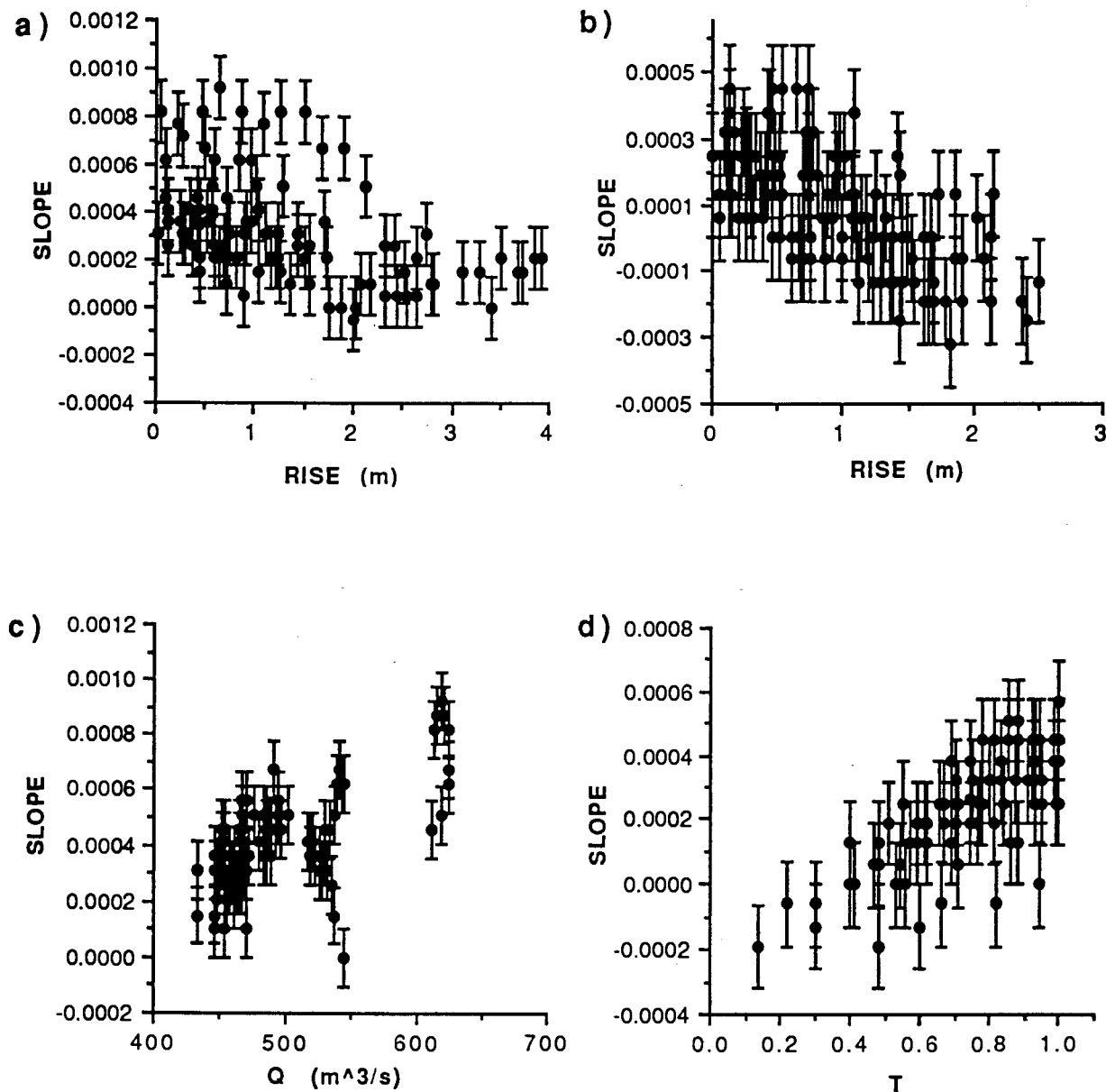


Fig. 4.6- a) L/B water-surface slope on flood tide vs. rise
 b) R/B water-surface slope on flood tide vs. rise
 c) L/B water-surface slope on ebb tide vs discharge
 d) R/B water-surface slope on ebb tide vs. T

4.3.2- Comparison of slope and speed

It is difficult to quantitatively link surface speed and water-surface slope in the study area because there was typically a difference of approximately 15 minutes between the two measurements. Differentiating between the ebb and flood tide allowed linear regression models to be fitted, but if the tides are not split, the shapes of the curves may offer some insight to the speed-slope relation.

The plots of water-surface slope over the tidal cycle at the right and left bank sites display some similarities, but there are also several important differences (Fig.4.7a,b). Both plots have steeper slopes and less variability on the flood tide, but the degree of time asymmetry is dissimilar. At the L/B, the slope minima occurs at approximately $T=1.6$, while the maxima occurs at approximately $T=0.95$. The slope minima occurs earlier in the tidal cycle at the R/B ($T=1.5$), as does the maxima ($T=0.85$). Also, at the L/B at $T=0$, note that the slope is not at zero, as it is at the LHT.

Although the sample sizes for the speed models may be inadequate, attributing all unexpected results to the small sample size is not appropriate. For instance, the data-scarce station 2 has a speed maximum that is on the flood tide (Fig.4.8a). Note, however, that the removal of that one point produces results more like those of L/B slope. Then, if the plot of the nearby station 3 is examined, it also appears that peak speeds (ignoring the absolute maxima) may have $T>1.0$ (Fig.4.8b). This might also be true for station 4 (Fig.4.8c). The stations at the R/B have maxima at approximately $T=0.9$, as does the R/B slope (Fig.4.7c,d). In fact, the large data set for station 5 allows a more reliable comparison between slope and speed.

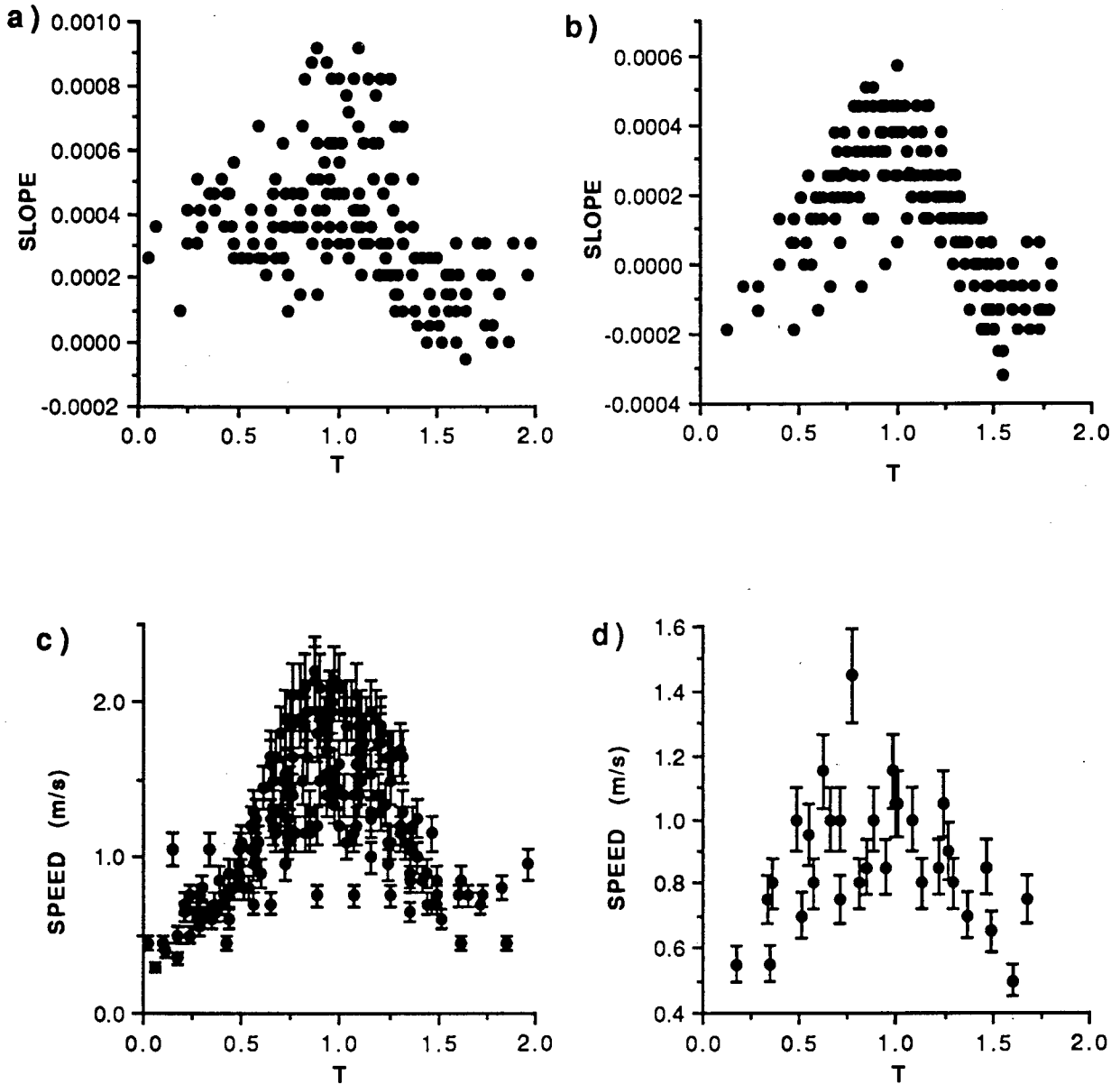


Fig. 4.7- a) L/B water-surface slope vs. T
 b) R/B water-surface slope vs. T
 c) Station 5 sfc. speed vs. T
 d) Station 6 sfc. speed vs. T

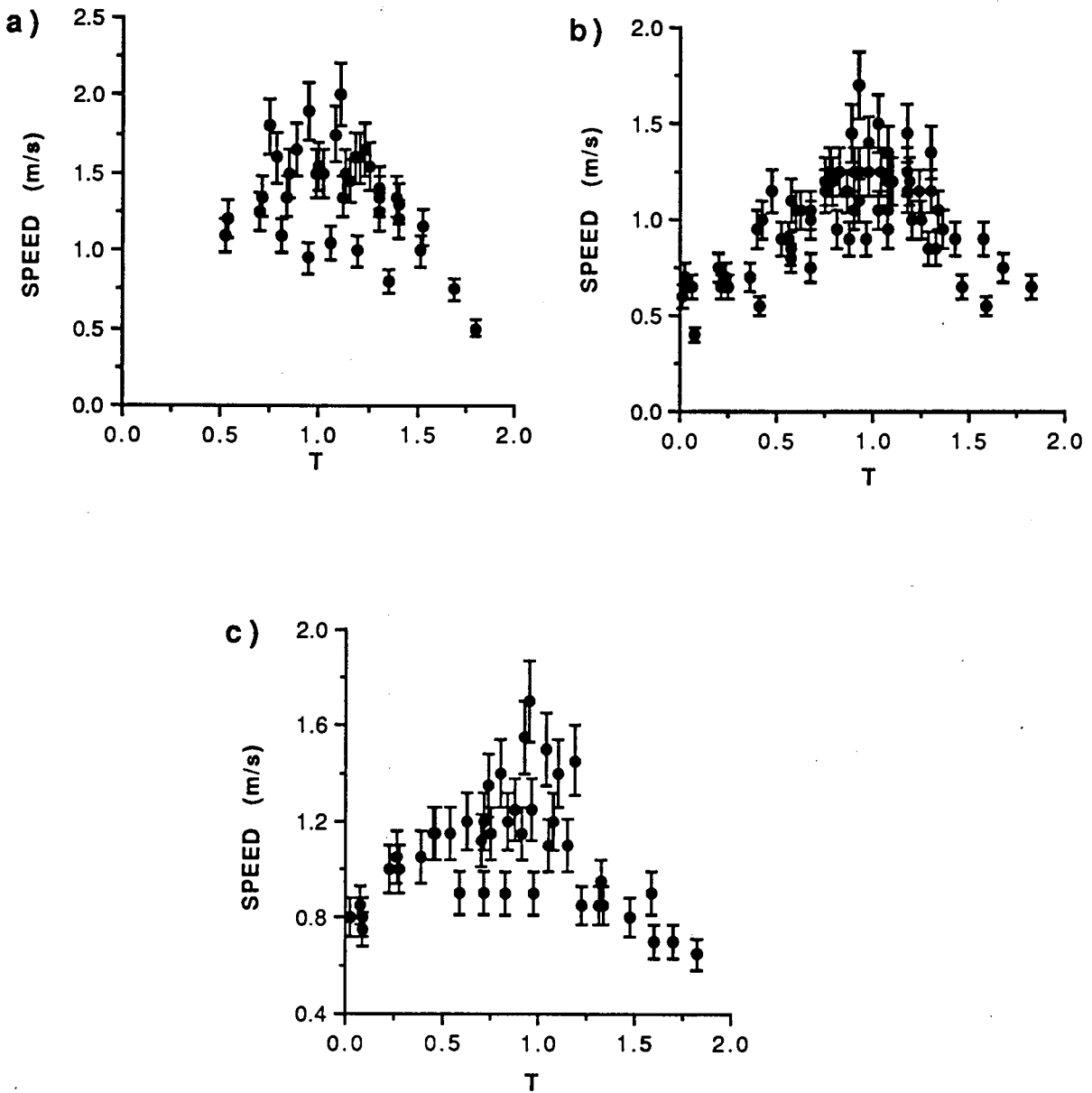


Fig. 4.8- Surface speed vs. T
 a) Station 2
 b) Station 3
 c) Station 4

At station 5, unlike the slope, speed displays a greater variability on the flood tide than the ebb tide. Also, there is not a minima found before LHT. However, the general shapes of the plots are similar, and the maxima occur at approximately the same T. If an envelope curve is drawn over both plots, they are near-identical. Upper envelope curves for the L/B slope and the speed stations near the L/B (#2-4) are also similar.

Plots of water-surface slope versus speed for these stations display poor correlation, even once differentiated by ebb and flood tide (Fig.4.9a-c). There is evidence of a linear trend for station 6, but this may be related to a paucity of data.

4.4- DISCUSSION

4.4.1- Current-speed model results

Due to small differentiated sample-sizes, the current-speed models seem unreliable. Examination of specific stations however, yielded interesting results and allowed inferences about the slope to be made. For the ebb-tide surface-speed models, the importance of Q in explaining variation in speed decreases in a downstream direction. This suggests that a transition zone exists between the fluvially-dominated and tidally-dominated regions. Only those stations with large sample sizes had outliers identified in the models. On the flood tide, sample size may not influence model fit as adversely as with the ebb-tide models, but the reliability tests for stations 3 and 5 suggest that the models may be unstable. Several variables selected in the flood-tide models are similar to those of the ebb tide, but the regions of fluvial versus tidal dominance are not as distinct. The importance of T diminishes in the upstream direction, but the combined effects of discharge and D or R on the current speed are not as evident.

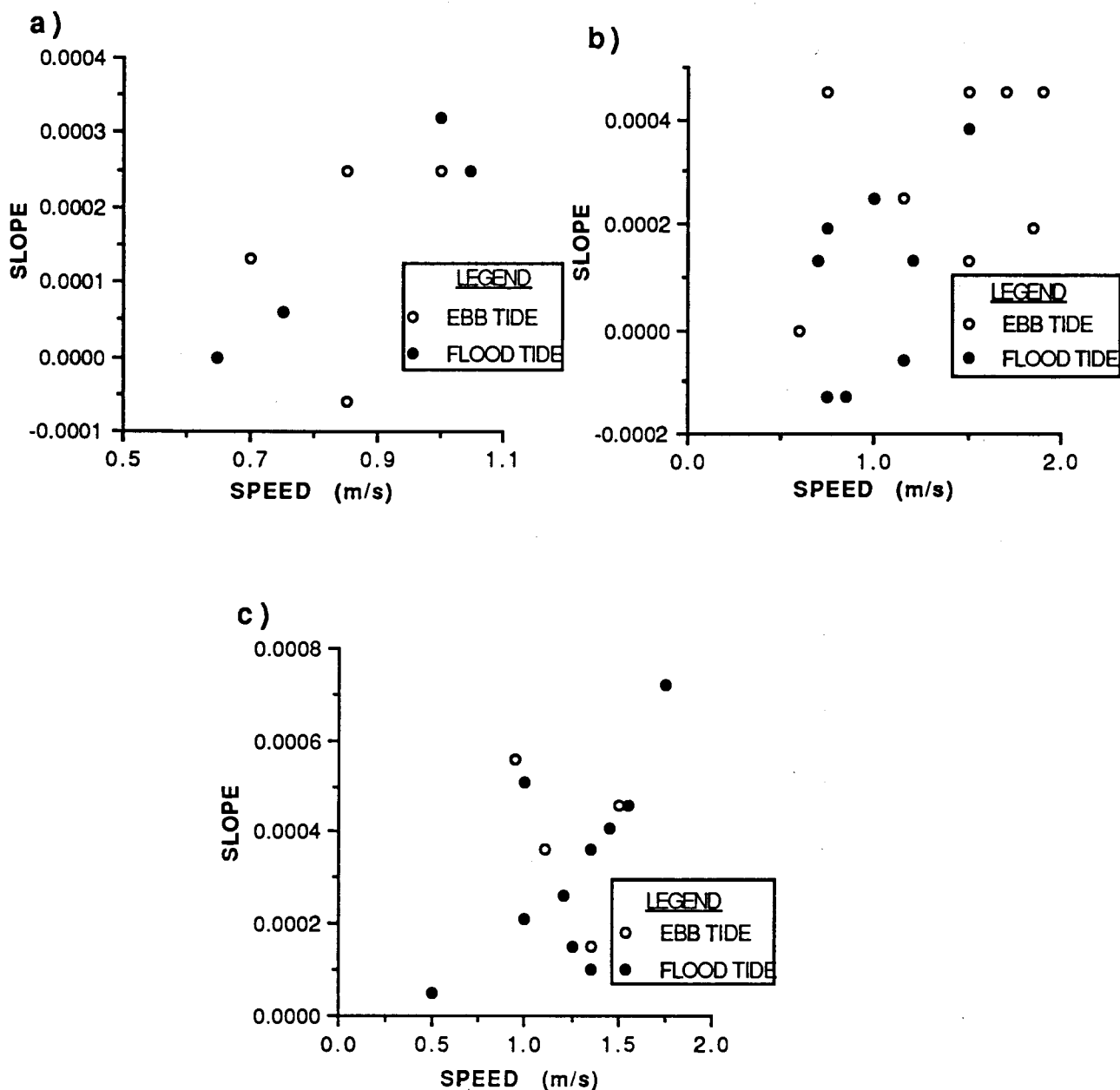


Fig. 4.9- Water-surface slope vs. current speed differentiated by ebb and flood tide:

- a) Station 6
- b) Station 5
- c) Stations 1 and 2

The models of U0.7d are based on small sample sizes, but the variables selected for the respective models at each station are similar to those of the surface speed. At station 2, Q dominates the model, but T is also important on the flood tide. D and R are important for stations 5 and 6, but T explains the most variation at station 6 on the flood tide. It was initially suspected that the variables in the models for U0.7d would differ from the surface-speed models (perhaps due to wind shear or bedforms), but this is not indicated in the results.

The extreme variability in current speed at 0.7d was not expected, but similar findings have been noted previously. Leighley (1934) (noted in Morisawa, 1985) concluded that zones of maximum turbulence are located at depths approximately 0.7-0.8d from the surface on either side of the cross-sectional maximum channel-depth.

The similarity of the variables selected in the models for speeds at both depths is encouraging, although the coefficients are based on small sample sizes, and the models are likely unstable. Whether there are more independent variables that should be considered, or a component of randomness, the models obtained are of limited predictive use. Nevertheless, the models do act to highlight the dominant controls on current speed.

Typically, as the data became more differentiated, the process of choosing variables for the model became more obvious since the decisions based on collinearity and parsimony did not need to be made. Note that, as the sample sizes diminish, the Kleinbaum et al.(1988) recommendation ($n > 5-10k$) may not be met. Statistically significant relations based on such small data sets are questionable.

The envelope curves that may be plotted on Fig.4.7c,d and Fig.4.8 are defined by the slope (Fig.4.7a,b) and are governed by the tidal wave propagation.

4.4.2- Tidal-wave Asymmetry

Plots of slope and surface-speed versus T (from HHT to LLT to LHT) highlight the spatial variability in tidal-wave asymmetry. From slope vs. T, there is a greater variability of slope values at both sites on the ebb tide. A hypothesis that will be explored in a subsequent chapter is that this is due to secondary circulation. The difference between the time of maximum slope between R/B and L/B is 0.10 T units. Also, the L/B data may be more skewed toward the ebb tide than the R/B data. As noted by Wright (1976), an upstream decrease in tidal amplitude is accompanied by a rapid increase in the tide wave asymmetry. The duration asymmetry is a manifestation of the finite-amplitude progressive wave characteristics. The Squamish River estuary is shallow compared to the tidal amplitude, and the celerity of the flood tidal-wave is faster than that of the ebb. The flood duration at the field site is approximately 80% of the ebb duration.

From the speed-T plots, the upstream stations (2,3,4) have velocity maxima after LLT, unlike the stations further downstream (5,6). There may be a shifting of the thalweg off the L/B as LLT nears, such that the core of the thalweg moves into the region of measurement (recall that at station 2, Q is negatively correlated with speed). When choosing the sites for speed measurement, it was assumed that the current speed in the thalweg would be relatively homogeneous over a lateral region of several meters. Thus, the rationale was to choose the most stable tree over a region (subjectively defined to be the thalweg) to which the buoy could be secured. Whether or not this decision has adversely affected the results cannot be ascertained for certain, but it does yield another cautionary note if attempting to utilize the regression models for prediction.

Effects of the lag of tidal parameters on flow hydraulics over time scales greater than a half-cycle are difficult to quantify. Kostaschuk et al. (1989b) note that identical values of tidal fall for similar river discharge could produce different effects dependent on the magnitude of the preceding tidal fall. Recall that LTH is an indication of the point in the fortnightly tidal cycle; the maximum Spring tide is at a LTH minimum and the maximum Neap tide is at a LTH maximum.

For the speed stations with large data sets (3 and 5), LTH is present in the models on both tides. This was not surprising because LTH was originally included in the regression models based on observations of differing boil activities with similar tidal drop and discharge at identical times in the diurnal tidal cycle (T). It is suspected that these effects could be recognized in the bedform records, but it will be difficult to isolate them due to the numerous complex hysteresis effects on smaller temporal scales.

It is often found that current speeds in an estuary ('horizontal tide') reverse earlier than the stage ('vertical tide'). This is known as 'time-velocity asymmetry' (Postma, 1961) or simply 'time asymmetry' (Hines, 1975). Rood and Hickin (1989) found that the velocity maximum occurred approximately 90 minutes before LLT at a site 1 km downstream of my R/B site. This value, however, is not only site specific, but dependent on the discharge and tidal characteristics at that time. The degree of phase shift depends on the effect of bottom friction and river discharge on the tide, a relationship for which a mathematical proof has been presented by van Rijn (1990). It is based on comparing the estuary discharge (from the equations of continuity and motion) to the tidal level from an oscillating solution of damped harmonic motion. Although the application of the formulae is not realistic due to assumptions being violated (e.g. constant cross-sectional area, hydraulic radius, Chezy C, water depth and bottom slope throughout the estuary), the physical explanation is still valid. Increasing bottom friction has the effect of

increasing time asymmetry, as does increasing river discharge. Knight (1977) found that the asymmetry of the hysteresis on the ebb tide increased moving upstream, which was also noted in Figs.4.7 and 4.8.

These effects are typically recognized in speed measurements, but they should also be evident in slope measurements. However, there have been few estuarine studies of water-surface slope made over multiple tidal cycles, so confirmation is difficult. Knight (1977) noted that slope values had a maximum before LLT, which was confirmed in this chapter (Figs.4.7a,b). A relation displaying a similar lag is that between current speeds near the bed (or shear velocities) and the surface speed.

It has been noted by several researchers that the Reynolds stresses at the bed are lagged relative to surface or mean-speed characteristics, resulting in a hysteresis (e.g. Gordon, 1975a, Anwar, 1983). Others note that turbulence intensity is greater during decelerating currents, which may or may not occur before low tide, depending on the degree of hysteresis in speed and stage (e.g. Knight, 1977). Van Rijn (1990) notes that there is a phase shift between the current speed at the surface and near the bed due to the effects of bottom friction. Since the pressure gradient generated by the water-level gradient (slope) is constant throughout the water column, the horizontal fluid momentum at depth can be overcome by the pressure gradient force sooner than the higher-momentum surface waters. This was put forth by Gordon (1975a) and confirmed by Davies (1977). Using shear velocity as an indication of flow turbulence, Kostaschuk et al.(1989a) found that there were enhanced shear velocities (u^*) during decelerating flows. A hysteresis relation between suspended-sediment concentration and mean velocity is attributed to this lag of turbulence (Thorn, 1975; Rood and Hickin, 1989). These findings cannot be verified using the speed measures obtained in this study. It is evident that the measured slope and

speed is not only controlled by simple tidal and discharge parameters, but it subject to a combination of many external forcings.

4.4.3- Current-speed time series

To ascertain the required duration of current-speed measurement at 0.7d necessary to approximate the long-term mean, the speed time series were filtered with a running mean, and the maximum deviations from the nine-minute mean were noted. The required duration was not only highly variable between measurement sites in the estuary, but could vary significantly at a site over short temporal scales. The time necessary ranged from 3.5 to 8 minutes at most sites, and exceeded 8 minutes on two occasions at the L/B U/S site.

Utilizing a similar technique for estimating the required duration of current-speed measurement, Savini and Bodhaine (1971) found that at most depths, a four-minute duration produced a value within 0.5% of the long term mean. It was concluded that the required duration varied temporally and spatially, which was noted previously by Dement'ev (1962). Dement'ev (1962) found that the required duration will not only vary between rivers, but even at a given point in the vertical will fluctuate with stage. He concluded that in order to obtain an accuracy of speed measurements within 2% of the long-term mean, the required duration will increase with depth, slope, bed material size and proximity to the banks. For steep rivers with coarse beds, required durations (depending on position in the transverse) are 1.5- 2 minutes at the surface, and 5-10 minutes at 0.8d. For rivers with low slopes and sandy beds, the times are approximately halved. Dement'ev implicitly equated bed-material size with resistance to flow, but did not consider the effect of bedforms.

The calculated values of TI and RTI were quite variable over short periods, but TI was correlated with $U0.7d$, most notably at the R/B. The intermittent maximas and minimas in water-surface slope previously noted could not be exclusively related to extremes of TI or RTI. Sokol'nikov (1936) (in Dement'ev, 1962) concluded that there are 'no regularities in probable values of current speed deviations from the mean, nor any relations to any factors'. Dement'ev (1962) concluded that the TI was positively correlated with the stage, as was the RTI, but only weakly. The correlations with stage were attributed to covariance with current speed, but with RTI, such a correlation could be spurious. In cross-section, the magnitude of the pulsation is inversely correlated with current speed at a point (thus increasing near the bed and banks). Similarly, at one point in the transverse, Savini and Bodhaine (1971) found that the maximum TI occurred at $0.75d$ and that the maximum RTI was found at $0.95d$. Rood (1980) suggests that such turbulence-intensity statistics are dominated by scales imported from upstream, and that large values of RTI are principally a result of declining local mean-velocities. I am unaware of any comparative downstream measurements of TI and RTI, but several studies indirectly confirm Rood's proposal.

Observations which may suggest that patterns in turbulence intensity are advected from upstream are given by current-speed measurements taken at a variety of depths in the flow. While such measures often indicate a close correlation between current-speed time series at various depths, there is frequently a lag whereby local maximas or minimas in the time series occur a few minutes earlier at the surface than near the bed (Dement'ev, 1962; Savini and Bodhaine, 1971). Perhaps this is related to eddies which are stretched asymmetrically in the vertical (ie. further downstream near the surface) due to skin or form resistance. Although current-speed fluctuations may be some relic of helical flow components imported from upstream, boil production may be associated with the

fluctuations. Simultaneous streamwise current-speed time series within the thalweg over short downstream separations (<10m) may elucidate this.

The magnitude of TI and RTI was not convincingly related to hourly fluctuations in stage and discharge. It may be that the temporal length of integration (1 hour) is too long to be an appropriate differentiator. The proposed relations between TI and the change in discharge in the hour preceding current-speed measurement may be present. As noted in section 4.1, previous studies relate the magnitude of current-speed fluctuations to variations in discharge, and this relation seems physically plausible. Although the data did not allow such investigation, the proposed relation between current-speed fluctuations and bedforms or bedload also seems possible. There are seemingly no causative links between discharge or tidal conditions (diurnal or fortnightly) and the *patterns* noted in the speed time series. In several instances, the patterns move from strongly-periodic to a random variation about the mean and back to periodic within a span of three samples over two hours.

These patterns noted in the current-speed time series included periods over temporal scales ranging from a few multiples of the sample interval to several minutes. Patterns of slow, unsteady increases in speed followed by a rapid decrease were occasionally noted. Rapid increases followed by slow, unsteady decreases were also observed, but considerably less frequently. These observations were made after a binomial filter was applied, but the filter did not significantly alter amplitudes, create phase shifts or polarity reversals. Similar patterns in current-speed may be noted in previous studies, but it is apparent that some periodicities were introduced by the filtering function used.

Rood (1980) noted from the findings of Dement'ev (1962) that the length of the longest period in current-speed records appeared to be partly dependent on river size and

discharge. However, the periods were on the order of the record length, and any shorter periods identified were simply small multiples of the shortest averaging interval. Tiffany (1950) also applied simple moving averages before data presentation. Although Rood (1980) recommends the use of spectral analysis for identification of periods in current-speed time series, he also notes that the spectral shape may be strongly dependent on conditions near the measurement site. Itakuri and Kishi (1980) relate variations in spectral shape to macroturbulence downstream of an artificial bedform in a flume. Williams et al. (1989) also conclude that the effect of surface wind, waves, pressure-gradients and suspended-sediment in the water column on turbulence spectra are not known. In such exploratory work, extensive use of synchronous plots of the time series is more appropriate than spectral analysis. Comparison of simultaneous time series of current speed and boil period are made in Chapter 6.

4.4.4- Implications

The regression analyses serve to indicate important variables at sites in the estuary and times in the tidal cycle. However, the forces controlling the hydraulic variables in the estuary are complex. The intermittent maximas and minimas in water-surface slope suggest that factors other than discharge or tidal parameters are influential. These factors may include wind shear or bedform passage (e.g. Znamenskaya, 1963). Models based on data collected over temporal scales less than the scales of the potential controlling factors (e.g. scour and fill) cannot be extrapolated in time. The regression models also highlighted the dangers of extrapolating the results spatially in the estuary.

Perhaps a maximum slope based on envelope curves could be used to predict some maximum velocity at a site, but the data display the complexity of such an endeavour. There are several factors which may act to decrease the measured speed and slope (e.g.

hysteresis effects, wind, high macroturbulence generated by bedforms). Therefore, placing a fitted regression line (or hyper-plane) through these data is not particularly useful for prediction of slope or speed. Thus, only the measured values (rather than any predicted values) of slope and speed will be used in calculations of scaling parameters in following chapters. Also, extrapolation of these values, spatially or temporally, will be limited.

As noted in Chapter 1, there are important feedback-type relations between mean flow, bedform geometry and turbulence (Leeder, 1983). These complex relationships appear to characterize Squamish estuary and are the subject of Chapters 5 and 6.

CHAPTER 5- BEDFORM ANALYSIS

5.1 - INTRODUCTION

There have been a variety of definitions for what constitutes a bedform (e.g. Jackson, 1975; Harms, 1969; Allen, 1976a), and even more proposals regarding bedform nomenclature. Structural differentiation is often based on descriptive attributes (Allen, 1968; Boothroyd and Hubbard, 1975; Southard, 1975) but more recently on genesis (Jackson, 1975; Leeder, 1983; Terwindt and Brouwer, 1986). In addition to the nomenclature problem, researchers often combine data from fluvial, marine and estuarine sources, which makes between-study comparisons difficult (Allen, 1983, 1985). Znamenskaya (1963) noted such difficulties three decades ago, but the inconsistency has worsened as workers choose those classifications which fit their data. Accepted definitions for terms such as dunes, megaripples or bars remain elusive.

All sedimentary structures of the estuary bed in this study are simply referred to as 'bedforms', not only to avoid the difficulty in nomenclature, but because my data are based on an indirect two-dimensional parameterization. Any bias introduced by grouping together structures which have differing forcing mechanisms (ie. lags) may be apparent from graphical analyses (e.g. Allen, 1985).

There is general agreement that the results of flume studies of bedforms often are not applicable to actual riverine, estuarine or marine environments. Allen (1983) noted the lack of understanding of bedforms in natural flows. Natural flows may be unsteady and/or nonuniform therefore they may have several characteristics not present in flumes. These include large variations in depth, discharge and velocity over short temporal and spatial scales (Coleman, 1969), and Reynolds numbers in excess of 10^6 (Lapointe, 1989).

Additionally, wind shear may affect bedform migration and shape and time-velocity curves (Terwindt and Brouwer, 1986).

Allen and Friend (1976a) concluded that the effects of flow unsteadiness on bedforms were highly complex and that each site has unique features. These may include flow unsteadiness that occurs so rapidly that the bedforms cannot respond immediately, and thus are out of phase with the flow, or 'lagged'. As a result, perceived differences of size and/or shape need not imply fundamental hydrodynamic differences (Allen, 1983).

As outlined by Allen (1974, 1976a, 1983) changes in bedform-size require erosion, transport and deposition of sediment. This produces a delayed bedform response to changes in flow conditions. This delay or lag is often measured in terms of temporal differences between maximum flow strength and peak bedform-size. However, there is not a commonly accepted definition of how 'time lag' should be measured (Terwindt and Brouwer, 1986). In fact, Jackson (1976) qualitatively defined lagged bedforms as those which did not produce the expected macroturbulence from measured flow conditions.

Time lag is dependent both on the kind of bedform, and the hydraulic and geometric characteristics of the environment (Allen, 1976b). Generally, larger bedforms are believed to show more lag than smaller ones (Collinson, 1970; Jackson, 1975). If lag is to be assessed quantitatively, bedforms must be studied on a time scale that is small compared to relevant time scales of changing flow conditions (Allen and Friend, 1976b). In a system such as the Squamish River estuary, there are several such temporal orders of flow variation.

An estuary will have components of both marine and fluvial influence, therefore lag related to both discharge and tidal variability may be expected. In fluvial systems, bedform

development may lag behind the rapid changes in discharge, most notably those systems dominated by a seasonal-snowmelt regime (due to the magnitude of the change in discharge) (Pretious and Blench, 1951; Allen 1973a; Kostaschuk et al., 1989b). In estuaries, discharge variations are superimposed on tidal fluctuations having two temporal scales: a semi-diurnal cycle and a fortnightly Spring-neap cycle.

Bedform lag after the turning of the tide on a diurnal scale is dependent upon the flow conditions, which in turn is affected by changes in tidal range over the fortnightly cycle. Separating the lag produced by these two scales is difficult, which is highlighted by the paucity of such studies. Allen (1976a) summarizes previous research, which is essentially qualitative and highly speculative. Recent attempts (Allen and Friend, 1976b; Knight, 1977; Boersma and Terwindt, 1981; Terwindt and Brouwer, 1986; Davis and Flemming, 1991) are more quantitative, but the study durations rarely exceed a few tidal cycles, and the frequency of data collection may be exceedingly low. The importance of these lags in the Squamish River estuary is examined, testing the observation of Dalrymple et al. (1978) that lag simply introduces variability without obscuring the basic hydraulic relations.

Quantitative relationships of bedform parameters with respect to apparent driving-forces are difficult to resolve in natural flows. Relations between bedform structure, hydraulic characteristics of the flow (e.g. depth, velocity, shear stress) and grain size in riverine and marine sites have been examined by many (e.g. Znamenskaya, 1963; Costello, 1974; Jackson, 1975; Knight, 1977). Although the flume-generated findings of Simons et al. (1966) and Yalin (1977) have been partially confirmed in some studies (summary in Knight, 1977), there is much variability about such relations.

These studies typically utilize graphical or bivariate regression analyses, and the proposed relations usually explain little variance in the bedform parameters (e.g. Korchokha, 1968;

Knight, 1977). Flow unsteadiness is typically blamed for the lack of correlation between dune dimensions and flow parameters, but Gabel (1993) noted that such data scatter is also observed during steady flows. She suggests that the influence of river-geometry on macroturbulence structure may also be important. Multivariate regression models are used in this thesis to predict the bedform height, wavelength and water depth, and the link in the generation of macroturbulent phenomenon may be elucidated (Chapter 6). Some researchers (e.g. Allen, 1983) have pondered the importance of flow resistance in bedform-hydraulics relations.

Allen (1976c) concluded that there are many methods for estimating flow resistance (e.g. Einstein and Barbarossa (1952), Engelund (1966), Simons and Richardson (1966), Smith (1968,1970)), but none consider form roughness. Allen (1983) notes that form roughness depends on size, shape and spacing of bedforms as well as on the flow itself. Several parameters to represent the resistance offered by bedforms have been suggested. These include bedform height (Brownlie, 1983), bedform steepness (Gabel, 1993) and relative roughness (Sayre and Albertson, 1961; Chang, 1970). Also, the longitudinal spacing of bedforms as a proportion of depth ('relative roughness spacing' or RRS) was suggested by Morris (1955). The complexities of bedform lag will also apply to variations in flow-resistance (Kinori and Mevorach, 1984).

Knight (1977) suggested that the resistance offered by three-dimensional bedforms may be greater than that for two-dimensional, but concedes to Allen's (1976c) conclusion of there being '...no acceptably reliable way of calculating the flow resistance of a large stream from the properties of its bedforms'. Recent work by Allen (1983) and Robert and Richards (1988) repeat the finding. Consideration of macroturbulence may be insightful.

This chapter addresses the applicability of predictive models for bedform parameters at various locations in the estuary over a wide range of tidal and discharge conditions. It is hypothesized that components of the mean flow-bedforms-turbulence feedback system will be elucidated.

5.2- RESULTS

5.2.1- Results of regression analyses

5.2.1.1- Data Inspection

For each reach, bedform height, wavelength and water depth versus LTH, Q, D, and T were examined. W and h are negatively correlated with LTH, displaying a weak linear trend in reaches 2,3,7, and strong linearity in reaches 1,4,5,6. There is also evidence that the variance in w and h decreases with increasing LTH. For w and h versus T, there is a general linear increase with T in reaches 1-3, 6 and 7, but w and h are relatively invariant with T for the downstream-most reaches (4 and 5) (Fig.5.1 a,b). There is also a positive correlation between T and the variance of w and h (Fig.5.1c). The variance of h is greatest between T= 1.0-1.4, and in several reaches, there appear to be peaks in w at T= 1.3 (and 0.3). In reaches 2,3, and 7, a lag is displayed in the early ebb such that w decreases between T= 0-0.3 (Fig.5.1d).

H and w may increase linearly with Q (Fig.5.2a), but it is masked by pronounced variance increase with Q, especially in reaches 4 and 5 (Fig.5.2b). Another notable feature is that, for every reach except #3, the variance in both h and w decreases once Q exceeds 650 m³/s. Lastly, for h and w versus D, there is a strong positive correlation (especially reaches 2 and 3) which may be non-linear, or linear up to a 3m drop and non-linear once D exceeds 3m (Fig.5.2c). In reaches 2 and 3 there is a suggestion that w and h decrease until D exceeds 1m (Fig.5.2d). In general, there are several trends that indicate that linear

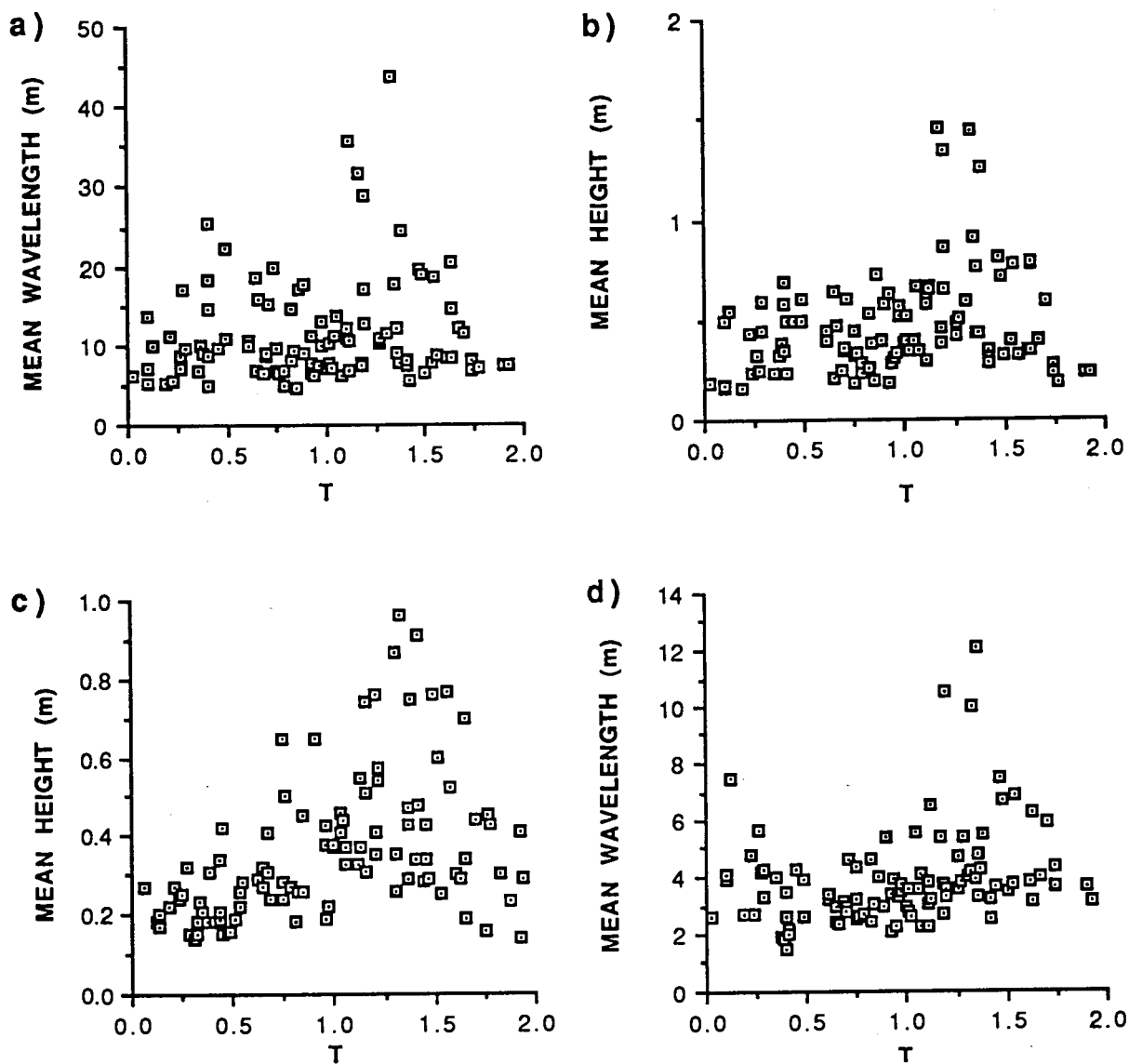


Fig. 5.1 Mean bedform-parameters vs. T

- a) Reach 4- wavelength
- b) Reach 4- height
- c) Reach 7- height
- d) Reach 2- wavelength

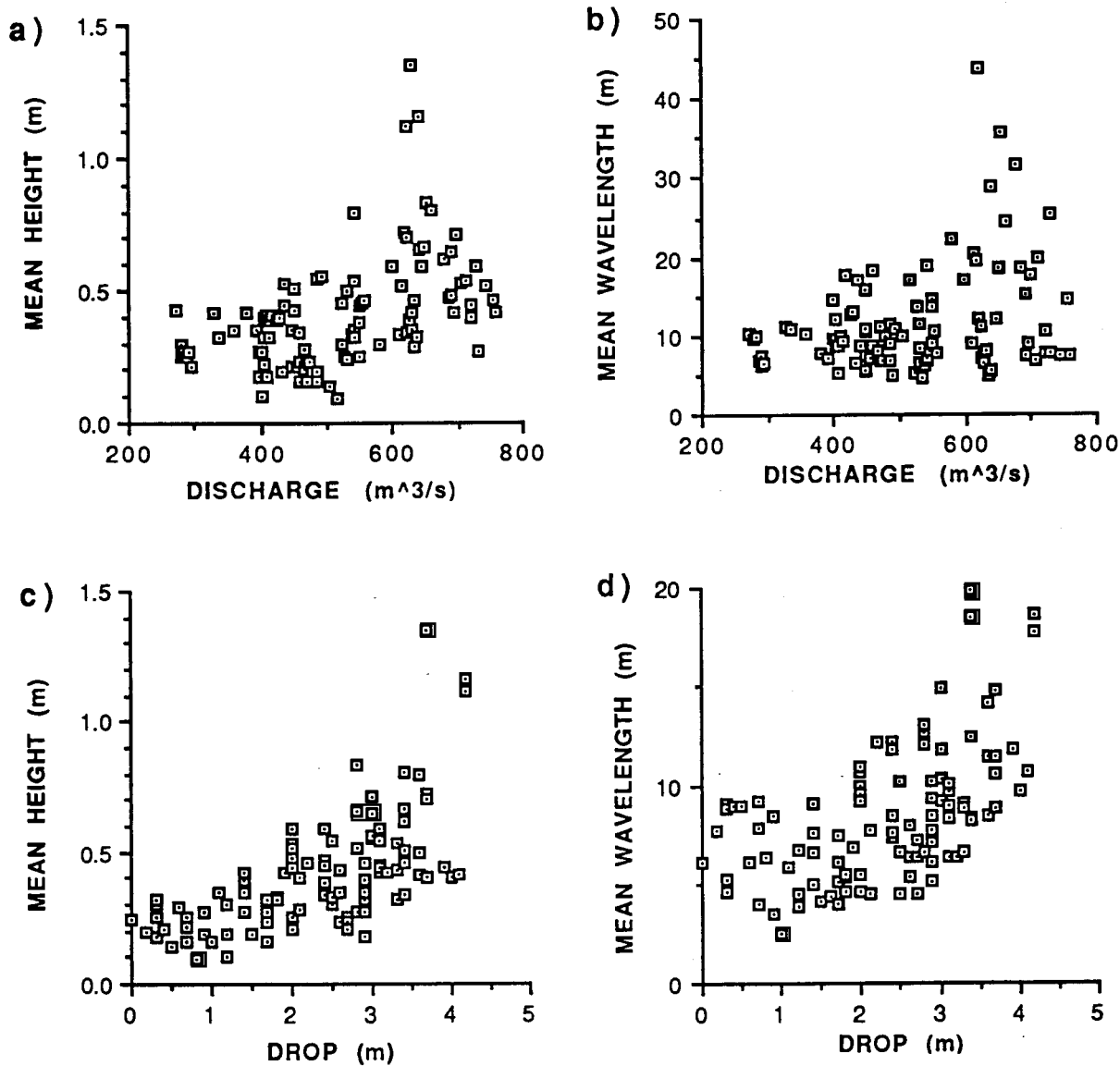


Fig. 5.2 a) Reach 2 mean bedform-height vs. discharge
 b) Reach 4 mean bedform-wavelength vs. discharge
 c) Reach 2 mean bedform-height vs. drop
 d) Reach 3 mean bedform-wavelength vs. drop

regression is not appropriate, but it will be assumed and residuals will be inspected for heteroscedasticity.

There are several trends apparent in the plots of depth versus the independent variables. A strong negative correlation is noted with D , although the variance increases significantly as D increases (Fig.5.3a,b). As expected, depth appears to be poorly correlated with Q , since the depth is so strongly controlled by the tides. The multiple regressions will determine if any of the variation is attributable to Q once the tidal effects are considered. Lastly, depth displays a strong linear relation with T (once the data are differentiated by ebb and flood tide), with variance greatest near LLT. Approaching LHT, the reaches furthest upstream display a tendency for the rate of increase of depth with T to diminish (Fig.5.3c,d).

Of those reaches which had high standard deviations (s.d. or σ) of wavelength or height, bedforms do not become progressively larger or smaller at any specific points in the reaches. Thus, high s.d. does not seem to be a result of heterogeneous differentiation of the transect, and reaches with high s.d. were not removed from the analysis. As the scale of the bedforms increases, the variability associated with the mean in that reach also increases. For h , the correlation with σ_h is strong, especially in reaches 2 and 3 (Fig.5.4a). In reaches 4 and 5, the variation in the standard deviation itself also increases with increasing h (Fig.5.4b). A similar pattern is exhibited by w (Fig.5.4c). For d , the s.d. is generally random, but there is a weak tendency for the maxima to occur at mid-depths in reaches 1,2,4,6 and 7 (Fig.5.4d).

In reach 6, many of the runs encountered submerged trees with root wads snagged on the river bottom. They are unstable, and although they can be identified when present at the time of the survey, it is uncertain if a recently eroded piece of debris had an effect on the bedforms. Results from this reach thus should be viewed cautiously.

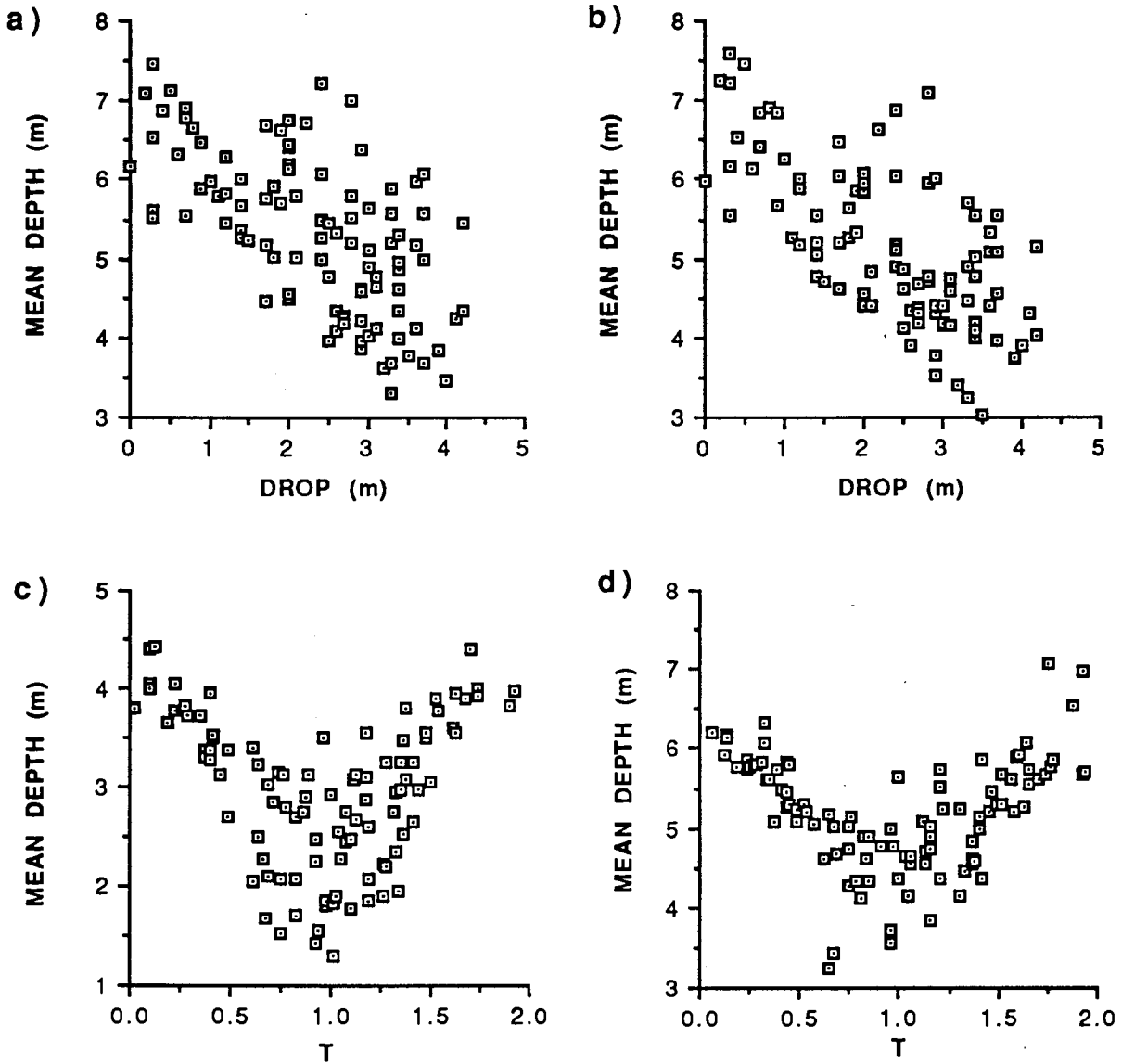


Fig. 5.3- a) Reach 5 mean water-depth vs drop
 b) Reach 4 mean water-depth vs. drop
 c) Reach 2 mean water-depth vs. T
 d) Reach 6 mean water-depth vs. T

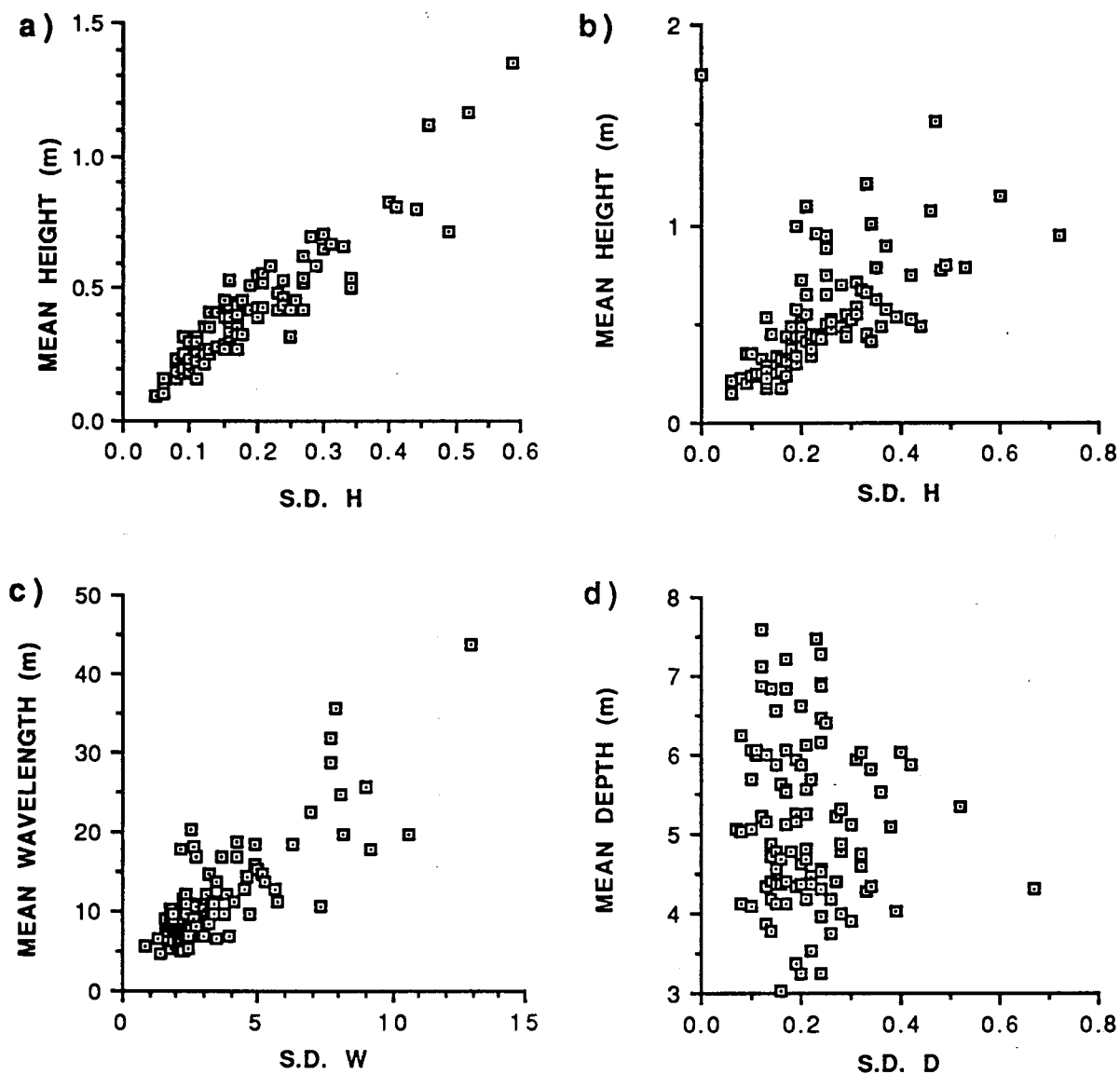


Fig. 5.4- Mean bedform-parameters or water depth vs. the standard deviations of the mean values:

- a) Reach 2 mean bedform-height
- b) Reach 5 mean bedform-height
- c) Reach 4 mean bedform-wavelength
- d) Reach 4 mean water-depth

There are three possible sources of error in the data, including sonar calibration, delineation of reach boundaries during data collection, and digitization of the profile. The echo sounder was calibrated at the beginning of the field season, so there should be no systematic errors; resolution of the equipment is 0.025m. Errors in delineating reach boundaries were carefully monitored in the field, and will be treated as random, thus summing to zero over the data-collection period. The largest errors occur with digitization.

Errors in bedform-height and water-depth are taken as one half the smallest measurement unit during digitization (± 0.05 ft.=0.015m). The error in w is not constant, but depends on the actual magnitude of the wavelength. It is 0.025cm on the graphic output, but once converted to actual distances, this value could be as high as 1.2m depending on the paper speed of the graphic-output and the length of reach. Since reach-averages are taken of each w , h and d measurement, it is assumed that these errors sum to zero over the collection period. An error that cannot be eliminated is the measurement of the reach-length, which will affect the value obtained for w . As indicated in Ch. 2, this error may be taken as ± 0.2 m. Although it would actually be significantly lower as an average error of the w (not the reach length), 0.2m will be used to account for possible differences between the distances measured on the shore versus those travelled along the river during profile measurement.

It may be argued that the error in measures of h , d and w should be significantly larger to account for potential problems with lateral boat movement, or bedform orientation that is non-perpendicular to transect path. It is not only difficult to assess this quantitatively, but there are even problems when measuring bedforms exposed on inter-tidal areas (Knight, 1977), especially if the bedforms are three-dimensional (Gabel, 1993). No account will be made of these types of errors.

5.2.1.2- Mean depth regressions

Differentiating the mean water-depth by ebb and flood tide allowed a reasonably good linear fit to the data (Tables 5.1 and 5.2 in App.1.1). On both the ebb and flood tide, the models for reaches 1,3,6 (furthest upstream sites) have both T as the most significant independent variable, and Q in the model. For reaches 1 and 6, the fit is comparatively poor with respect to the other reaches, but the models do explain in excess of 50% of the variance in depth. Note that the fit is better on the ebb tide in reach 6, and on the flood tide in reach 1. Reach 3 has R^2 values in excess of 0.8 on both tides. The flood-tide models for reaches 2 and 7 have identical explanatory variables to reach 3, explaining similar amounts of variation in d. The fit is best amongst these reaches for #2, especially on the ebb tide. The ebb-tide models for reach 2 and 7 included D, Q and LTH, but not T (due to collinearity with D). For both tides, the fit is better on the upstream transect(2) than the downstream transect(7). Multiple correlation coefficients meet or exceed 0.75 in reaches 2,3 and 7 on both tides.

The models predicted for the two reaches nearest the mouth are not similar to those for reaches upstream, but are strikingly similar to each other. On the ebb tide, reaches 4 and 5 have D, Q and LTH in the model, with D explaining most of the variation. On the flood tide, both reaches have T, Q and D in the model, with T as the most important dependent variable. Both reaches have better models on the ebb, with higher R^2 values and lower s.e.e. For all seven reaches on both tides, Wilkinson's Test indicates that the R^2 value is significant to a 99% confidence level.

On the ebb tide, only the reach 1, 6 and 7 models were found to contain outliers in the data. On the flood tide, data from all reaches contained 1 or 2 outliers. Outlier removal had

a minimal effect on the variables within the models; D entered the reach 1 and 6 ebb-tide models, and LTH entered the reach 6 flood-tide model. The improvements in R^2 of both ebb-tide models were approximately 0.1, while the flood-tide models of reaches 4 and 7 had improvements of 0.07 and 0.09 respectively. In other models, the improvement was quite minor. All other assumptions of linear regression were met based on the tests of residuals (Table 5.3 in App.1.1).

5.2.1.3-Mean bedform-wavelength and height regressions

The expected violations of linear regression produced by regressing the mean bedform-height and wavelength against the independent variables were confirmed by examining the residuals (Table 5.3). The models will not be discussed, but the data are presented for purposes of comparison (Tables 5.4, 5.5 in App.1.1) with the transformed data.

The tendency for the variance in bedform h or w to increase with increasing Q is evident in nearly every reach. Since Q is included in almost every model of the untransformed data, the residuals were frequently heteroscedastic. Also contributing to the heteroscedasticity is the power-function relation with D previously described. It is postulated that data transformation may solve these problems.

Transforming the independent variables while keeping the dependent variable untransformed was quite unsuccessful. However, transforming the dependent variable (Y) while keeping the independent variables untransformed produced useful results. A variety of transformations were investigated, including $\log Y$, Y^n (where $n=0.33, 0.5, 0.67$), and Y^{-1} . The transformation most successful in removing the heteroscedasticity was $\log Y$. A weighted least-squares (rather than ordinary least-squares) approach (ie. $Y'=y/x$; $X'=x^{-1}$) was not employed since the log transform worked adequately.

Trends in the log-transformed h and w indicate that most of the correlation between Q and the variance of h and w has been removed (Fig.5.5a). As outlined in section 5.2.1.1, this correlation was most strongly noted in reaches 4 and 5, but the transformation was successful (Fig.5.5b). Similar results are found for LTH (Fig.5.5c). The transformation was even more successful in removing the non-linear trend in the relations between h and w and D (Figs.5.5d,5.6a). However, there is still an indication of the lag in w in reaches 2 and 3 near HHT (Fig.5.6b).

Of the models for the log-transformed mean bedform-height, those for reaches 2 and 3 have the best fit, with identical explanatory variables and importance (Table 5.6 in App.1.1). D explains the most variation in h followed by Q and LTH. The reach 7 model also includes Q and D , but Q is the dominant explanatory variable. The fit of the models from reach 2 is better than those for reach 7, with higher R^2 and lower s.e.e (note that the s.e.e is expressed in log units (e.g. Kostaschuk et al.,1992)).

The models for reaches 1,4-6 all have LTH with the largest beta coefficient. Reaches 1,5 and 6 have T as the next most important variable, while it is Q for reach 4. Similarly, the R^2 value is greatest for reach 6 and poorest for reach 5. All models have significant R^2 values at the 99% confidence level according to Wilkinson's test.

Comparing the log-transformed models for predicting bedform height to the untransformed models, the explanatory variables in each model are very similar, except for reaches 1 and 6. For reaches 2-5 and 7, the variables with the two highest beta coefficients are identical between the transformed and untransformed models. Reaches 1 and 6 have a pronounced change- D dominates the untransformed models, but is absent from the transformed models due to collinearity with T . The fit also improved with the transformed

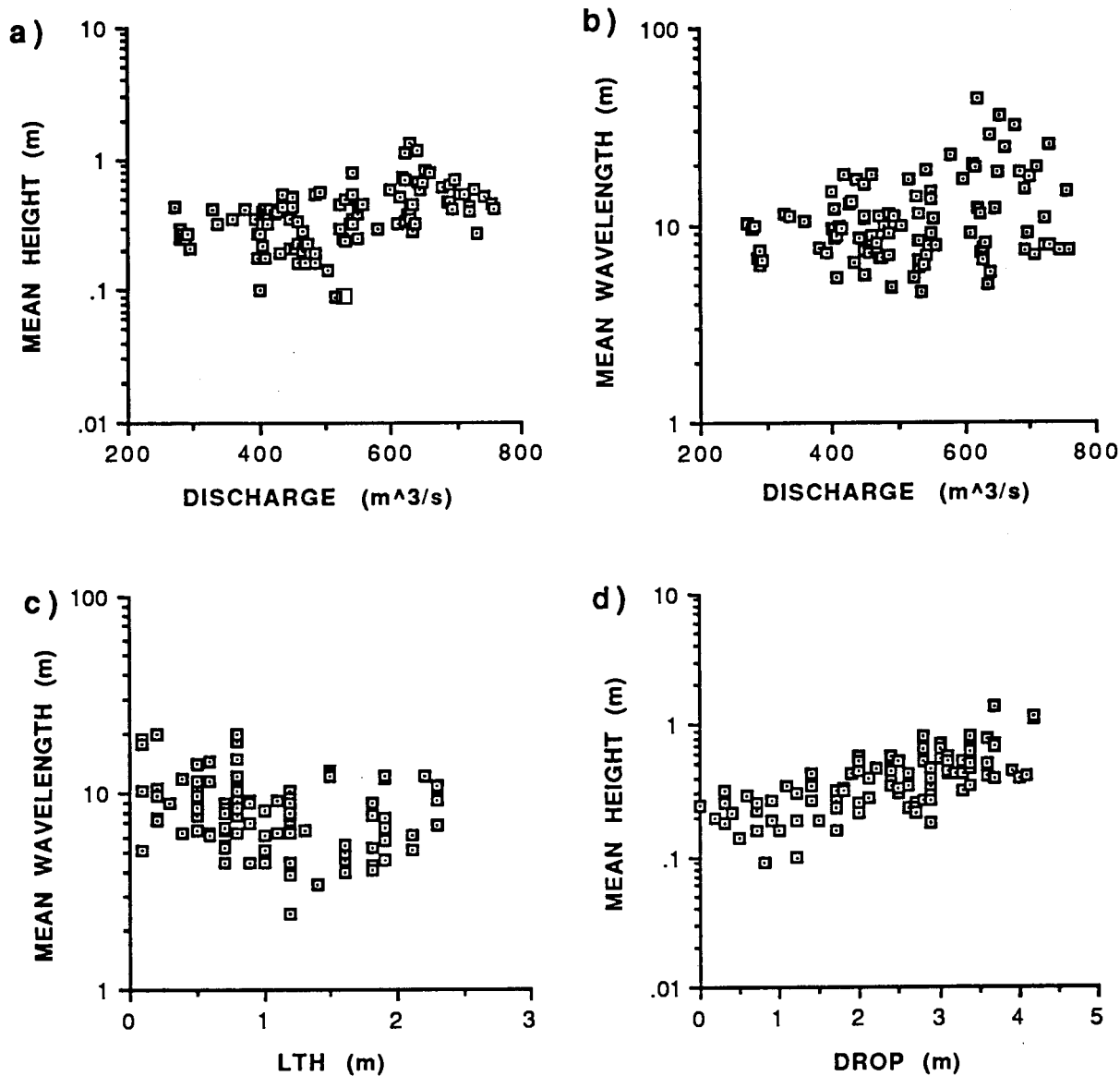


Fig. 5.5- a) Reach 2 log(bedform height) vs. discharge
 b) Reach 4 log(bedform wavelength) vs. discharge
 c) Reach 3 log(bedform wavelength) vs. LTH
 d) Reach 2 log(bedform height) vs. drop

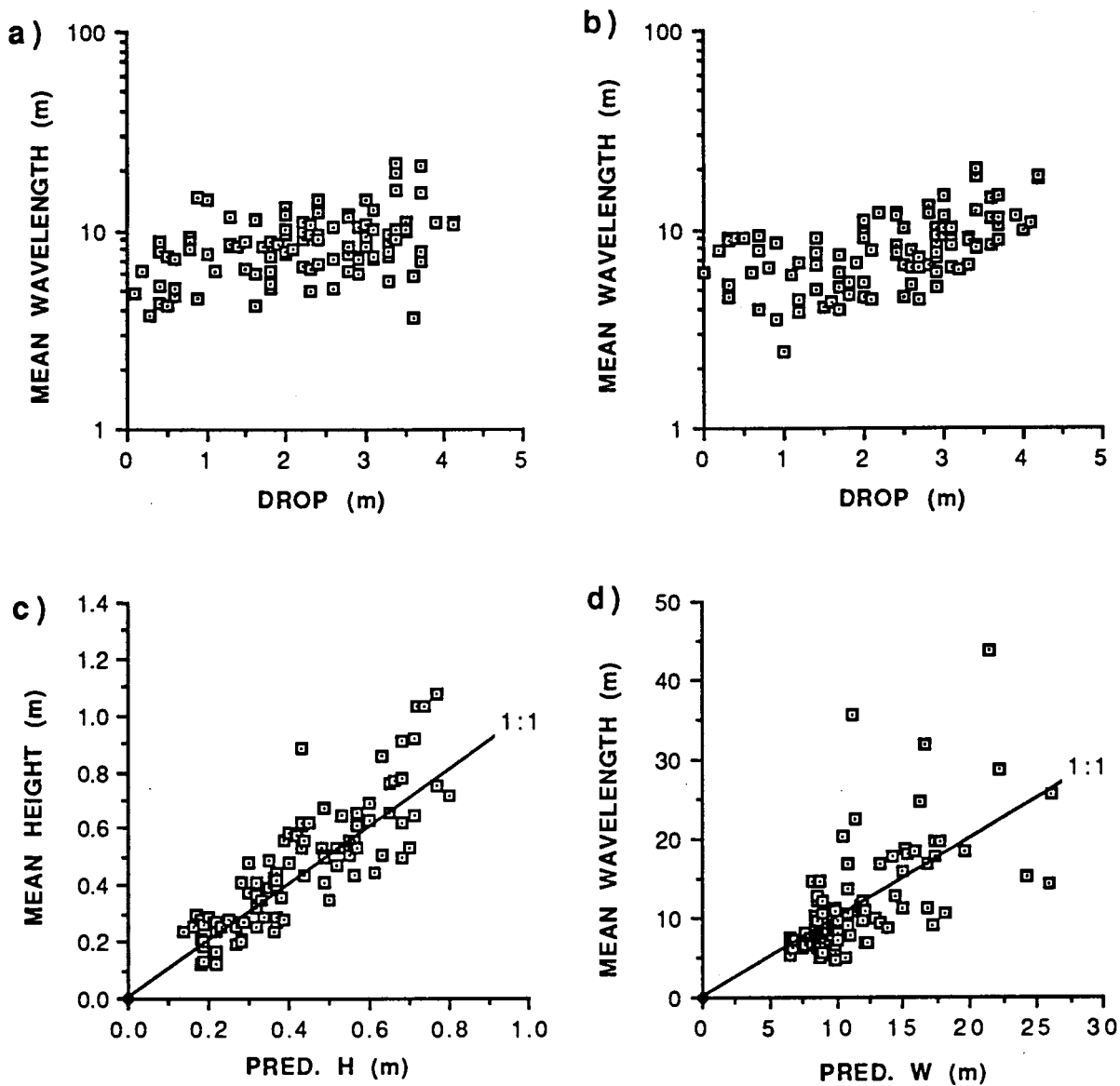


Fig. 5.6- a) Reach 6 log(bedform wavelength) vs. drop
 b) Reach 3 log(bedform wavelength) vs. drop
 c) Reach 3 mean bedform-height vs. values predicted from the full-regression model
 d) Reach 4 mean bedform-wavelength vs. values predicted from the full-regression model

models for all reaches except reach 5, presumably since the model of the transformed data has one fewer explanatory variable.

The models for h for each reach except #7 were found to contain at least one outlier (Table 5.7 in App.1.1). After removal of these data, the explanatory variables in the models did not change in any reach, and the improvement in fit was minimal (largest improvement was reach 6: R^2 increased by 0.076). Except for reaches 1 and 6, the residuals for the models of the log-transformed bedform-height display homoscedasticity. The two upstream-most reaches display a slight left-skewness to the frequency distribution of the residuals. All other assumptions of linear regression were met (Table 5.3).

The models for the log-transformed bedform-wavelength have poorer fits than height for every reach. Although the R^2 values do not exceed 0.5, Wilkinson's Test indicates that each w model is significant at the 99% level (Table 5.8 in App.1.1). LTH is the most significant explanatory variable in all models except reach 3. In every model, Q has the second-highest beta coefficient. T is included in some of the models (reach 1,2,6 and 7- indicating downstream and upstream path consistency), but D is only included in the model for reach 3. Unlike h , reaches 2 and 3 do not display significantly better fits than the other reaches. Reach 3 does have the highest R^2 value, but they are quite similar for all reaches.

The logarithmically-transformed models for predicting bedform w have the identical explanatory variables and importance to the corresponding untransformed models for each reach. The improvement in fit due to transformation was quite minimal, and for reaches 3 and 7, it appears to decrease.

The models for each reach contained at least one outlier, often two or three (Table 5.7), but once again, removal from the data sets had a minimal effect. T entered the model for

reach 4, but for all other reaches, the explanatory variables remained identical after outlier removal. The only notable improvements in fit were for reaches 1 and 6.

As a final note, there was an attempt to utilize nonlinear least-squares techniques (e.g. McCuen et al., 1990), but it was quite unsuccessful. It was very difficult to produce a model that had coefficients which predicted reasonably, seemingly due to the nature of the hyperplane fit to the data, which could contain many local minimas. Models had extremely poor fits, and typically, more than one hundred iterations were necessary. This required immense computational time, particularly with those models having more than two independent variables. This option was not pursued further.

5.2.1.4- Reliability Tests

Utilizing the split-sample test, the mean water-depth models had shrinkage values exceeding 0.1 for only two of the fourteen models. The split models were identical to the full models except for Q entering the reach 6 flood-tide model. The split-sample test for the model of the log-transformed h indicates that the shrinkage values are less than 0.1 for all reaches except 1 and 6. The models of the split-sample are similar to the full-sample models, although those variables with low beta coefficients were not found in the reach 1, 3 and 6 split-models. The split-sample test for the models of the log-transformed w had similar results, although the models may be more unstable. The shrinkage values are less than 0.1 for reaches 3-7, and less than 0.14 for reaches 1 and 2. The models of the split-samples have similar explanatory variables (and beta coefficients) to the full models for reaches 3-7. For reaches 1-2, the importance of variables in the split-sample models (based on beta coefficients) differ from the full models. The split-samples for w display more negative shrinkage values than those of h, perhaps indicating model instability.

The model reliability can also be directly inspected by plotting the actual parameters versus those predicted by the models. The models for bedform-height all tend to underpredict the actual height, and there is an indication that at extreme height values, the non-linear trend is still present (Fig.5.6c). These models have not had any outliers or values with high leverage removed. The model underprediction is not present for w , but there is generally much more scatter. The tendency for the variance in w to increase with w may still be present, or it may be the product of a few extreme observations (Fig.5.6d). With the split samples, the models of the mean bedform-wavelength tended to underpredict actual w , especially in reaches 1-3 (Fig.5.7a). The split-models of h displayed a better fit with less scatter (Fig.5.7b), but the nonlinear trend is again noted in reaches 2,4 and 7 (Fig.5.7c,d).

5.2.1.5- Alternative combinations of independent variables

A variety of combinations of variables were explored in order to elucidate potentially useful relationships. As noted in section 5.1, the option of using the 'absolute drop' was investigated. In each reach, for h , w and d , single variate linear regressions using D produced a more useful model than using absolute drop, without exception. Similarly for the stepwise multiple regressions, using absolute drop rather than D did not improve model fit for any reaches. The only positive aspect was a decrease in the residual heteroscedasticity for some reaches.

In another variation, the $Q \cdot D$ product (analogous to stream power) was investigated. The improvement in fit by using the product (rather than the two variables individually) was limited. No multivariate h models had a better fit, and for w , only the fit in reaches 2,3 and 7 improved. The improvement in these reaches may be related to having more variables in the model since the collinearity between T and D is eliminated. However, the degree of

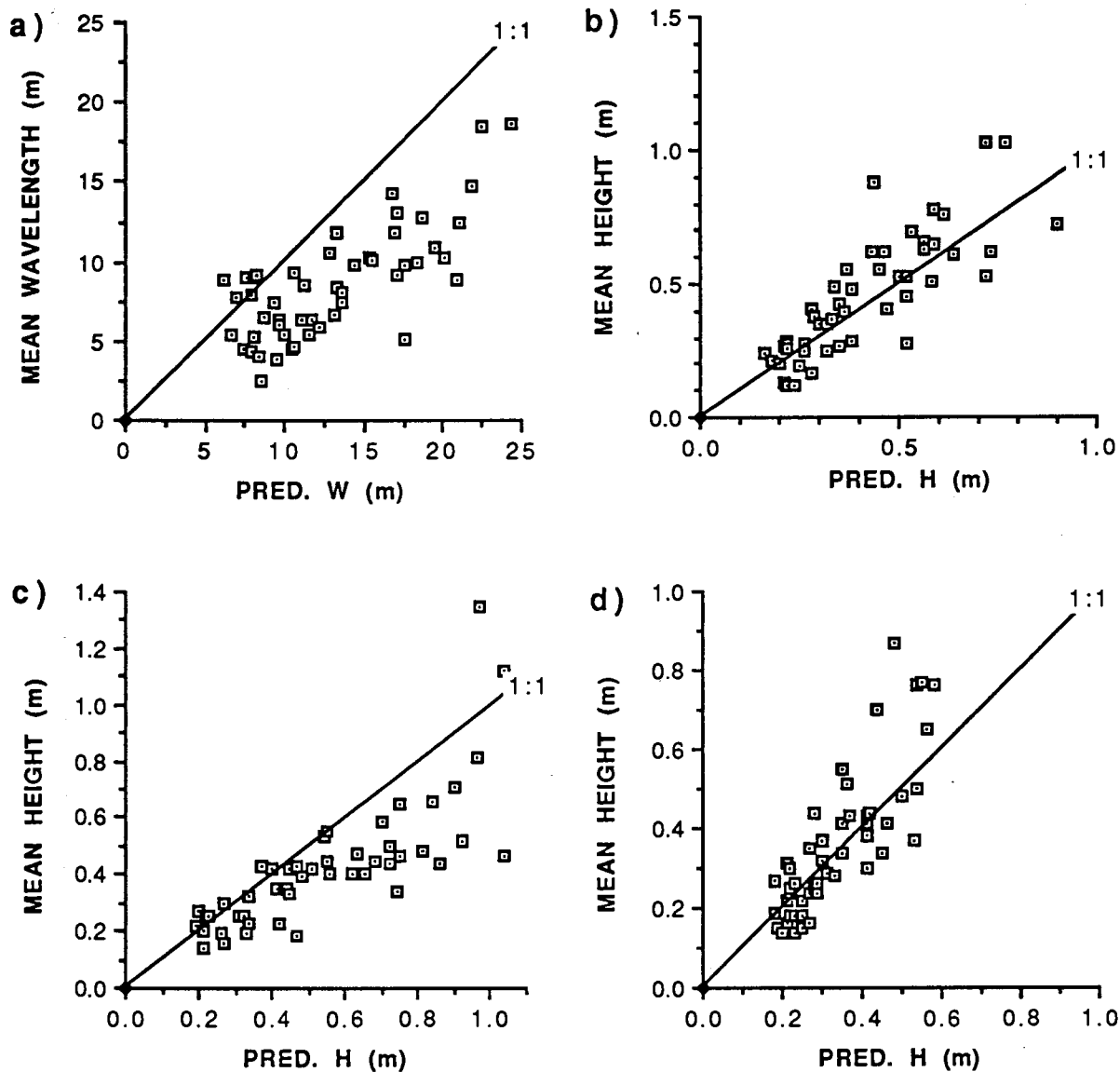


Fig. 5.7- Mean bedform-parameters vs. values predicted from split-sample regression models:

- a) Reach 3 wavelength
- b) Reach 3 height
- c) Reach 2 height
- d) Reach 7 height

correlation between h and w and $Q \cdot D$ in reaches 2,3 and 7 is notable (e.g. Fig.5.8a,b). Note also that the lag in h and w with small tidal-drop values is present in these plots.

If the bedform characteristics are plotted against scaling parameters such as the Froude number or the depth-slope product, the data sets are quite limited. The Froude number can only be compared with the bedforms in reaches 2, 4, 5 and 7 since only those reaches had current-speed measurements taken in the vicinity of the transect. Similarly, only reaches 1, 5 and 6 had slope measurements. The slope measurements had to be within 10 minutes of the transect being run, but the speed measurements were interpolated if there were bounding measurements taken within 90 minutes. This interpolation may not be strictly valid based on the findings of Chapter 4. Even with these liberal temporal limitations, there were typically only 10-15 data points for any particular reach.

Relations between the dependent variables (h,w,d) and the Froude number or depth-slope product were typically quite poor. For the depth-slope product, no regressions had R^2 values exceeding 0.15. However, if plotted against the relative roughness ($RR=h/d$), relative roughness spacing ($RRS=w/d$) or steepness ($S=h/w$), the correlation improved. For the Froude number, the RR and S fared best, albeit with limited degrees of freedom (Fig.5.8c,d).

5.2.2- Variability of results

5.2.2.1- Influence of vegetation and direction of travel

As outlined in Chapter 2, the reaches digitized were chosen so that several research hypotheses could be tested. One of these was the equality of parameters digitized from the upstream versus downstream-moving transects. The plots of h and w for reaches 1 and 2

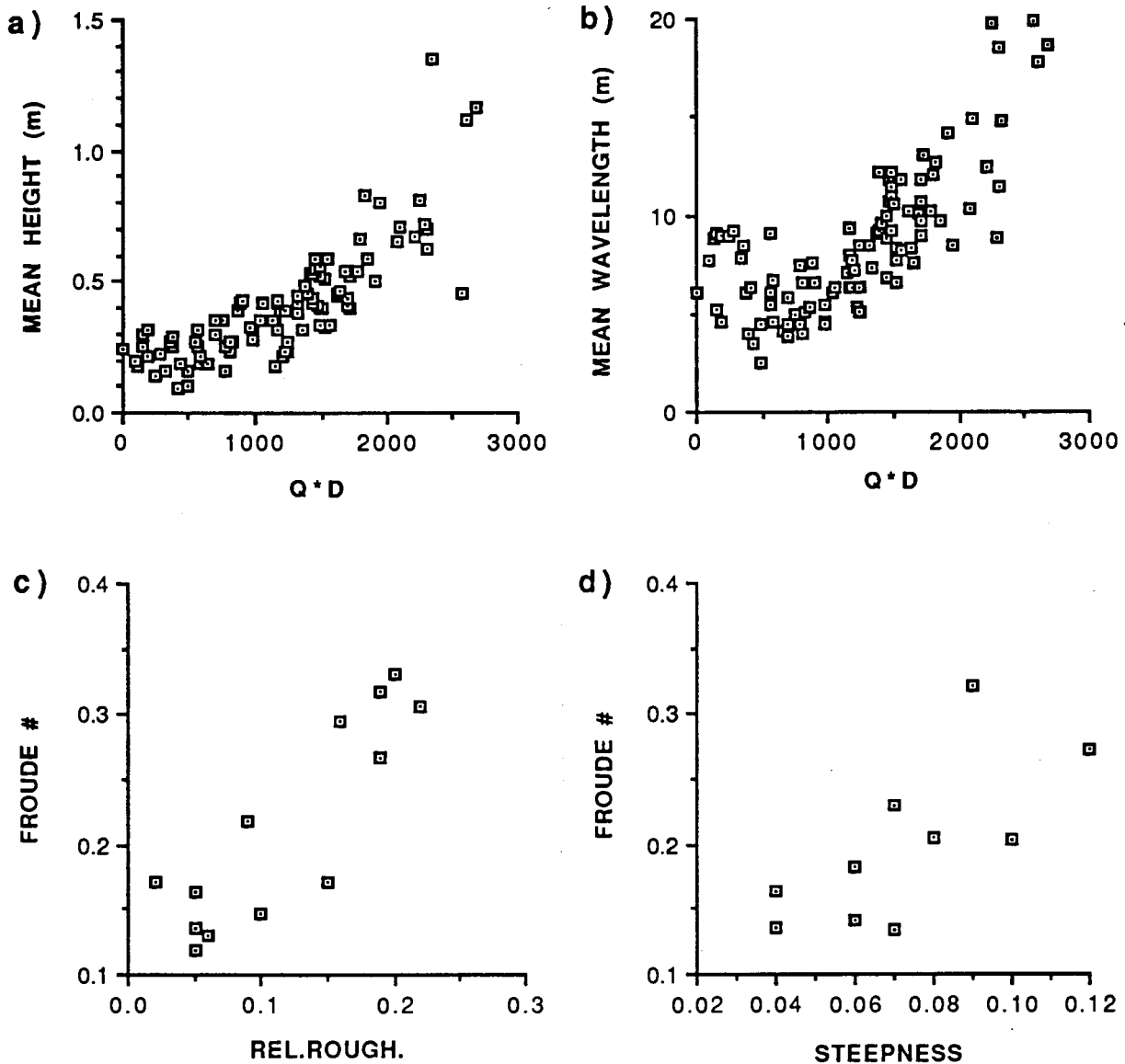


Fig. 5.8- a) Reach 2 bedform height vs.(discharge*drop)
 b) Reach 3 bedform wavelength vs.(discharge*drop)
 c) Reach 2 Froude number vs. relative roughness
 d) Reach 7 Froude number vs. bedform steepness

can be compared to reaches 6 and 7. Note however that the the transect path for reach 1 is slightly further streamward than reach 6.

To compare the paired values of h , w and d of reaches 1 vs. 6 and 2 vs. 7, a randomized Complete Blocks ANOVA analysis (Sokal and Rohlf, 1981) was performed. After the assumptions of the test were verified, a one-sided F-Test ($\alpha=0.05$) was utilized. The calculated F_s values for the reach 1 vs 6 analysis were 2.88, 4.30 and 16.48 for w , h and d respectively. For reach 2 vs 7, the values were 0.013, 0.34 and 22.93. With an $F_{crit(2,61)}=3.15$, the variance ratio between the up and downstream transects is significant for depth in both reaches and h for 1 vs 6.

The comparison of the up and downstream-moving transects may also be performed graphically. Generally, there is much more variability associated with reach 1 versus 6 compared to reach 2 versus 7. For both reaches, there is a tendency for the downstream-moving transects to produce a lower mean depth (Fig.5.9a,b). It is uncertain if this is a product of the different paths for reaches 1 vs. 6, but the results of reach 2 vs. 7 are confirmatory. Although not as obvious, it appears that h values may be larger on the downstream-moving transects for both reaches (Fig.5.9c,d). For w , the values appear larger on the downstream moving transect for 2 vs. 7, but smaller for 1 vs. 6 (Fig.5.10a,b). These findings are partially confirmatory of the ANOVA analysis.

The variability of the transect results were checked by running transects directly after one another on several days. Unfortunately, poor field conditions prevented reliable results for the majority of these runs. As a result, all reaches that were digitized were grouped together for the Randomized Complete Blocks ANOVA. The variation between the paired samples was found to be statistically insignificant at $\alpha=0.05$, with $F_{sample}= 1.58$, and $F_{crit(2,16)}=3.63$. There were limited degrees of freedom (16), but it seems safe to conclude

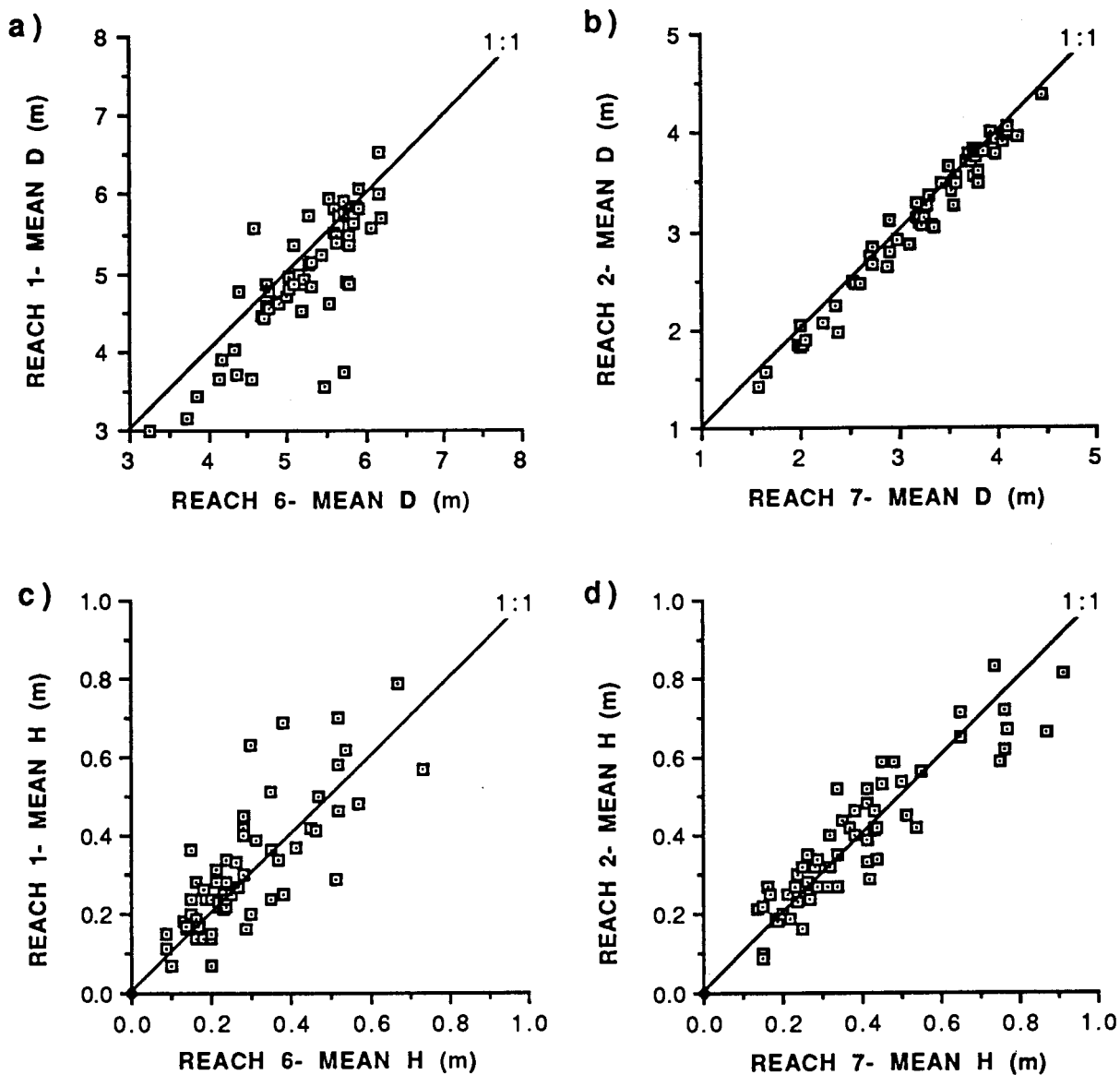


Fig. 5.9- a) Mean water-depth comparison-Reach 1 vs. 6
 b) Mean water-depth comparison-Reach 2 vs. 7
 c) Mean bedform-height comparison-Reach 1 vs. 6
 d) Mean bedform-height comparison-Reach 2 vs. 7

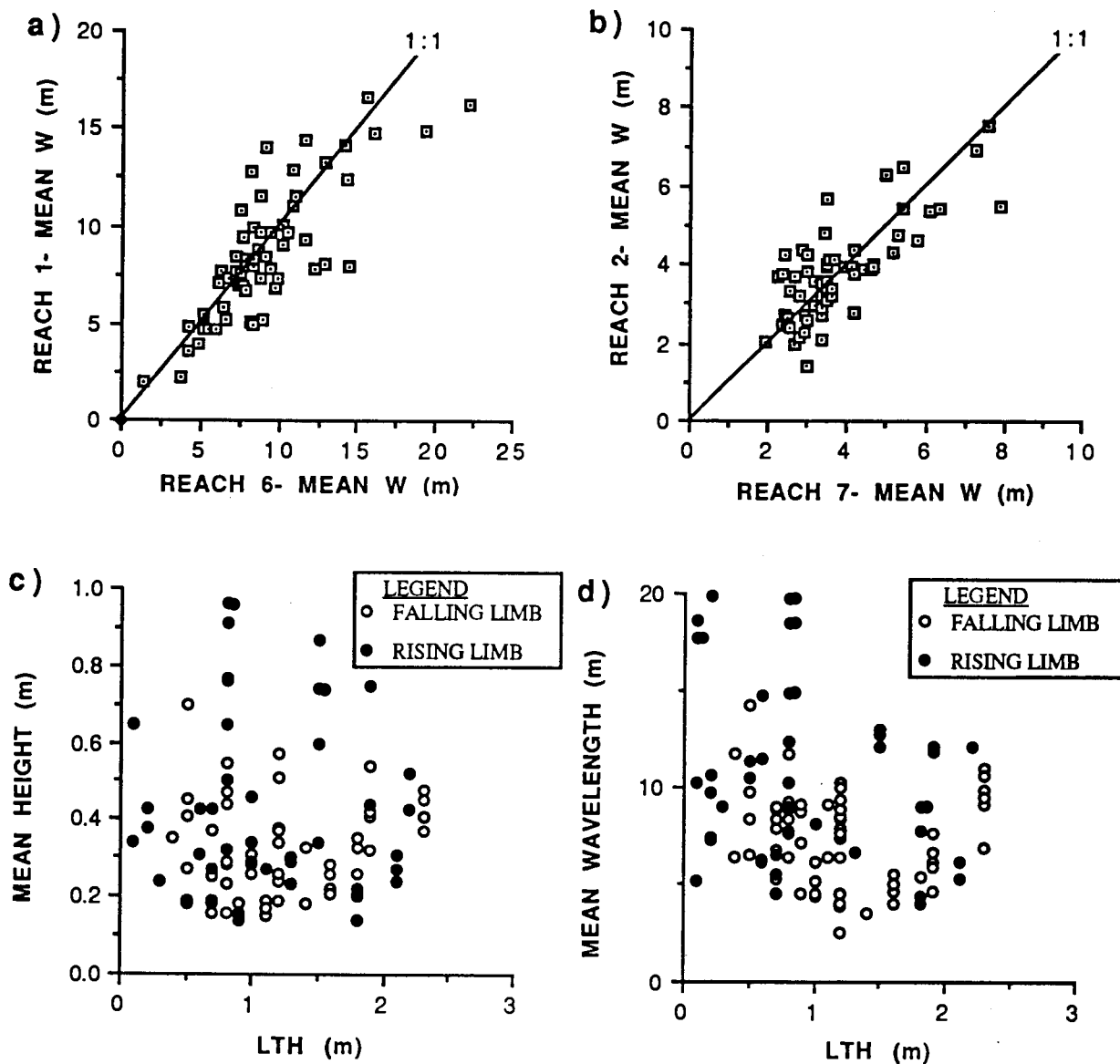


Fig. 5.10- a) Mean bedform-wavelength comparison-
Reach 1 vs. 6
b) Mean bedform-wavelength comparison-
Reach 2 vs. 7

Mean bedform height vs. LTH differentiated by
falling or rising limb of fortnightly tidal-cycle:
c) Reach 7
d) Reach 3

that the measurements were repeatable since a mean value over the reach was utilized, and the path could be followed very accurately along a line of stable trees and stumps in the river. The expected variance in bedform height and wavelength within short reaches is about 30-60% (Gabel, 1993), which is similar to the data collected in my study reaches.

The effects of the vegetation on the results of the mean bedform-characteristics in reaches 1 and 6 are difficult to quantify (as discussed in Chapter 2). In fact, the days and times noted to have debris entrenched on the river bottom were not exclusively outliers. Reach 1 was run several metres streamward of reach 6, to be just outside of the prime vegetation-snagging zone. This was attempted in order to study the effects of vegetation on the bedforms. Interestingly, the four runs in reach 1 where vegetation was noted on the graphic output fell within a one week period (see Appendix 2.4: July 28-Aug. 3). Removal from the analysis of these runs with debris on the bed (4% and 35% of runs digitized for reaches 1 and 6 respectively) was attempted and the model fit remained reasonably consistent, although the variables within the models differed slightly.

5.2.2.2- Lag effects

A potential source of uncertainty in predicting bedform characteristics in natural flows is the lag, and one may expect three potential sources of lag :

- 1) Freshet-related changes in Q producing hysteresis of h and w
- 2) Spring tides producing bedforms remaining for several tidal cycles
- 3) Minimum/maximum h and w (diurnally) occurring after HHT/LLT

It is difficult to isolate these lags, especially when Q is highly variable over short temporal periods, as is experienced in the research area. The plot of mean daily Q of the estuary from May to September, 1992 indicates a general rise and fall associated with the freshet.

However, the shorter-period (3-12 days) fluctuations associated with storms or isolated snowmelt events in the tributaries arguably dominated the hydrologic regime (Fig.5.11). On four distinct occasions, a level of $650 \text{ m}^3/\text{s}$ is exceeded, at which time the bed may have been significantly scoured. Note also that for two of these four events, the peak in Q corresponds to a tidal drop maxima in the Spring-neap tidal cycle so that the seasonal hysteresis may not be recognizable.

From inspection of the data, reaches 1-5 would be poorly suited for an analysis of this type since they were not monitored until the second week in June. Vegetation may make the results of reach 6 questionable, therefore only reach 7 will be examined. At approximately two-week intervals (as the data allow), mean bedform-wavelengths were inspected at several times in the diurnal tidal-cycle, with similar tidal drops and low tide heights. Wavelength will be used rather than height since it is less sensitive to short-term changes in depth (diurnal scale lag), and the tidal conditions are chosen to approximate LLT on a Spring tide. The standards are for T between 0.75 and 1.25, $LTH \leq 1.0\text{m}$, and $D > 3.0\text{m}$ (these standards were slightly violated for July 28 and August 10). Table 5.9 indicates that the wavelength follows the discharge quite well, inferring that there is no lag in wavelength on a scale longer than two weeks.

Isolating the lag associated with the Spring-neap tidal cycle was attempted two ways. The first was to simply examine mean bedform-characteristics at similar T , Q , LTH and D on either limb of a Spring-neap cycle. This is dependent on discharge being reasonably constant over this period. There were seven Spring-neap cycles between May and September, but data was not collected during one of the cycles. For five others, there were discharge values exceeding $650 \text{ m}^3/\text{s}$, so bed scour may have occurred. As a result, there was only one choice: mid-July. Table 5.10 shows that for reaches 1-5 (6 and 7 were

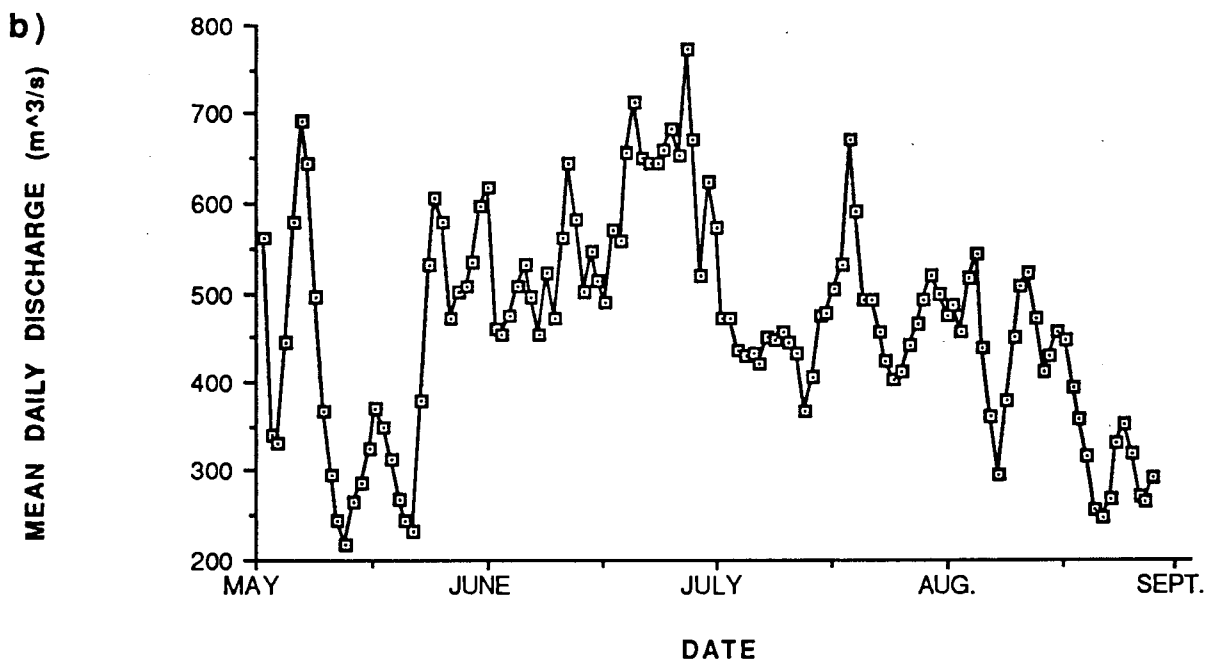
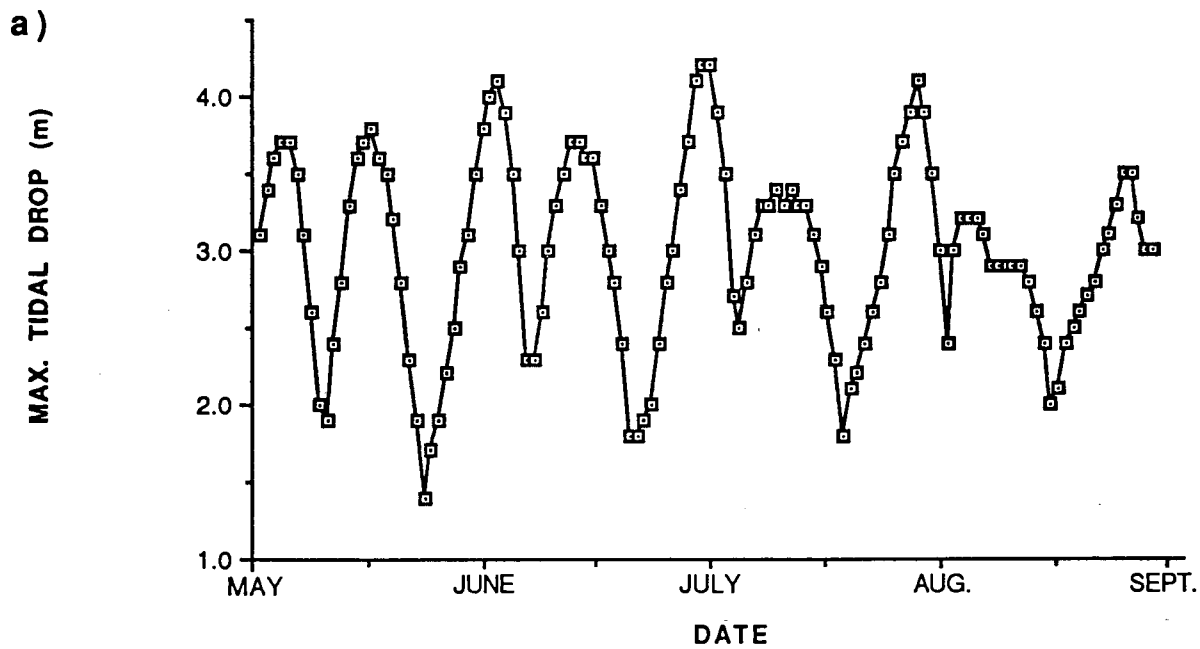


Fig. 5.11- a) Maximum daily tidal drop at Pt Atkinson:
May-Sept. 1992
b) Squamish River estuary mean daily discharge:
May-Sept. 1992

<u>Date</u>	<u>Wavelength(m)</u>	<u>I</u>	<u>Q (m³/s)</u>	<u>Drop (m)</u>	<u>LTH (m)</u>
MAY 15	1.57	0.96	270	3.5	0.7
JUNE 11	3.33	1.03	465	3.5	1.0
JUNE 27	6.36	1.20	674	3.4	0.8
JULY 13	3.50	1.06	441	3.3	0.7
JULY 28	3.50	0.74	417	2.9	0.3
AUG. 10	2.89	1.15	285	2.9	1.0
AUG. 26	3.46	0.96	327	3.4	0.6

Table 5.9- Analysis of seasonal-scale lag in bedform wavelength

DATE & TIME	LIH(m)	I	Q(m ³ /s)	DROPE(m)	— MEAN HEIGHT (m)					MEAN WAVELENGTH (m)				
					1	2	3	4	5	1	2	3	4	5
JULY 12 1256	0.7	1.27	449	3.4	0.52	0.51	0.62	0.51	0.78	8.84	3.79	8.38	10.99	10.39
JULY 17 1533	1.2	1.26	449	2.6	0.35	0.43	0.45	0.42	0.55	6.73	4.71	7.89	10.66	7.89

Table 5.10- Analysis of bedform lag induced by fortnightly-scale lags

fouled and not digitized), h and w were greater on the rising limb of the Spring-neap cycle than the falling limb for 90% of the data.

The second method of investigation was to differentiate the h and w data from every reach based on whether the date it was taken from was on the rising limb of a Spring-neap cycle or the falling limb, and then plot the data against LTH. Figure 5.10c,d indicate that indeed a hysteresis-type relation exists between the rising and falling limbs. In reaches 2,3,7 and 4(weakly), the bedform parameters appear to be larger at any given LTH on the rising limb of the Spring-neap cycle than on the falling limb. This becomes more apparent near the Spring tides. An ANOVA based on regressions through the data of falling and rising limbs found that in each of reaches, the relations were not significant at $\alpha=0.05$. This is due to the variance in the relations which are likely attributable to differences in discharge. Although these results were not statistically significant, both methods produce consistent results.

In order to investigate the lag on a diurnal scale, data from reaches 2 and 3 were utilized since they exhibit bedform parameters that are best explained by the variation in the independent variables used. Those days over the research period with a minimum of three transects run between $T=0.65$ and 1.45 were studied in order to quantitatively approximate the degree of lag of h and w after LLT. Table 5.11 indicates the sample times, times of peak h and w , and the Q and D values for that period. In general, peak T_h and w occur at $T=1.15-1.25$. However, on days with $D < 2.0\text{m}$, the peak values seem to occur closer to $T=1.0$. This observation is more distinct in the reach 3 data. In fact, reach 3 generally shows a better correlation between times of peak h and w than does reach 2. However, for both reaches, there are not distinguishable trends of Q or D between days when the correlation does or does not occur. For both reaches, the tendency for bedform height to peak with the

DATE	DROP (m)	Q (m ³ /s)	SAMPLE T	REACH 2		REACH 3	
				T @ PEAK H	T @ PEAK W	T @ PEAK H	T @ PEAK W
JUNE 20	1.8	540	0.78, 1.07, 1.41	1.07	1.40	1.07	1.07
JUNE 21	1.4	625	0.76, 1.00, 1.18	1.18	1.00	1.00	1.00
JUNE 22	2	730	0.96, 1.18, 1.37	1.37	1.37	1.18	1.18
JUNE 27	3.4	670	0.74, 0.89, 1.17, 1.38	1.38	1.54	1.17	1.38
JUNE 30	4.2	660	0.71, 1.19, 1.33	1.19	1.19	1.19	1.19
JULY 17	2.6	450	0.82, 1.26, 1.41	1.26	1.26	1.26	1.26
JULY 29	4.1	425	0.66, 0.97, 1.34	1.34	1.34	1.34	1.34
AUG 7	3.1	550	0.93, 1.05, 1.07	1.05	1.07	1.05	1.07
AUG 10	2.9	290	0.68, 0.94, 1.11, 1.26	1.11	0.68	1.11	1.11
				BEACH2	BEACH3		
T@PEAK W=T@PEAK H				44.4%	77.7%		
T@PEAK W>T@PEAK H				33.3%	22.2%		
IST@PEAK H THE FIRST RUN AFTER T=1.0 ?				66.6%	100.0%		
IST@PEAK W THE FIRST RUN AFTER T=1.0 ?				44.4%	77.7%		

Table 5.11- Analysis of bedform lag induced by diurnal-scale lags

first sample time after low tide is better than that for w . While these findings are far from indisputable, the results obtained are as would be expected from physical reasoning.

5.3- DISCUSSION

5.3.1- Multiple regression models

The apparent bed scour at discharges in excess of $650 \text{ m}^3/\text{s}$ will affect not only the models for predicting d , h and w , but also the models for slope, current speed, stage and other rating-curve relations (Leopold and Maddock, 1953; Dinehart, 1992). Other data from natural environments on the effects of scour on bedforms is extremely limited.

Znamenskaya (1963) postulated a relation between the ratio of mean velocity to scouring velocity and the relative roughness exhibited by the bedforms. As well, Wjibenga and Klaassen (1983) noted that data of Nasner (1978) showed a decrease in bedform height as discharge increased. It was not noted, however, if bed scour was occurring or if the result was attributable to tidal effects. Allen (1983) indicated that Nasner's (1974) data showed an *eight* month lag of bedform-height to changes in discharge. The hysteresis could also be a result of bed scour once Q exceeded some critical level (it is a freshet-dominated system). Then, with time, the bed recovered and returned to an equilibrium sediment-transport regime.

The relative importance of the independent variables in the mean water-depth models indicate that the reaches can be broken into 'zones' related to proximity to the mouth. The ebb-tide models for reaches 1, 3 and 6 are dominated by T and Q , reaches 2 and 7 have D explaining the most variation in depth followed by T and Q , and reaches 4 and 5 are dominated by D . The flood-tide models for each reach were quite similar, with T having the highest beta coefficient for each reach, and Q also important. The beta coefficient for D increases in the reaches downstream. This degree of spatial variability is not unexpected

since similar results were found in Chapter 4 for current speed. This degree of variation has also been reported in other estuarine studies (e.g. Boersma and Terwindt, 1981; Terwindt and Brouwer, 1986).

The transformation did not fully remove the residual heteroscedasticity for the h models from reaches 4 and 5, and there was still lag in w near HHT for reaches 2 and 3. However, the results are useful and correlate well with findings in previous studies. The h models for reaches 2, 3 and 7 have D as the independent variable explaining the most variation in h . Apparently, in these shallow reaches, the bedform height responds relatively quickly to the D . The model fit of these three reaches is better than those for reaches 1 and 4-6. Many previous studies of bedforms have successfully used the hydraulic conditions on the dominant tide to describe the bedform parameters throughout the tidal cycle (e.g. Knight, 1977; Terwindt and Brouwer, 1986). For reaches 1,4-6, the bed is slower to respond, therefore the average change in tidal height over the diurnal cycle (LTH) is the best explanatory variable.

Bedform wavelength has been found to respond more slowly to flow instability than bedform height (e.g. Gabel, 1993), and my results confirm this. LTH is the most significant explanatory variable in all reaches except #3. Perhaps this is related to reach 3 being away from the thalweg (unlike the other reaches). Unlike bedform height, the wavelength models do not fit much better in the shallow reaches, and the fit is poorer for w compared to h . It is postulated that this is related to lag effects which may continue over several tidal cycles.

From the outliers of the models predicting w and h (Table 5.7), there were secondary bedforms present on the larger features for just over 25% of the outliers (Appendix 2.4), but these are almost exclusively limited to $T < 0.4$ and > 1.5 . There also seem to be specific

days that many reaches had bedforms not described well by the models. In fact, almost every outlier occurred at times in the Spring-neap tidal cycle when the maximum daily tidal drop was near a minima or a maxima (Fig.5.11). For w , the dates of outliers at a minima were June 19-20, July 17-18, and July 31. The dates of maxima were May 14, June 13 and June 30. Similarly for h , the dates of the outliers at a minima were July 17, August 1 and 8, and the maxima were at June 10, 13 and 30. Although it has been suggested that the presence of more than one order of bedforms is linked to flow instability (e.g. Knight, 1977; Allen, 1983), these opinions are not unanimous (Jackson, 1976).

Tests of reliability of the models for predicting d and h were quite successful for reaches 2-5 and 7 (shrinkage <0.1), but to a lesser extent for reaches 1 and 6. The models for predicting w were generally more unstable, once again, especially for reaches 1 and 6. The plots of Y vs. predicted Y for h and w found that the models typically underpredicted the actual values. For h , this was attributable to the apparent non-linear trend which was not noted in the residuals.

Any previous studies similar to this one are either of limited duration (in terms of tidal cycles) or the interval between measurements is too long compared to dune activity. As noted by Davis and Flemming (1991), studies of bedform-morphology over numerous diurnal and fortnightly cycles are quite rare. Even remotely comparable studies have only been performed in strictly fluvial or tidal environments, so there are not standards to directly compare the results and fit of the models determined. Dalrymple et al. (1978) related the wavelength and height of bedforms, producing correlation coefficients up to 0.627. However, attempts to relate this same data to independent variables produced R^2 values <0.3 (Knight, 1977).

Of the more exotic combinations of 'independent' variables attempted, the $Q \cdot D$ product and the Froude number had the best correlations with the bedform parameters, especially for the shallow reaches. Kostaschuk et al. (1990) concluded that $Q \cdot D$ was a poor measure of stream power due to lag effects of the Spring-neap tidal cycle. This seems a valid explanation for the poor fit of the deeper reaches. Researchers have found that RRS is an inverse function of Froude number (Allen, 1984) and that RR has a direct linear relationship with the Froude number (Robert and Richards, 1988). Although the analysis could typically only be performed for a few reaches, the findings seem to indicate future study may be worthwhile.

5.3.2- Variability of results

From the comparison of the data obtained from reach 1 versus 6 and 2 versus 7, the tendency for the downstream-moving transect to produce a lower mean depth suggests that the more-rapid boat speed moving downstream results in a poorer sonar resolution near the bed. Comparisons involving h and w suggest that the differences are not statistically significant (at the 95% confidence level), and although the plots seem to indicate subtle trends, the predictive models are usually quite similar. The effects of the vegetation on h , w and d were not conclusive, but suggest that the disturbance to the mean bedform parameters over the reach length is insignificant.

It is likely that much of the unexplained variance in the dependent variables of the models presented can be attributed to wind and lag effects (Boersma and Terwindt, 1981; Allen, 1986). The effects of wind on the slope of the water surface were postulated in Chapter 4, and a key point is that the dominant winds have maximum speeds in the afternoon. They create waves with heights nearing 1m in reaches 4 and 5, but the sharp bend in the estuary just upstream acts as a wind barrier. Thus, wave heights rarely exceeded 0.5m for reaches

2, 3 and 7 and 0.2m for 1 and 6. As the Neap tides approach in the fortnightly cycle, LLT tends to occur in late afternoon, and the effect on the bedforms in the shallow water will be significant (in fact, the tendency for the maxima in σ_d to occur at mid-depths may be related to the depth at low tide during Neap tides, when the lags will be large). Much care was taken not to include wave-fouled data in the analysis, even when only wind ripples were noted on the surface. However, there were occasions when short-lived storms may have produced waves in the estuary before we arrived in the morning, thus their presence and influence on the bed would have been unrecognized. These storms often produced wave heights exceeding 1m.

The lag of bedform response in the estuary was identified, and a more quantitative analysis was attempted. A study of the lag of bedform h and w behind seasonal changes in discharge (ie. freshet) requires minimal tidal influence and relatively steady discharge over shorter temporal scales. Neither of these conditions are met in the field site. Although the results showed that w followed discharge when the tidal forcings were held reasonably constant, the result may simply be fortuitous. Previous results indicate that the degree of lag decreases with decreasing river and bedform size (Allen, 1983), with a lag perhaps on the order of days for bedforms comparable in size to the ones in the field site (Jackson, 1976).

The investigation of lag over the fortnightly cycle was conducted in two ways, producing consistent results. It was presumed that the bedforms would show maximum values a few cycles after high Spring tide, producing larger mean values for the falling limb.

Unexpectedly, it was found that bedform parameters were larger on the rising limb of the Spring-neap cycle (ie. as the tidal drop from HHT to LLT increased). While it is possible that the actual maximum values indeed occurred on the falling limb, but the bedforms then

diminished quickly as Neap tides approached, this hypothesis could not be examined due to variations in discharge and gaps in the data.

Terwindt and Brouwer (1986), noted that several researchers have concluded that h 'increases up to Spring tide and decreases towards Neap tide' (e.g. Allen and Friend (1976b), Boersma and Terwindt (1981)). The references (as well as Davis and Flemming, 1991) simply state that h will be greater at Spring tides than at Neap tides, but do not state if maximum bedform parameters occur at peak Spring tide or a few cycles later. However, Terwindt and Brouwer (1986) indeed found that for three-dimensional bedforms, maximum h and w occurs at 1-3 tides after max. Spring tide. Allen (1973a) further notes that the degree of lag in the Gironde estuary depends on the particular Spring-neap cycle chosen, which is cyclic on a period of 6 months (Allen, 1985). This issue remains unresolved.

On a diurnal scale, the lag in h and w after LLT was noted to increase with increasing D , and it was (weakly) demonstrated that peak bedform height tends to occur sooner after LLT than peak wavelength. Researchers have noted this latter finding (e.g. Allen, 1973a, 1983; Knight, 1977), but there are relatively few data sets that have been collected. Some workers have ignored bedform-lag effects (e.g. Green, 1975), but typically, lags are simply acknowledged without serious consideration. This is no doubt related to the difficulties in obtaining reliable data.

The complex feedback relations between components of the flow, bedforms and macroturbulence have been suggested in Chapters 1-5. Chapter 6 will quantitatively examine the relation of bedform parameters (such as periodicity and intensity) to hydraulic and bedform variables.

CHAPTER 6- ANALYSIS OF BOIL PARAMETERS

6.1- INTRODUCTION

Quantitative analyses of boil parameters have rarely been attempted, and this scarcity may be related to difficulties in obtaining reliable data. Boil 'strength' might be best quantified by the elevation upon eruption at the surface, but the influence on the surrounding flow may be more appropriately described by the boil size or sediment content. In studies to date, boil elevation has only been visually estimated, and no researchers have followed Matthes' (1947) suggestion to estimate boil elevation by the rate of subsequent expansion.

Boil size upon eruption has been related to the mean water-depth (Jackson, 1977), or the Strouhal number (Korchokha, 1968). Boils may also be larger, with longer durations and inter-event periods during decelerating current speeds as opposed to accelerating speeds (Anwar, 1981). Such complexities may be partially responsible for limiting most quantitative analyses of boils to inspection of frequency distributions or mean periods between successive boils.

There have been several studies of the application of the Strouhal Law to a mean burst period (quantified as deviations of $u'w'$) in tidal, estuarine and fluvial environments (e.g. Gordon 1975a; Anwar, 1983; Lapointe, 1989). Lapointe (1989) implies that the findings of these studies are debatable due to subjective burst-intensity thresholds, and interactions with bedforms or other macroturbulent phenomena. Laboratory studies have suggested that burst periods are related to the passage of larger-scale features which may be governed by a similar frequency law (Nychas et al., 1973; Praturi and Brodkey, 1978; Bridge and Best, 1988). Many researchers (e.g. Lapointe, 1989; Williams et al., 1989)

question the presumed relations between bursting and boils based on the similarity of their frequency characteristics (Jackson, 1976).

There are few studies of the temporal characteristics of macroturbulent phenomena in rivers. Korchokha (1968) and Jackson (1976, 1977) noted that the mean period between the appearance of boils was well described by the Strouhal Law, but Jackson used the dune wavelength for the length scale while Korchokha used height. Jackson (1976, 1977) concluded that boils were the surficial expression of fluid 'bursting' which had been ascertained in laboratory flumes to follow a similar frequency law. Levi (1984) suggested that many periodic motions of fluids follow the Strouhal Law, and doubted Jackson's (1976, 1977) assertion that bursting and river boils must be different aspects of the same phenomenon. Kostaschuk and Church (1993) also question Jackson's finding, claiming that the range of values he used in the frequency law was not precise enough to be a useful discriminator between candidate length scales. They also emphasize the importance of choosing appropriate length and speed scales, but the disparities they note between some predicted and measured boil periods may be related to the inability to attribute boils to a specific production site. In fact, Rood and Hickin (1989) questioned the applicability of the scaling equation to a single production site as opposed to a broad water-surface area. There may be additional complexities associated with multiple boil-production mechanisms.

Investigation of the temporal characteristics of boils based on data obtained by current meters and sonar has indicated that there may be several boil-generation mechanisms. Kostaschuk and Church (1993) claim that the period determined by Strouhal's Law depends on appropriate choice of length and velocity scales for the particular generating mechanism. A similar, but more basic finding was noted in a flume study by Itakura and Kishi (1980). Strouhal's Law may serve to describe mean boil-periodicities adequately,

but it seems only a partial explanation when boil periods are noted to fluctuate on longer periods.

Kostaschuk and Church (1993) present a time-series plot of boil periods which displays repeated cyclicity on scales of several minutes. Although a simultaneous plot of current-speed is not included, other data presented suggest that the current speed could fluctuate on similar scales. There must be some minimal duration over which the boil period and current speed must be averaged in order for Strouhal's Law to apply, presumably over several such cycles of current-speed and boil-period. If so, there must be some mechanism which is producing this variability on similar scales in both time series. Levi (1983b) claims that the boil periodicity is governed by Strouhal's Law due to excitation by an outer-flow perturbation with wavelength = $2\pi d$.

In order to obtain a continuous record of the boil activity in conjunction with current-speed in Squamish River estuary, the surficial expression of macroturbulence was videotaped for later digitization. Video footage has been used previously to study macroturbulence (Znamenskaya, 1963) or other phenomena in rivers (summary in Drake et al., 1988). The boil period was taken as representative of the macroturbulence intensity, and time series examination highlights any correlation with the current speed measured at 0.7d.

During initial observations at the field site, not only were there notable fluctuations in current-speed, but there was also a distinct intermittency in macroturbulent activity. Periodic changes in flow character associated with the presence or absence of standing waves were also observed in Mamquam River just upstream of the confluence with Squamish River.

Observations made on Mamquam River several hundred metres upstream of the Squamish River confluence suggest relations between macroturbulence and flow unsteadiness on scales of several minutes. Standing waves would intermittently appear on the outside bank, and intense boil activity was generated in the wave troughs. These boils were transported in the troughs towards the center of the channel, typically entraining fine sediment. After several minutes, the standing waves would dissipate, and subdued macroturbulence would fill the entire channel. Again, after several more minutes, the standing waves would reappear, beginning at the downstream end of the reach, and gradually forming further upstream. These cycles repeated many times during the period of observation. Similar observations were made on subsequent days, but the persistence, wavelength and height of the standing waves could be quite variable.

A similar observation by Iseya and Ikeda (1983) was related to the unsteady nature of bedload transport, which has been quantitatively (though not convincingly) related to fluctuations in current speed by Korchokha (1968). The influence of bedforms and secondary flow patterns (Jackson, 1977) upon boil generation has also been pondered.

Boil generation has been linked to dunes by several researchers (Lane, 1944; Matthes, 1947; Coleman, 1969). Boils are typically concluded to originate in the lee (Znamenskaya, 1963; Korchokha, 1968; Rood and Hickin, 1989), but may be ramped off the stoss side (Kostaschuk and Church, 1993). Matthes (1947) adopted the term 'kolk' to describe the subsurface turbulent feature associated with boils. Dyer (1986) believes that kolks result from intermittent flow separation in the lee of dunes and that a minimum steepness(S) of 0.07 is required for flow separation. However, the finding is based on flume studies, and Dyer notes that separation may occur at lower S if the bedforms are sharp-crested. Kostaschuk et al. (1991) found that kolk generation occurred in the absence of flow separation and was consistently associated with only a few bedforms ($S=$

0.02-0.05). Other researchers have found that bedforms are not even required for boil generation (Jackson, 1976; Allen, 1985). This may be related to Kelvin-Helmholtz mechanisms (Kostaschuk and Church, 1993). This proposal may satisfy Lapointe's (1989) skepticism that two-dimensional bedforms can produce 'outer-flow burst structures' that have a scale considerably less than channel width. Studies in energetic systems such as Squamish River estuary may resolve this issue. Such analyses may also shed light upon the proposed relations between bedforms, macroturbulence and flow resistance.

Secondary upwellings within a boil structure (Rood and Hickin, 1989) and multiple boil morphologies (Korchokha, 1968) may also affect the scaling equations. Integration of boil-parameter data from a variety of sources may have introduced scatter in such scaling relations (e.g. Jackson, 1976). Elucidation of these relations may require a classification of boil structures. In Chapter 3, it was suggested that there are two types of boils in the estuary, but a closer inspection based on quantitative parameters may reveal production mechanisms.

Rood (1980) noted that the classification of macroturbulent structures attempted by Matthes (1947) was based purely on observable properties. It is evident that there is a lack of quantitative data with respect to boil strength, size, expansion rates and periodicity under a variety of hydraulic and bedform conditions. The variability of hydraulic and bedform parameters over short temporal and spatial scales in Squamish River estuary allows efficient study of boil properties. The boil presence, morphology, intensity and periodicity are related to a variety of hydraulic and bedform parameters, for both Type 1 (reaches 2,3 and 7) and Type 2 boils (reaches 1, 4-6).

6.2- ANALYSIS OF TYPE 1 BOILS

6.2.1- Relations between bedforms and Type 1 boil intensity

6.2.1.1- Graphical differentiation based on field observations

As noted in Chapter 5, direct examination of the relations between bedform h and w and depth (eliminating representation of independent variables), has been utilized by many researchers (e.g. Jackson, 1976; Knight, 1977). The parameter used to differentiate such plots will be the intensity of the macroturbulence observed at the water surface during the transect for each reach. Although the appearance of the features within a reach may be temporally intermittent, the intensity was generally quite spatially homogenous within the thalweg. For each reach, the boil-intensity differentiated plots of w vs. h , d vs. h and w vs. d are examined, and the quantitative limits of particular intensity levels noted.

From an examination of all 7 plots of w versus h , there appear to be two distinct populations with a separate at $h=0.5-0.6\text{m}$. A pattern noted in reaches 2,3 and 7 is for the w vs. h relation to display a high variance with $h<0.5-0.6\text{m}$, but then a tight linear pattern once height exceeds 0.6m . The sediment-laden boils (Intensity levels 1 and 2) are associated with the latter population. In reach 2, the sediment-laden boils are associated with the higher values of dune steepness within this latter population (Figs.6.1a,b and 6.2a).

Examination of the w versus d plots does not yield such a consistent separate. For reaches 2,3 and 7, it appears that sediment entrainment within the macroturbulent features may depend on the RRS. A separate at $\text{RRS}=0.8$ for reaches 2 and 7 is suggested, but most of the sediment-laden features occur in $d<3.25\text{m}$ (Fig.6.2b, 6.3a). The RRS dependence seems more strongly developed in reach 3, where the separate may

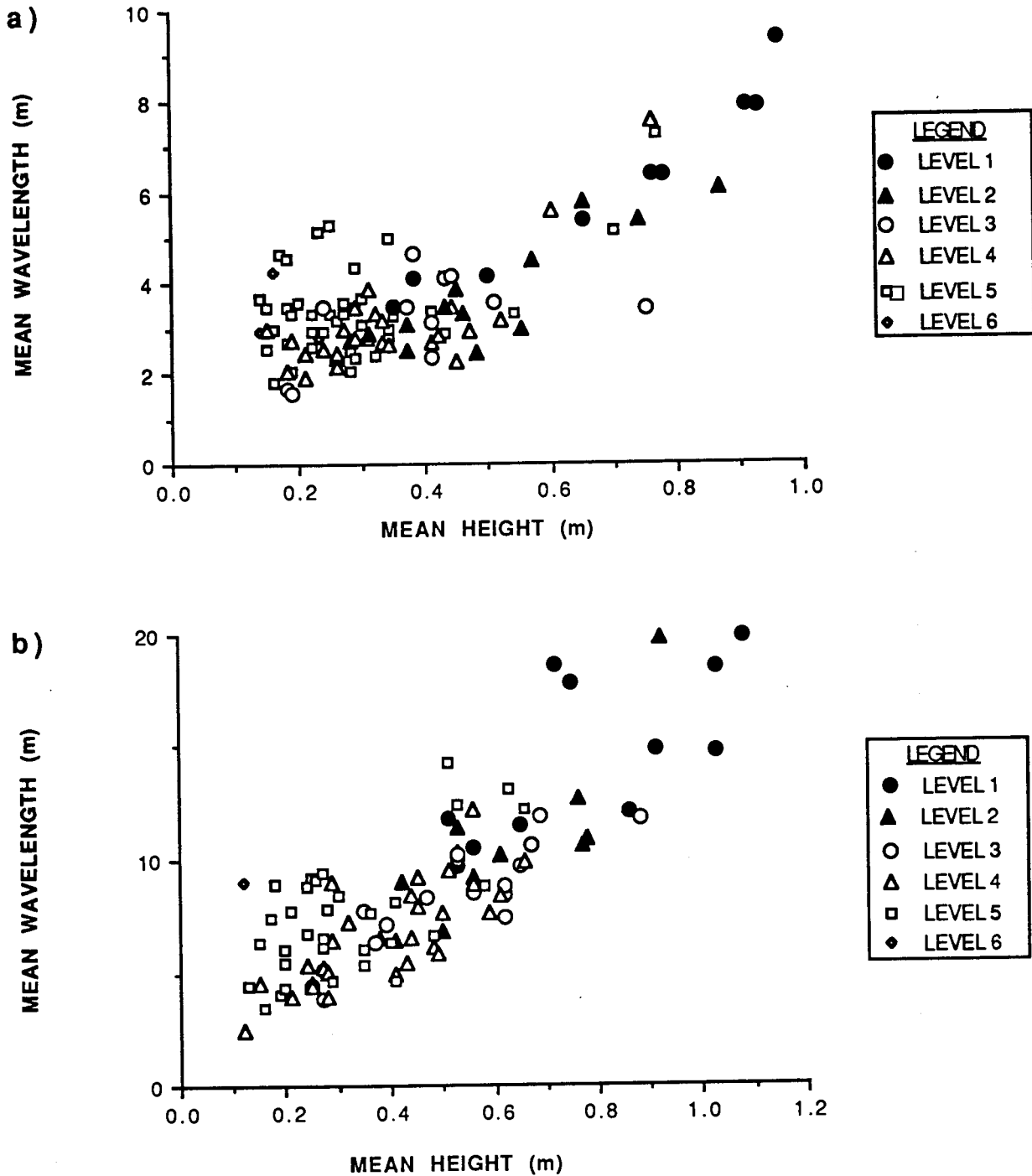


Fig. 6.1- Boil intensity as a function of mean bedform-wavelength and height:
 a) Reach 7
 b) Reach 3

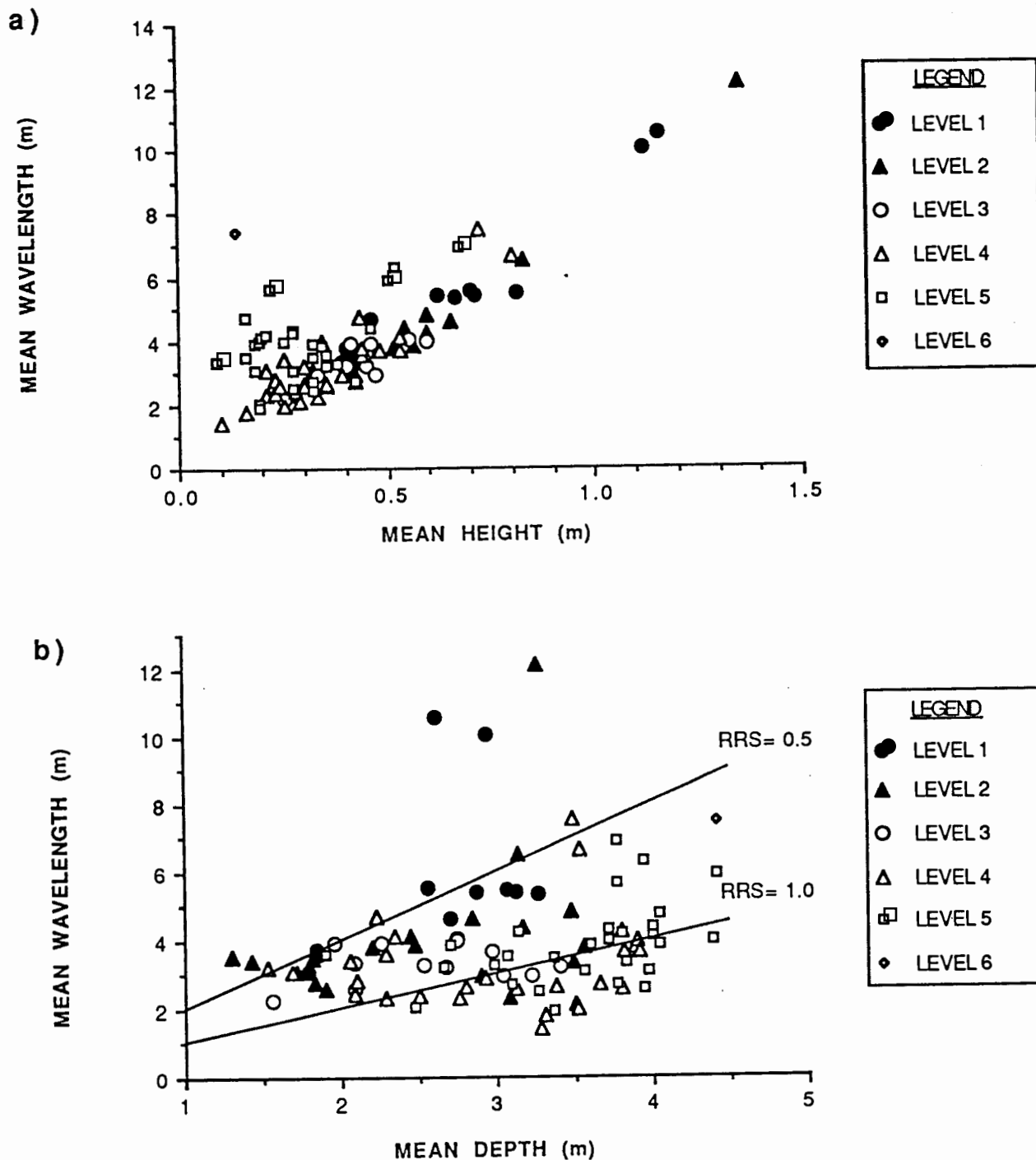


Fig. 6.2- Reach 2 boil intensity as a function of mean bedform-wavelength and:
 a) mean bedform-height
 b) mean water-depth

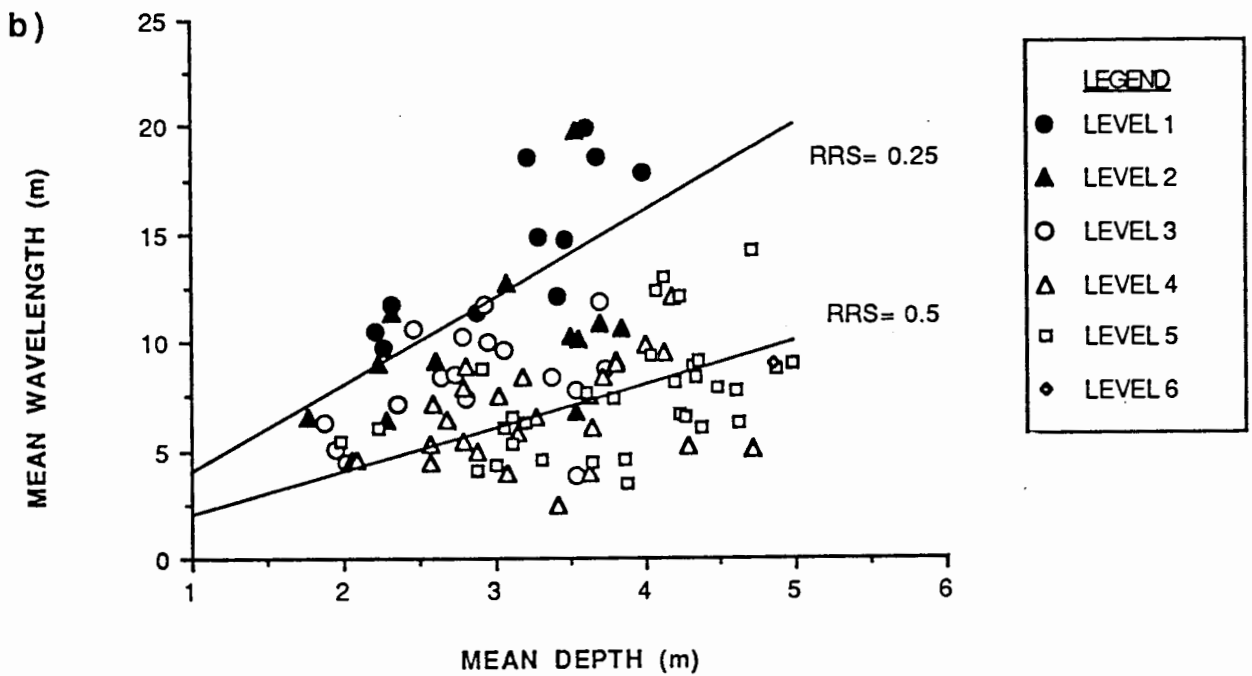
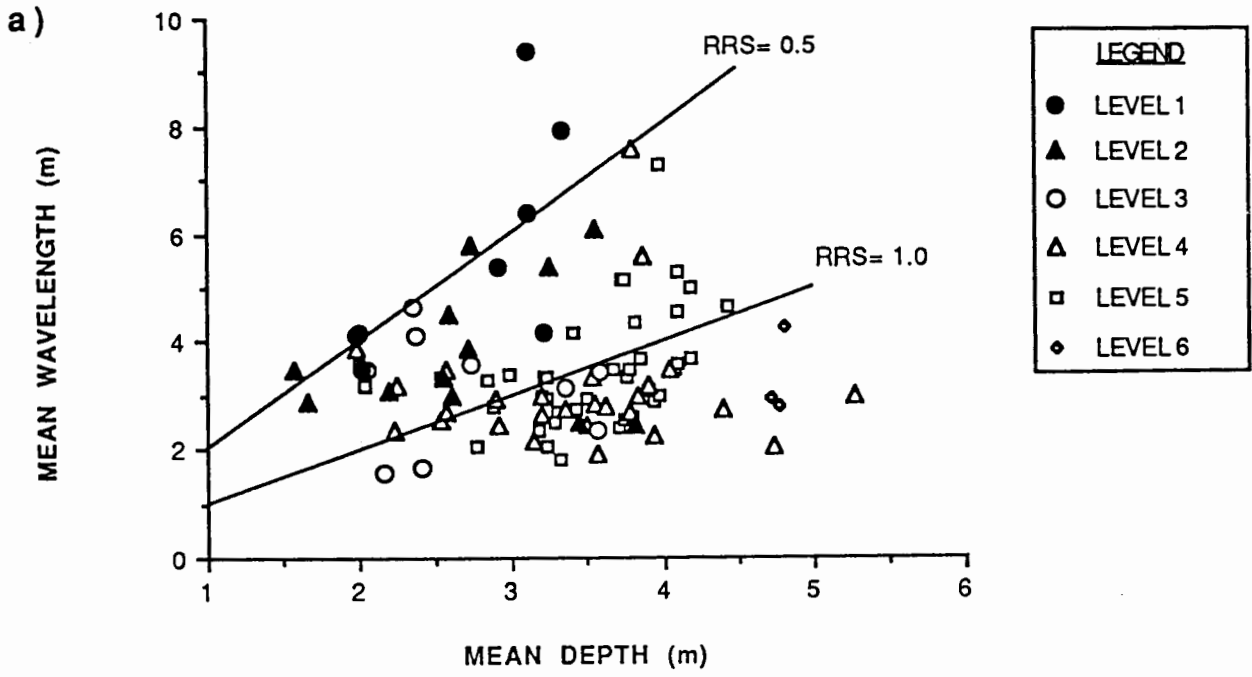


Fig. 6.3- Boil intensity as a function of mean bedform-wavelength and mean water-depth:
 a) Reach 7
 b) Reach 3

arguably fall between $RRS=0.25-0.35$ (Fig.6.3b). No RRS differentiation (or depth) with respect to intensity levels 3 and 4 was recognizable.

From the plots of d vs. h , reach 7 data indicate that sediment-laden features dominate when $RR>0.2$. Then as RR decreases, the features with intensity levels 1-4 concentrate with $d<3m$, and the proportion of lower intensities increases (Fig.6.4a). For reach 2, the dominance of intensity levels 1 and 2 with $RR>0.2$ is also noted. There may also be an increase of weaker macroturbulent features as the RR diminishes, but these reach 2 relations are not as distinct as with reach 7 (Fig.6.4b). Reach 3 displays a dominance of sediment-laden features with $RR>0.25$, and as RR decreases, the gradation into progressively weaker boil intensities is again evident (Fig.6.5). Note however, that as RR decreases, the intensity levels 1 and 2 are confined to depths $<2.5m$ and $>3.5m$. This gap is also visible in reach 2 and 7, albeit slightly weaker and between 2-3m depths.

6.2.1.2- Graphical differentiation based on sonar inspection

A second way to graphically differentiate the plots of w , h and d is based upon features noted on the graphic output of the bed profiles which appear to be columns of sediment rising from the bed (Fig.2.3). Whether these are analagous to the kolks described by Kostaschuk et al. (1991) and other researchers is debatable, but it was noted during the transects that these features corresponded to boils at the surface. This analysis is performed only for the Type 1 boils because the data of reaches 1 and 4-6 is not adequate.

This differentiation will not be performed for reach 6 since, inevitably, there was a disturbed band on the chart near the shallow upstream limit of the reach. It was concluded to be a high suspended-sediment concentration associated with disturbance by the propellor during the upstream transect since it was never noted moving upstream.

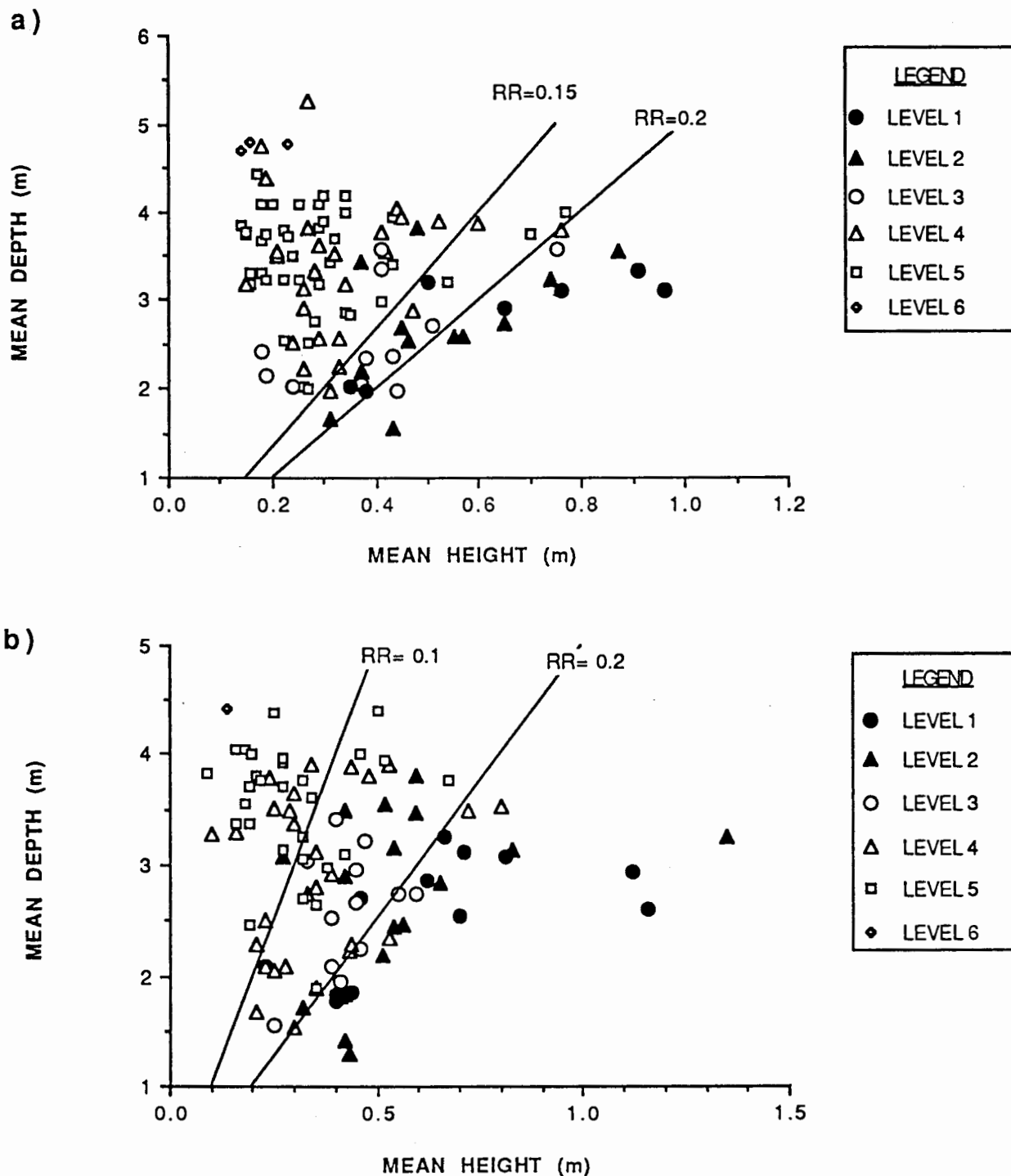


Fig. 6.4- Boil intensity as a function of mean water-depth and mean bedform-height:
 a) Reach 7
 b) Reach 2

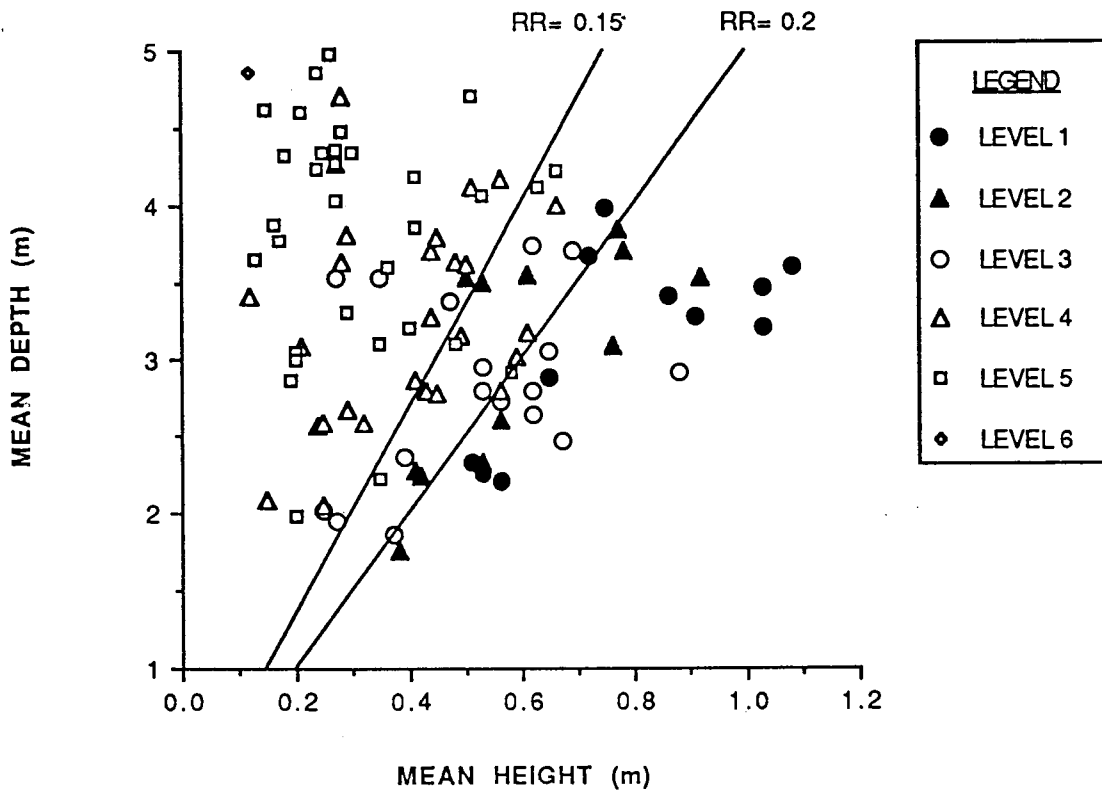


Fig. 6.5- Reach 3 boil intensity as a function of mean water-depth and mean bedform-height:

The differentiation is not performed for reach 1 either since the kolks were never noted there. For reaches 4 and 5, the features were only noted on less than 5 transects each, therefore the graphs are not discussed. However, for reaches 2,3 and 7, this technique produces results strikingly similar to those of section 6.2.1.1. The sediment-laden features in this section correspond to #1 and 2 in the notes column (Appendix 2.4).

For w vs. h , the vertical separative noted previously at $h=0.5-0.6\text{m}$ might be placed at 0.3m based on Fig.6.6. Also, once $h>0.5\text{m}$ at reach 2, the tendency for the kolks to be produced from bedforms with higher steepness is noted. For w vs d , the previously noted separative at $RRS=0.8$ is recognizable in reaches 2 and 7, and similarly for reach 3 at $RRS=0.25-0.35$ (Fig.6.7). Lastly, from d vs h , the concentration of kolks at $RR>0.175$ is recognizable in all three reaches (Fig.6.8).

This correspondance with results from section 6.2.1.1 is confirmed by utilizing a Spearman's Test ($\alpha=0.005$). The null hypothesis is no rank correlation between the visual recognition of kolks on the graphical output and observations of surface sediment-laden boils made during the transects. Based on critical values of Spearman's Rank Correlation Coefficient (Ebdon, 1988, p.219), the null hypothesis is rejected for all 5 reaches. However, if considering the adjustment for ties, the null hypothesis is accepted at $\alpha=0.005$ for reach 5.

6.2.2- Type 1 boil parameters

6.2.2.1- Boil Presence, Morphology and Intensity

Examination of the presence, morphology and intensity of the Type 1 boils is based on observations made during the transects of reaches 2, 3 and 7 digitized in Chapter 5. From plots of bedform-height and wavelength versus T , it is evident that boil presence is

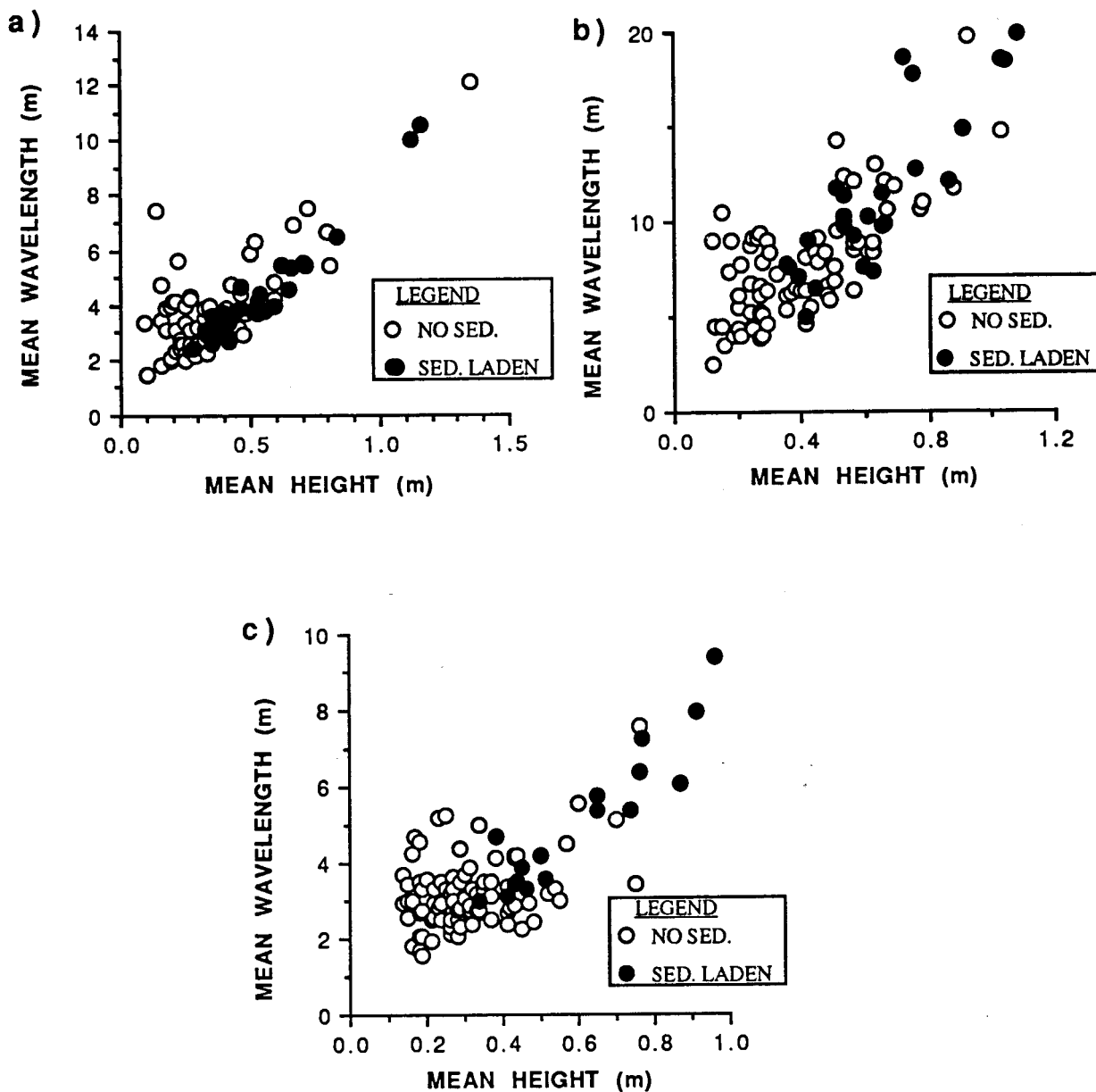


Fig. 6.6- Identification of sediment entrainment on sonar graphical-output as a function of mean bedform-wavelength and height:

- a) Reach 2
- b) Reach 3
- c) Reach 7

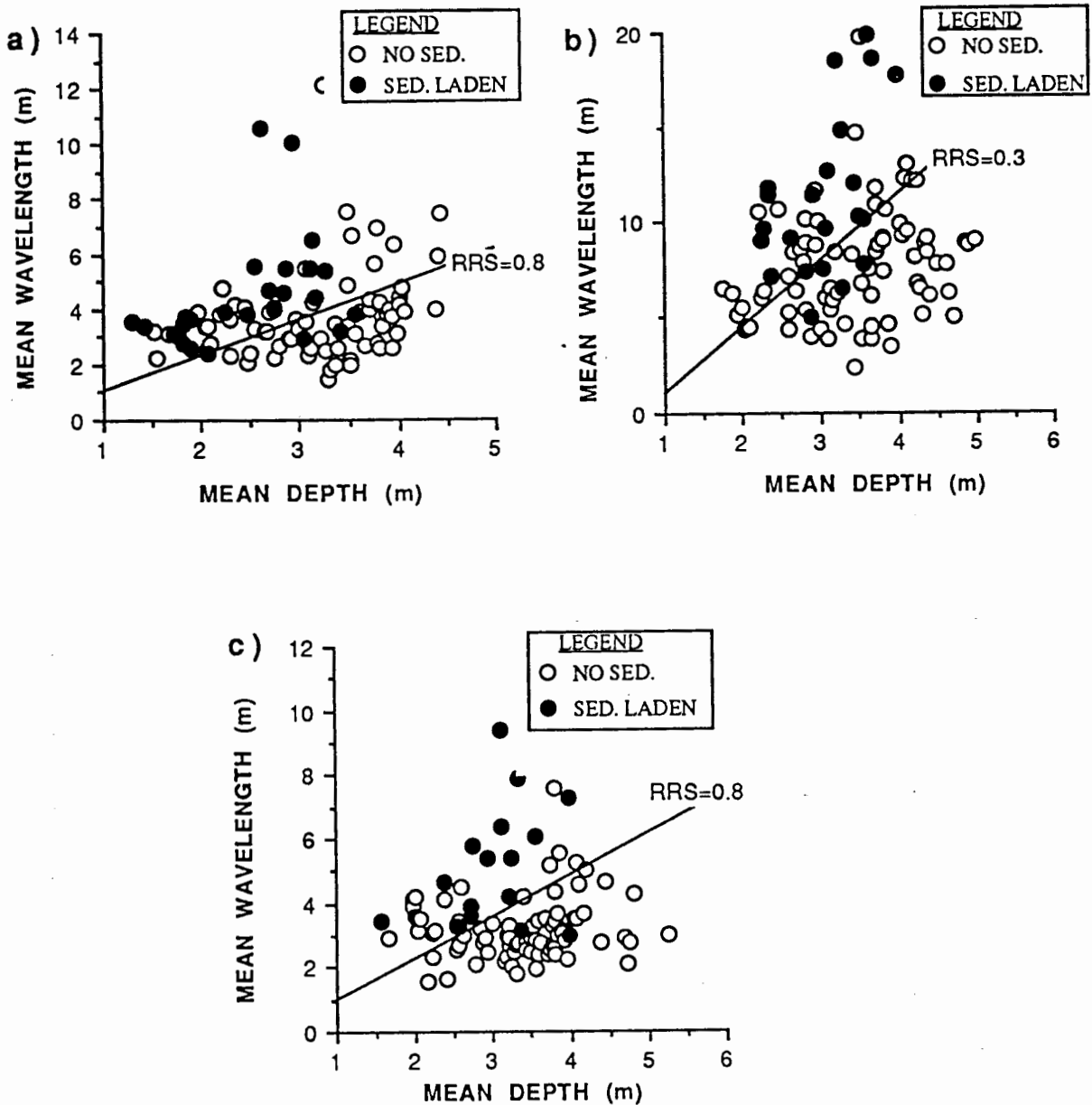


Fig. 6.7- Identification of sediment entrainment on sonar graphical-output as a function of mean bedform-wavelength and mean water-depth:

- a) Reach 2
- b) Reach 3
- c) Reach 7

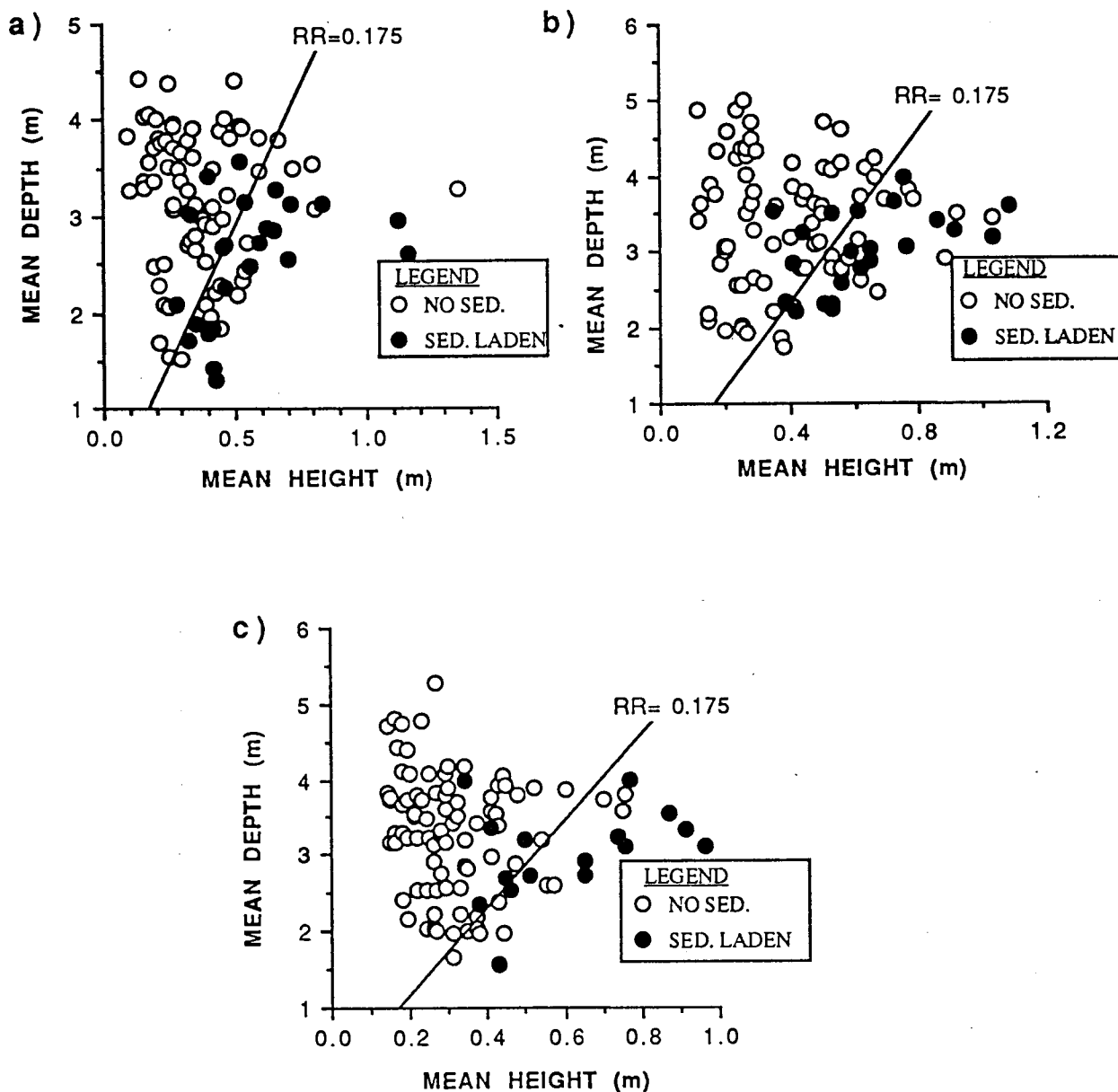


Fig. 6.8- Identification of sediment entrainment on sonar graphical output as a function of mean water-depth and mean bedform-height:

- a) Reach 2
- b) Reach 3
- c) Reach 7

related to tidal conditions. Although boils with intensity levels 4, 5 and 6 may be observed over the entire semi-diurnal tidal cycle, stronger boil activity is limited to short temporal ranges surrounding LLT.

In Fig.6.9a, boil activity of levels less than 4 are restricted to several hours surrounding LLT, with $T=0.5-1.5$. These data were collected throughout the Spring-neap cycle, thus boil activity of levels 4 and 5 occurring near LLT are associated with Neap tides, and the intensity levels less than 4 occur during Spring tides. Intensity levels less than 3 are only found with $T=0.7-1.4$. Similar results are displayed in all three reaches (e.g. Figs.6.9b, 6.9c).

The results of section 6.2.1 suggested that boil intensity in reaches 2, 3 and 7 was strongly related to bedform parameters and water depth. Bedform parameters are likely correlated with the current speed and/or water-surface slope within these reaches, but data to test this hypothesis were not collected. Although it can only be generally summarized that boil activity is strongest near LLT (especially during Spring tides), field observations suggested that the morphologies of Type 1 boils may occur under specific conditions.

Typically, there was a single dominant boil morphology and intensity noted over a surface area of tens of square metres at any particular time. Of the 300 digitized transect portions for reaches 2, 3 and 7, only a few displayed surficial macroturbulence patterns that were not dominated by the simple quasi-circular upwellings described in the Coleman/Jackson model (Appendix 2.4). Although the sample sizes for the cauliflower, roller and roller-horn morphologies are small, it is likely that graphical analyses would yield similar conclusions for all three reaches.

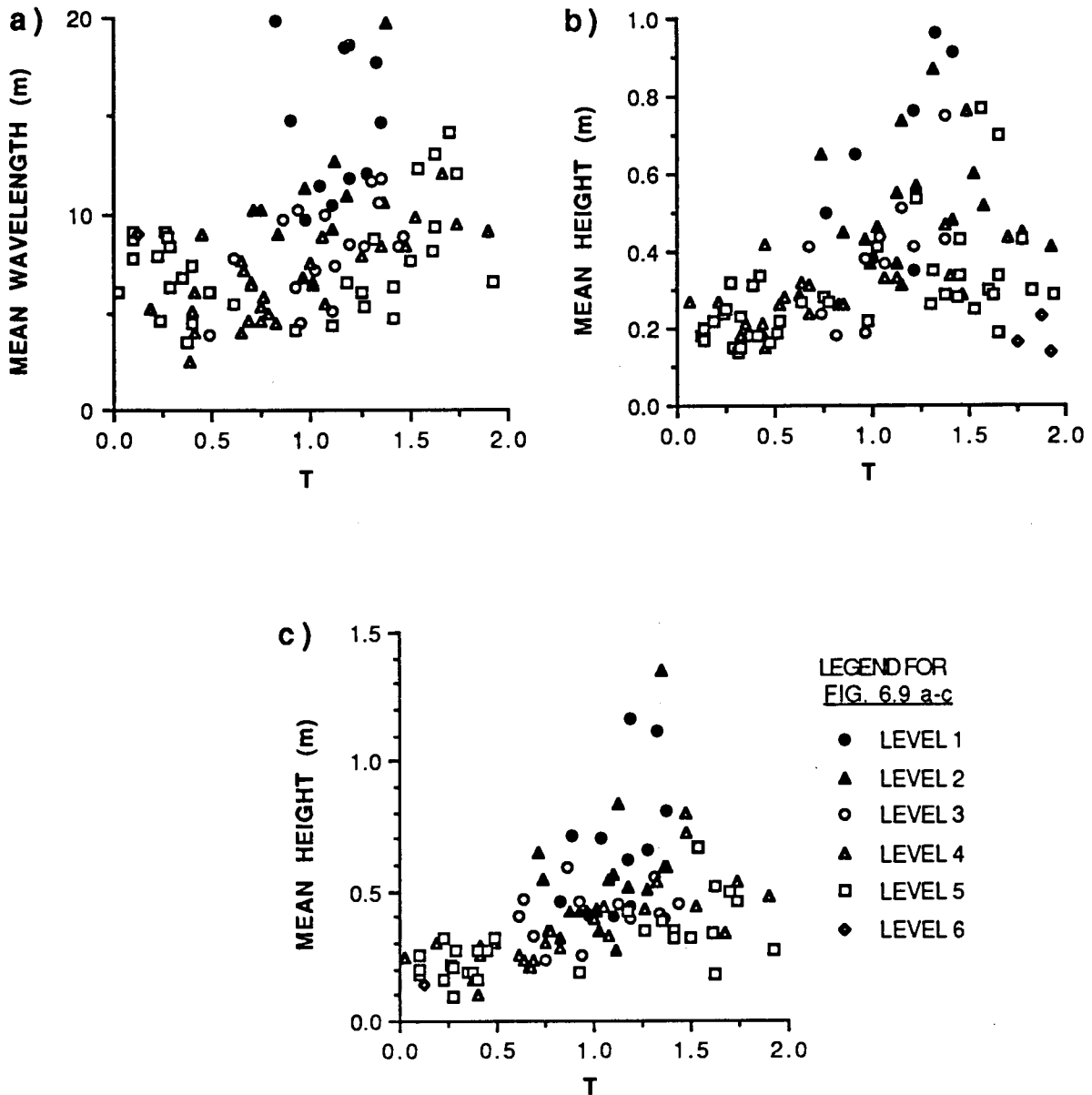


Fig. 6.9- Mean bedform-parameters vs. T differentiated by boil intensity:

- a) Reach 3 wavelength
- b) Reach 7 height
- c) Reach 2 height

From the plots of water depth versus bedform height differentiated by boil morphology, it is evident that some structures tend to occur only under very specific conditions. The Coleman/Jackson morphology is present over the full range of hydraulic and bedform conditions, but it dominates all three reaches as depth shallows and relative roughness increases (Figs.6.10a,b and 6.11a). The cauliflower shape only occurred when the mean depth was less than 2.5m and the relative roughness exceeded 0.17. There were very few times when the reaches were dominated by rollers that did not evolve into horns. When it was noted, the mean depth did not exceed 3.0m and the relative roughness was greater than 0.15. More frequently, the rollers that did evolve into horns dominated the reaches, but the conditions of their occurrence were more variable. Generally, the mean depth did not exceed 3.5m and the relative roughness was less than 0.10.

It was suspected that the tendency for rollers to evolve into horns may be related to scour holes formed as bedform steepness increases. However, this was not apparent for any of the reaches (e.g. Fig.6.11b). Examination of the data in Appendix 2.4 is not useful for confirmation of the hypothesis either. Fluctuations in current-speed may also influence boil morphology, although observations of boil morphology at a single site over extended durations could not reliably confirm or refute this notion.

To test whether boil presence and/or intensity was related to the intrusion and retreat of a body of saline water, water samples were collected at a variety of tidal heights and discharges. Utilizing a systotic pump, 500 ml samples were obtained within 1m of the river bed at current speed measurement station #6 (Fig.2.1) from July 26 to August 4, 1992 at HHT and LLT. Subsequent analysis utilizing a YSI Model 33 S-C-T meter indicated that all water samples had salinity values of 0 ppt.

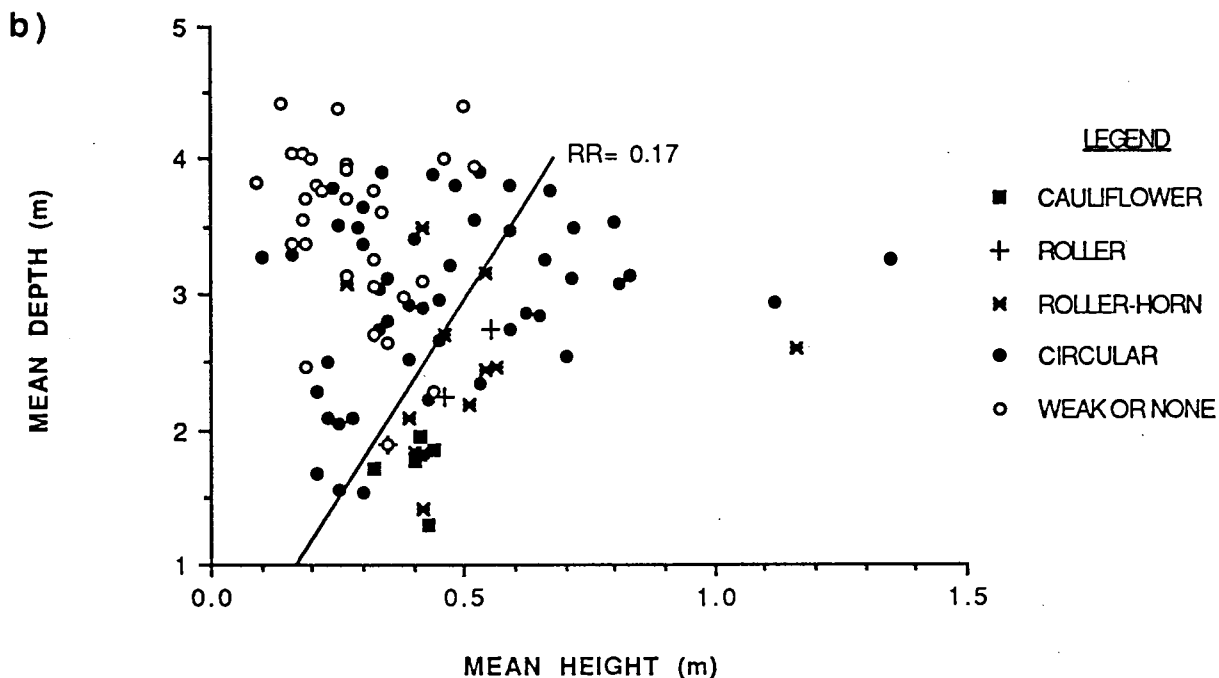
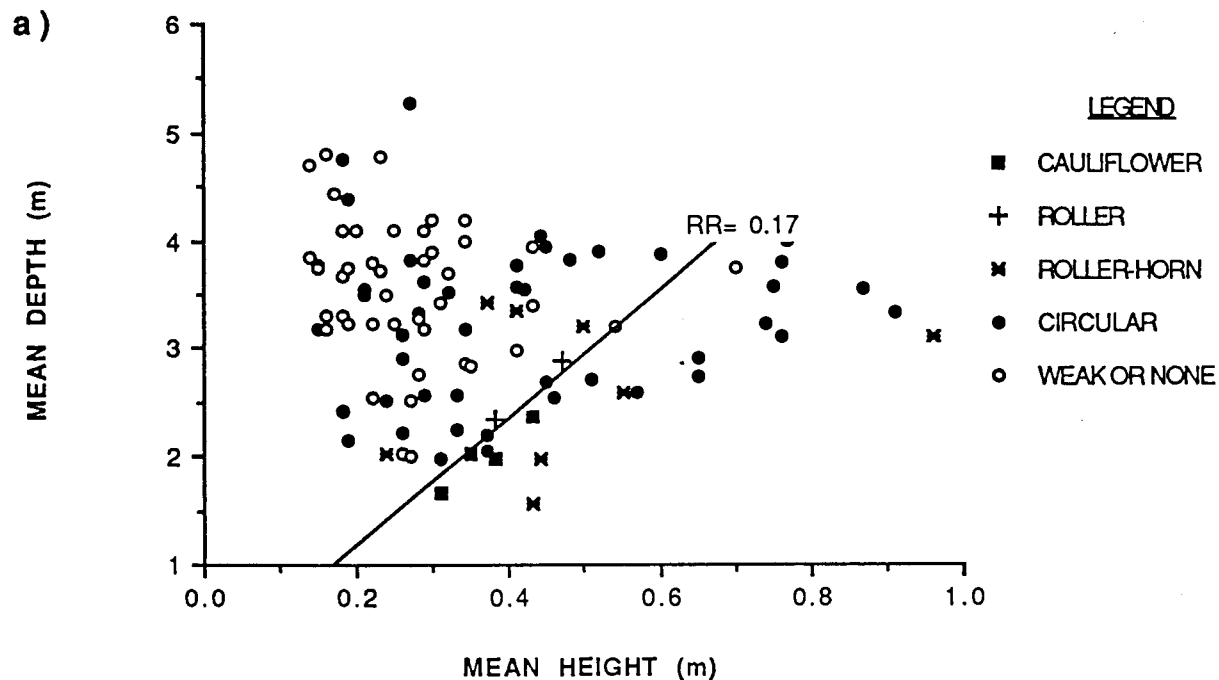
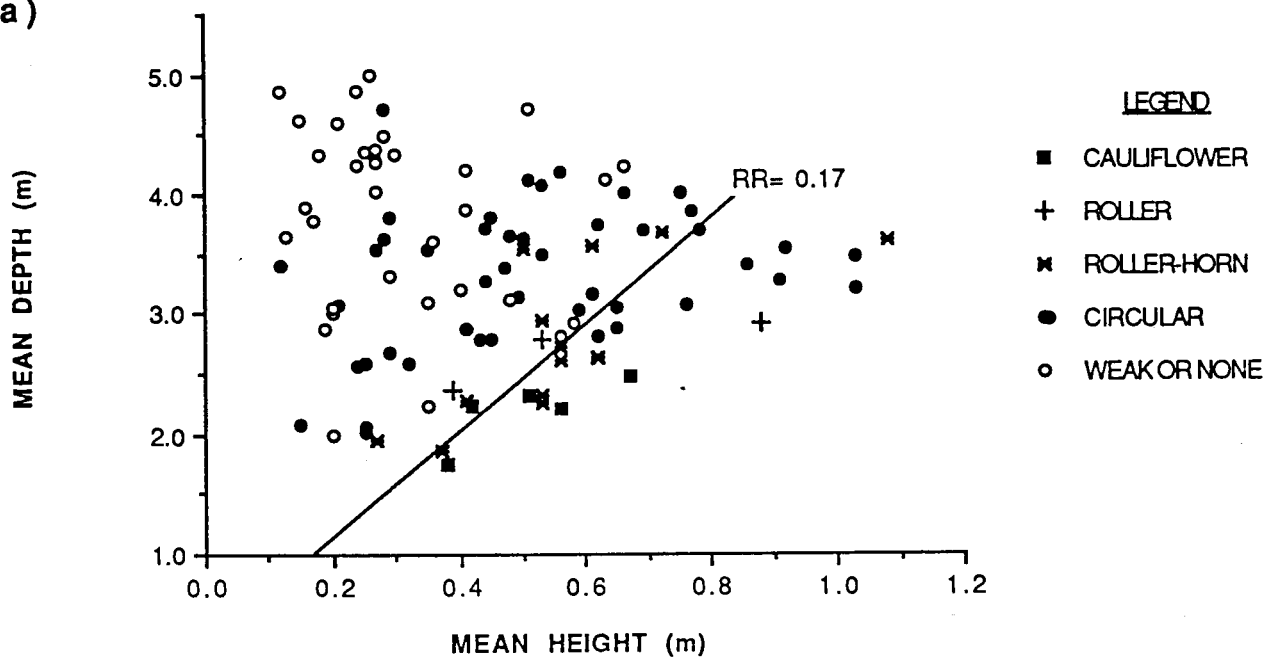


Fig. 6.10- Boil morphology as a function of mean water-depth and mean bedform-height:

a) Reach 2

b) Reach 7

a)



b)

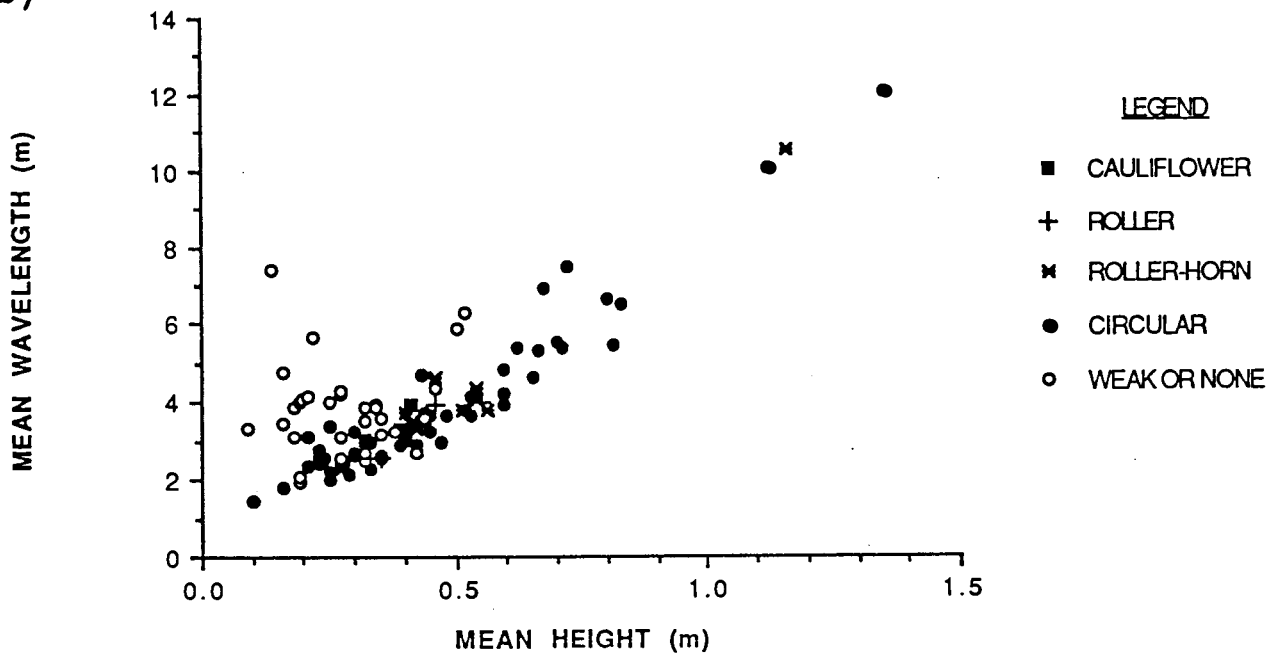


Fig. 6.11- Boil morphology as a function of mean bedform-height and mean depth or mean wavelength:

a) Reach 3

b) Reach 2

6.2.2.2- Mean boil-period

Initial observations in the lower estuary suggested that in the hours surrounding LLT when boil activity was strong, the macroturbulence was intermittent, and relatively periodic when present. Examples of the boil-period time series highlight the intermittent and periodic qualities (Fig.6.12a,b). The period between boils shed by a production site was similar to the period of nearby production sites, but this similarity often diminished as the separation increased. Current speed (and presumably bedform parameters) could be variable over small spatial distances (particularly in the transverse), so given some governing law as Strouhal's, variation in boil-period was not unexpected.

The collection of boil periodicity data in the lower estuary and reaches 2, 3 and 7 was sporadic for several reasons. There were a limited number of days in which the strong boils were present without any wind or wave disturbance and there was usually other data collection required elsewhere in the estuary. As well, these data were to be collected in the final month of the field season, but the boil activity diminished significantly due to lower tidal drops and discharge. Finally, there were numerous electrical difficulties with the current meter in July which ultimately forced the current-speed data collection to be abandoned in early August. In total, there were only 11 measures of mean boil periodicity which also had measures of depth, bedform-height and current-speed.

All boil-period time series were found to be positively skewed, and only one displayed bimodality (Table 6.1). Many of the frequency distributions appeared log-normal. To test this, the logarithms of the frequency distributions (differentiated by 1 second intervals) were obtained, and the chi-square test ($\alpha=0.01$ level) was used to examine the similarity between the observed distributions and normal distributions. The acceptance level utilized was noted by Hassan et al. (1991) to bias the test so that 'irregular data

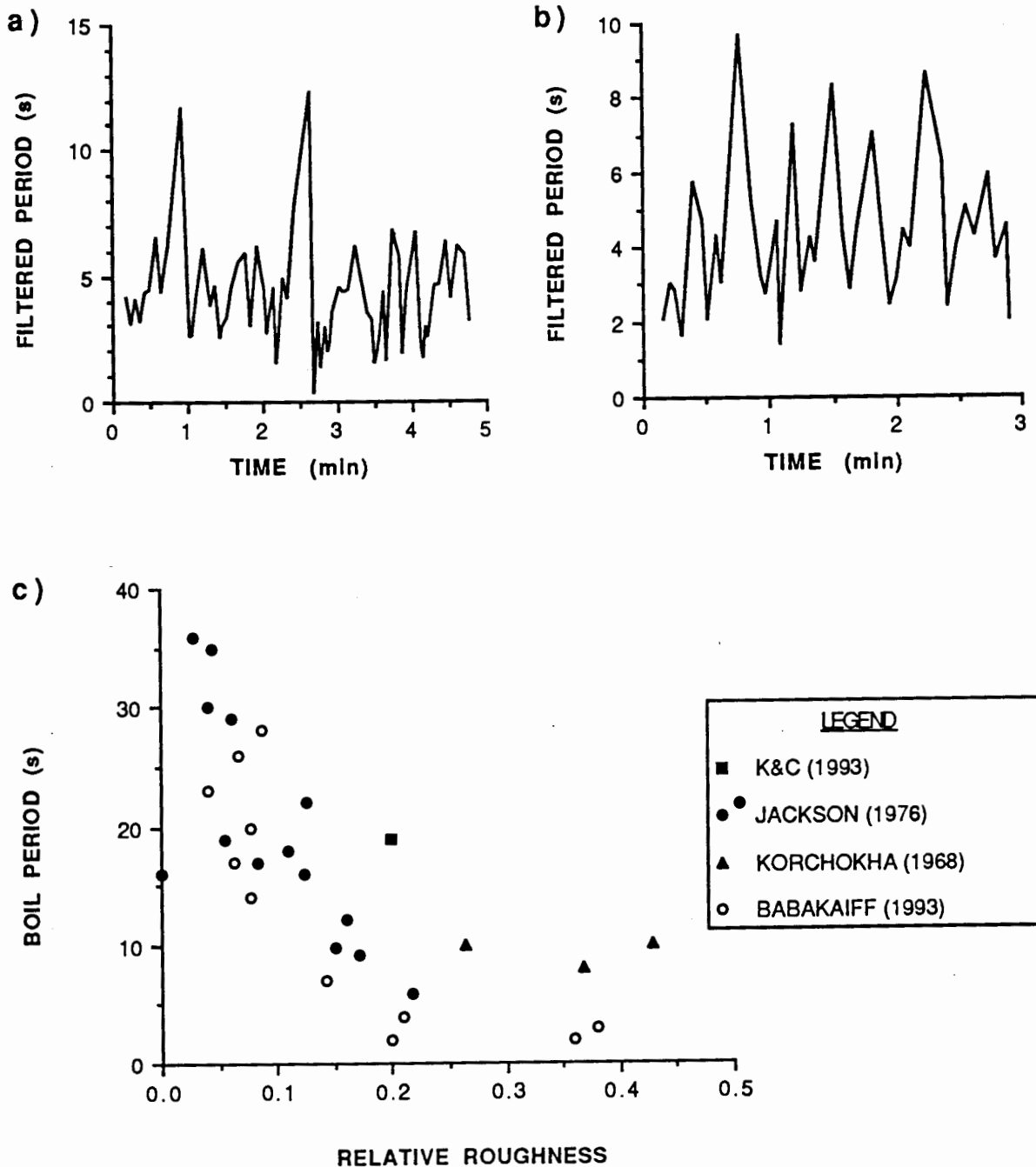


Fig. 6.12- a) Filtered boil-period time series: July 29 1239-44
 b) Filtered boil-period time series: July 29 1245-48
 c) Boil period vs. relative roughness (data from four studies)

DATE AND TIME	SKEWNESS	BIMODAL?	CHI-SQUARED TEST FOR LOG-NORMALITY			CHI-SQR. TEST: DIGITIZATION REPETITION	D.F.	χ^2	CRIT(0.01)	ACCEPT?
			D.F.	χ^2	CRIT(0.01)					
<u>LOWER ESTUARY</u>										
MAY 3 1312	0.863	N	5	1.7	15.1	Y	6	7.6	16.8	Y
MAY 5 1600	1.134	N	7	4.3	18.5	Y	6	4.9	16.8	Y
MAY 5 1617	0.850	N	6	8.1	16.8	Y	5	3.1	15.1	Y
MAY 9 1636	0.529	N	5	5.2	15.1	Y	5	3.8	15.1	Y
MAY 3 1451	0.993	N	5	17.3	15.1	N	N/A	N/A	N/A	N/A
MAY 5 1630	1.546	N	7	4.6	18.5	Y	N/A	N/A	N/A	N/A
JUNE 15 1248	1.972	N	5	9.2	15.1	Y	N/A	N/A	N/A	N/A
AUG 11 1012	0.610	N	5	2.6	15.1	Y	N/A	N/A	N/A	N/A
AUG 11 1114	0.811	N	5	7.2	15.1	Y	N/A	N/A	N/A	N/A
AUG 11 1221	1.608	N	5	16.4	15.1	N	N/A	N/A	N/A	N/A
<u>SPEED SITE#2</u>										
JULY 29 1239	2.048	Y	5	7.0	15.1	Y	5	2.1	15.1	Y
JULY 29 1245	0.715	N	5	5.0	15.1	Y	5	1.4	15.1	Y
JULY 29 1251	2.107	N	6	3.3	16.8	Y	5	9.0	15.1	Y
JULY 30 1423	1.341	N	5	0.7	15.1	Y	5	0.9	15.1	Y

Table 6.1- Chi-squared tests of Type 1 boil-period frequency distributions

would not obscure possibly interesting results'. The degrees of freedom (D.F.= #categories-1) had to be manipulated for each test such that the assumptions of the chi-square test could be met. The key assumption was that no category could have a relative frequency <1%, and no more than 20% of the categories could have relative frequencies <5%. The results of the chi-square test indicate that all but two time series have log-normal frequency distributions.

In order to test the reliability of the technique for determining boil period, each video time series was digitized a second time. Then, the frequency distribution for the repeat-digitization was compared to that of the original distribution, using the chi-square test ($\alpha=0.01$). All Type 1 boil-period time series obtained from video footage were found to have frequency distributions which could be duplicated with repeat digitization. With respect to boil morphology, the structures observed on May 3 and 5 and July 29-30 were cauliflower, and the other dates were dominated by circular upwellings with the occasional roller.

To test the applicability of Strouhal's Law to the mean boil periodicities displayed, the predicted length scales were calculated (based on $L=UT/2\pi$) and compared to the mean water-depth and the bedform height (Table 6.2). For the speed site #2, the predicted length scales fall between the dune heights and water depths. Interestingly, for the lower estuary sites, the predicted length scales exceed the water depth for all time series except those obtained when the bed was planar with occasional deep scour holes. The negative dune heights represent scour holes identified on the sonar record (Fig.6.13). Strong boils erupted at the water surface a few metres downstream of the scour hole as it progressed past the survey boat.

DATE AND TIME	BOIL PERIOD (s)	U sfc (m/s)	U0.7d (m/s)	DEPTH (m)	HEIGHT (m)	R.R.	PREDICTED LENGTH SCALES (m) from U sfc	PREDICTED LENGTH SCALES (m) from U0.7d
<u>SPEED SITE#2</u>								
JULY 29 1239	4	1.70	1.40	1.9	0.4	0.21	1.08	0.89
JULY 29 1245	4	1.70	1.30	1.9	0.4	0.21	1.08	0.82
JULY 29 1251	4	1.70	1.35	1.9	0.4	0.21	1.08	0.86
JULY 30 1423	7	1.45	1.10	2.1	0.3	0.14	1.62	1.23
<u>LOWER ESTUARY</u>								
MAY 3 1451	2	1.00	-	1.0	-0.2	0.20	0.32	-
MAY 3 1312	26	0.60	-	1.5	0.1	0.07	2.48	-
MAY 5 1600	14	0.85	-	1.3	0.1	0.08	1.89	-
MAY 5 1617	20	0.85	-	1.3	0.1	0.08	2.71	-
MAY 5 1630	3	1.50	-	1.6	-0.6	0.38	0.71	-
JUNE 15 1248	2	1.40	-	1.5	-0.5	0.36	0.45	-
AUG 11 1012	17	0.65	0.35	1.4	0.1	0.06	1.75	0.95
AUG 11 1114	28	0.75	0.50	1.4	0.1	0.09	3.34	2.23
AUG 11 1221	23	0.75	0.45	1.5	0.1	0.04	2.75	1.65

Table 6.2- Applicability of Strouhal's Law to Type 1 boils

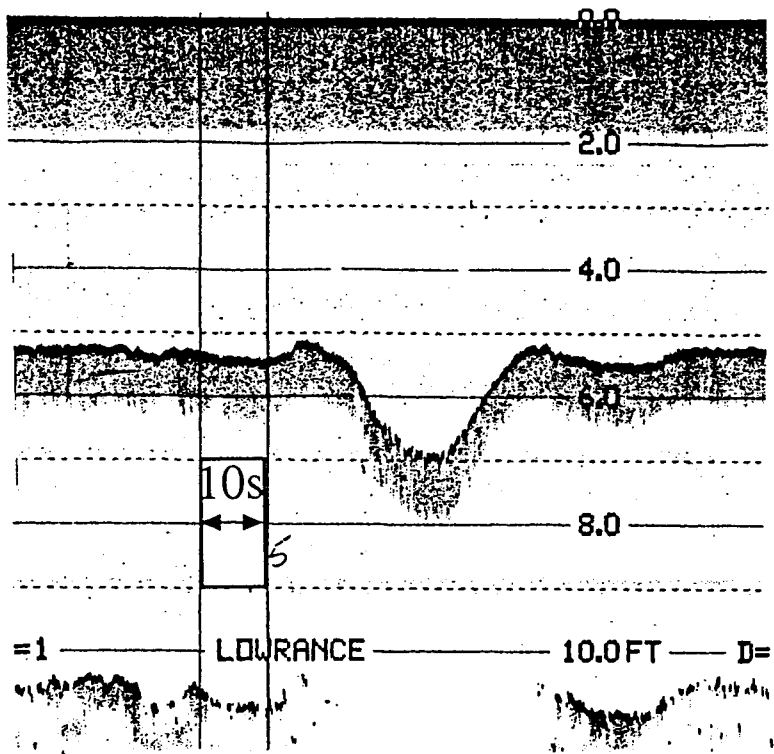


Fig. 6.13- Sonar record of scour hole moving past research vessel anchored in lower estuary

Table 6.2 also includes the calculated relative roughness with the depth of the scour hole taken as the length scale compared to mean water-depth. Data in Jackson (1976) (including that of Korchokha (1968)) allows calculation of the relative roughness. Kostaschuk and Church (1993) also include relative roughness and boil-period data. Although there is a bit of scatter in Fig.6.12c, it is evident that as the relative roughness increases, the boil period diminishes rapidly, and becomes constant as $RR > 0.2$. There may also be evidence of separate curves for the Jackson (1976) data and that of this study; the Jackson data seems to be displaced upwards by approximately 5s.

6.2.2.3- Secondary upwellings within Type 1 boils

It was noted that the Type 1 boil events are often associated with several distinct secondary upwellings near the original structure, typically within the first few seconds. From initial observations, it was postulated that the number of upwellings within each event may be related to the period between each boil event. Since the duration of boil shedding at a particular site rarely exceeded 5 minutes, data were collected from several sites. Over a three-day period, data were collected at 14 sites, but not one time series displayed a relation between the number of upwellings per boil event and the inter-boil period (either preceding or following the boil).

6.2.2.4- Type 1 boil size and persistence

The size and persistence of boil events were expected to be simple to quantify, but proved to be quite problematic. Attempts were made to take photos normal to the water surface in order to avoid difficulties with rectification. Standing on the roof of the research boat with the camera lens at its widest setting did not allow enough of the water surface to be shown, thus the camera was affixed onto an extendable pole. As the camera

elevation above the water surface increases, the length of the boil life-cycle able to be photographed also increased. However, the pole constructed to elevate the camera above the surface was too heavy and awkward to operate safely at elevations greater than 7m above the water surface. The wind and instability of the boat also produced conditions not conducive to keeping the pole stable. Even at maximum elevation, the combination of rapid surface current-speeds and the relatively slow refractory period of the camera produced only two, and on rare occasions, three photos of the boil before it was transported out of camera range.

There were also difficulties associated with boil production. Since the production sites did not last longer than ten minutes, repositioning the boat each time a production site became inactive was not feasible. An alternative was to remain anchored and move towards any production sites created near the boat, using a series of lead weights dropped to the bed to restabilize. This was not successful since the winds and current could move the boat several metres in any direction. There were also a limited number of days with tidal drops large enough to produce strong boil activity. If the weather and lighting conditions were not ideal on those days, the structures could not be identified in non-oblique angle photos. Typically, only the initial photo in the series showed the whole structure, particularly if secondary upwellings occur. The secondary upwellings also complicated any scaling of boil size or expansion rates with hydraulic or bedform variables. Due to these complications, boil size and expansion rate quantification from the photos was abandoned. The option of utilizing low-level balloon photography was pursued, but could not be organized before the research period ended.

6.3- ANALYSIS OF TYPE 2 BOILS

6.3.1- Relations between bedforms and Type 2 boil intensity

As in section 6.2.1, the relations of w , h and d are differentiated by the boil intensity. In general, the Type 2 boil intensities are not as well described by relations between w , h and d as the Type 1 boil intensities. For the w vs. h plots, in reaches 4 and 5, the $h=0.5\text{m}$ separative marks an increased variance (similar to reaches 2,3 and 7), but it is the bedforms with $h<0.5\text{m}$ that display a strong linear correlation (Fig.6.14a). There are no recognizable relations between the boil intensity and the bedform conditions, however. For reaches 1 and 6, the separative is not as obvious, and again there are no relations between the appearance of boils and the bed conditions.

The w vs. d plots suggest that for reaches 1 and 6, the majority of boils occur with $d<5.25\text{-}5.5\text{m}$, due to velocity patterns associated with diurnal tidal control. Similarly, for reaches 4 and 5, the dependence of boil intensity on RRS is poorly developed and the majority of boil intensities of level 1-4 occur at $d<5.5\text{m}$. From the plots of d vs. h , reaches 1 and 6 do not display any patterns of macroturbulence intensity with RR, nor do the boils occur at any critical height or depth. In reaches 4 and 5, there is a suggestion of a separative for boils (level 1-4) at $RR=0.1$, but the stronger trend is the dominance of these features at $d<4.25\text{m}$ (Fig.6.14b).

6.3.2- Type 2 boil parameters

6.3.2.1- Boil presence and intensity

The presence and intensity of Type 2 boils is based on video footage and observations made during transects, and water-surface slope and current-speed data collection. When boils were present, the intensity was qualitatively assessed. As noted in Chapter 2, this

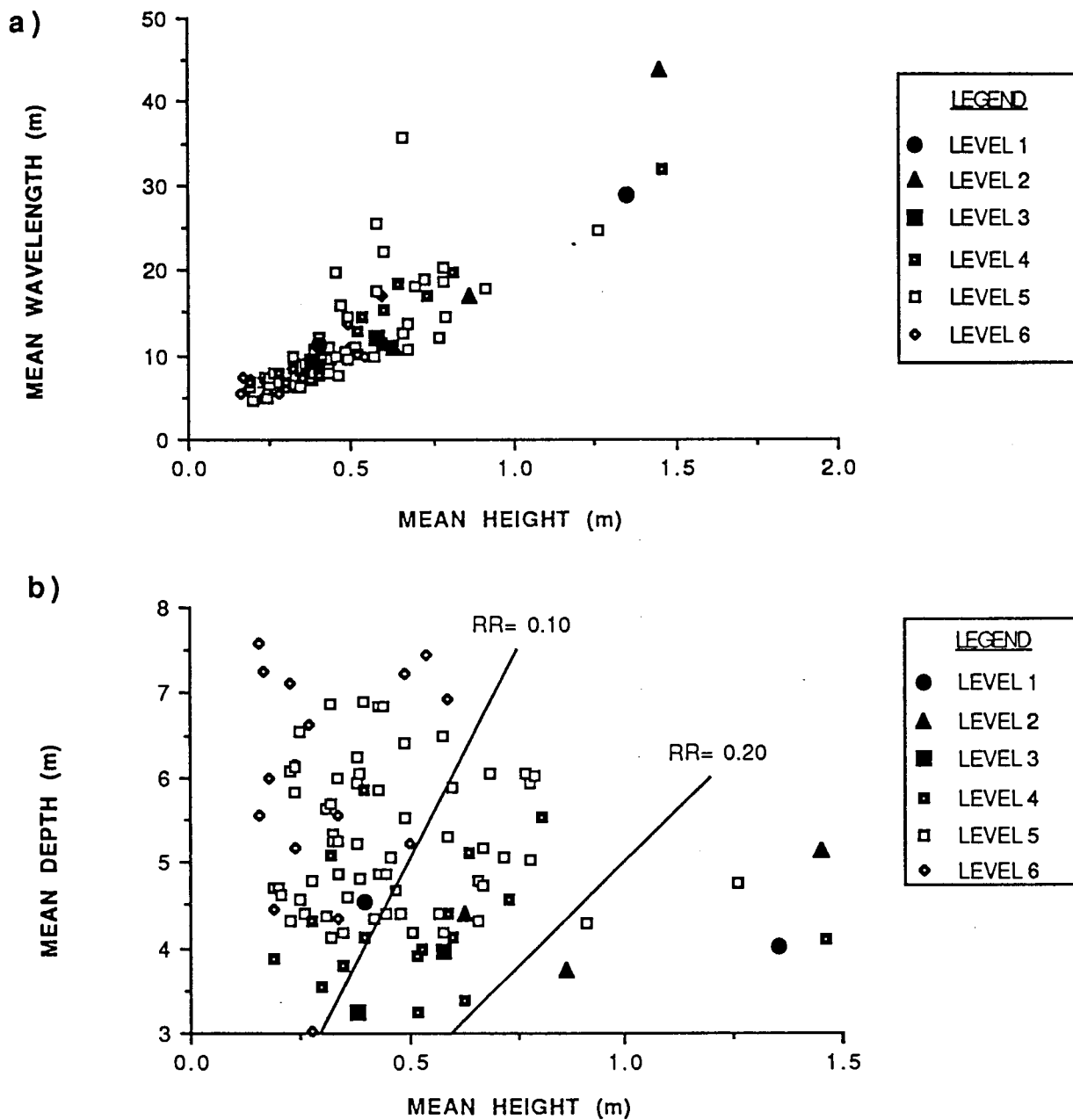


Fig. 6.14- Reach 4 boil intensity as a function of mean bedform-height and:
 a) mean bedform-wavelength
 b) mean water-depth

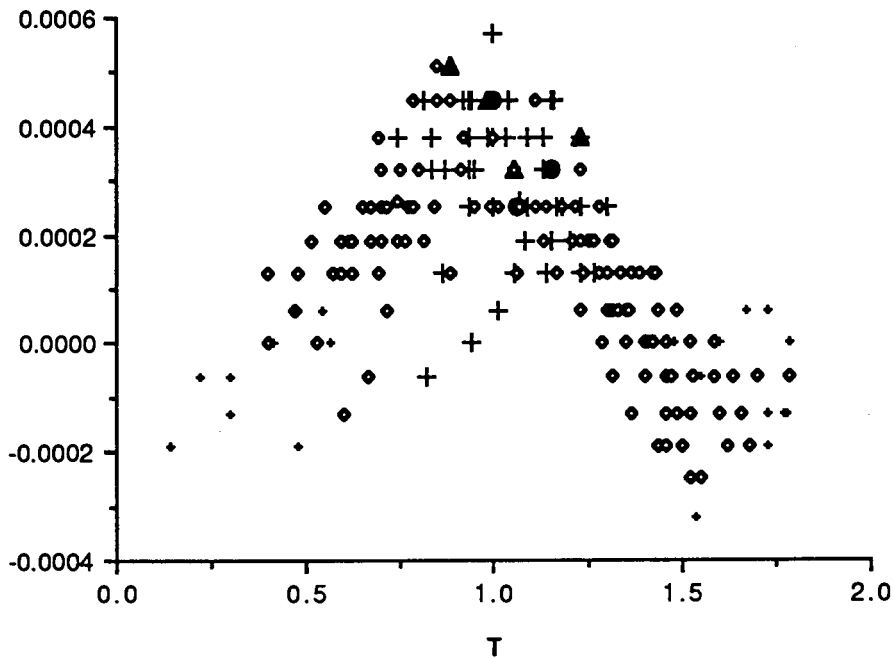
intensity rating is a scale with bounding conditions of no evidence of surface macroturbulence (Level 6) to intense eruptions seen to entrain sediment and organics (Level 1). Hereafter, intensity levels ≥ 5 are known as 'weak' Type 2 boils, and intensity levels ≤ 4 are 'strong' (examples are shown in Figs.3.14a-d, and 3.15a-d respectively).

As with the Type 1 boils, the presence and intensity of Type 2 boils were noted to be strongly related to tidal conditions. At HHT during Spring tides, the river surface would be quite mirror-like. As the water level began to drop, weak gleams (patches of smooth water) would be produced at a variety of sites. During Neap tides, these gleams would be present at HHT presumably because the imposed tidal heights were lower and the degree of ponding upstream was not as extensive. As a result, current speeds and water-surface slopes would not diminish as greatly.

In Chapter 4, the changes in current speed during the tidal cycle were noted to follow those of water-surface slope. Due to a variety of complex lag effects, it may not be possible to determine if the increase in boil activity is simply related to increased current speed, or if it is also related to shear stress at the bed, increases in RR, and/or some feedback relation with flow resistance. Graphical analyses of the maximum observed intensity of boil activity versus the water-surface slope, current speed and tidal forcings at a variety of sites may offer insight.

At both the R/B and L/B sites, plots of water-surface slope versus T indicate that strong boil activity concentrates near LLT (Fig.6.15a,b). Strong boil activity is found at the R/B site between $T=0.8-1.25$, but occurs slightly later at the L/B site at $T=0.9-1.5$. Only intensity levels <4 occur with steeper slopes imposed during Spring tides and times of high discharge.

a)



b)

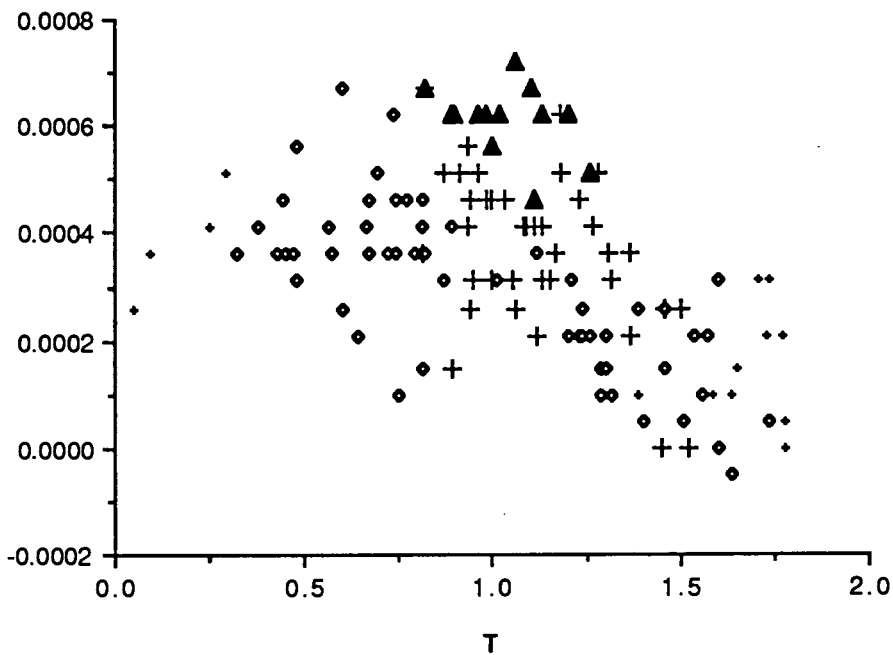


Fig. 6.15- Boil intensity as a function of slope and T:
 a) R/B site
 b) L/B site

Plots of the surface current speed versus T which are differentiated by boil intensity indicate that strong boil activity concentrates near LLT. For the R/B U/S and L/B D/S sites, the strong boil activity (especially < level 4) tends to concentrate in the early flood tide (Fig.6.16a,b). This tendency is not noted at the other two sites (e.g. Fig.6.16c), but this may be related to a general lack of strong boil activity. There is an indication at the R/B U/S site that strong boil activity may be positively correlated with current speed. However, it generally seems that the maximum level of boil activity noted in a given period does not correlate well with a median surface current-speed obtained over a 30s period. Utilizing the nine-minute mean of current speed at 0.7d rather than U_{sfc} does not alter the conclusions. Again, the strong boil activity concentrates near LLT, but not necessarily during high current speeds.

6.3.2.2- Boil size and morphology

Attempts to photograph and videotape the Type 2 boils within the transportation zones in order to determine the size and morphology of the structures met with several difficulties. It was postulated that the orientation or morphology of the Type 2 boils could be related to hydraulic or tidal parameters. The most frequently observed morphology was an oval stretched in accordance with the streamwise and lateral shear, with the sites of vigorous downwelling on the downstream side (Fig.6.17). However, observations indicated a lack of consistency between structures over short periods; even successive boils often had their long axes displaced by up to 90° (Fig.3.11b).

The shape of the Type 2 boil could be strongly influenced by the strength, number and duration of the upwellings within it. Furthermore, these factors dictated the size and duration of the boil agglomeration. Observations suggested that, where the upwellings within a Type 2 boil were of comparable strength and size, the size of the Type 2 boil

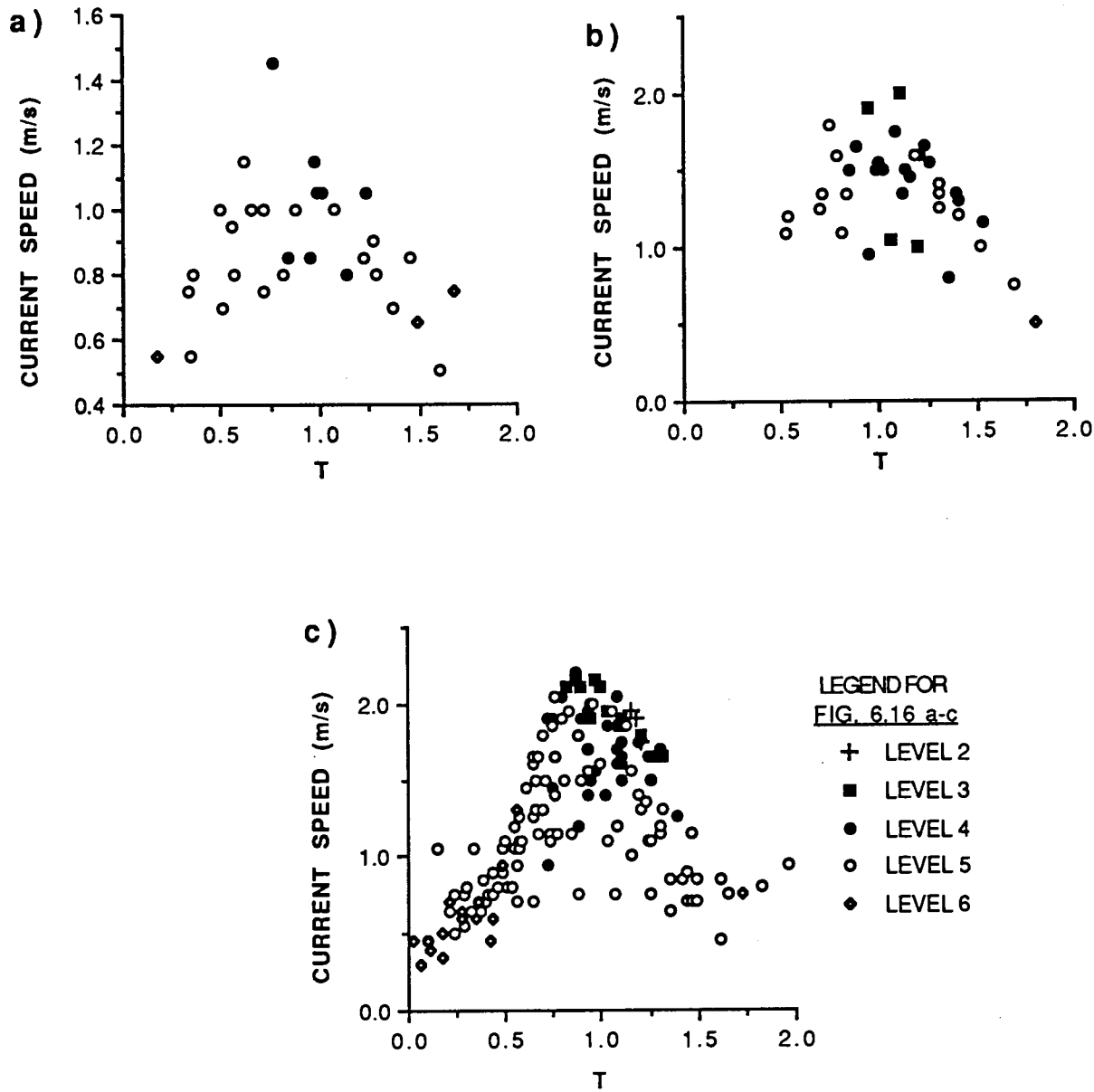


Fig. 6.16- Boil intensity as a function of surface current speed and T:

- a) R/B U/S site
- b) L/B D/S site
- c) R/B D/S site



Fig. 6.17- Type 2 boil with strongest downwelling on R/B D/S side (flow direction is towards upper right side of photo; boil is approx. 15m long)

agglomeration may be related to the number of upwellings within. Numerous time-series photos were taken in hopes of quantitatively verifying this relation. Unfortunately, these photos were also affected by the factors noted in section 6.2.2.4. Identification of the upwellings within the Type 2 boils was also influenced by the location of the structure in relation to the camera focal point in the streamwise and transverse direction. Estimation of the number of upwellings and the surface areas of the agglomerations was attempted, but repeat digitizations of the time series produced inconsistent results.

The morphology, size and evolution of the Type 2 boils was also influenced by the hydraulic and tidal conditions within the estuary. There seemed to be some critical intensity of upwellings which, once exceeded, would segment the boil agglomeration. This was observed most frequently near LLT, particularly during Spring tides. During weak ebb tides the boils would preferentially diffuse, but on the flood tide elongation was more likely to occur.

6.3.3- Type 2 Boil-period time series

6.3.3.1- Frequency distributions

The boil-period analysis of Type 2 boils is based on video footage of production sites and preferential upwelling sites within transportation zones. Upwelling locations at the production sites were fixed, but within the transportation zone, upwelling locations could vary between time series. Also, once the site of upwelling to be analyzed in the transportation zone was chosen, the boil agglomeration that would advect past often seemed to induce stronger and more frequent upwellings. As noted previously, the boundaries between successive Type 2 boils could not always be identified, and whether or not an upwelling was induced by a Type 2 boil could not be determined with certainty.

Current speed varies slightly within Type 2 boils, but the current direction is much more variable. The directional current meter indicated that the upstream and downstream edges of a Type 2 boil could have current direction which differed by up to 70° . Such levels of vorticity were typically noted down to $0.7d$, where separation zones behind bedforms and obstacles could be affected. Since it was not possible to differentiate those upwellings which were produced 'independently' of the Type 2 boils from those that were not, the boil-period time series and mean quantities include both populations. All boil-period frequency histograms display a positive skewness (Table 6.3). Some histograms display bimodality, but these were limited to the R/B U/S site, save for one example at the R/B D/S site (Fig.6.18a).

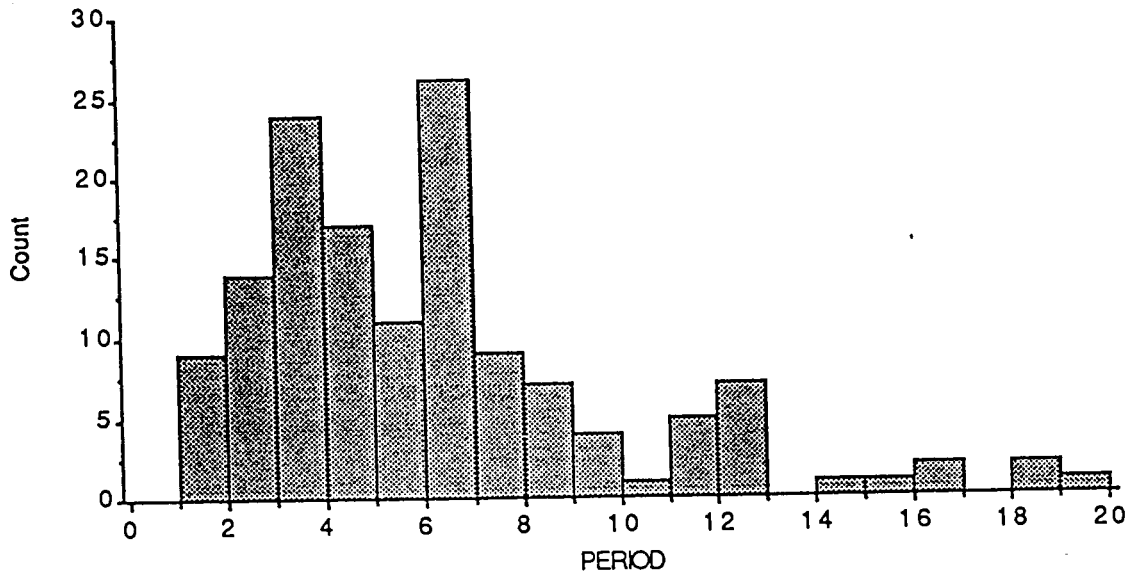
Many of the histograms appear to display a log-normal distribution (e.g. Fig.6.18b). To test if the frequency distributions were log-normally distributed, the technique described in section 6.2.2.2 was again employed. The assumptions could be met for all but one of the time series. At the L/B, the observed distributions are concluded to be log-normal for only 20% of the data. These are similarly proportioned amongst the U/S and D/S sites (Table 6.3). For the R/B sites, more distributions are concluded to be log-normal (approximately 36%), and again the proportions are similar between the U/S and D/S sites. Those time series that were well described by the log-normal distribution were dispersed over a wide range of days, discharges and tidal conditions. Those time series which were not well described by the log-normal distribution often had secondary modes or long tails. Truncation of these tails improved the results for several, but not all time series.

If the number of boils occurring in a given time span was a random phenomenon, the frequency distribution of the inter-event periods may follow the Poisson distribution. Previous results indicated that distributions often followed the log-normal distribution,

DATE AND TIME	SKEWNESS	BIMODAL?	CHI-SQUARED TEST FOR LOG-NORMALITY	CHI-SQR. TEST: DIGITIZATION REPETITION						
			DF.	χ^2	CRIT	ACCEPT?	DF.	χ^2	CRIT	ACCEPT?
<u>L/B U/S</u>										
JUNE 5 1536	0.866	N	6	26.5	18.8	N	5	132.9	15.1	N
JUNE 5 1634	1.803	N	5	16.4	15.1	N	5	43.3	15.1	N
JUNE 7 1535	1.941	N	6	8.8	16.8	Y	5	12.6	15.1	Y
JUNE 7 1642	1.551	N	5	25.8	15.1	N	6	14.7	16.8	Y
JUNE 7 1727	2.582	N	5	15.7	15.1	N	N/A	-	-	-
<u>L/B D/S</u>										
JUNE 11 0821	1.468	N	6	26.6	16.8	N	5	8.4	15.1	Y
JUNE 11 0923	0.876	N	5	21.7	15.1	N	7	35.5	18.5	N
JUNE 11 1012	0.684	N	7	82.3	18.5	N	6	4.6	16.8	Y
JUNE 11 1117	0.536	N	6	34.5	16.8	N	5	131.4	15.1	N
JUNE 13 0923	1.436	N	7	15.6	18.5	Y	6	7	16.8	Y
<u>R/B U/S</u>										
JUNE 18 1255	1.335	N	6	12.6	16.8	Y	7	9.7	18.5	Y
JUNE 18 1355	1.406	N	9	53.3	21.7	N	5	12.8	15.1	Y
JUNE 18 1456	1.396	Y?	9	9.1	21.7	Y	7	23.6	18.5	N
JUNE 22 0538	3.465	Y?	9	20.8	21.7	Y	N/A	-	-	-
JUNE 22 0651	1.648	N	6	23.6	16.8	N	5	8.8	15.1	Y
JUNE 22 0759	3.346	Y?	7	32.4	18.5	N	N/A	-	-	-
JUNE 24 0557	0.874	Y?	6	31.3	16.8	N	5	7.5	15.1	Y
JUNE 24 0710	2.413	Y?	7	22.9	18.5	N	N/A	-	-	-
JUNE 24 0825	1.738	Y?	7	30.2	18.5	N	6	226.2	16.8	N
JUNE 26 0708	1.177	Y?	-	N/A	-	-	6	40.4	16.8	N
JUNE 26 0825	1.263	N	6	27.5	16.8	N	6	3.4	16.8	Y
JUNE 26 0950	1.758	Y?	6	5.9	16.8	Y	5	29.3	15.1	N
<u>R/B D/S</u>										
JUNE 23 0638	2.074	N	6	15.2	16.8	Y	6	15.2	16.8	Y
JUNE 23 0800	2.083	N	5	15.3	15.1	N	5	5.9	15.1	Y
JUNE 27 0618	2.235	N	6	29.4	16.8	N	6	11	16.8	Y
JUNE 27 0708	2.007	Y	6	24.9	16.8	N	5	14.1	15.1	Y
JUNE 27 0817	1.952	N	5	63.4	15.1	N	5	76.2	15.1	N
JUNE 27 0946	1.586	N	8	13.1	20.1	Y	5	83.2	15.1	N
JUNE 28 0818	2.343	N	5	58.1	15.1	N	N/A	-	-	-
JUNE 28 1038	1.461	N	6	6.6	16.8	Y	N/A	-	-	-

Table 6.3- Chi-squared tests of Type 2 boil-period frequency distributions

BOIL PERIOD FOR JUNE 27 0708-0723



BOIL PERIOD FOR JUNE 18 1255-1310

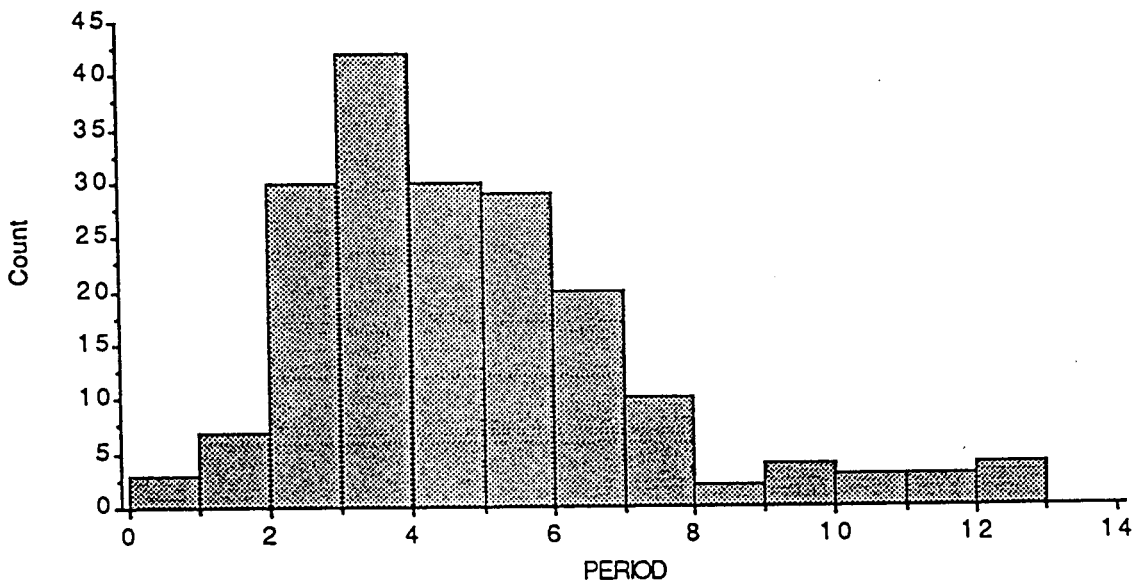


Fig. 6.18- Boil-period(s) histograms for:
 a) June 27 0708-0723
 b) June 18 1255-1310

and my field observations indicated that assumptions of the Poisson distribution may be violated (e.g. independence of boil events). However, a liberal approach was taken, and the chi-square test ($\alpha=0.01$) was again utilized. For every time series, the test indicated an unsuccessful fit. Again, truncation of the tails often improved the similarity between the observed and Poisson distributions, but not to the extent that the null hypothesis could be rejected.

6.3.3.2- Mean boil-periods

As noted in Chapter 2, the mean boil-period was calculated over the 15 minute span of each digitized time series. For the L/B sites, the period remained essentially constant between time series, albeit slightly shorter for the D/S site. These results seem attributable to similar U_{sfc} and water depth (Table 6.4). Note, however, that the $U_{0.7d}$ varied considerably. For the R/B sites, there is more variability in the mean period, essentially ranging from 4-8 seconds. For the R/B U/S site, on June 18 the increase in period seems to follow the decrease in $U_{0.7d}$ and depth. If the current speed used in Strouhal's Law is the surface measure, a decrease in depth would instead be expected to produce a decrease in period. For June 22 and 24, depth and current speed remained steady on both days, but with larger current speeds and shallower depths on the 24th. The mean boil-period was also generally shorter on June 24, which would be expected from Strouhal's Law. Note that data from June 26 is excluded due to data fouling (non-stationarity).

Similar results emerged from the data of the R/B D/S site, with the mean boil-periods of June 28 much shorter than those of June 23 or 27. Note that there were no notable differences in current speed or depth. Although the noted variations in speed, depth and period are relatively small, the lack of consistent patterns seems to imply that Strouhal's

DATE AND TIME	AVG. BOIL PERIOD(s)	U@0.7d (m/s)	S.D. U@0.7d (m/s)	C.V. U@0.7d	USFC (m/s)	DEPTH (m)	LENGTH SCALE(m): STROUHAL LAW	
							from U	from U sfc
L/B U/S								
JUNE 5 1536	4	0.81	0.10	0.10	0.75	3.7	0.52	0.48
JUNE 5 1634	4	1.02	0.09	0.08	0.85	4.7	0.65	0.54
JUNE 7 1535	5	0.75	0.08	0.10	0.80	4.3	0.60	0.64
JUNE 7 1642	4	0.63	0.10	0.16	0.70	4.9	0.40	0.45
JUNE 7 1727	5	0.67	0.11	0.17	0.75	4.9	0.53	0.60
L/B D/S								
JUNE 11 0821	3	0.96	0.09	0.09	1.10	3.7	0.46	0.53
JUNE 11 0923	3	1.15	0.12	0.10	0.95	3.4	0.55	0.45
JUNE 11 1012	3	1.27	0.16	0.13	1.05	4.0	0.61	0.50
JUNE 11 1117	3	0.67	0.26	0.40	1.00	4.3	0.32	0.48
R/B U/S								
JUNE 18 1255	5	1.51	0.22	0.04	1.50	5.2	1.20	1.19
JUNE 18 1355	6	1.46	0.23	0.16	1.50	4.6	1.39	1.43
JUNE 18 1456	7	1.38	0.21	0.15	1.50	4.0	1.54	1.67
JUNE 22 0538	6	1.20	0.18	0.15	1.50	6.7	1.15	1.43
JUNE 22 0651	5	1.21	0.19	0.16	1.20	6.7	0.96	0.95
JUNE 22 0759	6	1.11	0.21	0.19	-	6.6	1.06	-
JUNE 24 0557	6	1.54	0.18	0.12	1.65	4.6	1.47	1.58
JUNE 24 0710	4	1.58	0.20	0.13	1.70	4.6	1.01	1.08
R/B D/S								
JUNE 23 0638	8	0.68	0.09	0.14	0.85	2.4	0.87	1.08
JUNE 23 0800	7	0.67	0.10	0.15	0.80	2.7	0.75	0.89
JUNE 27 0618	7	0.54	0.09	0.18	0.95	3.0	0.60	1.06
JUNE 27 0708	6	0.64	0.11	0.18	1.00	2.7	0.61	0.95
JUNE 27 0817	6	0.58	0.10	0.17	0.80	2.1	0.55	0.76
JUNE 27 0946	8	0.74	0.18	0.25	1.15	1.8	0.94	1.46
JUNE 28 0818	4	0.55	0.08	0.14	0.75	2.4	0.35	0.48
JUNE 28 1038	5	0.78	0.17	0.22	1.05	1.8	0.62	0.84

Table 6.4- Calculated length scales based on Strouhal's Law

Law does not fully explain mean boil-periodicities at the field sites based on the data employed.

6.3.3.3- Reliability of digitization technique

The repeat digitization technique employed in section 6.2.2.2 was again used to test the reliability of the technique for determining boil period. Unfortunately, violations of the test assumptions disqualified 20% of the comparisons. Of those that could be tested, just over 40% were concluded to have frequency distributions that were not similar in the repeat digitization (Table 6.3). Most of these failures could be related to poor video quality, and it cautions against ready acceptance of the conclusions of sections 6.3.3.1 and 6.3.3.2 based on these time series. The results from these time series which had frequency distributions dissimilar to the repeat digitization are excluded from further analyses.

The repeat time series that could not be analyzed with the chi-square test were inspected graphically. Typically, the repeated time series were quite similar (e.g. Fig.6.19a), but there were changes in the longer periodicities in the series. This skew of the frequency distribution again prevents the meeting of the chi-square test assumptions. Again, a liberal approach was taken, and these six time series were retained for further analyses.

6.3.3.4- Graphical inspection of boil-period time series

As in Chapter 4, time series are presented in which a 7-term binomial filter has been run through the data. This is even more crucial for the boil-period time series due to fluctuations on scales as short as several seconds. Trends in the boil-period time series are strikingly similar to those of the current speed, displaying variability on similar

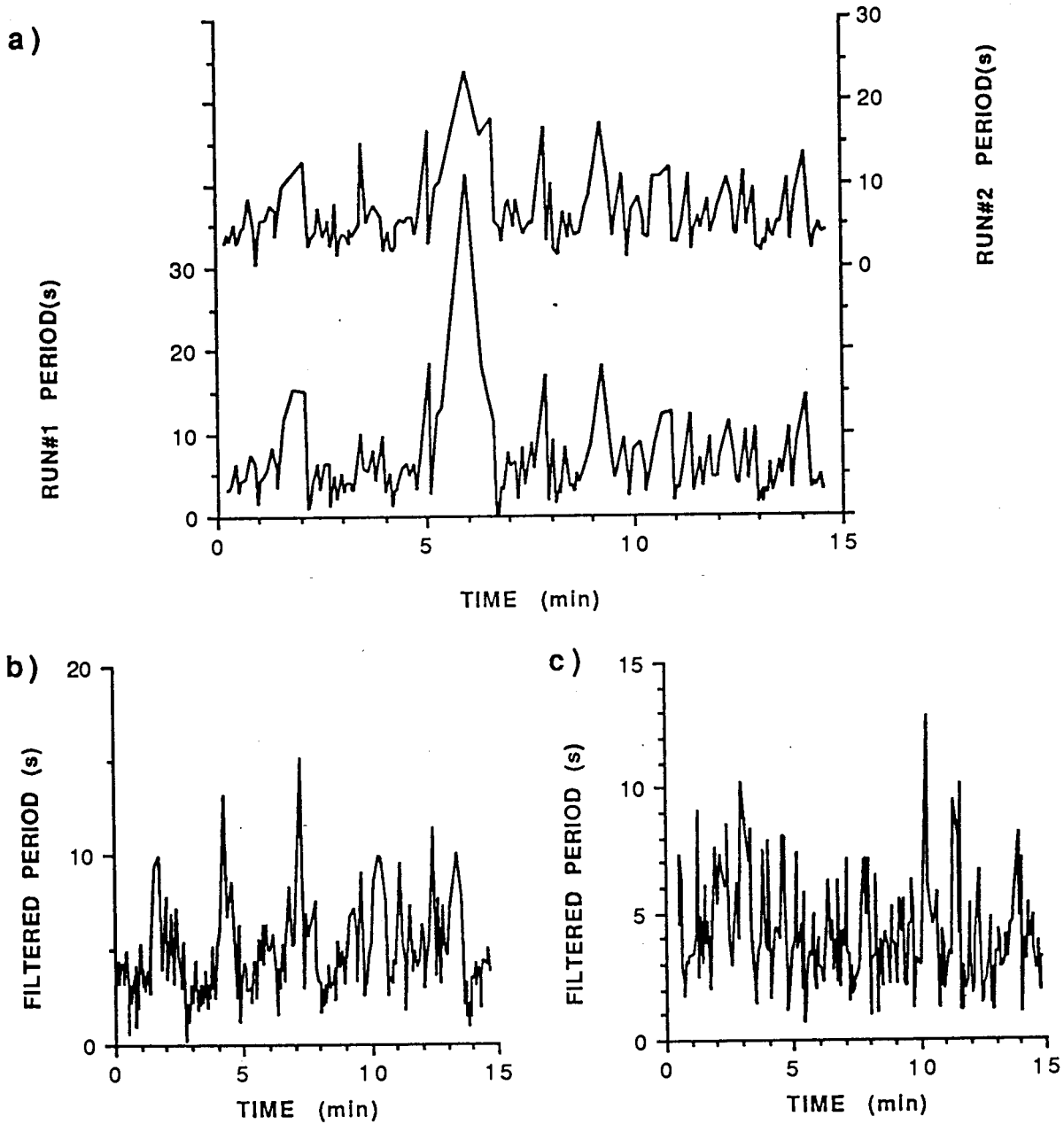


Fig. 6.19- a) Filtered boil-period time series for repeat digitizations: June 22 0759-0814

Filtered boil-period time series:

b) June 7 1642-1657

c) June 26 0708-0723

temporal scales, and sequences where the boil period becomes progressively shorter followed by a rapid increase (Fig.6.19b,c).

6.3.4- Comparison of speed and Type 2 boil-period time series

6.3.4.1- Graphical correlation

There were twenty simultaneous current-speed and boil-period time series which were inspected. The number is too sparse for any confident differentiation based on site, discharge or tidal conditions. Although several interesting trends (both within and between correlations) were noted, these are essentially limited to the R/B sites, likely due to the vastly superior video footage.

Several simultaneous time series displayed the tendency for the peaks in boil-period to correspond to troughs in current-speed. However, not every trough in the speed series is associated with a peak in the boil-period series. There is also a lag often displayed between these apparent corresponding variations in the time series. Typical examples are shown in Fig.6.20a,b. Note that the longer scale variability (Fig.6.20a) or non-stationarity (Fig.6.20b) in speed does not have corresponding patterns in the boil-period time series.

In portions of some plots, the sequence of shorter-period fluctuations also appear to correspond, which produces an inverted 'reflection' (e.g. minutes 3-11 of Fig.6.21a). It should also be noted, however, that some time series such as Fig.6.21b have a generally poor correspondence, but still display fluctuations on similar temporal scales (45-60 s). Curiously, all time series with peaks in the boil period corresponding strongly with current speed troughs came from the R/B U/S site.

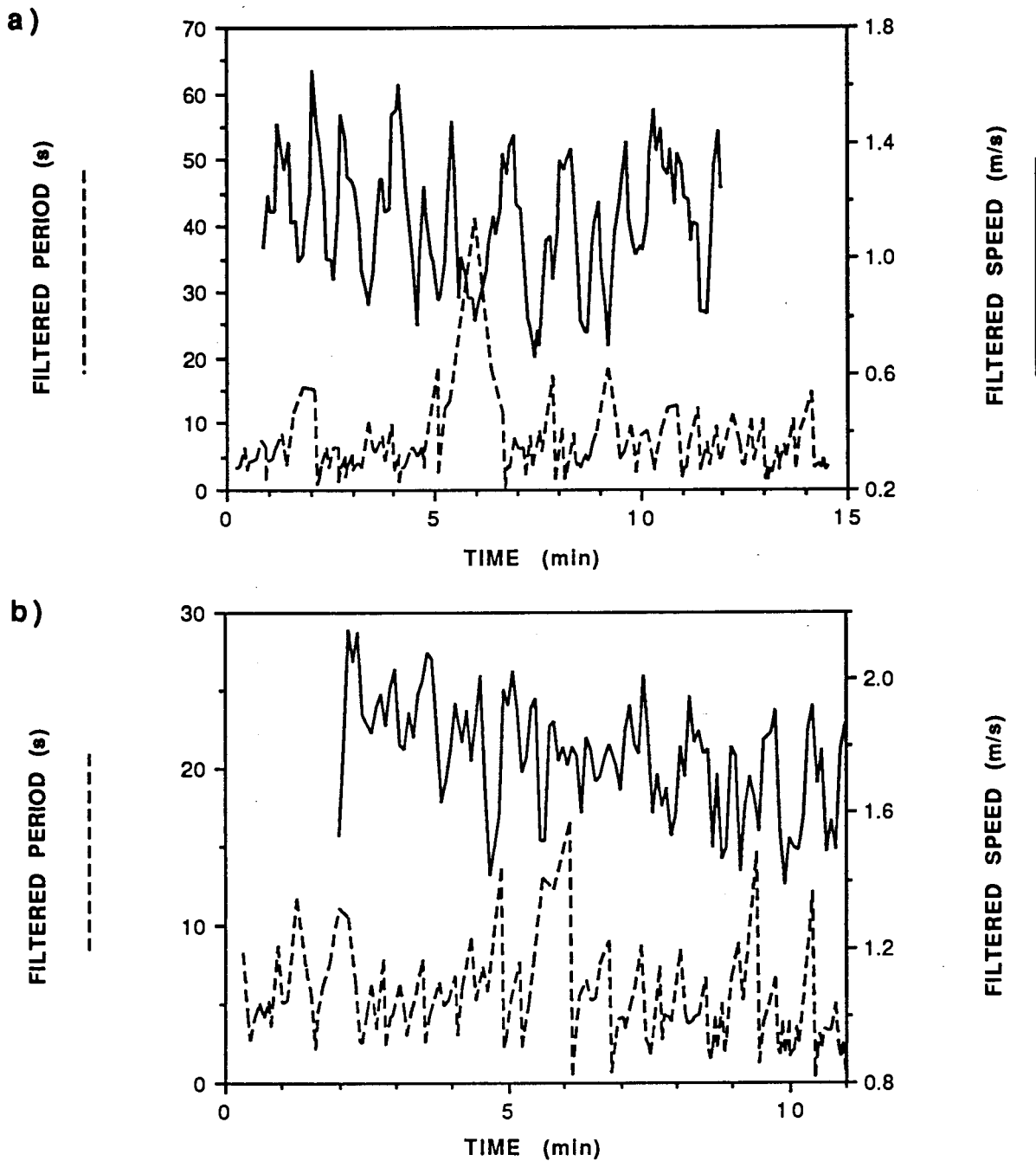


Fig. 6.20- Comparative plot of filtered boil-period and current-speed time series:

a) June 22 0759-0814

b) June 26 0950-1001

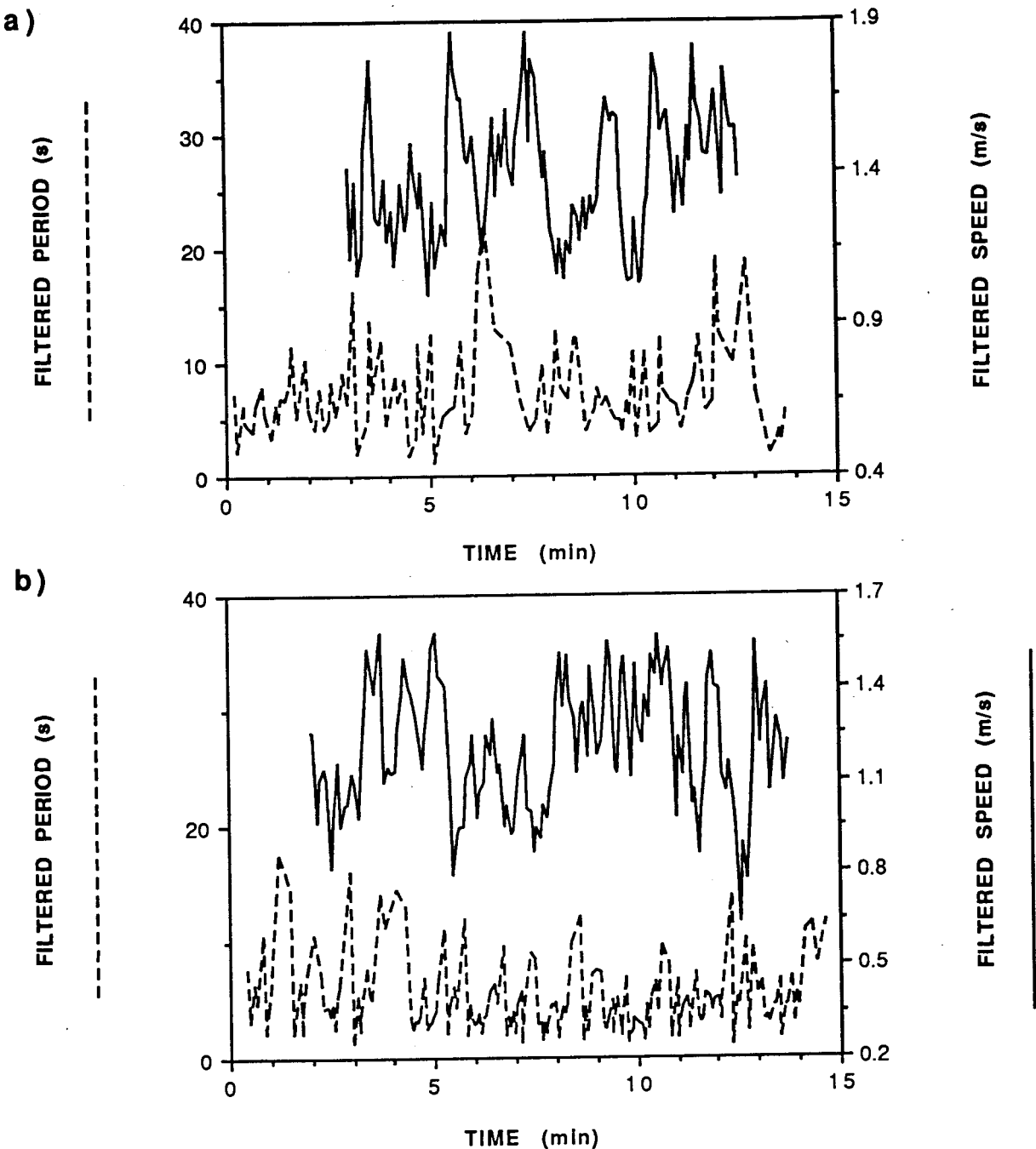


Fig. 6.21- Comparative plot of filtered boil-period and current-speed time series:

a) June 18 1456-1510

b) June 22 0651-0706

There were also time series in which the peaks in boil period appeared to correspond to both peaks and troughs in the current speed. Typical examples are shown in Fig.6.22a,b. In Fig.6.22a, the current speed peaks that appear to correspond with peaks in period may actually be local minimas. In Fig.6.22b, the time series vary on such short scales that it is difficult to discern whether the peaks in period correspond to the current speed troughs or the peaks which occur 20-30 s later. The boil period peaks appear to correspond to the speed troughs early in the record (minutes 3, 4.5) and to peaks later (minutes 7, 8.5, 11.5, 12.5). All time series that displayed these patterns were limited to the R/B D/S site.

In Chapter 4 it was noted that some speed time series had a slow unsteady increase followed by a rapid decline. Conversely, some boil-period time series had a slow unsteady decrease followed by a rapid increase. In Fig.6.23a, the patterns in boil period (minutes 4-8, 8-12) precede the speed patterns (minutes 6-9, 9-13), as do the shorter-scale boil peaks versus speed troughs (minutes 3.5, 5.25, 8, 9, 9.5). A similar pattern is displayed in Fig.6.21a (minutes 5,7). In Fig.6.23b, the similarity of temporal scales of speed and boil-period fluctuations, and the correspondence of peaks in boil-period with current-speed troughs are again noted. However, an interesting longer-scale pattern is also apparent. As both the magnitude and variation in current-speed increase, the boil-period diminishes, along with its variability. Then, after minutes 8-9, the magnitude and variability of current-speed decreases, but the boil-period magnitude and variability increases.

6.3.4.2- Quantitative correlation

In an effort to quantitatively assess the correlation between the unfiltered current-speed and boil-period time series, the cross-correlation feature in SYSTAT was used. In order to perform the cross-correlation, the time-series data must be set up as paired samples.

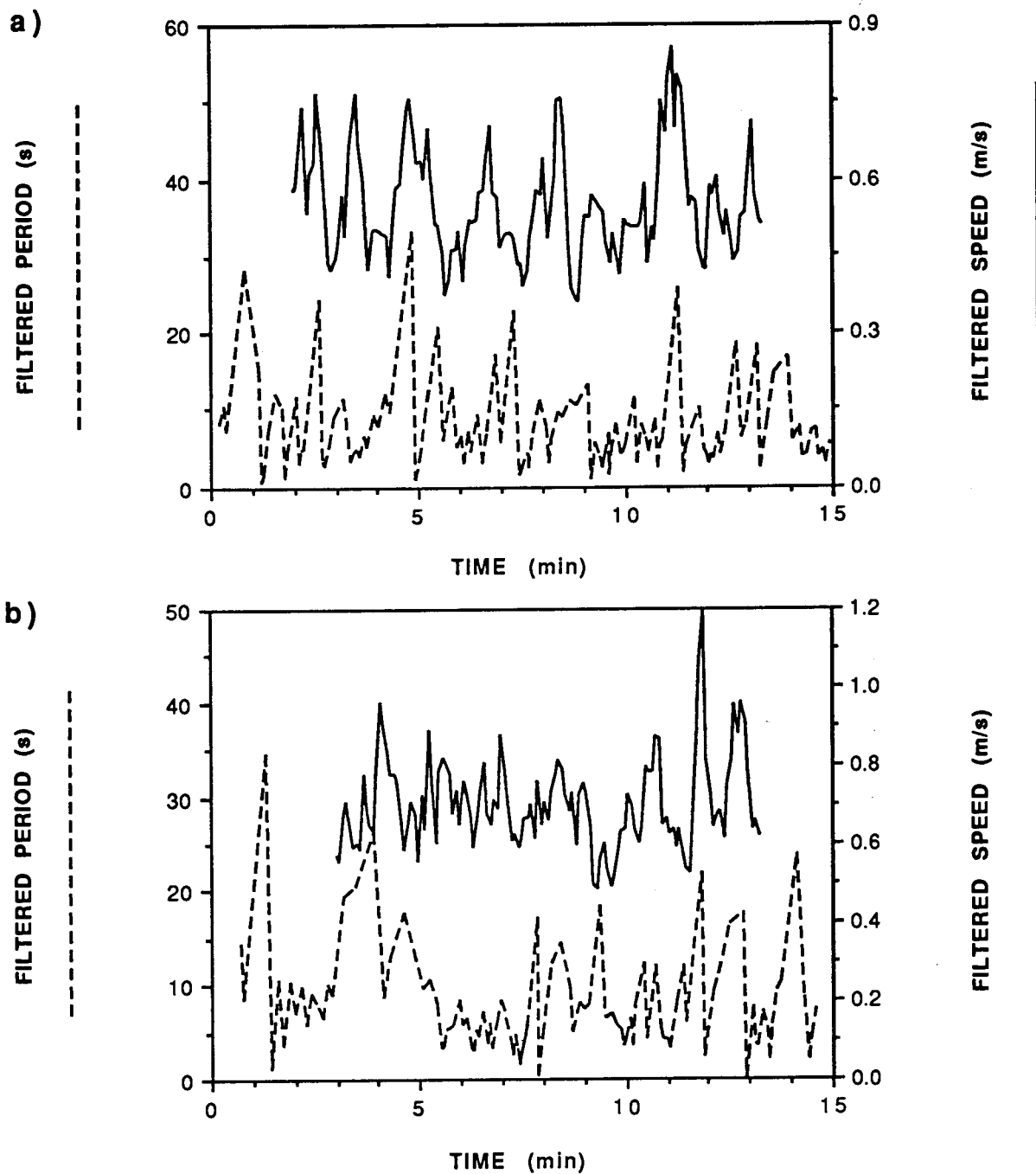


Fig. 6.22- Comparative plot of filtered boil-period and current-speed time series:

a) June 27 0618-0633

b) June 23 0638-0653

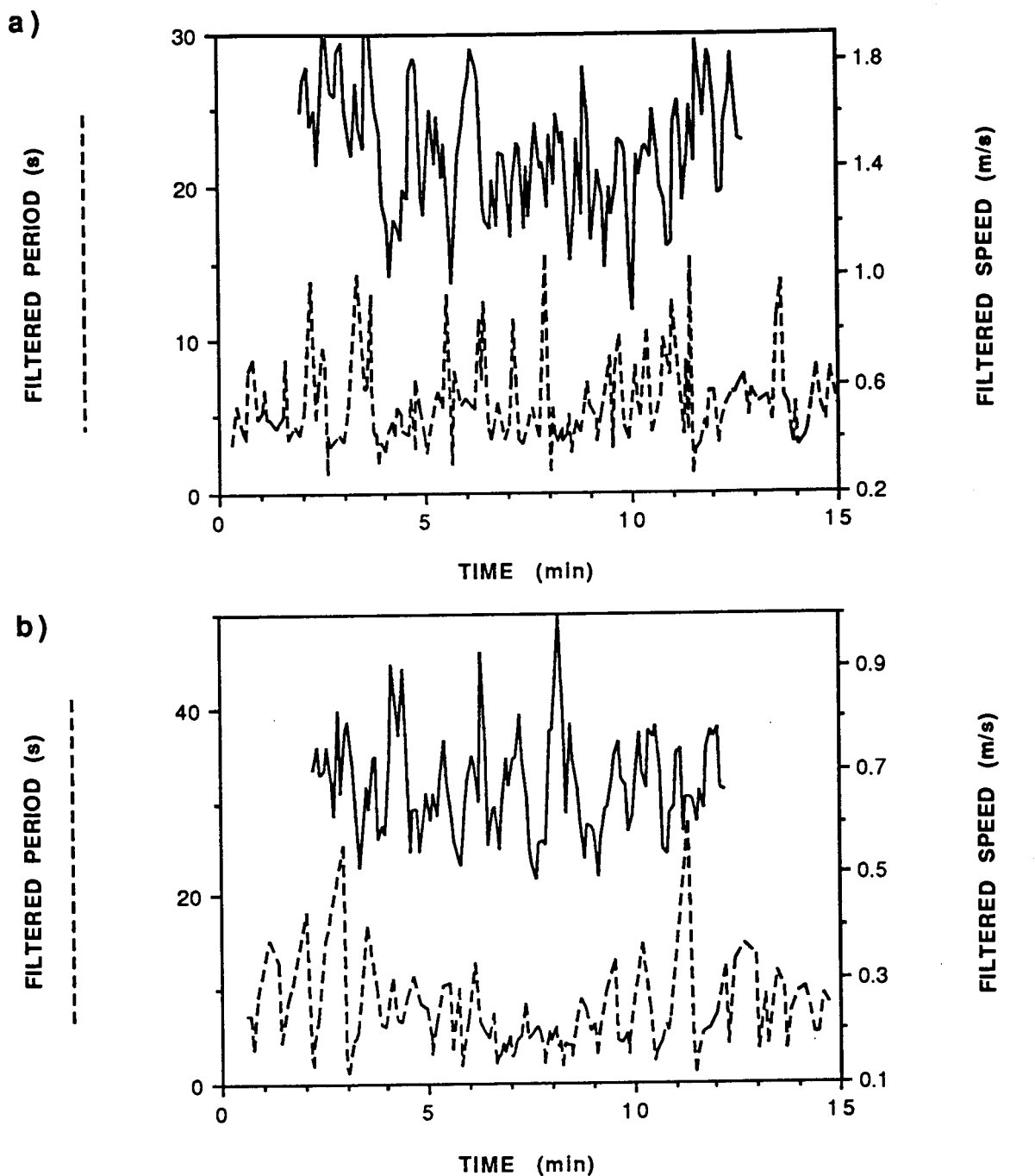


Fig. 6.23- Comparative plot of filtered boil period and current-speed time series:

a) June 18 1355-1410

b) June 23 0800-0815

Two techniques for obtaining these paired samples were employed. Since the current speed was sampled at 5 second intervals, the number of boils erupting at the surface within each 5 second interval were counted. The other technique was to interpolate the current speed for each boil, and correlate these values with the period between each boil.

From the first technique, the correlation between the number of boils per 5 seconds and the current speed was not strong. It was not improved by correlating the number of boils per 10 or 20 seconds with the average speed per 10 or 20 seconds respectively.

Correlation coefficients did not exceed 0.35, and the time lag of maximum correlation coefficient occurred over a wide range of values for each site. The lags calculated are seemingly unrelated to the spatial separation of the measurement sites of the time series with respect to the mean current-speed. It was noted that the range of values determined for the number of boils per 5, 10 or 20 seconds was typically quite small, so it was postulated that interpolation of the current speed for each boil would produce a stronger correlation. In fact, the correlation coefficients generally diminished, with none exceeding 0.3, and again, no apparent pattern in the lag values.

6.4- DISCUSSION

6.4.1- Quantitative analyses of boil parameters

In order to quantitatively assess the presence, morphology and intensity of Type 1 and 2 boils, a variety of graphical analyses were utilized. For both boil types, it was concluded that their presence and intensity were related to tidal conditions on semi-diurnal and fortnightly scales. Type 1 boil intensity was related to bedform parameters, which in turn are influenced by the hydraulic and tidal variables. Attempts to relate the dominant Type 1 structure observed within a reach to the bedform parameters and water depth were not conclusive. The cauliflower and roller structures were limited to specific relative

roughness and depth domains which were consistent in all three reaches. The Coleman/Jackson structures could also be noted within these domains, so there may be some degree of randomness involved or perhaps dependence on variables not measured such as secondary circulation or bedform shape. Gabel (1993) related the size and vigor of boil eruptions to the curvature of dune crestlines.

For calculation of the average period between Type 1 boil events, the duration of measurement (and subsequent averaging) was the lifespan of the production site. The boil periods do not become progressively shorter or longer as a production site ceases; it is an abrupt ending that may be concluded with a few boils of diminished strength. All Type 1 boil-period time series were found to be positively skewed, and only one displayed bimodality. Based on the chi-square analysis, the majority of the time series were concluded to be log-normally distributed. A log-normal distribution has been used to describe the distribution of periodicities of turbulent phenomena in previous studies of bursting in flume studies (Rao et al., 1971; Nakagawa and Nezu, 1977; Ikeda and Asaeda, 1983) and boils in rivers (Jackson, 1976; Kostaschuk and Church, 1993).

Those time series that were obtained from video footage were all found to have frequency distributions which could be repeated with subsequent digitization based on the results of the chi-square test. The quality of video records of the macroturbulence was noted to be strongly dependent on the weather and lighting conditions during filming. The problems with video quality had also been noted in previous studies (e.g. Drake et al., 1988), and the reliability of the data obtained in less than ideal conditions was questionable. In fact, the frequency distributions of Type 2 boil periods was found to be non-repeatable for several time series obtained during poor weather or lighting conditions. These time series were removed from the analysis, and the records were not

analyzed further. The trends which the removed time series shared with the time series that remain are noted.

The frequency distributions for all Type 2 boil period time series displayed a positive skewness. Histograms displaying a bimodality were restricted to the R/B U/S site, with one exception at the R/B D/S site. As noted by Kostaschuk and Church (1993), turbulent phenomena in a wide variety of environments have been found to be positively skewed (e.g. Jackson, 1976; Ikeda, 1980; Thorne et al., 1989), often exceeding skewness values of 2.0 (Williams et al., 1989). Bimodal distributions have been found in a variety of studies (e.g. Fukuoka and Fukushima, 1980; Ikeda, 1980; Kostaschuk and Church, 1993), but explanations among researchers vary.

Fukuoka and Fukushima (1980) propose that boil production depends on a concentration and subsequent release of vorticity in the boundary layer. They imply that there is some critical level of boil strength which once exceeded, induces more frequent boil production. More recently, Kostaschuk and Church (1993) postulate that the histogram may be divided into two subpopulations with periods that can be approximated by using different length scales in Strouhal's Law. The shorter-period subpopulation utilizes length scales based on dune height and is noted to be associated with persistent wave instability on the lee side of dunes. The longer-period subpopulation utilizes length scales based on the internal boundary layer (two to three times the dune height), and is believed to be associated with intermittent ejections from this boundary layer.

Dyer (1986) notes that the length of time over which turbulent phenomena are averaged is crucial, but some researchers (e.g. Jackson, 1976) do not justify their choices. As well, the appropriate speed and length scales to be used in the calculations are still uncertain. The surface velocity has commonly been employed for the speed scale, but the length

scales have included water depth (e.g. Ikeda, 1980), mean bedform-wavelength (Jackson, 1976) or height (Itakura and Kishi, 1980).

These hypotheses could not be examined for the Type 2 boils since the height of the obstructions producing the boils could not be estimated. In fact, the range of the Type 2 mean boil periods was quite limited. There was a range of 3-8 seconds at the R/B, and slightly shorter periods with a smaller range at the L/B.

A limited analysis of the applicability of the Strouhal Law was performed for the Type 1 boils, producing inconclusive results. At current-speed measurement station 2, the predicted length scales based on U_{sfc} underestimated the depth in both instances. Using the speed at $0.7d$, the predicted length scales are within 2-4 times the bedform height. For the lower estuary sites, utilizing U_{sfc} produces length scales which exceed the depth in all but three cases. In all three instances, the river bed was essentially planar except for scour holes which were propagated downstream. For all three, the predicted length scale approximates the depth of the scour hole quite well.

Only a few comparative measures of current speed at $0.7d$ were collected and all have predicted length scales which exceed the dune height by a wide margin. These length scales, and those based on U_{sfc} which also overestimated depth, may in fact be estimates of the bedform wavelength. This postulation cannot be tested with certainty since the wavelengths are not known. However, the heights are known, and if one assumes a bedform steepness of .03-.06, the length scales are similar to the estimated wavelength. This finding and the one noted in the previous paragraph may be fortuitous, but if not, it implies that there may be mechanisms other than those addressed by Kostaschuk and Church (1993) which can generate boil activity.

Based on data from this research, and from values presented in Jackson (1976) and Kostaschuk and Church (1993), there appears to be a relation between the relative roughness and the boil period. As relative roughness increases, the boil period diminishes rapidly, becoming asymptotic at $RR > 0.2$. This invariance in the relation beyond $RR = 0.2$ may explain why Korchokha (1968) concluded that boil period is invariant with depth. In fact, Rood (1980) postulated that Korchokha's observations may have been related to bedform properties. Although there is much scatter, it also appears that there may be separate curves for Jackson's data, and that of Squamish River estuary. This curve displacement may be physically based (ie. grain size or water viscosity), or related to differences in averaging times of boil periods. Regardless, this general relation has not been reported previously and deserves future study.

The scatter in the relation may also be a function of the number or strength of secondary upwellings. However, attempts to relate the number of secondary upwellings to the boil period were not successful. Again, this may be related to bedform shape or some other unknown factor.

Kostaschuk and Church (1993) suggest that the presence of boils in lower Fraser River estuary is related to the advance and retreat of a saline body of water near the bed. Extreme seasonal fluctuations in water salinity have been noted in Squamish River estuary: 27 ppt in Winter and < 4 ppt during Spring and Summer. Although the upstream penetration of saline water depends on the tidal and discharge fluctuations, when Q exceeds $500 \text{ m}^3/\text{s}$, the salt wedge does not penetrate the river mouth (Levings, 1980). Similar findings were put forth by Smythe (1987). In fact, the progression even a few kilometers upstream may require discharges much lower. Water samples collected at discharges between 395 and $525 \text{ m}^3/\text{s}$ and at a variety of tidal heights during the Spring-

neap cycle suggest that the intrusion and retreat of a body of saline water did not influence boil presence during the study period.

Attempts to estimate the size and expansion rates of both Types of boils based on low-level photographs met with a variety of difficulties. Resolving the problems described for Type 1 boils may simply require a taller, more lightweight pole with a wide-angle lens on the camera. However, for both boil Types, low-altitude balloon photography may be more appropriate with respect to required elevations and stability. If lighting and weather conditions allowed, photos from elevations exceeding 10m may even capture several boils simultaneously. With this type of data, quantitative estimates of boil densities over an area of the water surface could also be obtained. Coleman (1969) notes the value of aerial reconnaissance for observing patterns in macroturbulence on the water surface, but of course, the optimal techniques depend on the scale of the features studied.

Studies of boil periodicities to date have concentrated on obtaining a mean value over some time span and then attempting to scale this value with other measured hydraulic variables. To my knowledge, the plot by Kostaschuk and Church (1993) is the only presentation of boil-period time series in any previous studies. Their plot and the data presented in section 6.3 indicates that patterns noted in the Type 2 boil time series may fluctuate on temporal scales similar to the current-speed time series.

6.4.2- Comparison of speed and Type 2 boil-period time series

From comparative plots of the time series, there were several corresponding patterns which were noted. The peaks in the boil-period time series correspond to troughs in speed at the R/B U/S site, and to troughs (and perhaps peaks) in speed at the R/B D/S site. A lag of boil-period changes after current-speed fluctuations was noted in some time

series at the R/B U/S site, as expected from the separation in measurement sites. The times of weak boil activity seemed to be more exclusively associated with the times of low current speed at the R/B U/S versus the R/B D/S site. It may be fortuitous, but both the R/B U/S and the L/B D/S sites are within the Type 2 boil transportation zones rather than the production sites.

It was noted that the upwellings seemingly induced by the Type 2 boils within the transportation zone consist of the rollers and the Coleman/Jackson structures. At the Type 2 boil production sites, the upwelling is slowly stretched downstream but continues upwelling for several seconds before 'detaching' as a discrete structure. During digitization of the video footage, it was the period between successive upwellings that was timed, but the proportional duration of the upwelling within that period could be quite variable. This variability in upwelling duration was also noted at the transportation zones, but upon arrival at the surface, the structure is inevitably swept downstream rapidly, and the duration of the upwelling seems to depend on energy sources unrelated to its original locale.

It is not known if the physical mechanism(s) which create(s) the upwellings within the Type 2 boil transport zones are even partially attributable to the agglomerations themselves, or if they are created by the same mechanism(s) creating the boils in reaches 2, 3 and 7, and the lower estuary. The variable nature of the upwellings between the Type 2 production and transportation sites however, may imply differing production mechanisms.

The production sites of Type 2 boils are limited to the concave bank during strong currents, and it is under these conditions that a strong helical flow component may be expected. Several figures presented in Thompson (1986) based on flume studies and

field observations indicate secondary flow and bed morphology patterns similar to those observed in Squamish River estuary. Tamai et al.(1986) conclude that a shear layer in the lateral velocity profile will shed eddies periodically, but the production sites of Type 2 boils were always in the wake of an obstruction. This obstruction could presumably deflect helical flow towards the surface, particularly if the obstruction has trapped sediment and other material on its upstream face. Whether the Type 2 boil eventually stretches, diffuses or segments may also be related to the strength of a helical flow component. The rotation within the Type 2 boils that had been attributed to lateral shear could also be imposed by the helical flow at the production site. Observations made to test this hypothesis proved inconclusive.

Figures 2 and 4b in Thompson (1986) display tight helical cells along the concave bank which produce several sites of upwelling. In Squamish River estuary, there were 4-6 sites of Type 2 boil production per concave bank, each separated by several hundred metres. They remained essentially stationary on a daily basis but were noted to shift position in late July and August, 1992. This variability may be attributed to variations in the length of the helical flow as discharge diminished (Thompson, 1986). However, it is more likely related to changes in bed morphology, channel obstructions, or lateral erosion which were all observed in late summer.

Summarizing the postulation, the upwellings at the production sites along the concave banks may be related to helical flow, and subsequent upwellings within the transportation zone could be (at least partially) produced by the Strouhal Law-governed perturbation of a wave-like oscillation travelling with the current . Unfortunately, this notion cannot be conclusively proven with the data collected. Fukuoka and Fukushima (1980) conclude that 'flow separation induces intensive ascending currents which in turn aspire to bring forth new ascending currents'. However, the interaction of flow separation and helical

flow cells with the wave-like oscillation proposed by Levi (1983a,b) is unknown. Our knowledge of secondary flows is still incomplete (Allen, 1985), and the study of boil-generation mechanisms is still in its infancy. It may even be possible that sites of unexplained consistent boil production noted in previous studies (e.g. Lane, 1944; Kostaschuk and Church, 1993) are related to some persistent secondary flow cell.

Previous studies of turbulent phenomenon found that burst frequency could be scaled by $U/2\pi d$. Levi (1983b) postulated that this was not a primary property of the bursts, but rather the result of an outer oscillatory perturbation of wavelength $= 2\pi d$ as governed by Strouhal's Law. Such a perturbation would have a wavelength $= tU$, therefore assuming that d remains constant, boil period must be inversely proportional to current speed. Thus, the times of high current-speed should produce short boil periods, and the troughs in current speed would correspond to the peaks in boil period. This hypothesis implies that the shifts in mean current-speed are controlled by some independent factor(s).

An alternative proposal depends not only on the Strouhal Law, but assumes that there is some critical level of boil activity which, once exceeded, creates such resistance to flow within the water column that the mean current-speed is diminished (this component of flow resistance is known as impact resistance). Then, once the current speed decreases to the point that the boil activity (quantified as the boil period) slackens and offers less resistance to flow, the current speed will begin to increase again, and the cycle repeats. Such a feedback relation would be highly complex over a variety of temporal and spatial scales. Generally, the current speed would be expected to increase slowly, but diminish rapidly once that critical level of macroturbulence is exceeded. The peaks in current-speed would still correspond to the troughs in boil-period, but there would be identifiable patterns in the time series that this hypothesis could explain. Such patterns were noted in Figs.6.21a and 6.23a,b, but these findings are quite tentative and require much more

study. Notions similar to this hypothesis have quietly existed in the fluvial literature for some time.

McQuivey (1973b) postulated that bedforms and the magnitude of resistance to flow in alluvial channels seem to be byproducts of turbulence. Subsequently, Jackson (1977) proposed that long-period oscillations in current speed may be related to dunes, or perhaps even bursting. The data of Tiffany (1950) indicates that of the three sites of simultaneous measure of current-speed and pressure-fluctuations near the river bed, it was not the site with the highest mean current speed that produced the greatest speed fluctuations, but the one with the maximum changes in pressure. This variability in pressure may be attributable to macroturbulent phenomena.

Qualitatively, it may be concluded that the boil activity is a maximum in the few hours preceding and following LLT, but to quantify a precise time based on surface observations would be difficult. Complexities include the intermittency, bedform lags and the relation of boil activity to discharge fluctuations and tidal conditions over the Spring-neap cycle. Such an endeavour would require reliable data obtained over a wide range of conditions. The reliance on adequate lighting and weather conditions further complicates data collection.

Unfortunately, a general relation between boil period and current speed is not obtainable due to the narrow range of speed values in which this technique could be utilized. Based on the results obtained, however, the existence of such a relation seems questionable. From Figs.6.20-6.23, the variation in boil-period seems only partially attributable to variations in current-speed, and the applicability of Strouhal's Law may be questionable. The fluctuations in the time-series on the order of a few minutes appear to correspond,

but there may be some independent longer-scale variability in current-speed, perhaps related to channel geometry or meander wavelength.

Lapointe (1992) attempted mathematical cross-correlation between time series of estimated suspended-sediment concentration and vertical flow velocities. Even though the records appeared well correlated, the R^2 value was only 0.31. Lapointe claimed that this rather weak level of association is not unusual in turbulent mixing. In this chapter, visual comparison suggested that the local minimas and maximas in the time series were correlated, but the absolute maximas and minimas in either time series were rarely correlated. It may not be the magnitude of current-speed and boil-period which are linked, but perhaps the *change* in the magnitude. The applicability of Strouhal's Law when high amplitude and/or low frequency fluctuations in current speed are present is debatable. Such a hypothesis cannot be addressed by the data collected in this study, but should be examined in future research. It is also uncertain if Strouhal's Law appropriately describes the periodicity of all non-continuous, discrete macroturbulent phenomena displayed in natural flows. Past studies invoking the Strouhal Law to describe boil periodicities (e.g. Znamenskaya, 1962; Jackson, 1976; Kostaschuk and Church, 1993) seem to refer to Type 1 boils.

6.4.3- Postulated boil-production mechanisms

The bedform qualities were found to be poor descriptors of the intensity of Type 2 boils. Alternatively, the water-surface slope and current speed were hypothesized to control the presence and intensity of these structures. Based on the results of this chapter, and from field observations and video footage, it is apparent that some simple scaling relation between water-surface slope and boil intensity is unlikely. This conclusion is based on fluctuations in boil intensity on scales of several minutes which the water-surface slope

does not exhibit. Although such fluctuations are noted in the time series of current-speed, the complexity that such a relation may exhibit was apparent. Thus, it was not surprising that the correlation of a 'maximum observed intensity' to a current speed collected over a 30-second period (section 6.3.2.1) would not be strong. The correlation between the intensity and the nine-minute mean current speed at 0.7d was not significantly better.

All four current-speed measurement sites along the concave bank exhibit the most intense boil activity near LLT. However, for only the R/B U/S and L/B D/S sites, intense boil activity seems to preferentially concentrate in the early flood tide. This lag may be explained by the hysteresis in turbulent intensity with respect to current speed (e.g. Gordon, 1975b). As well, in the deeper reaches (1, 4-6), bedform wavelength may respond more slowly than height to changing hydraulic conditions, producing a lag (e.g. Fig.6.14a). The lags may also be related to properties of the boil activity at these sites compared to the R/B D/S and L/B U/S sites (section 6.4.2). Unlike the Type 2 boils, Type 1 boils seem closely related to bedform wavelength and height.

From the comparative plots of w , h and d using the intensity of macroturbulence as a differentiator, several interesting findings are noted. For w vs. h , the separation of the data at $h=0.5-0.6\text{m}$ was strongly recognized in reaches 2, 3 and 7. There was a strong linear structure and decreased variance in the data greater than the critical height. It is postulated that once bedform height exceeds this critical level, troughs begin to be scoured and steepness increases markedly. The values of steepness that are found seem exceedingly high compared to previous studies. This is attributed to the fine sediment, high discharges, a large ratio of tidal amplitude to estuary depth, and a relatively narrow estuary width at low tide resulting in extremely high shear at the bed (as noted in Chapter 4, accurate measures of shear were not obtainable). Once the three-dimensional bedforms create separation zone vortices and detached rollers, sediment is entrained in the

macroturbulent features. This may be controlled by current velocity but the data cannot shed light on this.

Increased steepness has been related to the formation of scour pits in the lee of the bedforms and increased three-dimensionality (Green, 1975; Dalrymple et al., 1978) and scour pits have been found to increase with high Spring tides (Terwindt and Brouwer, 1986). Znamenskaya (1963) relates the occurrence and intensity of macroturbulence to dune steepness and Froude number, and found that for macroturbulent features to be noted at the surface, S had to exceed 0.04. Terwindt and Brouwer (1981) concluded that tidal bedforms with $S > 0.044$ will be three-dimensional. The evolution of tidal bedforms from two-dimensional to three-dimensional, with grain sizes between 0.2 and 0.5 mm, was found to occur at a peak depth-averaged current-speed of 0.8 m/s (Dalrymple et al., 1978; Terwindt and Brouwer, 1986). This finding could not be examined with the data collected in this study.

On Aug 25, 1993, particularly low discharges exposed portions of the bed within the estuary that were typically covered with a metre of water at LLT during maximum Spring tides. Approximately 1-3 hours previous to the bed exposure, boils were noted above the bed, occasionally entraining sediment. The photos show prominently two-dimensional forms, but there are some sinewy crestlines with gravels in the dune troughs, and scours in the lee which may have been the dunes producing the sediment-laden boils (Fig.6.24).

Ikeda (1980) noted that as ripples become three-dimensional, the amount of sediment put into suspension increases ten-fold without an increase in shear velocity. Similarly, Ikeda and Asaeda (1983) found increased sediment suspension in the lee of bedforms as they become three-dimensional. Coleman (1969) noted that the surface turbulence is more prevalent when scour exists in the lee of bedforms. Korchokha (1968) and

a)



b)



Fig. 6.24- Bedforms exposed on inter-tidal area:

- a) Dominantly two-dimensional (looking downstream)
- b) Scour holes and spurs observed in region of intense boil activity before exposure (note wristwatch for scale in lower left corner; river flow was from left to right)

Znamenskaya (1963) conclude that 'eddy formations' (ie. boils) require 'warped dunes', but also act to shape the warped dunes in a feedback mechanism. A similar idea by Yalin (1977) theoretically related the average path-length of macroturbulent eddies to dune wavelength, and Jackson (1976) echoes the idea of a feedback mechanism between bursts and bedforms.

From w versus d , sediment entrainment within the macroturbulent features may be related to $RR > 0.8$ for reaches 2 and 7 and $RR > 0.25-0.35$ for reach 3. Furthermore, it seems that most sediment-laden features occur when the depth of water is below some critical level. A similar hypothesis for reaches 1,4-6 was suggested, but at a less-shallow depth.

For d versus h , reaches 1 and 6 do not display any patterns of Type 2 boil intensity with RR or depth. Data of reaches 4 and 5 suggest a $RR > 0.1$ separative (for intensities entraining sediment and organics), but more apparent is the dependence of these features on the depth of water. However, reaches 2, 3 and 7 display a gradation of decreasing Type 1 boil intensities with decreasing relative roughness.

Sediment-laden features are noted most strongly with $RR > 0.2$. However, as RR decreases, a 'gap' in the sediment-laden features between $d=2.3-3.5\text{m}$ for reach 3 and $d=2-3\text{m}$ for reaches 2 and 7 is noted. The sediment-laden features at the greater depths correspond to conditions of high discharges (Appendix 2.4). For reaches 2-5 and 7, if the models from Chapter 5 predict $h > 0.5-0.6\text{m}$ and depths less than the critical depth for any particular reach, it should be expected that macroturbulent features will be seen to contain sediment at the surface. However, the sediment-laden features found at greater depths than expected (from bedform height) are surely related to bed scour once discharges

reach $650 \text{ m}^3/\text{s}$. Thus, these models should be utilized cautiously when Q meets or exceeds such levels.

The dependence of the sediment content of boils on flow depth may explain the finding of Rood and Hickin (1989) that the sediment content of boils will be greater during decelerating flows. The hysteresis noted may be related to the current speed peaking two hours before LLT, but the water depth continuing to diminish because all data was obtained on the ebb tide.

Similar results based on features identified on the graphic-output of the transects were noted, although the RR and RRS separatrix are at slightly lower values than those identified from the surficial Type 1 boil observations. Similarly, the separatrix noted at $h=0.5\text{-}0.6\text{m}$ is instead found at $h=0.3\text{m}$. This may indicate that sediment entrainment within such features actually begins once $h>0.3\text{m}$, but for it to be noted at the water surface, larger dune heights are required. Thus, the sediment-laden features noted at the surface are a truncated sample of those features below the water surface from sonar inspection. A similar finding for kolks based on comparative techniques of sonar versus current-speed excursions was noted by Kostaschuk and Church (1993).

From my findings, the critical parameter for Type 1 boil intensity would seem to be relative roughness, but the dune steepness also appears to be crucial. Robert and Richards (1988) conclude that since bedforms tend towards a steepness which maximizes flow resistance (e.g. Yalin, 1977; Davies and Sutherland, 1980), determination of flow resistance should rely on the relative roughness.

As noted in section 5.1, estimating the form resistance component of the flow resistance from bedform parameters is still an enigma. The portion of the stress which is carried by

form drag is related to bedform steepness and flow separation, with several studies concluding that maximum resistance to flow of bedforms occurs when $S = 0.075-0.1$ (Dyer, 1986). It seems quite likely, however, that a significant amount of flow resistance within the water column would be related to the macroturbulent features, which are related to the bedform parameters. Korchokha (1968) concluded that maximum flow resistance occurs several days after maximum discharge, but relations with bedforms or macroturbulence were not made explicit. Tamai et al. (1986) noted that when large eddies are present in open channel flow, the additional resistance decelerates the flow, reducing the discharge capacity of the channel by up to 15%. Matthes (1947) concluded that macroturbulent features such as boils and pulsations represent expenditures of energy in overcoming channel roughness. Although this chapter has contributed quantitative evidence to associate Type 1 boils and relative roughness, links between Type 2 boils and current speed and/or secondary flow patterns have also been suggested. At this stage, there are still far more questions than answers.

CHAPTER 7- CONCLUSION

7.1-SUMMARY OF FINDINGS

The main research objective of this thesis was to relate macroturbulent properties observed at the surface to the hydraulic and bedform parameters in Squamish River estuary. This study was designed to address the main objective by inspecting specific components of the interrelations between flow hydraulics, bedforms and macroturbulence. It is the principal task of this final chapter to revisit the questions posed in Chapter 1, and to consider the extent to which they have been answered by evidence presented in Chapters 3 to 6:

1) Is there evidence of more than one type of boil in Squamish River estuary?

Based on qualitative observations, there are at least two distinct types of boils in the study area. Type 1 boils are noted in the lower estuary and where the thalweg crosses from the left to the right banks. Boil production is typically intermittent, but periodic when present. The production sites have durations of less than 10 minutes, and the boil morphologies either follow the Coleman /Jackson model, or appear as 'rollers' or 'cauliflower' structures.

Type 2 boils are noted where the thalweg moves alongside the outside bank. The production sites are in the wakes of obstacles; the four to six dominant production sites along each bank are separated by several hundred metres. These production sites remained relatively unchanged throughout the research period. As the upwelling arrives at the surface at the production site, it is stretched downstream for several seconds before detaching. As it is advected downstream, it is revitalized with numerous upwellings such that it becomes a boil 'agglomeration'. Its size and shape fluctuate with each upwelling, and these upwellings include rollers and Coleman/Jackson structures.

2) Can current speed, water-surface slope and water depth at various sites in the estuary be reliably predicted based on multivariate regressions?

Multivariate regression analyses of current speed and depth yielded many interesting findings, but only the models for depth are recommended for predictive use. Short-duration slope changes which are not attributable to discharge or tidal fluctuations introduced much unexplained variation and a regression analysis was not attempted. Limited sample sizes and data ranges may have biased the current-speed models, but another concern was the variability in current speed over short periods. At 0.7d from the surface, the required duration of current-speed measurements necessary to approximate the long-term mean was highly variable between measurement sites, and over short temporal scales at a site. Graphical analyses of current-speed time series indicated periodicities over temporal scales ranging from a few multiples of the sample interval to several minutes. There were also patterns of slow, unsteady increases in speed followed by rapid decreases. These patterns were discussed in Chapter 6.

The speed and depth models suggest that there are regions in the estuary (related to proximity to the river mouth) with hydraulic characteristics controlled by specific independent variables. This regionality is most strongly noted on the ebb tide, but some patterns persist into the flood tide. In the predictive models of current-speed and water-depth, the importance of Q decreases in the downstream direction, while the importance of D increases. The importance of T is greatest in the middle reaches of the study region for current-speed models, and in the upstream reaches for depth models.

3) Can bedform height and wavelength in various reaches in the estuary be reliably predicted based on multivariate regressions?

The multivariate regression analyses of bedform height and wavelength produced models recommended for predictive use providing channel morphology remains unchanged. When Q exceeds $650 \text{ m}^3/\text{s}$, bed scour may take place and the model reliability diminishes. The most important explanatory variables in the models seem related to the ability of the bed to respond quickly to changes in water depth. For predicting bedform height, the models of the shallow reaches near the thalweg crossing describe the data well and are dominated by D . The models of the deeper reaches near the outside banks have the most variation in h explained by LTH . Previous studies suggest that bedform w requires more time to respond to changes in hydraulic conditions than h . This is confirmed here, with LTH explaining the most variation in w for all reaches except the shallow #3. The poorer fit of the w models compared to the h models is likely related to bedform lag effects continuing over several tidal cycles. The importance of the fortnightly tidal cycle is also highlighted by examination of the outliers in the models of h and w . Almost every outlier occurred at times when the diurnal tidal drop was a maxima or minima in the Spring-neap cycle.

4) Can lags in bedform wavelength and height behind changing hydraulic and tidal conditions over a variety of temporal scales be identified?

The lags in bedform parameters occur on a variety of temporal scales, and they are difficult to separate. The lag related to the freshet cannot be isolated since there are short-term, high-magnitude fluctuations in discharge superimposed on the seasonal trend. Investigation of lag on fortnightly tidal scales suggested that bedform parameters were larger on the rising limb of the Spring-neap cycle than on the falling limb. This is contrary to physical reasoning, but two analyses produced consistent results. On the semi-diurnal tidal scale, the lags in h and w after LLT increase with increasing D , and peak bedform-height appears to occur sooner after LLT than peak bedform-wavelength.

5) Can properties of the macroturbulence noted at the surface be related to bedform and hydraulic parameters in Squamish River estuary?

Several notable findings were produced by differentiating the plots of bedform parameters and water depth by boil intensity noted at the water surface. For reaches 2,3 and 7, plots of w vs. h become strongly linear at $h > 0.5-0.6\text{m}$, and there is little variance about the best-fit line. Also, sediment is entrained in the boils noted at the surface once this critical h is exceeded. I suggest that when h exceeds $0.5-0.6\text{m}$, bedform troughs become scoured, and the steepness increases markedly as the bedform becomes three-dimensional. These relations do not apply in reaches 1 and 4-6, presumably because the Type 2 boils have a generating mechanism unrelated to bedforms, or because the lags were large.

For reaches 2,3 and 7, plots of w vs. d suggest that most sediment-laden boils occur when d is less than some critical depth for the reach. Similar, but more poorly defined relations are present in reaches 1 and 4-6. Plots of d vs. h yield findings similar to the previous analyses, again best defined for reaches 2,3 and 7. If the regression models predict $h > 0.5-0.6\text{m}$ and $d < d_{\text{crit}}$, it is expected that the macroturbulent features will be seen to contain sediment. This finding is less reliable when Q exceeds $650\text{ m}^3/\text{s}$. Attempts to relate the dominant observed Type 1 structure to the bedform height, wavelength and water depth were not conclusive. Although the cauliflower and roller structures were limited to specific relative roughness and depth domains (which were consistent in all three reaches), the Coleman/Jackson structures were also noted in these domains. There may be some degree of randomness involved, or dependence on factors not considered (e.g. bedform shape).

The applicability of the Strouhal Law could not be examined for the Type 2 boils since neither the height of the obstructions nor the water depth at the site of boil-production could

be estimated. For the Type 1 boils, the results varied depending on the current-speed measure employed. When $U0.7d$ was used, some predicted length scales were within 2-4h. Using U_{sfc} (and some $U0.7d$ measures), when the predicted length scale exceeded depth, it may actually be an estimate of bedform wavelength. As well, for scour holes observed to shed boils, the length scale described by Strouhal's Law was similar to the depth of the scour hole. The results suggest that there may be several mechanisms of boil production associated with the various length scales predicted by Strouhal's Law.

A relation not noted in previous studies of macroturbulence is that as relative roughness increases, the Type 1 boil period diminishes rapidly. As $RR > 0.2$, boil period becomes asymptotic with the period = 1-10s. Although the plot displays some scatter, a rating curve such as this may prove more useful than models which require measurements of current speed, depth or bedform parameters. The scatter may be due to integration of data from dissimilar environments; the plotted data of Jackson (1976) is displaced from the data of Squamish estuary by approximately 5 seconds.

It may be that patterns in the simultaneous time series of Type 2 boil period and current speed indicate that boil periodicity is not governed by current speed, but that boil activity may also influence current speed in a feedback-type relation. Perhaps once some critical level of boil activity is exceeded, there is such resistance to flow within the water column that the mean current-speed is diminished. As a result, boil activity soon decreases and the macroturbulence offers less resistance to flow to be succeeded in turn by current speed increases and greater boil activity, and the cycle repeats. These findings are highly speculative, and it cannot be definitely ascertained if the current-speed fluctuations are produced (or influenced) by intense boil activity, or if they are independent of boils.

7.2- DISCUSSION AND SUGGESTIONS FOR FUTURE WORK

Complex and inter-related processes are in operation in an estuarine environment, and analyses of the fluvial and tidal activities must consider all relevant factors- including interactions with bedforms and macroturbulent phenomena. The simplistic engineering studies completed in the 1970s in Squamish River estuary must be avoided. For instance, a study by Zrymiak and Durette (1979) was performed to monitor the impact of the water diversion and dredging on the lower estuary. The conclusions were based on bed survey differentials, but there were only three surveys taken over five years, with no consideration of:

- tidal effects (diurnal or fortnightly scale)
- bed scour or fill related to high Q levels
- bedforms (heights may be >> measured differentials in some reaches)
- required length of time to complete the survey
- variability of water-surface slope within the 5 km study area

As a general recommendation for future studies, not only must all the above-listed factors be considered, one should also not assume that relations established in previous studies will persist indefinitely.

It was disappointing that quantitative estimates of the size, expansion rates and densities of boils over some surface area could not be obtained. Such measures would not only be useful for elucidating boil geometry relations and production mechanisms, but scaling relations with several variables (e.g. T, D, h, w, U) may be possible. Attempts to estimate boil size and expansion rates from low-level photographs met with a variety of difficulties. It is likely that low-altitude balloon photography would be most appropriate to meet the elevation and stability requirements. Boil densities would also be useful in association with measurements of the sedimentary-content of boils.

It is apparent that the injection of sediment in discrete packages (such as boils) to levels above the bed creates suspended-sediment transport that is not well described by general eddy diffusion theories of sediment suspension (e.g. Rouse, 1937). The diffusion-based theories are the preferred means of predicting the concentrations of suspended-sediment in open channel flow, having been found reasonably accurate both in lab and field studies (Pizzuto, 1984). However, the application of such theories in flows which do not display a characteristic decrease in suspended-sediment size nor concentration away from the bed must certainly be questioned.

Analyses of the sedimentary content of boils might ultimately allow prediction of sediment-transport rates when these macroturbulent features are present. Such an analysis should seek quantitative estimates of the sediment concentration and texture within boils as a function of the boil parameters (e.g. type, size, presence of secondary upwellings, time after initial upwelling), hydraulic and tidal variables, and the location within the estuary. Although Hickin (1989) produced predictive models of average sediment-fluxes through Squamish River estuary on an annual and seasonal basis, estimates on a daily or flood-event scale may also be possible.

Pizzuto (1984) concluded that further study is required to develop accurate models of sediment-suspension for natural streams with sandy, dune-covered beds. Kalinske (1943) suggested that turbulent fluctuations in rivers are more important than mean flow-parameters in predicting sediment entrainment and suspension. Future theories of sediment-suspension in a fluvial or estuarine environment must include some consideration of macroturbulence.

The critical parameter for determining whether macroturbulent features in Squamish estuary entrain sediment seems to be the relative roughness. As well, several studies suggest that relative roughness is the key parameter for describing the flow resistance in open channel flow when bedforms are present. However, Kinori and Mevorach (1984) point out that, in deformable channels, the parameters affecting flow resistance are interrelated and not easily separated for independent analysis. They claim that the experimental information remains inconclusive with large scatter, and that proposed analytical methods are unreliable. Several findings in this thesis suggest that a greater understanding of macroturbulence may improve the estimation of flow resistance in natural channels with bedforms.

The dependence of Type 1 boil periodicity and sediment content on bedform parameters suggests that observations of surficial boil characteristics may provide efficient and inexpensive estimates of both the macroturbulence intensity within the water column and the relative roughness. This may then lead to estimates of the flow resistance. Gabel (1993) emphasizes that the relations between water flow, sediment transport and dune geometry are poorly understood, and are fundamental for prediction of flow resistance and sediment transport rates. Hypotheses incorporating macroturbulence certainly deserve future investigation.

A greater knowledge of bedform lag would not only aid in the analyses described above, but would also improve predictions of river stage during flooding. This will require measurement periods shorter than any temporal scales of variability of relevant factors, at a sufficient intensity and duration compared to discharge (and, if necessary, tidal) fluctuations. Gabel (1993) recommends defining dune lag as a geometrical deviation from equilibrium conditions rather than as a temporal difference between maximum discharge and maximum bedform-height or length. The costs of such studies may be prohibitive.

The notion that more than one type of boil, or more than one boil-generating mechanism could exist has been suggested in many previous studies. It is only recent studies such as Rood and Hickin (1989) and Kostaschuk and Church (1993) that approach the topic quantitatively. The findings in this thesis suggest that Type 1 boils may be produced by a Strouhal-Law governed mechanism, and Type 2 boils may be dependent on helical flow. Type 1 boil-morphologies and periodicities also imply that Strouhal's Law could predict a variety of length scales- each of which may be the result of specific production mechanisms. Examination of bedform shape on intertidal areas where macroturbulent features are noted previous to bed exposure may also be useful. Frequency distributions of boil-periods may also offer boil production insights.

Many of the postulations of this chapter regarding boil production and feedback relations with bedforms and hydraulic parameters are based on inconclusive data, and require further field work to confirm or refute. With the extensive lateral erosion presently occurring in Squamish River estuary, it is questionable whether the specific predictive models produced for hydraulic and bedform parameters will remain applicable. It may also be advisable for future studies to avoid the estuarine environment. The complexities of bedform lag induced by tidal fluctuations may outweigh the benefits of a concentrated boil production at certain stages in the tidal cycle. A sand-bed river with a hydrologic regime dominated by a single, high-magnitude snowmelt event may be ideal.

Observations suggest that boils are common amongst high-energy sand-bed rivers. There is still much to be discovered about the importance of these macroturbulent features to the fluid dynamics and sediment transport of rivers and estuaries.

Appendix 1.1

REGRESSION	n	X VAR.	COEFF.	TOL	β COEFF.	R SQ. A. R. SQ. R	S.E.E.	C.V.	Wilkinson's	F
ALL	227	constant	0.540			0.535	0.294	25.9%	99%	258
		D	0.336	1.000	0.731	0.533				
ALL (no outliers)	219	constant	0.514			0.598	0.269	23.6%	99%	323
		D	0.349	1.000	0.773	0.596				
SITE#1	7	constant	2.191			0.462	0.105	13.9%	99%	4.295
		Q	-0.00336	1.000	-0.680	0.354				
SITE#2	14	constant	0.589			0.582	0.187	13.2%	99%	16.70
		Q	0.00441	1.000	0.763	0.547				
SITE#3	41	constant	-0.384			0.742	0.143	14.7%	99%	53.21
		Q	0.00173	0.832	0.365	0.728				
SITE#3 (no outliers)	39	T	0.887	0.832	0.955					
		constant	-0.317			0.777	0.124	12.6%	99%	64.40
SITE#4	30	Q	0.00189	0.813	0.372					
		T	0.832	0.813	0.957	0.607	0.149	13.7%	99%	18.54
SITE#4 (no outliers)	28	constant	0.050			0.696	0.132	11.9%	99%	23.37
		Q	0.00209	0.873	0.475	0.574				
SITE#5	117	T	0.625	0.873	0.845					
		constant	0.151			0.67	0.132	11.9%	99%	23.37
SITE#5 (no outliers)	112	Q	0.00076	0.857	0.412					
		T	0.623	0.857	0.898	0.779	0.231	18.7%	99%	206
SITE#5	117	constant	-0.064			0.828	0.216	17.7%	99%	181
		Q	0.00132	0.890	0.145	0.775				
SITE#6	18	T	0.400	0.309	0.209					
		D	0.403	0.291	0.741					
SITE#6 (no outliers)	112	constant	-0.237			0.828	0.216	17.7%	99%	181
		Q	0.00083	0.902	0.136	0.828	0.216	17.7%	99%	181
SITE#6	18	T	0.466	0.316	0.238					
		D	0.507	0.295	0.724					
SITE#6	18	constant	0.621			0.453	0.171	18.9%	99%	13.29
		D	0.147	1.000	0.673	0.419	0.171	18.9%	99%	13.29

Table 4.1- Regression Tables: Surface speed on ebb tide

REGRESSION	n	X VAR.	COEFF.	TOL	β COEFF.	R SQ.	A. R. SQ.	SEE	C.V.	Wilkinson's test	F
ALL	160	constant T	2.738 -1.224	1.000	-0.632	0.400	0.396	0.306	25.8%	99%	105
ALL (no outliers)	154	constant T	2.854 -1.304	1.000	0.688	0.473	0.470	0.280	23.4%	99%	136
SITE#2	23	constant Q T	1.108 0.00389 -1.385	0.972 0.972	0.457 -0.804	0.733	0.707	0.189	14.5%	99%	27.50
SITE#3	27	constant T Q LTH	1.683 -0.968 0.00243 -0.181	0.386 0.827 0.274	-0.843 0.464 -0.331	0.808	0.782	0.114	11.0%	99%	17.59
SITE#3 (no outliers)	26	constant T Q LTH	1.603 0.002 -0.969 -0.137	0.389 0.834 0.278	0.488 -0.869 -0.242	0.850	0.831	0.100	10.4%	99%	28.62
SITE#4	14	constant Q T	1.777 0.0012 -1.049	0.962 0.962	0.401 -0.901	0.832	0.802	0.136	13.3%	99%	27.31
SITE#5	77	constant T	3.468 -1.713	1.000	-0.746	0.556	0.550	0.299	23.0%	99%	89.10
SITE#5 (no outliers)	75	constant T	3.625 -1.821	1.000	-0.777	0.604	0.598	0.277	21.2%	99%	111
SITE#6	13	constant T	1.455 -0.487	1.000	-0.690	0.476	0.428	0.120	14.5%	99%	9.996

Table 4.2- Regression Tables: Surface speed on flood tide

SITE	n	X VAR.	COEFF	TOL	β COEFF.	RSQR.	ADJ R2	SEE.	C.V.	Wilkinson's	F
<u>EBBTIDE:</u>											
ALL	49	constant	0.635			0.148	0.130	0.310	32.9%	95%	8.167
	T		0.409	1.000	0.385						
SITE#1	7	constant	0.472			0.689	0.627	0.101	13.3%	n/a	11.086
	D		0.196	1.000	0.830						
SITE#2	12	constant	0.799			0.772	0.721	0.117	11.0%	99%	15.201
	Q		0.00312	0.959	0.691						
	T		0.576	0.959	0.420						
SITE#5	16	constant	0.315			0.314	0.265	0.250	32.6%	<95%	6.412
	D		0.698	1.000	0.561						
SITE#5	15	constant	0.303			0.420	0.376	0.193	25.2%	95%	9.422
(no outliers)	D		0.653	1.000	0.648						
SITE#6	14	constant	0.522			0.289	0.230	0.329	29.2%	<95%	4.873
	T		0.383	1.000	0.537						
<u>FLOODTIDE:</u>											
ALL	52	constant	1.846			0.279	0.264	0.242	27.4%	99%	19.331
	T		-0.754	1.000	0.528						
ALL	51	constant	1.849			0.316	0.302	0.227	25.6%	99%	22.592
(no outliers)	T		-0.766	1.000	0.562						
SITE#2	20	constant	2.514			0.736	0.687	0.167	17.5%	99%	14.872
	Q		-2.417	0.203	1.364						
	R		0.323	0.203	0.652						
	T		0.002	0.967	0.334						
SITE#5	16	constant	1.271			0.481	0.444	0.217	22.1%	99%	12.989
	R		-0.363	1.000	0.694						
SITE#6	13	constant	1.239			0.524	0.481	0.098	14.6%	95%	12.102
	T		-0.442	1.000	0.724						

Table 4.3- Regression Tables: 9-minute mean speed at 0.7d

	n	X VAR.	COEFFICIENT	TOL.	β COEFF.	R SQ.	A.R. SQ.	SEE	C. OF V.	Wilkinson's Test	F
REACH 1	50	constant	4.204			0.658	0.643	0.475	10.0%	99%	45.124
		T	-1.875	0.993	-0.672						
		Q	0.003160	0.993	0.514						
REACH 2	51	constant	3.344			0.911	0.905	0.249	8.3%	99%	160.230
		LTH	-0.554	0.597	-0.422						
		Q	0.003195	0.936	0.517						
		D	-0.816	0.617	-1.055						
REACH 3	50	constant	3.453			0.853	0.847	0.337	9.8%	99%	136.403
		T	-2.590	0.993	-0.857						
		Q	0.002827	0.993	0.424						
REACH 4	53	constant	7.179			0.807	0.795	0.503	9.5%	99%	68.310
		LTH	-0.559	0.621	-0.304						
		Q	0.001287	0.938	0.148						
		D	-1.111	0.642	-1.043						
REACH 5	53	constant	5.907			0.787	0.774	0.489	9.0%	99%	60.295
		LTH	-0.321	0.621	-0.188						
		Q	0.002870	0.938	0.357						
		D	-0.921	0.642	-0.934						
REACH 6	52	constant	5.182			0.771	0.757	0.362	7.1%	99%	53.888
		T	-1.270	0.205	-0.461						
		Q	0.002235	0.962	0.381						
		D	-0.252	0.204	-0.350						
REACH 7	51	constant	4.434			0.746	0.730	0.404	12.5%	99%	46.127
		LTH	-0.691	0.589	-0.521						
		Q	0.001760	0.935	0.279						
		D	-0.806	0.619	-1.052						

Table 5.1- Regression Tables: Mean water-depth on ebb tide

	n	X VAR.	COEFFICIENT	TOL.	B COEFF.	RSQR	A.R. SQR.	S.EE	C. OF V.	Wilkinson's Test	F
REACH 1	50	constant	0.671			0.778	0.763	0.372	7.7%	99%	53.680
		LTH	0.229	0.787	0.184						
		T	1.946	0.897	0.603						
		Q	0.002423	0.826	0.390						
REACH 2	49	constant	-1.318			0.883	0.780	0.355	12.0%	99%	81.744
		T	2.154	0.961	0.688						
		Q	0.002589	0.961	0.434						
REACH 3	50	constant	-0.778			0.814	0.806	0.305	9.4%	99%	102.635
		T	2.092	0.953	0.715						
		Q	0.002338	0.953	0.415						
REACH 4	47	constant	2.435			0.657	0.634	0.563	11.3%	99%	27.506
		T	2.127	0.957	0.572						
		Q	0.001853	0.875	0.245						
		D	-0.462	0.901	-0.343						
REACH 5	47	constant	2.309			0.727	0.708	0.526	10.1%	99%	38.244
		T	2.452	0.958	0.640						
		Q	0.001795	0.875	0.227						
		D	-0.480	0.902	-0.340						
REACH 6	48	constant	2.351			0.567	0.558	0.426	8.1%	99%	60.312
		T	2.016	1.000	0.753						
REACH 7	50	constant	-1.127			0.764	0.754	0.381	11.6%	99%	75.970
		T	2.493	0.995	0.849						
		Q	0.001667	0.995	0.279						

Table 5.2- Regression Tables: Mean water-depth on flood tide

TABLE 5.3- RESIDUAL ANALYSIS

	REACH	Normal Dist.	Independence	Common Linear Model
<u>Wavelength:</u>	1	negative skew	√	√
	2	slight neg. skew	X	√
	3	slight neg. skew	√	√
	4	slight neg. skew	X	√
	5	negative skew	X	√
	6	negative skew	X?	√
	7	negative skew	X	√
<u>Height:</u>	1	√	X	√
	2	slight neg. skew	X?	√
	3	√	√	√
	4	slight neg. skew	X	√
	5	negative skew	X	√
	6	negative skew	X	√
	7	√	X	√
<u>Depth: ebb tide</u>	1	√	√	√
	2	√	√	√
	3	√	√	√
	4	√	√	√
	5	√	√	√
	6	√	√	√
	7	√	√	√
<u>Depth: flood tide</u>	1	√	√	√
	2	√	√	√
	3	√	√	√
	4	√	√	√
	5	√	√	√
	6	√	√	√
	7	√	√	√
<u>Log Wavelength:</u>	1	√	√	√
	2	√	√	√
	3	slight neg. skew	√	√
	4	√	√	√
	5	slight pos. skew	√	√
	6	√	√	√
	7	√	√	√
<u>Log Height:</u>	1	slight neg. skew	X	√
	2	slight neg. skew	√	√
	3	√	√	√
	4	√	√	√
	5	√	√	√
	6	negative skew	X	√
	7	slight neg. skew	√	√

Note: √=yes
X=no

	n	X VAR.	COEFFICIENT	TOL.	B COEFF.	RSQR.	A.R. SQR.	SEE	C. OF V.	Wilkinson's Test	F
REACH 1	100	constant	6.026			0.371	0.352	3.366	35.3%	99%	18.887
		LTH	-3.953	0.914	-0.576						
		T	1.512	0.967	0.169						
		Q	0.012200	0.907	0.369						
REACH 2	100	constant	1.563			0.318	0.297	1.456	37.2%	99%	14.940
		LTH	-1.270	0.897	-0.447						
		T	0.988	0.972	0.266						
		Q	0.005360	0.890	0.393						
REACH 3	100	constant	-2.455			0.500	0.490	2.571	30.1%	99%	48.476
		Q	0.131000	1.000	0.459						
		D	1.814	1.000	0.539						
REACH 4	100	constant	4.777			0.416	0.404	5.181	44.5%	99%	34.609
		LTH	-6.583	0.897	-0.596						
		Q	0.027000	0.897	0.504						
REACH 5	100	constant	6.721			0.308	0.294	7.280	59.7%	99%	21.603
		LTH	-7.716	0.897	-0.541						
		Q	0.026700	0.897	0.387						
REACH 6	100	constant	4.113			0.386	0.367	2.737	30.6%	99%	20.109
		LTH	-3.178	0.826	-0.532						
		T	1.753	0.971	0.261						
		Q	0.013700	0.827	0.506						
REACH 7	101	constant	2.080			0.322	0.301	1.126	31.8%	99%	15.349
		LTH	-1.180	0.860	-0.503						
		T	0.592	0.980	0.226						
		Q	0.000451	0.862	0.423						

Table 5.4- Regression Tables: Mean bedform-wavelength

	n	X VAR.	COEFFICIENT	TOL.	β COEFF.	RSQR.	A.R. SQR.	SEE	C. OF V.	Wilkinson's Test	F
REACH 1	100	constant	0.118			0.372	0.365	0.143	40.3%	99%	57.969
		D	0.103	1.000	0.610						
REACH 2	100	constant	-0.316			0.628	0.620	0.133	32.3%	99%	81.815
		Q	0.000826	1.000	0.488						
		D	0.128	1.000	0.633						
REACH 3	100	constant	-0.367			0.696	0.690	0.123	27.2%	99%	110.926
		Q	0.001040	1.000	0.593						
		D	0.121	1.000	0.587						
REACH 4	100	constant	0.221			0.415	0.397	0.200	42.3%	99%	22.762
		LTH	-0.257	0.890	-0.605						
		T	0.139	0.970	0.258						
		Q	0.000766	0.886	0.373						
REACH 5	100	constant	0.418			0.265	0.242	0.252	48.6%	99%	11.549
		LTH	-0.244	0.890	-0.512						
		T	0.126	0.970	0.207						
		Q	0.000477	0.886	0.207						
REACH 6	100	constant	0.079			0.432	0.415	0.104	35.7%	99%	24.376
		LTH	-0.062	0.653	-0.262						
		Q	0.000281	0.816	0.264						
		D	0.064	0.779	0.500						
REACH 7	101	constant	-0.277			0.596	0.588	0.118	42.1%	99%	72.389
		Q	0.000876	0.998	0.604						
		D	0.089	0.998	0.510						

Table 5.5- Regression Tables: Mean bedform-height

	n	X VAR.	COEFFICIENT	TOL	β COEFF.	R SQ.	A.R. SQ.	SEE	Wilkinson's Test	F
REACH1	100	constant	-0.701			0.435	0.417	0.170	99%	24.598
		LTH	-0.202	0.914	-0.551					
		T	0.205	0.967	0.430					
		Q	0.000381	0.907	0.216					
REACH2	100	constant	-1.280			0.723	0.715	0.115	99%	83.698
		LTH	0.062	0.644	0.176					
		Q	0.000757	0.875	0.448					
		D	0.156	0.712	0.771					
REACH3	100	constant	-1.342			0.745	0.737	0.116	99%	93.546
		LTH	0.083	0.649	0.226					
		Q	0.000906	0.893	0.507					
		D	0.156	0.703	0.741					
REACH4	100	constant	-0.581			0.444	0.426	0.161	99%	25.520
		LTH	-0.223	0.890	-0.638					
		T	0.118	0.970	0.266					
		Q	0.000607	0.886	0.359					
REACH5	100	constant	-0.255			0.259	0.244	0.194	99%	16.964
		T	0.102	0.983	0.219					
		LTH	-0.180	0.983	-0.489					
REACH6	100	constant	0.075			0.512	0.497	0.142	99%	33.572
		LTH	-0.210	0.826	-0.604					
		T	0.198	0.971	0.508					
		Q	0.000403	0.827	0.257					
REACH7	101	constant	-1.249			0.643	0.635	0.123	99%	88.086
		Q	0.001010	0.998	0.628					
		D	0.102	0.998	0.529					

NOTE: coefficients for the constant term are adjusted by $10 \times 0.5(SEE)^2$ and SEE is expressed in log units

Table 5.6- Regression Tables: Log (mean bedform-height)

<u>REACH #</u>	<u>DATE AND TIME</u>
<u>Log Wavelength</u>	1 June 19 1120, June 20 1134, July 18 1019
	2 June 13 1353, July 31 0728
	3 July 17 0940
	4 June 25 0923
	5 June 19 1538, June 27 1251, June 30 1437
	6 May 14 1615, (June 30 0745), July 18 1034
	7 May 30 0745
<u>Log Height</u>	1 July 18 1019
	2 June 13 1130, (June 30 0734), Aug 1 0924, Aug 8 1352
	3 July 17 0940, (June 30 0734)
	4 June 10 1448
	5 June 24 1028
	6 June 10 1531, (June 30 0745)
	7 none
<u>Depth-ebb tide</u>	1 July 18 1019
	2 none
	3 none
	4 none
	5 none
	6 May 17 0744, Aug.26 0817, Aug.25 0705,(June 22 0610, Aug.3 1520)
	7 May 17 0744, May 18 0734, June 22 0610
<u>Depth-flood tide</u>	1 (Aug. 22 1405)
	2 Aug. 10 1119, (Aug. 22 1405)
	3 June 22 1234, (Aug. 22 1405)
	4 June 11 1258, (Aug. 22 1405)
	5 (Aug. 22 1405)
	6 May 14 1615
	7 May 14 1615, June 22 1247

note: dates and times with high leverage values are displayed in brackets

	n	X VAR.	COEFFICIENT	TOL.	B COEFF.	R SQR.	A.R. SQR.	SEE	Wilkinson's Test	F
REACH1	100	constant	0.797		0.421	0.403	0.148	99%	23.259	
		LTH	-0.192	0.914	-0.612					
		T	0.093	0.967	0.228					
		Q	0.000541	0.907	0.358					
REACH2	100	constant	0.336		0.330	0.309	0.134	99%	15.727	
		LTH	-0.114	0.897	-0.433					
		T	0.105	0.972	0.305					
		Q	0.000489	0.890	0.387					
REACH3	100	constant	0.379		0.475	0.464	0.130	99%	43.822	
		Q	0.000608	1.000	0.430					
		D	0.090	1.000	0.539					
REACH4	100	constant	0.867		0.468	0.457	0.148	99%	42.612	
		LTH	-0.219	0.897	-0.661					
		Q	0.000782	0.897	0.488					
REACH5	100	constant	0.973		0.377	0.364	0.177	99%	29.372	
		LTH	-0.229	0.897	-0.626					
		Q	0.000636	0.897	0.360					
REACH6	100	constant	0.727		0.407	0.388	0.124	99%	21.937	
		LTH	-0.155	0.826	-0.566					
		T	0.085	0.971	0.275					
		Q	0.000614	0.827	0.495					
REACH7	101	constant	0.390		0.286	0.264	0.124	99%	12.934	
		LTH	-0.120	0.860	-0.477					
		T	0.065	0.980	0.230					
		Q	0.000434	0.862	0.380					

NOTE: coefficients for the constant term are adjusted by $10^{0.5(SEE)^2}$ and SEE is expressed in log units

Table 5.8- Regression Tables: Log (mean bedform-wavelength)

APPENDIX 1.2- SYMBOLS FOR VARIABLES AND OTHER ABBREVIATIONS**VARIABLES**

d	=	mean water-depth (m)
dQ/dt	=	change in discharge with respect to time
ds/dt	=	change in stage with respect to time
D	=	tidal drop (m)
h	=	mean bedform-height (m)
k	=	number of independent variables in a model
L	=	length scale (m)
LTH	=	low tide height (m)
Q	=	estuary discharge (m ³ /s)
R	=	tidal rise (m)
RR	=	relative roughness (=h/d)
RRS	=	relative roughness spacing (=w/d)
RTI	=	relative turbulence intensity (= $\sigma U_{0.7d} / U_{0.7d}$)
	=	<u>standard deviation of streamwise current-speed at 0.7d</u>
		9-min. mean streamwise current-speed at 0.7d
S	=	bedform steepness (=h/w)
t	=	boil period (s)
T	=	'time'
	=	<u>time interval between t and HHT</u>
		time interval between HHT and LLT
TI	=	standard deviation of streamwise current speed (= $\sigma U_{0.7d}$) (m/s)
U	=	streamwise current-speed (m/s)
U _{0.7d}	=	(9-minute) mean current-speed at 0.7d from the water surface (m/s)
U _{sf}	=	current speed at the water surface (m/s)
w	=	mean bedform-wavelength (m)

OTHER ABBREVIATIONS

CHS	-	Canadian Hydrographic Service
D.F.	-	degrees of freedom
HHT	-	High high tide
HLT	-	High low tide
L/B	-	left bank (facing downstream)
LHT	-	Low high tide
LLT	-	Low low tide
m	-	metres
m ³ /s	-	cubic metres per second
n	-	number of dunes in each reach
R ²	-	multiple correlation coefficient
R/B	-	right bank (facing downstream)
s.d.or σ	-	standard deviation
s.e.e.	-	standard error of the estimate
WSC	-	Water Survey of Canada
χ^2	-	Chi-squared test value

APPENDIX I.3- 1992 DAILY DATA COLLECTION									
MONTH	DAY	DAILY Q RANGE (m3/s)	TIDAL RANGE (m)	SLOPE	U0.7d	Usfc	DATA COLLECTION		
							BEDFORM	BOIL VIDEO	BOIL PHOTOS
5	3	375.5- 313.6	3.6			X			
5	6	734.3- 662.4	3.5			X			
5	7	695.6- 579.1	3.1			X			
5	8	556.4- 431.5	2.6			X			
5	9	428.6- 326.9	2			X			
5	10	325.0- 266.3	1.9			X			
5	11	264.8- 230.4	2.4			X			
5	21	289.9- 246.9	2.3				X		
5	26	628.2- 588.2	2.2				X		
5	27	646.5- 514.0	2.5				X		
5	30	541.5- 480.4	3.5				X		
5	31	573.6- 508.2	3.8				X		
6	1	695.5- 561.6	4				X		
6	2	716.9- 502.1	4.1	X			X		
6	3	497.5- 432.8	3.9	X		X	X		
6	4	477.0- 445.1	3.5	X	X	X	X	X	
6	5	496.5- 449.7	3	X	X	X	X	X	
6	6	532.9- 483.6	2.3	X	X	X	X	X	
6	7	554.9- 513.1	1.5	X	X	X	X	X	
6	8	537.4- 446.2	2.6	X	X	X	X	X	
6	9	463.0- 445.9	3	X		X	X	X	
6	10	546.3- 467.2	3.3	X	X	X	X	X	
6	11	524.5- 433.4	3.5	X	X	X	X	X	
6	12	629.5- 490.7	3.7	X	X	X	X	X	
6	13	682.9- 622.9	3.7	X			X	X	
6	14	667.0- 514.4	3.6	X	X	X	X	X	
6	15	532.5- 479.0	3.6	X			X		
6	16	564.8- 529.4	3.3	X			X		
6	17	557.8- 478.8	3	X			X	X	
6	18	545.4- 451.9	2.8	X	X	X	X	X	
6	19	605.7- 542.2	2.4	X	X	X	X	X	
6	20	604.6- 542.2	1.8	X	X	X	X	X	
6	21	728.7- 624.3	1.4	X	X	X	X	X	
6	22	767.0- 646.3	2	X	X	X	X	X	
6	23	703.1- 602.2	2.2	X	X	X	X	X	
6	24	698.0- 593.3	2.4	X	X	X	X	X	
6	25	692.1- 598.2	2.8	X			X	X	
6	26	701.8- 612.8	3	X		X	X	X	
6	27	731.4- 636.8	3.4	X	X	X	X	X	
6	28	718.8- 596.9	3.7		X	X	X	X	
6	29	847.0- 668.0	4.1				X	X	
6	30	839.1- 559.7	4.2		X	X	X	X	
7	9	443.6- 395.9	3.3				X		
7	11	467.7- 425.0	3.4			X	X		
7	12	485.3- 435.9	3.3				X		
7	13	462.5- 428.7	3.4			X	X		
7	14	479.1- 392.6	3.3			X	X		X

7	15	405.5- 354.2	3.1			X	X		X
7	16	465.7- 385.7	2.9			X	X		X
7	17	500.1- 445.3	2.6			X	X		X
7	18	509.3- 444.0	2.3			X	X		X
7	19	538.9- 474.7	1.8			X	X		X
7	20	576.4- 496.7	1.3			X	X		X
7	21	710.9- 599.3	2.2				X		X
7	22	658.8- 536.2	2.4				X		X
7	23	540.8- 454.7	2.6				X		X
7	24	529.0- 453.2	2.8				X		X
7	25	492.3- 422.0	3.1				X		X
7	26	463.2- 391.0	3.5			X	X		X
7	27	429.8- 373.4	3.7			X	X		X
7	28	446.7- 386.8	3.9			X	X		X
7	29	473.4- 410.2	4.1			X	X		X
7	30	501.6- 429.9	3.9			X	X		X
7	31	538.1- 453.7	3.5			X	X		X
8	1	556.1- 480.7	3			X	X		X
8	2	561.9- 449.5	2.4			X	X		X
8	3	514.9- 431.4	3			X	X		X
8	4	532.4- 445.9	3.2				X		X
8	5	501.8- 414.3	3.2				X		X
8	6	675.2- 431.5	3.2				X		X
8	8	503.1- 394.2	3.1			X	X		X
8	9	453.2- 299.5	2.9			X	X		X
8	10	334.8- 277.3	2.9			X	X		X
8	11	436.3- 347.1	2.9			X	X		X
8	22	382.1- 268.6	2.8	X			X		
8	23	284.9- 232.5	3	X			X		
8	25	295.9- 248.0	3.3	X			X		
8	26	370.2- 303.3	3.5	X			X		

MONTH	DATE	TIME	SLOPE	T	DROP (m)	RISE (m)	LTH (m)	Q (m ³ /s)
6	2	1148	0.00082	0.83	3.4		0.4	624.3
6	2	1205	0.00087	0.87	3.57		0.4	620.7
6	2	1222	0.00092	0.90	3.69		0.4	617.7
6	2	1237	0.00087	0.94	3.85		0.4	615.1
6	2	1253	0.00082	0.97	3.98		0.4	612.2
6	2	1309	0.00082	1.01		0.06	0.4	607.0
6	2	1323	0.00077	1.04		0.23	0.4	600.8
6	2	1339	0.00082	1.08		0.46	0.4	593.7
6	2	1356	0.00092	1.11		0.63	0.4	586.2
6	2	1414	0.00082	1.15		0.86	0.4	580.5
6	2	1430	0.00077	1.19		1.09	0.4	576.1
6	2	1446	0.00082	1.22		1.27	0.4	571.6
6	2	1501	0.00082	1.26		1.5	0.4	567.6
6	2	1515	0.00067	1.29		1.67	0.4	565.5
6	2	1535	0.00067	1.33		1.9	0.4	562.6
6	2	1553	0.00051	1.37		2.13	0.4	559.9
6	2	1615	0.00026	1.42		2.42	0.4	557.1
6	2	1630	0.00005	1.46		2.65	0.4	555.3
6	2	1646	0.00010	1.49		2.82	0.4	553.4
6	2	1707	0.00015	1.54		3.11	0.4	551.1
6	2	1723	0.00015	1.57		3.28	0.4	549.6
6	2	1739	0.00021	1.61		3.51	0.4	548.2
6	2	1756	0.00015	1.65		3.74	0.4	546.7
6	3	800	0.00010	0.21	0.82		0.7	470.7
6	3	815	0.00031	0.25	0.98		0.7	469.9
6	3	832	0.00031	0.29	1.13		0.7	469.0
6	3	844	0.00041	0.31	1.21		0.7	468.4
6	3	900	0.00046	0.35	1.37		0.7	467.5
6	3	915	0.00046	0.38	1.48		0.7	466.7
6	3	930	0.00051	0.42	1.64		0.7	465.9
6	3	948	0.00046	0.46	1.79		0.7	464.9
6	3	1000	0.00026	0.48	1.87		0.7	464.3
6	3	1017	0.00026	0.52	2.03		0.7	463.3
6	3	1030	0.00026	0.55	2.15		0.7	462.5
6	3	1045	0.00031	0.58	2.26		0.7	461.6
6	3	1103	0.00026	0.62	2.42		0.7	460.5
6	3	1117	0.00031	0.66	2.57		0.7	459.3
6	3	1130	0.00026	0.69	2.69		0.7	458.3
6	3	1145	0.00026	0.72	2.81		0.7	457.1
6	3	1200	0.00021	0.75	2.93		0.7	455.9
6	3	1215	0.00036	0.79	3.08		0.7	454.4
6	3	1230	0.00046	0.82	3.2		0.7	452.9
6	3	1302	0.00036	0.89	3.47		0.7	449.7
6	3	1330	0.00036	0.96	3.74		0.7	447.0
6	3	1400	0.00036	1.02		0.12	0.7	444.0
6	3	1430	0.00036	1.09		0.52	0.7	441.9
6	3	1500	0.00036	1.16		0.92	0.7	439.7
6	3	1542	0.00031	1.25		1.44	0.7	437.3
6	3	1605	0.00021	1.30		1.73	0.7	436.0
6	3	1835	0.00015	1.64		3.68	0.7	434.7
6	4	1006	0.00041	0.38	1.33		0.5	452.7

6	4	1028	0.00036	0.43	1.51		0.5	451.7
6	4	1047	0.00031	0.48	1.68		0.5	450.8
6	4	1128	0.00036	0.57	2		0.5	449.4
6	4	1200	0.00021	0.64	2.24		0.5	448.5
6	4	1246	0.00010	0.75	2.63		0.5	447.1
6	4	1313	0.00015	0.81	2.84		0.5	446.6
6	4	1346	0.00015	0.89	3.12		0.5	446.3
6	4	1415	0.00031	0.95	3.33		0.5	446.2
6	4	1457	0.00031	1.05		0.27	0.5	446.0
6	4	1528	0.00021	1.12		0.65	0.5	446.2
6	4	1615	0.00021	1.23		1.24	0.5	446.1
6	4	1642	0.00010	1.29		1.56	0.5	445.5
6	4	1954	0.00021	1.73		3.92	0.5	451.4
6	5	903	0.00036	0.09	0.27		0.8	484.0
6	5	1008	0.00041	0.25	0.75		0.8	478.9
6	5	1130	0.00036	0.45	1.35		0.8	472.4
6	5	1233	0.00026	0.60	1.8		0.8	467.4
6	5	1258	0.00041	0.66	1.98		0.8	465.5
6	5	1334	0.00036	0.74	2.22		0.8	461.6
6	5	1405	0.00036	0.82	2.46		0.8	458.3
6	5	1452	0.00041	0.93	2.79		0.8	453.6
6	5	1520	0.00046	1.00	3		0.8	451.9
6	5	1557	0.00041	1.09		0.45	0.8	450.2
6	5	1624	0.00031	1.15		0.75	0.8	449.9
6	5	1701	0.00021	1.24		1.2	0.8	449.7
6	5	1723	0.00021	1.30		1.5	0.8	451.3
6	5	1853	0.00005	1.51		2.55	0.8	454.0
6	5	2038	0.00021	1.77		3.85	0.8	466.2
6	6	1129	0.00051	0.29	0.67		1.3	501.3
6	6	1227	0.00046	0.44	1.01		1.3	495.9
6	6	1246	0.00056	0.48	1.1		1.3	494.1
6	6	1333	0.00067	0.60	1.38		1.3	490.7
6	6	1401	0.00046	0.67	1.54		1.3	488.9
6	6	1438	0.00046	0.77	1.77		1.3	486.7
6	6	1456	0.00046	0.81	1.86		1.3	485.6
6	6	1533	0.00051	0.91	2.09		1.3	484.4
6	6	1556	0.00051	0.96	2.21		1.3	483.7
6	6	1642	0.00041	1.08		0.35	1.3	484.9
6	6	1700	0.00041	1.13		0.57	1.3	485.4
6	6	1734	0.00031	1.21		0.92	1.3	488.7
6	6	1803	0.00015	1.29		1.27	1.3	491.5
6	6	2022	0.00010	1.64		2.8	1.3	507.6
6	6	2120	0.00000	1.78		3.41	1.3	514.8
6	7	1124	0.00026	0.05	0.08		1.9	534.4
6	7	1300	0.00036	0.32	0.48		1.9	526.7
6	7	1355	0.00036	0.47	0.71		1.9	522.2
6	7	1426	0.00041	0.56	0.84		1.9	520.8
6	7	1506	0.00036	0.67	1.01		1.9	519.4
6	7	1524	0.00036	0.72	1.08		1.9	518.8
6	7	1558	0.00041	0.81	1.22		1.9	517.8
6	7	1625	0.00041	0.89	1.34		1.9	517.0
6	7	1707	0.00031	1.01		0.04	1.9	515.8
6	7	1748	0.00036	1.12		0.42	1.9	515.2
6	7	1926	0.00010	1.39		1.37	1.9	513.1

6	7	2038	0.00010	1.59		2.07	1.9	513.7
6	8	708	0.00046	0.98	2.55		2.1	530.3
6	8	749	0.00041	1.08		0.12	2.1	527.4
6	8	828	0.00036	1.17		0.26	2.1	524.0
6	8	858	0.00026	1.24		0.36	2.1	521.2
6	8	923	0.00015	1.30		0.45	2.1	519.0
6	8	959	0.00026	1.39		0.59	2.1	515.8
6	8	1029	0.00026	1.46		0.69	2.1	513.4
6	8	1104	0.00021	1.54		0.81	2.1	510.6
6	8	1129	0.00031	1.60		0.9	2.1	508.5
6	8	1230	0.00031	1.74		1.11	2.1	503.2
6	9	650	0.00036	0.81	2.43		1.7	452.4
6	9	719	0.00031	0.87	2.61		1.7	453.2
6	9	748	0.00026	0.94	2.82		1.7	453.8
6	9	815	0.00031	1.00	3		1.7	454.4
6	9	841	0.00026	1.06		0.14	1.7	455.0
6	9	912	0.00031	1.13		0.29	1.7	455.5
6	9	942	0.00021	1.20		0.45	1.7	455.6
6	9	1011	0.00021	1.26		0.59	1.7	455.9
6	9	1038	0.00010	1.32		0.72	1.7	456.5
6	9	1112	0.00005	1.40		0.9	1.7	457.4
6	9	1140	0.00015	1.46		1.04	1.7	458.2
6	10	736	0.00036	0.81	2.67		1.3	529.9
6	10	835	0.00046	0.94	3.1		1.3	533.8
6	10	915	0.00046	1.03		0.09	1.3	534.9
6	10	948	0.00041	1.11		0.34	1.3	535.6
6	10	1022	0.00051	1.18		0.56	1.3	536.1
6	10	1045	0.00046	1.23		0.72	1.3	536.3
6	10	1121	0.00036	1.31		0.97	1.3	535.1
6	10	1145	0.00021	1.37		1.16	1.3	533.7
6	10	1226	0.00026	1.46		1.44	1.3	531.6
6	10	1247	0.00026	1.50		1.56	1.3	530.7
6	10	1328	0.00000	1.60		1.88	1.3	528.9
6	10	1349	-0.00005	1.64		2	1.3	528.1
6	10	1431	0.00005	1.74		2.31	1.3	537.3
6	10	1450	0.00005	1.78		2.44	1.3	543.2
6	11	745	0.00046	0.74	2.59		1.0	493.2
6	11	810	0.00036	0.79	2.77		1.0	485.9
6	11	845	0.00051	0.87	3.05		1.0	475.8
6	11	912	0.00056	0.93	3.26		1.0	470.0
6	11	946	0.00056	1.00	3.5		1.0	466.2
6	11	1035	0.00046	1.11		0.43	1.0	460.6
6	11	1104	0.00051	1.26		1.01	1.0	457.4
6	11	1147	0.00041	1.27		1.05	1.0	453.0
6	11	1212	0.00031	1.32		1.24	1.0	450.5
6	11	1309	0.00000	1.45		1.74	1.0	445.1
6	11	1343	0.00000	1.52		2.02	1.0	442.2
6	11	1401	0.00010	1.56		2.17	1.0	440.7
6	11	1439	0.00015	1.65		2.52	1.0	438.0
6	11	1510	0.00031	1.71		2.75	1.0	436.0
6	12	808	0.00051	0.69	2.55		0.7	537.5
6	12	825	0.00062	0.73	2.7		0.7	538.5
6	12	909	0.00067	0.82	3.03		0.7	540.8
6	12	943	0.00062	0.90	3.33		0.7	542.1

6	12	1021	0.00062	0.98	3.63		0.7	544.0
6	12	1057	0.00072	1.06		0.28	0.7	545.9
6	12	1129	0.00062	1.13		0.6	0.7	548.8
6	12	1154	0.00062	1.18		0.83	0.7	551.1
6	12	1238	0.00051	1.28		1.3	0.7	554.7
6	12	1322	0.00036	1.37		1.71	0.7	558.8
6	12	1420	0.00026	1.50		2.31	0.7	564.4
6	12	1451	0.00021	1.57		2.64	0.7	566.7
6	13	945	0.00067	0.82	3.03		0.6	623.9
6	13	1021	0.00062	0.89	3.29		0.6	623.6
6	13	1052	0.00062	0.96	3.55		0.6	623.6
6	13	1118	0.00062	1.02		0.1	0.6	623.4
6	13	1154	0.00067	1.10		0.49	0.6	623.0
6	13	1242	0.00062	1.20		0.98	0.6	624.0
6	16	1608	0.00013	1.43		2.15	0.6	545.9
6	17	1006	0.00019	0.51	1.53		0.8	519.6
6	17	1105	0.00025	0.65	1.95		0.8	511.6
6	17	1147	0.00038	0.74	2.22		0.8	508.7
6	17	1225	0.00038	0.83	2.49		0.8	505.3
6	17	1247	0.00051	0.88	2.64		0.8	503.0
6	17	1342	0.00045	1.00	3		0.8	498.0
6	17	1406	0.00025	1.06		0.29	0.8	495.9
6	17	1444	0.00032	1.15		0.71	0.8	492.6
6	17	1519	0.00038	1.23		1.09	0.8	489.6
6	17	1551	0.00025	1.30		1.43	0.8	486.8
6	17	1631	0.00013	1.39		1.85	0.8	485.0
6	18	1033	0.00006	0.48	1.34		0.9	487.1
6	18	1101	0.00006	0.54	1.51		0.9	485.6
6	18	1130	0.00019	0.61	1.71		0.9	484.4
6	18	1206	0.00019	0.70	1.96		0.9	482.5
6	18	1230	0.00032	0.75	2.1		0.9	479.7
6	18	1312	0.00045	0.85	2.38		0.9	473.0
6	18	1347	0.00045	0.93	2.6		0.9	463.5
6	18	1414	0.00038	1.00	2.8		0.9	458.1
6	18	1452	0.00038	1.09		0.42	0.9	453.0
6	18	1523	0.00045	1.16		0.74	0.9	453.2
6	18	1548	0.00025	1.22		1.02	0.9	454.5
6	18	1627	0.00019	1.31		1.43	0.9	457.9
6	18	1732	0.00000	1.46		2.13	0.9	464.5
6	18	1758	-0.00030	1.52		2.41	0.9	467.1
6	19	1049	0.00000	0.41	0.98		1.2	581.3
6	19	1144	0.00025	0.55	1.32		1.2	575.1
6	19	1210	0.00019	0.61	1.46		1.2	572.0
6	19	1245	0.00025	0.70	1.68		1.2	567.8
6	19	1321	0.00045	0.78	1.87		1.2	563.9
6	19	1349	0.00045	0.85	2.04		1.2	561.0
6	19	1418	0.00038	0.92	2.21		1.2	558.5
6	19	1451	0.00038	1.00	2.4		1.2	555.8
6	19	1535	0.00045	1.11		0.45	1.2	552.5
6	19	1603	0.00025	1.18		0.74	1.2	550.6
6	19	1625	0.00019	1.23		0.95	1.2	550.2
6	19	1700	0.00006	1.32		1.32	1.2	549.5
6	19	1743	0.00013	1.42		1.73	1.2	548.7
6	19	1809	0.00006	1.49		2.02	1.2	548.8

6	20	1052	-0.00010	0.30	0.54		1.6	552.8
6	20	1130	0.00000	0.40	0.72		1.6	550.0
6	20	1158	0.00006	0.47	0.85		1.6	547.9
6	20	1245	0.00019	0.59	1.06		1.6	545.3
6	20	1315	0.00019	0.67	1.21		1.6	543.7
6	20	1357	0.00025	0.77	1.39		1.6	541.6
6	20	1423	0.00025	0.84	1.51		1.6	540.5
6	20	1448	0.00032	0.91	1.64		1.6	539.5
6	20	1520	0.00025	0.99	1.78		1.6	538.7
6	20	1551	0.00025	1.07		0.25	1.6	538.2
6	20	1621	0.00025	1.14		0.51	1.6	537.9
6	20	1647	0.00019	1.21		0.76	1.6	537.8
6	20	1722	0.00013	1.30		1.09	1.6	539.6
6	20	1801	0.00000	1.40		1.45	1.6	542.9
6	20	1825	0.00000	1.46		1.67	1.6	546.1
6	21	1046	-0.00020	0.14	0.2		1.9	639.6
6	21	1116	-0.00006	0.22	0.31		1.9	637.4
6	21	1143	-0.00006	0.30	0.42		1.9	635.9
6	21	1222	0.00013	0.40	0.56		1.9	633.4
6	21	1249	0.00013	0.48	0.67		1.9	631.6
6	21	1322	0.00013	0.57	0.8		1.9	629.9
6	21	1358	0.00025	0.67	0.94		1.9	628.4
6	21	1500	0.00025	0.84	1.18		1.9	626.4
6	21	1542	0.00025	0.95	1.33		1.9	624.9
6	21	1620	0.00032	1.05		0.16	1.9	625.3
6	21	1649	0.00019	1.13		0.42	1.9	626.8
6	21	1732	0.00019	1.25		0.81	1.9	633.3
6	21	1806	0.00006	1.35		1.14	1.9	639.9
6	22	524	0.00013	0.88	1.76		2.5	763.6
6	22	553	0.00025	0.95	1.9		2.5	759.6
6	22	618	0.00025	1.01		0.01	2.5	756.1
6	22	640	0.00013	1.06		0.05	2.5	753.1
6	22	713	0.00025	1.14		0.12	2.5	747.8
6	22	727	0.00013	1.17		0.15	2.5	745.2
6	22	752	0.00006	1.23		0.2	2.5	740.4
6	22	821	0.00006	1.30		0.26	2.5	734.9
6	22	847	0.00006	1.36		0.32	2.5	730.0
6	22	920	0.00006	1.44		0.39	2.5	724.8
6	22	954	0.00000	1.52		0.46	2.5	720.1
6	22	1023	0.00000	1.59		0.52	2.5	715.5
6	22	1108	-0.00006	1.70		0.61	2.5	707.8
6	22	1148	-0.00006	1.79		0.69	2.5	699.4
6	23	538	-0.00006	0.82	1.8		2.2	697.4
6	23	628	0.00025	0.93	2.05		2.2	691.2
6	23	700	0.00025	1.00	2.2		2.2	687.3
6	23	738	0.00025	1.09		0.11	2.2	680.1
6	23	816	0.00025	1.17		0.21	2.2	672.9
6	23	845	0.00013	1.24		0.3	2.2	667.5
6	23	922	0.00019	1.32		0.4	2.2	660.6
6	23	941	0.00013	1.37		0.46	2.2	657.0
6	23	1010	0.00013	1.43		0.54	2.2	652.0
6	23	1033	0.00000	1.48		0.6	2.2	648.5
6	23	1100	-0.00006	1.55		0.69	2.2	644.4
6	23	1125	0.00000	1.60		0.75	2.2	641.7

6	23	1154	0.00006	1.67		0.84	2.2	638.5
6	23	1222	0.00006	1.73		0.91	2.2	633.4
6	23	1249	0.00000	1.79		0.99	2.2	628.1
6	24	531	0.00025	0.71	1.7		1.9	691.1
6	24	553	0.00032	0.75	1.8		1.9	688.0
6	24	618	0.00045	0.81	1.94		1.9	684.5
6	24	648	0.00032	0.87	2.09		1.9	680.2
6	24	708	0.00045	0.92	2.21		1.9	677.2
6	24	735	0.00045	0.98	2.35		1.9	673.0
6	24	806	0.00032	1.05		0.09	1.9	668.1
6	24	846	0.00032	1.13		0.24	1.9	661.4
6	24	907	0.00025	1.18		0.34	1.9	658.0
6	24	931	0.00038	1.23		0.43	1.9	654.4
6	24	949	0.00019	1.27		0.51	1.9	651.7
6	24	1024	0.00000	1.35		0.66	1.9	646.3
6	24	1047	-0.00006	1.40		0.75	1.9	642.7
6	24	1114	-0.00006	1.46		0.86	1.9	638.1
6	24	1145	-0.00006	1.53		0.99	1.9	632.5
6	24	1217	-0.00010	1.60		1.13	1.9	626.5
6	24	1247	-0.00010	1.66		1.24	1.9	620.6
6	24	1315	-0.00010	1.73		1.37	1.9	615.5
6	24	1338	-0.00010	1.78		1.46	1.9	611.5
6	25	550	0.00019	0.67	1.88		1.5	683.1
6	25	612	0.00006	0.71	1.99		1.5	680.4
6	25	641	0.00025	0.78	2.18		1.5	676.4
6	25	711	0.00025	0.84	2.35		1.5	672.2
6	25	751	0.00032	0.93	2.6		1.5	666.2
6	25	818	0.00038	0.98	2.74		1.5	662.2
6	25	848	0.00013	1.05		0.13	1.5	657.8
6	25	918	0.00025	1.11		0.29	1.5	653.0
6	25	948	0.00025	1.18		0.47	1.5	647.9
6	25	1033	0.00013	1.28		0.74	1.5	641.4
6	25	1102	0.00013	1.34		0.89	1.5	637.4
6	25	1142	0.00000	1.42		1.1	1.5	630.4
6	25	1212	-0.00010	1.49		1.29	1.5	624.9
6	25	1242	-0.00030	1.55		1.44	1.5	619.1
6	25	1311	-0.00020	1.62		1.63	1.5	613.7
6	25	1343	-0.00020	1.68		1.79	1.5	608.4
6	25	1405	-0.00020	1.73		1.92	1.5	605.1
6	26	610	0.00019	0.62	1.86		1.2	693.1
6	26	645	0.00038	0.69	2.07		1.2	689.4
6	26	706	0.00019	0.74	2.22		1.2	687.2
6	26	737	0.00032	0.80	2.4		1.2	684.1
6	26	814	0.00045	0.88	2.64		1.2	679.7
6	26	842	0.00045	0.94	2.82		1.2	675.6
6	26	910	0.00057	1.00	3		1.2	671.3
6	26	931	0.00045	1.04		0.14	1.2	668.0
6	26	1012	0.00038	1.13		0.44	1.2	661.6
6	26	1027	0.00045	1.16		0.54	1.2	659.3
6	26	1058	0.00032	1.23		0.78	1.2	654.5
6	26	1125	0.00025	1.28		0.95	1.2	650.1
6	26	1157	0.00006	1.35		1.18	1.2	644.8
6	26	1224	0.00000	1.41		1.38	1.2	640.8
6	26	1249	-0.00010	1.46		1.55	1.2	637.2

6	26	1307	-0.00020	1.50		1.69	1.2	634.4
6	26	1325	-0.00030	1.54		1.82	1.2	631.3
6	27	609	0.00000	0.53	1.8		0.8	728.9
6	27	637	0.00013	0.59	2.01		0.8	723.2
6	27	706	0.00025	0.65	2.21		0.8	717.6
6	27	728	0.00032	0.70	2.38		0.8	713.9
6	27	807	0.00045	0.78	2.65		0.8	707.4
6	27	840	0.00051	0.85	2.89		0.8	701.8
6	27	919	0.00038	0.93	3.16		0.8	695.2
6	27	1004	0.00038	1.03		0.13	0.8	687.7
6	27	1103	0.00045	1.15		0.64	0.8	678.0
6	27	1138	0.00025	1.23		0.98	0.8	672.4
6	27	1208	0.00000	1.29		1.23	0.8	667.5
6	27	1238	0.00000	1.35		1.49	0.8	662.8
8	22	921	0.00006	1.33		1.07	1.3	331.8
8	22	955	0.00000	1.40		1.3	1.3	326.8
8	22	1031	-0.00006	1.47		1.53	1.3	321.7
8	22	1056	-0.00010	1.52		1.69	1.3	318.1
8	22	1130	-0.00006	1.59		1.92	1.3	313.2
8	22	1154	-0.00006	1.64		2.08	1.3	309.8
8	22	1235	-0.00020	1.73		2.37	1.3	303.3
8	22	1255	-0.00010	1.77		2.5	1.3	300.2
8	23	724	0.00032	0.95	2.85		1.1	278.1
8	23	827	0.00026	1.07		0.26	1.1	273.1
8	23	857	0.00013	1.14		0.53	1.1	271.0
8	23	929	0.00019	1.20		0.75	1.1	268.2
8	23	955	0.00007	1.25		0.94	1.1	266.0
8	23	1030	-0.00006	1.32		1.2	1.1	263.0
8	23	1054	-0.00010	1.37		1.39	1.1	261.0
8	23	1129	-0.00020	1.44		1.65	1.1	258.5
8	25	644	-0.00010	0.60	1.98		0.7	281.3
8	25	715	-0.00006	0.66	2.18		0.7	280.7
8	25	751	0.00026	0.74	2.44		0.7	279.3
8	25	823	0.00019	0.81	2.67		0.7	277.7
8	25	846	0.00013	0.86	2.84		0.7	276.5
8	25	923	0.00000	0.94	3.1		0.7	274.5
8	25	954	0.00006	1.01		0.05	0.7	272.8
8	25	1028	0.00019	1.08		0.37	0.7	270.6
8	25	1101	0.00019	1.15		0.69	0.7	268.3
8	25	1134	0.00013	1.23		1.06	0.7	266.0
8	25	1156	0.00013	1.27		1.25	0.7	264.4
8	25	1232	0.00000	1.35		1.62	0.7	262.0
8	25	1254	-0.00006	1.40		1.85	0.7	260.5
8	25	1323	-0.00020	1.46		2.13	0.7	258.5
8	26	659	-0.00020	0.48	1.68		0.6	335.1
8	26	732	0.00000	0.56	1.96		0.6	333.9
8	26	756	0.00013	0.62	2.17		0.6	333.0
8	26	826	0.00013	0.69	2.42		0.6	332.0
8	26	856	0.00019	0.76	2.66		0.6	330.9
8	26	926	0.00032	0.83	2.91		0.6	329.4
NOTE:								
-	The water-surface slope values from June 2-13 are from the L/B site							
	and those from June 17-Aug. 26 are from R/B site							

MONTH	DATE	TIME	CODE	SPEED (m/s)	Q (m ³ /s)	T	DROP (m)	RISE (m)	LTH (m)
6	4	1106	2	1.10	450.0	0.52	1.82		0.5
6	4	1225	2	1.25	447.8	0.70	2.45		0.5
6	4	1319	2	1.35	446.5	0.83	2.89		0.5
6	4	1434	2	1.55	446.1	1.00	3.50		0.5
6	4	1553	2	1.60	446.4	1.18		0.96	0.5
6	4	1651	2	1.35	445.3	1.31		1.68	0.5
6	5	1204	1	0.75	469.7	0.53	1.58		0.8
6	5	1308	1	1.00	464.4	0.68	2.05		0.8
6	5	1427	1	0.80	456.1	0.87	2.62		0.8
6	5	1535	1	0.75	451.2	1.04		0.18	0.8
6	5	1637	1	0.85	449.9	1.19		0.93	0.8
6	5	1736	1	0.85	450.7	1.33		1.64	0.8
6	6	1306	2	1.20	492.4	0.53	1.23		1.3
6	6	1417	2	1.35	488.0	0.71	1.64		1.3
6	6	1506	2	1.50	485.2	0.84	1.93		1.3
6	6	1619	2	1.50	484.2	1.02		0.10	1.3
6	6	1709	2	1.45	486.3	1.15		0.65	1.3
6	6	1813	2	1.25	492.6	1.31		1.36	1.3
6	7	1320	1	0.65	525.1	0.38	0.56		1.9
6	7	1442	1	0.60	520.3	0.60	0.90		1.9
6	7	1533	1	0.80	518.6	0.74	1.12		1.9
6	7	1639	1	0.70	516.5	0.93	1.39		1.9
6	7	1725	1	0.75	515.5	1.06		0.19	1.9
6	8	807	2	1.35	525.9	1.12		0.18	2.1
6	8	928	2	1.40	518.5	1.31		0.47	2.1
6	8	1006	2	1.20	515.2	1.40		0.60	2.1
6	8	1054	2	1.00	511.4	1.52		0.65	2.1
6	8	805	2	1.65	533.0	0.88	2.90		2.1
6	10	850	2	1.50	534.2	0.98	3.23		1.3
6	10	1000	2	1.50	535.9	1.13		0.42	1.3
6	10	1055	2	1.55	536.4	1.26		0.80	1.3
6	10	1200	2	1.30	532.8	1.40		1.25	1.3
6	10	1300	2	1.15	530.1	1.53		1.67	1.3
6	10	1412	2	0.75	531.3	1.69		2.17	1.3
6	10	1500	2	0.50	546.3	1.80		2.50	1.3
6	11	820	2	1.10	483.0	0.81	2.85		1.0
6	11	922	2	0.95	468.9	0.95	3.32		1.0
6	11	1010	2	1.05	463.5	1.05		0.21	1.0
6	11	1113	2	1.00	456.5	1.19		0.75	1.0
6	11	1225	2	0.80	449.3	1.35		1.36	1.0
6	12	848	2	1.60	539.7	0.78	2.88		0.7
6	12	1105	2	1.75	546.6	1.08		0.35	0.7
6	12	1200	2	1.60	551.7	1.20		0.90	0.7
6	12	1330	2	1.35	559.7	1.39		1.81	0.7
6	14	950	2	1.80	605.3	0.74	2.68		0.5
6	14	1120	2	1.90	594.4	0.94	3.40		0.5
6	14	1229	2	2.00	584.8	1.10		0.50	0.5
6	14	1328	2	1.65	573.5	1.23		1.17	0.5
6	18	1147	5	1.25	483.7	0.65	1.82		0.9
6	18	1256	5	1.50	476.7	0.81	2.28		0.9
6	18	1354	5	1.50	461.6	0.95	2.66		0.9
6	18	1456	5	1.50	452.4	1.10		0.45	0.9
6	18	1603	5	1.10	455.5	1.25		1.18	0.9
6	18	1645	5	0.65	459.8	1.35		1.63	0.9

6	19	1100	5	0.60	580.2	0.44	1.05		1.2
6	19	1223	5	0.70	570.4	0.64	1.54		1.2
6	19	1359	5	0.75	560.0	0.88	2.10		1.2
6	19	1517	5	0.75	553.9	1.07		0.27	1.2
6	19	1632	5	0.75	550.0	1.26		1.06	1.2
6	19	1749	5	0.70	548.6	1.44		1.80	1.2
6	20	1110	5	0.60	551.5	0.35	0.62		1.6
6	20	1220	5	0.80	546.5	0.53	0.96		1.6
6	20	1341	5	1.10	542.4	0.73	1.32		1.6
6	20	1354	5	1.15	541.8	0.77	1.38		1.6
6	20	1426	5	1.15	540.4	0.85	1.53		1.6
6	20	1535	5	1.10	538.4	1.03		0.09	1.6
6	20	1626	5	1.00	537.9	1.16		0.57	1.6
6	20	1743	5	0.85	541.4	1.35		1.28	1.6
6	21	1057	6	0.55	638.6	0.17	0.24		1.9
6	21	1203	6	0.55	634.7	0.35	0.49		1.9
6	21	1300	6	0.70	630.9	0.51	0.71		1.9
6	21	1413	6	1.00	627.9	0.71	0.99		1.9
6	21	1518	6	1.00	625.8	0.88	1.24		1.9
6	21	1629	6	1.00	625.8	1.08		0.27	1.9
6	21	1745	6	0.80	635.7	1.29		0.97	1.9
6	22	535	5	1.50	762.1	0.90	1.80		2.5
6	22	650	5	1.20	751.7	1.08		0.07	2.5
6	22	756	5		738.9	1.25		0.22	2.5
6	22	937	5	0.85	722.0	1.49		0.43	2.5
6	22	1046	5	0.75	711.3	1.65		0.57	2.5
6	23	548	6	0.85	696.3	0.84	1.85		2.2
6	23	638	6	0.85	690.0	0.95	1.91		2.2
6	23	758	6	0.80	676.3	1.13		0.16	2.2
6	23	900	6	0.90	664.7	1.27		0.34	2.2
6	23	1036	6	0.65	648.0	1.49		0.61	2.2
6	23	1200	6	0.75	637.8	1.68		0.85	2.2
6	24	554	5	1.65	687.4	0.76	1.83		1.9
6	24	713	5	1.70	678.5	0.93	1.30		1.9
6	24	827	5	1.60	674.3	1.09		0.17	1.9
6	24	1007	5	1.20	649.0	1.31		0.59	1.9
6	24	1117	5	1.15	637.5	1.47		0.87	1.9
6	24	1221	5	0.85	625.7	1.61		1.14	1.9
6	24	1318	5	0.75	615.0	1.73		1.37	1.9
6	26	627	5	1.30	691.3	0.66	1.97		1.2
6	26	710	5	1.85	686.8	0.75	2.24		1.2
6	26	822	5	1.90	678.5	0.90	2.70		1.2
6	26	949	5	1.70	665.1	1.08		0.28	1.2
6	26	1140	5	1.30	647.6	1.21		0.72	1.2
6	27	618	6	0.95	727.1	0.55	1.88		0.8
6	27	708	6	1.00	717.3	0.66	2.24		0.8
6	27	815	6	0.80	705.4	0.81	2.75		0.8
6	27	941	6	1.15	691.6	0.98	3.34		0.8
6	27	1142	6	1.05	671.7	1.24		1.00	0.8
6	27	1327	6	0.85	655.1	1.46		1.97	0.8
6	27	1436	6	0.50	645.9	1.60		2.56	0.8
6	28	712	6	0.80	690.6	0.57	2.12		0.5
6	28	817	6	0.75	678.5	0.71	2.63		0.5
6	28	1037	6	1.05	651.0	1.01		0.05	0.5
6	28	1220	6	0.85	634.3	1.22		1.08	0.5
6	28	1332	6	0.70	621.8	1.37		1.82	0.5
6	30	702	6	0.75	739.6	0.33	1.37		0.1

6	30	712	6	0.80	736.6	0.36	1.46		0.1
6	30	815	6	1.00	717.8	0.49	2.03		0.1
6	30	914	6	1.15	701.3	0.62	2.56		0.1
6	30	1019	6	1.45	683.7	0.77	3.14		0.1
6	30	1200	6	1.05	657.9	0.99	4.05		0.1
7	11	930	3	1.10	451.4	0.92	3.02		0.9
7	11	1000	3	1.25	449.7	0.98	3.23		0.9
7	11	1028	3	1.25	447.6	1.04		0.17	0.9
7	11	1058	3	1.20	445.4	1.10		0.44	0.9
7	11	1139	3	1.20	441.9	1.19		0.82	0.9
7	11	1206	3	1.15	439.6	1.24		1.07	0.9
7	11	1233	3	1.15	437.7	1.30		1.32	0.9
7	11	1302	3	0.95	435.6	1.36		1.58	0.9
7	13	618	5	0.45	483.6	0.42	1.41		0.7
7	13	817	5	1.15	473.9	0.67	2.28		0.7
7	14	815	3	1.15	459.8	0.47	1.56		0.7
7	14	927	3	1.05	451.3	0.63	2.09		0.7
7	14	1035	3	1.20	443.3	0.79	2.60		0.7
7	14	1138	3	1.25	436.1	0.93	3.06		0.7
7	14	1328	3	1.15	423.8	1.18		0.83	0.7
7	14	1442	3	1.05	416.6	1.34		1.62	0.7
7	15	735	5	0.55	401.9	0.28	0.87		0.8
7	15	832	5	0.75	398.2	0.41	1.28		0.8
7	15	937	5	0.95	393.8	0.56	1.74		0.8
7	15	1038	5	1.30	389.4	0.70	2.18		0.8
7	15	1330	5	1.60	375.2	1.10		0.48	0.8
7	15	1423	5	1.35	370.2	1.23		1.05	0.8
7	16	730	5	0.35	393.0	0.17	0.48		0.9
7	16	835	5	0.65	398.2	0.32	0.93		0.9
7	16	942	5	0.90	402.7	0.48	1.39		0.9
7	16	1048	5	1.25	405.8	0.64	1.85		0.9
7	16	1140	5	1.40	406.7	0.76	2.21		0.9
7	16	1308	5	1.55	407.3	0.97	2.82		0.9
7	16	1353	5	1.60	405.7	1.08		0.35	0.9
7	16	1440	5	1.40	403.3	1.19		0.86	0.9
7	17	857	5	0.65	489.5	0.27	0.70		1.2
7	17	1007	5	0.75	483.0	0.44	1.15		1.2
7	17	1057	5	1.25	477.6	0.57	1.48		1.2
7	17	1153	5	1.50	470.8	0.71	1.84		1.2
7	17	1300	5	1.80	463.8	0.88	2.28		1.2
7	17	1349	5	1.60	458.7	1.00		0.00	1.2
7	17	1450	5	1.55	452.5	1.15		0.62	1.2
7	17	1554	5	1.15	447.9	1.31		1.28	1.2
7	18	916	5	0.70	485.5	0.21	0.48		1.4
7	18	950	5	0.80	481.8	0.30	0.69		1.4
7	18	1046	5	0.90	475.0	0.44	1.02		1.4
7	18	1142	5	1.10	468.2	0.59	1.36		1.4
7	18	1242	5	1.45	461.7	0.75	1.71		1.4
7	18	1353	5	1.40	453.4	0.93	2.14		1.4
7	18	1426	5	1.40	450.9	1.02		0.06	1.4
7	18	1455	5	1.40	448.9	1.09		0.35	1.4
7	18	1551	5	1.10	445.5	1.24		0.92	1.4
7	18	1703	5	0.85	444.1	1.42		1.64	1.4
7	19	922	5	0.45	505.5	0.10	0.18		1.8
7	19	1014	5	0.75	499.0	0.24	0.43		1.8
7	19	1106	5	0.85	492.8	0.38	0.69		1.8
7	19	1216	5	1.05	486.6	0.57	1.03		1.8

7	19	1315	5	1.15	481.8	0.73	1.31		1.8
7	19	1357	5	1.30	479.1	0.84	1.52		1.8
7	19	1444	5	1.35	476.8	0.97	1.75		1.8
7	19	1522	5	1.40	475.5	1.07		0.25	1.8
7	19	1556	5	1.25	474.8	1.16		0.56	1.8
7	19	1703	5	1.05	475.5	1.35		1.17	1.8
7	20	937	5	1.05	530.8	0.00	0.00		2.1
7	20	1032	5	1.05	524.9	0.15	0.20		2.1
7	20	1133	5	1.05	518.4	0.33	0.43		2.1
7	20	1233	5	1.10	512.2	0.50	0.65		2.1
7	20	1328	5	1.20	507.1	0.66	0.86		2.1
7	20	1424	5	1.15	502.4	0.82	1.07		2.1
7	20	1525	5	1.20	498.3	1.00	1.30		2.1
7	26	818	5	2.15	442.0	0.87	3.06		0.7
7	26	851	5	1.90	439.0	0.94	3.29		0.7
7	26	935	5	1.85	434.5	1.03		0.14	0.7
7	26	1015	5	1.75	430.3	1.11		0.51	0.7
7	26	1118	5	1.65	423.4	1.24		1.08	0.7
7	26	1222	5	1.20	416.1	1.37		1.67	0.7
7	27	640	5	1.20	426.6	0.55	2.04		0.5
7	27	735	5	1.65	422.9	0.67	2.47		0.5
7	27	832	5	1.90	418.2	0.79	2.91		0.5
7	27	855	5	1.95	416.2	0.83	3.08		0.5
7	27	956	5	2.00	410.7	0.96	3.55		0.5
7	27	1027	5	1.85	407.5	1.03		0.13	0.5
7	27	1057	5	1.85	404.4	1.09		0.44	0.5
7	27	1136	5	1.75	398.2	1.21		1.05	0.5
7	27	1220	5	1.50	395.7	1.26		1.30	0.5
7	27	1248	5	1.30	392.8	1.32		1.59	0.5
7	27	1322	5	1.00	389.6	1.39		1.95	0.5
7	27	1418	5	0.60	384.9	1.51		2.53	0.5
7	28	630	5	0.55	430.0	0.41	1.61		0.3
7	28	740	3	0.85	424.2	0.57	2.20		0.3
7	28	830	3	1.05	419.8	0.67	2.63		0.3
7	28	938	3	1.25	413.7	0.82	3.20		0.3
7	28	1050	3	1.40	407.5	0.98	3.82		0.3
7	28	1219	3	1.25	400.1	1.17		0.92	0.3
7	28	1320	3	1.35	396.0	1.30		1.64	0.3
7	28	1418	3	0.90	392.2	1.43		2.31	0.3
7	29	706	5	0.65	460.7	0.37	1.51		0.2
7	29	756	5	1.05	455.2	0.48	1.97		0.2
7	29	853	5	1.45	449.1	0.61	2.49		0.2
7	29	913	5	1.65	446.7	0.65	2.67		0.2
7	29	945	5	1.90	442.9	0.72	2.96		0.2
7	29	1018	5	2.05	438.7	0.80	3.26		0.2
7	29	1051	5	2.20	434.2	0.87	3.56		0.2
7	29	1117	5	1.95	431.0	0.93	3.80		0.2
7	29	1202	5	1.95	425.7	1.03		0.15	0.2
7	29	1304	5	1.95	420.6	1.16		0.93	0.2
7	29	1324	5	1.80	419.4	1.21		1.18	0.2
7	29	1352	5	1.65	417.6	1.27		1.53	0.2
7	29	1416	5	1.65	416.1	1.32		1.83	0.2
7	29	1445	5	1.25	414.3	1.39		2.19	0.2
7	29	1507	5	0.90	413.0	1.44		2.46	0.2
7	30	805	5	0.70	478.6	0.36	1.42		0.4
7	30	857	5	0.95	472.3	0.49	1.90		0.4
7	30	928	5	1.30	467.6	0.56	2.18		0.4

7	30	1000	5	1.60	462.6	0.64	2.48		0.4
7	30	1022	5	1.80	459.6	0.69	2.68		0.4
7	30	1053	5	2.05	455.3	0.76	2.96		0.4
7	30	1120	5	2.10	451.6	0.82	3.21		0.4
7	30	1223	5	2.15	443.9	0.97	3.79		0.4
7	30	1319	5	1.90	438.6	1.10		0.56	0.4
7	30	1350	5	1.90	436.2	1.18		0.95	0.4
7	30	1446	5	1.70	432.0	1.31		1.66	0.4
7	30	1554	5	0.70	430.0	1.47		2.52	0.4
7	30	1605	5	0.70	430.0	1.49		2.66	0.4
7	31	644	5	0.45	511.6	0.02	0.08		0.7
7	31	703	3	0.40	509.0	0.07	0.25		0.7
7	31	712	4	0.75	507.6	0.09	0.32		0.7
7	31	719	5	0.40	506.5	0.11	0.39		0.7
7	31	757	5	0.65	500.5	0.21	0.72		0.7
7	31	813	3	0.65	498.2	0.25	0.86		0.7
7	31	827	5	0.75	496.2	0.28	0.98		0.7
7	31	903	5	0.65	491.1	0.37	1.30		0.7
7	31	957	5	0.80	483.4	0.51	1.77		0.7
7	31	1017	3	0.90	480.6	0.56	1.94		0.7
7	31	1024	5	1.10	479.6	0.57	2.00		0.7
7	31	1058	5	1.50	474.9	0.66	2.30		0.7
7	31	1132	5	1.90	470.8	0.74	2.60		0.7
7	31	1202	5	2.10	467.2	0.82	2.86		0.7
7	31	1234	5	2.10	464.0	0.90	3.14		0.7
7	31	1312	5	2.10	460.4	0.99	3.47		0.7
7	31	1341	3	1.05	458.1	1.07		0.33	0.7
7	31	1348	5	2.05	457.5	1.08		0.42	0.7
7	31	1430	5	1.75	455.1	1.19		0.96	0.7
7	31	1458	5	1.65	453.8	1.26		1.32	0.7
8	1	748	5	0.45	528.9	0.03	0.10		1.1
8	1	800	3	0.65	527.4	0.06	0.19		1.1
8	1	808	4	0.80	526.4	0.09	0.26		1.1
8	1	845	5	0.50	521.8	0.18	0.55		1.1
8	1	907	3	0.70	518.9	0.24	0.72		1.1
8	1	915	4	1.05	517.8	0.26	0.78		1.1
8	1	920	5	0.60	517.1	0.27	0.82		1.1
8	1	954	5	0.70	512.3	0.36	1.08		1.1
8	1	1018	3	1.00	508.9	0.42	1.27		1.1
8	1	1027	4	1.15	507.6	0.45	1.34		1.1
8	1	1033	5	0.80	506.8	0.46	1.39		1.1
8	1	1106	5	1.05	502.3	0.55	1.64		1.1
8	1	1125	3	1.05	499.9	0.60	1.79		1.1
8	1	1133	4	1.20	498.9	0.62	1.85		1.1
8	1	1213	5	1.55	494.5	0.72	2.17		1.1
8	1	1219	4	1.35	494.0	0.74	2.21		1.1
8	1	1224	3	1.15	493.5	0.75	2.25		1.1
8	1	1256	5	1.65	490.7	0.83	2.50		1.1
8	1	1314	4	1.25	489.2	0.88	2.64		1.1
8	1	1321	3	1.25	488.7	0.90	2.70		1.1
8	1	1329	5	1.85	488.0	0.92	2.76		1.1
8	1	1409	5	1.95	484.8	1.02		0.11	1.1
8	1	1433	3	1.20	483.2	1.09		0.40	1.1
8	1	1440	4	1.40	482.7	1.10		0.48	1.1
8	1	1445	5	1.75	482.4	1.12		0.54	1.1
8	2	847	3	0.70	514.3	0.02	0.05		1.6
8	2	909	4	0.85	510.4	0.08	0.19		1.6

8	2	918	5	0.45	508.9	0.10	0.25		1.6
8	2	955	3	0.65	502.5	0.21	0.49		1.6
8	2	1022	4	1.00	497.8	0.28	0.67		1.6
8	2	1029	5	0.60	496.6	0.30	0.72		1.6
8	2	1107	3	0.95	490.0	0.40	0.97		1.6
8	2	1129	4	1.15	486.3	0.46	1.11		1.6
8	2	1137	5	0.90	484.9	0.48	1.16		1.6
8	2	1209	3	1.10	479.7	0.57	1.37		1.6
8	2	1300	4	1.20	472.6	0.71	1.71		1.6
8	2	1307	5	1.25	471.6	0.73	1.76		1.6
8	2	1315	3	1.20	470.4	0.75	1.81		1.6
8	2	1408	3	1.05	462.8	0.90	2.16		1.6
8	2	1432	4	1.25	460.4	0.96	2.31		1.6
8	2	1438	5	1.45	459.8	0.98	2.35		1.6
8	2	1515	3	1.20	456.2	1.08		0.33	1.6
8	2	1539	4	1.10	454.0	1.15		0.82	1.6
8	2	1545	5	1.30	453.4	1.16		0.83	1.6
8	2	1617	3	1.00	451.3	1.25		1.41	1.6
8	2	1644	4	0.95	450.2	1.33		1.94	1.6
8	2	1653	5	1.05	449.8	1.35		1.97	1.6
8	3	952	3	0.60	471.0	0.01	0.01		1.8
8	3	1001	4	0.80	469.7	0.03	0.05		1.8
8	3	1009	5	0.30	468.4	0.06	0.09		1.8
8	3	1058	3	0.75	460.4	0.20	0.32		1.8
8	3	1108	4	1.00	458.7	0.23	0.37		1.8
8	3	1113	5	0.50	457.8	0.24	0.39		1.8
8	3	1153	3	0.70	450.8	0.36	0.58		1.8
8	3	1201	4	1.05	449.5	0.39	0.62		1.8
8	3	1207	5	0.70	448.6	0.40	0.64		1.8
8	3	1247	3	0.90	443.2	0.52	0.83		1.8
8	3	1254	4	1.15	442.2	0.54	0.87		1.8
8	3	1301	5	0.70	441.3	0.56	0.90		1.8
8	3	1342	3	1.00	437.3	0.68	1.09		1.8
8	3	1349	4	1.12	436.6	0.70	1.12		1.8
8	3	1355	5	0.95	436.0	0.72	1.15		1.8
8	3	1435	4	1.20	433.1	0.84	1.34		1.8
8	3	1442	3	1.15	432.6	0.86	1.37		1.8
8	3	1450	5	1.20	432.1	0.88	1.41		1.8
8	3	1538	3	1.05	431.4	1.02		0.08	1.8
8	3	1547	4	1.10	431.4	1.05		0.16	1.8
8	3	1553	5	1.15	431.4	1.07		0.22	1.8
8	3	1638	3	1.00	431.5	1.20		0.65	1.8
8	3	1644	4	0.85	431.5	1.22		0.71	1.8
8	3	1650	5	0.95	431.6	1.24		0.76	1.8
8	7	702	3	1.45	558.9	0.89	2.76		1.2
8	7	719	4	1.55	557.1	0.93	2.88		1.2
8	7	724	5	2.00	556.6	0.94	2.91		1.2
8	7	807	3	1.50	552.2	1.03		0.11	1.2
8	7	815	4	1.50	551.5	1.04		0.15	1.2
8	7	821	5	1.95	550.9	1.05		0.18	1.2
8	7	919	3	1.45	544.5	1.18		0.65	1.2
8	7	926	4	1.45	543.5	1.19		0.69	1.2
8	7	930	5	1.85	543.0	1.20		0.73	1.2
8	7	1231	3	0.90	516.3	1.58		2.10	1.2
8	7	1238	4	0.90	515.6	1.59		2.14	1.2
8	7	1242	5	0.75	515.3	1.60		2.18	1.2
8	7	1323	3	0.75	512.9	1.68		2.47	1.2

8	7	1333	4	0.70	512.5	1.70		2.54	1.2
8	7	1338	5	0.70	512.4	1.71		2.57	1.2
8	8	703	3	1.25	455.2	0.78	2.25		1.2
8	8	715	4	1.40	453.4	0.80	2.33		1.2
8	8	724	5	1.85	452.1	0.82	2.38		1.2
8	8	817	3	1.70	444.4	0.93	2.70		1.2
8	8	825	4	1.70	443.2	0.95	2.75		1.2
8	8	832	5	1.95	442.2	0.96	2.79		1.2
8	8	929	3	1.35	433.7	1.08		0.31	1.2
8	8	937	4	1.40	432.5	1.10		0.38	1.2
8	8	953	5	1.85	430.1	1.13		0.51	1.2
8	8	1126	3	0.85	415.5	1.33		1.26	1.2
8	8	1133	4	0.85	414.5	1.34		1.32	1.2
8	8	1140	5	0.90	413.6	1.35		1.37	1.2
8	8	1231	3	0.65	407.3	1.46		1.78	1.2
8	8	1238	4	0.80	406.5	1.48		1.84	1.2
8	8	1243	5	0.75	405.9	1.49		1.88	1.2
8	8	1335	3	0.55	400.3	1.59		2.30	1.2
8	8	1340	4	0.70	399.8	1.60		2.34	1.2
8	8	1347	5	0.45	399.1	1.62		2.40	1.2
8	9	715	3	0.75	400.9	0.68	1.98		1.1
8	9	728	4	0.90	398.5	0.71	2.06		1.1
8	9	733	5	1.15	392.9	0.77	2.25		1.1
8	9	817	3	0.95	389.2	0.81	2.36		1.1
8	9	825	4	0.90	387.6	0.83	2.41		1.1
8	9	833	5	1.20	386.1	0.85	2.46		1.1
8	9	924	3	0.90	376.4	0.96	2.77		1.1
8	9	934	4	0.90	374.6	0.98	2.83		1.1
8	9	942	5	1.20	373.2	0.99	2.88		1.1
8	10	715	3	0.80	296.4	0.57	1.66		1.0
8	10	723	4	0.90	296.1	0.59	1.71		1.0
8	10	730	5	0.90	295.9	0.60	1.75		1.0
8	10	822	3	0.80	293.5	0.72	2.08		1.0
8	10	835	4	1.15	292.8	0.75	2.17		1.0
8	10	843	5	1.40	292.3	0.76	2.22		1.0
8	10	937	3	0.90	290.1	0.88	2.56		1.0
8	10	951	4	1.15	289.6	0.91	2.65		1.0
8	10	957	5	1.55	289.4	0.93	2.69		1.0
8	10	1100	3	0.95	286.1	1.07		0.28	1.0
8	10	1108	4	1.20	285.8	1.08		0.35	1.0
8	10	1115	5	1.65	285.6	1.10		0.42	1.0
8	10	1242	3	0.85	281.9	1.29		1.23	1.0
8	10	1250	4	0.85	281.5	1.31		1.31	1.0
8	10	1259	5	1.10	281.0	1.33		1.39	1.0
NOTE:									
CODE 1= L/B U/S									
CODE 2= L/B D/S									
CODE 3= L/B D/S #2									
CODE 4=THALWEG CROSSING									
CODE 5= R/B U/S									
CODE 6= R/B D/S									

MONTH	DATE	TIME	CODE	U0.7d (m/s)	S.D.U0.7d	C.V.U0.7d	Q (m ³ /s)	T	DROP (m)	RISE (m)	LTH (m)
6	4	1109	1	0.85	0.17	0.19	450.0	0.52	1.82		0.5
6	4	1228	1	0.75	0.19	0.25	447.8	0.70	2.45		0.5
6	4	1438	1	1.06	0.24	0.23	446.1	1.00	3.50		0.5
6	4	1557	1	1.09	0.24	0.22	446.4	1.18		0.96	0.5
6	4	1653	1	1.13	0.19	0.17	445.3	1.31		1.68	0.5
6	5	1208	2	0.73	0.10	0.14	469.7	0.53	1.58		0.8
6	5	1312	2	0.98	0.12	0.12	464.4	0.68	2.05		0.8
6	5	1428	2	0.95	0.11	0.12	456.1	0.87	2.62		0.8
6	5	1538	2	0.91	0.10	0.10	451.2	1.04		0.18	0.8
6	5	1639	2	1.02	0.09	0.08	449.9	1.19		0.93	0.8
6	5	1743	2	0.90	0.10	0.11	450.7	1.33		1.64	0.8
6	6	1310	1	0.95	0.19	0.20	492.4	0.53	1.23		1.3
6	6	1420	1	1.02	0.23	0.23	488.0	0.71	1.64		1.3
6	6	1509	1	1.00	0.22	0.22	485.2	0.84	1.93		1.3
6	6	1622	1	1.19	0.25	0.21	484.2	1.02		0.10	1.3
6	6	1712	1	0.97	0.23	0.24	486.3	1.15		0.65	1.3
6	6	1815	1	0.76	0.19	0.25	492.6	1.31		1.36	1.3
6	7	1325	2	0.52	0.10	0.20	525.1	0.38	0.56		1.9
6	7	1445	2	0.76	0.11	0.15	520.3	0.60	0.90		1.9
6	7	1537	2	0.75	0.08	0.10	518.6	0.74	1.12		1.9
6	7	1644	2	0.63	0.10	0.16	516.5	0.93	1.39		1.9
6	7	1729	2	0.67	0.11	0.17	515.5	1.06		0.19	1.9
6	8	811	1	1.17	0.20	0.17	526.0	1.12		0.18	2.1
6	8	933	1	0.80	0.14	0.17	518.5	1.31		0.47	2.1
6	10	854	1	1.13	0.40	0.35	534.2	0.98	3.23		1.3
6	10	1004	1	1.00	0.25	0.25	535.9	1.13		0.42	1.3
6	10	1100	1	0.99	0.19	0.20	536.4	1.26		0.80	1.3
6	10	1204	1	0.42	0.26	0.62	532.8	1.40		1.25	1.3
6	10	1304	1	0.51	0.14	0.27	530.1	1.53		1.67	1.3
6	10	1417	1	0.55	0.12	0.22	531.3	1.69		2.17	1.3
6	11	823	1	0.96	0.09	0.09	483.0	0.81	2.85		1.0
6	11	926	1	1.15	0.12	0.10	468.9	0.95	3.32		1.0
6	11	1015	1	1.27	0.16	0.13	463.5	1.05		0.21	1.0
6	11	1120	1	0.67	0.27	0.40	456.5	1.19		0.75	1.0
6	11	1326	1	0.50	0.07	0.14	449.3	1.35		1.36	1.0
6	12	850	1	1.13	0.24	0.21	539.7	0.78	2.88		0.7
6	12	1115	1	1.31	0.30	0.23	546.6	1.08		0.35	0.7
6	12	1212	1	1.23	0.27	0.22	551.7	1.20		0.90	0.7
6	12	1338	1	1.06	0.23	0.22	559.7	1.39		1.81	0.7
6	14	954	1	1.21	0.43	0.36	605.3	0.74	2.68		0.5
6	14	1125	1	1.63	0.36	0.22	594.4	0.94	3.40		0.5
6	14	1236	1	1.37	0.29	0.21	584.8	1.10		0.50	0.5
6	14	1330	1	1.15	0.23	0.20	573.6	1.23		1.17	0.5
6	18	1149	3	1.16	0.21	0.18	483.7	0.65	1.82		0.9
6	18	1258	3	1.51	0.22	0.14	476.7	0.81	2.28		0.9
6	18	1357	3	1.46	0.23	0.16	461.6	0.95	2.66		0.9
6	18	1459	3	1.38	0.21	0.15	452.4	1.10		0.45	0.9
6	18	1604	3	1.03	0.14	0.14	455.5	1.25		1.18	0.9
6	18	1649	3	0.84	0.12	0.15	459.8	1.35		1.63	0.9
6	19	1104	3	0.52	0.06	0.11	580.2	0.44	1.05		1.2
6	19	1225	3	0.54	0.07	0.13	570.4	0.64	1.54		1.2
6	19	1519	3	0.84	0.16	0.19	553.9	1.07		0.27	1.2

6	19	1635	3	0.65	0.12	0.19	550.0	1.26		1.06	1.2
6	19	1752	3	0.56	0.09	0.15	548.6	1.44		1.80	1.2
6	20	1115	3	0.62	0.13	0.21	551.5	0.35	0.62		1.6
6	20	1223	3	1.05	0.16	0.15	546.5	0.53	0.96		1.6
6	20	1343	3	1.38	0.17	0.12	542.4	0.73	1.32		1.6
6	20	1429	3	1.39	0.17	0.12	540.4	0.85	1.53		1.6
6	20	1536	3	1.46	0.18	0.12	538.4	1.03		0.09	1.6
6	20	1628	3	1.17	0.20	0.18	537.9	1.16		0.57	1.6
6	20	1745	3	0.75	0.13	0.17	541.4	1.35		1.28	1.6
6	21	1059	4	0.42	0.07	0.17	638.6	0.17	0.24		1.9
6	21	1207	4	0.51	0.07	0.13	634.7	0.35	0.49		1.9
6	21	1301	4	0.58	0.08	0.14	630.9	0.51	0.71		1.9
6	21	1415	4	1.41	0.14	0.10	627.9	0.71	0.99		1.9
6	21	1520	4	1.18	0.12	0.10	625.8	0.88	1.24		1.9
6	21	1631	4	0.78	0.14	0.18	625.8	1.08		0.27	1.9
6	21	1748	4	0.77	0.13	0.16	635.7	1.29		0.97	1.9
6	22	540	3	1.20	0.18	0.15	762.1	0.90	1.80		2.5
6	22	653	3	1.21	0.19	0.16	751.7	1.08		0.07	2.5
6	22	800	3	1.11	0.21	0.19	738.9	1.25		0.22	2.5
6	22	940	3	0.87	0.16	0.18	722.0	1.49		0.43	2.5
6	22	1049	3	0.88	0.18	0.21	711.3	1.65		0.57	2.5
6	22	1203	3	0.89	0.15	0.17	696.9	1.82	1.64		2.5
6	22	1304	3	0.97	0.16	0.17	685.6	1.96	1.76		2.5
6	23	540	4	0.66	0.08	0.12	696.3	0.84	1.85		2.2
6	23	641	4	0.68	0.09	0.14	690.0	0.95	1.93		2.2
6	23	802	4	0.67	0.10	0.15	676.3	1.13		0.16	2.2
6	23	904	4	0.67	0.12	0.17	664.7	1.27		0.34	2.2
6	23	1040	4	0.54	0.07	0.14	648.0	1.49		0.61	2.2
6	23	1202	4	0.47	0.06	0.12	637.8	1.68		0.85	2.2
6	24	557	3	1.54	0.18	0.12	687.4	0.76	1.83		1.9
6	24	715	3	1.58	0.20	0.13	678.5	0.93	1.30		1.9
6	24	1009	3	1.48	0.14	0.09	649.0	1.31		0.59	1.9
6	24	1224	3	0.85	0.14	0.16	625.7	1.61		1.14	1.9
6	24	1323	3	0.65	0.13	0.19	615.0	1.73		1.37	1.9
6	27	620	4	0.54	0.09	0.18	727.1	0.55	1.88		0.8
6	27	710	4	0.64	0.11	0.18	717.3	0.66	2.24		0.8
6	27	819	4	0.58	0.10	0.17	705.4	0.81	2.75		0.8
6	27	948	4	0.74	0.18	0.25	691.6	0.98	3.34		0.8
6	27	1148	4	0.90	0.12	0.13	671.7	1.24		1.00	0.8
6	27	1330	4	0.63	0.09	0.15	655.1	1.46		1.97	0.8
6	27	1438	4	0.40	0.11	0.27	645.9	1.60		2.56	0.8
6	28	820	4	0.55	0.08	0.14	678.5	0.71	2.63		0.5
6	28	1040	4	0.78	0.17	0.22	651.0	1.01		0.05	0.5
6	28	1222	4	0.68	0.14	0.21	634.3	1.22		1.08	0.5
6	28	1335	4	0.72	0.10	0.14	621.8	1.37		1.82	0.5
6	30	712	4	0.68	0.14	0.21	736.6	0.36	1.46		0.1
6	30	819	4	0.73	0.10	0.14	717.8	0.49	2.03		0.1
6	30	915	4	0.86	0.10	0.12	701.3	0.62	2.56		0.1
6	30	1023	4	0.98	0.20	0.20	683.7	0.77	3.14		0.1
6	30	1202	4	1.25	0.19	0.15	657.9	0.99	4.05		0.1
NOTE:											
CODE 1=				L/B	D/S						
CODE 2=				L/B	U/S						
CODE 3=				R/B	U/S						
CODE 4=				R/B	D/S						

APPENDIX 2.4: BEDFORM DATA

MONTH	DATE	TIME	REACH	mean w	s.d. w	mean h	s.d. h	mean d	s.d. d	S	RR	RFS	n	BOIL LEVEL	NOTES	LTH	T	Q	DROP
			(m)	(m)	(m)	(m)	(m)	(m)								(m)		(m ³ /s)	(m)
5	14	1615	6	3.60	2.53	0.20	0.17	7.06	0.47	0.06	0.03	2.98	51	6	3	0.9	1.75	242.8	3.6
5	14	1615	7	4.28	2.78	0.16	0.07	4.81	0.09	0.04	0.03	1.48	16	6	3	0.9	1.75	242.8	3.6
5	14	1724	6	5.86	3.30	0.37	0.29	6.97	0.43	0.07	0.05	1.48	28	6	3	0.9	1.92	245.9	3.6
5	14	1724	7	2.92	1.47	0.14	0.08	4.71	0.69	0.06	0.03	1.95	24	6	3.5	0.9	1.92	245.9	3.6
5	15	1112	6	9.90	3.15	0.45	0.30	3.56	0.65	0.05	0.13	0.40	24	3	1	0.7	0.96	269.9	3.5
5	15	1112	7	1.57	0.59	0.19	0.08	2.15	0.20	0.12	0.09	1.38	44	3		0.7	0.96	269.9	3.5
5	16	1044	6	7.37	2.59	0.33	0.22	4.13	0.26	0.04	0.08	0.63	32	3	1	0.5	0.81	287.9	3.1
5	16	1044	7	1.67	0.51	0.18	0.10	2.41	0.22	0.11	0.08	1.55	41	3		0.5	0.81	287.9	3.1
5	17	744	6	6.21	3.58	0.16	0.11	6.31	0.40	0.03	0.03	1.31	32	6	4	0.5	0.32	327.0	1.1
5	17	744	7	2.08	0.62	0.18	0.08	4.74	0.26	0.09	0.04	2.47	33	4		0.5	0.32	327.0	1.1
5	17	838	6	11.41	4.17	0.51	0.31	5.26	0.55	0.04	0.10	0.54	20	4		0.5	0.44	327.4	1.6
5	17	838	7	2.76	0.59	0.19	0.09	4.39	0.26	0.07	0.04	1.69	26	4		0.5	0.44	327.4	1.6
5	17	935	6	10.09	6.25	0.36	0.22	5.06	0.36	0.04	0.07	0.69	23	4		0.5	0.57	327.6	2.0
5	18	734	7	3.01	0.59	0.27	0.14	5.27	0.31	0.09	0.05	1.82	23	4		0.5	0.21	389.9	0.7
5	18	934	6	8.20	5.80	0.29	0.33	5.23	0.60	0.03	0.05	0.89	28	3	4	0.5	0.49	387.6	1.7
6	6	1837	6	10.71	3.32	0.45	0.25	4.60	0.46	0.04	0.10	0.48	22	5		1.3	1.37	495.3	2.3
6	6	1837	7	2.33	0.59	0.29	0.11	3.17	0.16	0.13	0.09	1.49	30	5		1.3	1.37	495.3	2.3
6	10	1531	7	2.80	0.78	0.23	0.12	4.77	0.29	0.08	0.05	1.86	25	6		1.3	1.87	543.7	3.3
6	10	745	6	6.26	1.54	0.25	0.13	4.61	0.20	0.04	0.05	0.78	34	4		1.3	0.83	531.0	2.8
6	10	754	4	4.54	1.43	0.20	0.12	4.70	0.21	0.04	0.04	1.17	22	5		1.3	0.85	532.1	2.8
6	10	754	5	4.31	1.08	0.23	0.11	5.52	0.17	0.06	0.04	1.36	21	5		1.3	0.85	532.1	2.8
6	10	1230	6	7.37	4.38	0.23	0.17	5.45	0.28	0.04	0.04	1.01	35	4	1	1.3	1.46	531.5	3.3
6	10	1230	7	2.80	0.72	0.29	0.17	3.62	0.30	0.10	0.08	1.38	25	4		1.3	1.46	531.5	3.3
6	10	1241	4	6.66	1.31	0.32	0.14	5.69	0.22	0.05	0.06	0.89	15	5		1.3	1.49	531.0	3.3
6	10	1241	5	7.13	2.36	0.43	0.23	5.88	0.22	0.06	0.07	0.95	13	5		1.3	1.49	531.0	3.3
6	10	1332	6	9.61	3.75	0.34	0.22	5.92	0.36	0.03	0.06	0.75	24	5	1	1.3	1.60	528.8	3.3
6	10	1332	7	3.68	0.90	0.30	0.15	4.18	0.18	0.08	0.07	1.21	19	5		1.3	1.60	528.8	3.3
6	10	1344	4	8.34	1.78	0.34	0.19	4.88	0.28	0.04	0.07	0.62	13	5		1.3	1.63	528.3	3.3
6	10	1344	5	5.90	1.53	0.24	0.12	5.58	0.22	0.04	0.04	1.01	15	5		1.3	1.63	528.3	3.3
6	10	1434	6	8.89	4.17	0.26	0.20	5.68	0.63	0.03	0.05	0.80	24	5		1.3	1.74	538.2	3.3
6	10	1448	4	7.08	1.68	0.19	0.07	4.46	0.22	0.03	0.04	0.67	14	6		1.3	1.77	542.6	3.3
6	10	1531	5	5.35	1.46	0.22	0.08	5.22	0.40	0.04	0.04	1.04	16	6		1.3	1.87	543.7	3.3
6	10	1531	6	5.53	2.78	0.15	0.16	6.55	0.28	0.02	0.02	1.50	35	6	5	1.3	1.87	543.7	3.3
6	11	755	6	5.05	1.79	0.19	0.12	4.75	0.24	0.04	0.04	1.07	43	5	1	1.0	0.75	490.8	2.6
6	11	755	7	2.07	0.55	0.28	0.11	2.76	0.26	0.14	0.10	1.44	33	5		1.0	0.75	490.8	2.6
6	11	803	4	4.86	2.11	0.23	0.15	4.31	0.67	0.05	0.05	1.02	21	5		1.0	0.78	487.9	2.7
6	11	803	5	4.35	1.56	0.26	0.16	4.18	0.48	0.06	0.06	1.08	20	5		1.0	0.78	487.9	2.7

APPENDIX 2.4: BEDFORM DATA

6	11	958	6	10.09	3.89	0.21	0.19	4.64	0.27	0.02	0.05	0.53	23	3	1	1.0	1.03	464.8	3.5
6	11	958	7	3.33	0.67	0.46	0.22	2.55	0.26	0.14	0.08	0.79	21	2	1	1.0	1.03	464.8	3.5
6	11	1246	6	10.97	4.75	0.46	0.29	5.00	0.41	0.04	0.09	0.57	21	4	4	1.0	1.40	447.3	3.5
6	11	1246	7	2.67	0.71	0.34	0.22	3.19	0.25	0.12	0.10	1.30	26	4		1.0	1.40	447.3	3.5
6	11	1258	4	5.55	0.86	0.28	0.07	3.02	0.16	0.05	0.09	0.56	18	6		1.0	1.42	446.1	3.5
6	11	1258	5	6.22	1.81	0.23	0.10	3.78	0.41	0.04	0.06	0.65	14	6		1.0	1.42	446.1	3.5
6	11	1342	6	7.03	3.72	0.20	0.14	5.31	0.63	0.03	0.04	0.93	33	4	4.5	1.0	1.52	442.3	3.7
6	11	1354	4	8.55	2.41	0.32	0.15	5.09	0.38	0.04	0.06	0.64	12	4		1.0	1.56	440.0	3.7
6	11	1354	5	10.24	2.55	0.46	0.20	6.06	0.19	0.04	0.08	0.63	9	4		1.0	1.56	440.0	3.7
6	11	1437	6	7.82	4.70	0.30	0.29	6.08	0.26	0.03	0.05	1.23	29	6	4	1.0	1.64	438.1	3.7
6	12	1357	7	4.17	1.16	0.43	0.14	3.40	0.24	0.11	0.13	0.87	17	5		0.7	1.45	562.6	3.7
6	13	1130	1	21.91	6.17	0.84	0.26	4.47	0.28	0.04	0.19	0.23	11	3	1	0.6	1.04	623.3	3.7
6	13	1130	2	5.53	1.51	0.70	0.28	2.55	0.20	0.14	0.27	0.27	13	1	1	0.6	1.04	623.3	3.7
6	13	1130	3	11.44	4.44	0.65	0.35	2.88	0.28	0.05	0.22	0.30	15	1	1	0.6	1.04	623.3	3.7
6	13	1130	4	11.33	5.76	0.40	0.36	4.54	0.24	0.04	0.09	0.53	9	1		0.6	1.04	623.3	3.7
6	13	1130	5	15.53	3.38	0.62	0.35	4.98	0.26	0.04	0.12	0.34	6	1		0.6	1.04	623.3	3.7
6	13	1353	1	15.87	6.93	0.59	0.42	4.60	0.36	0.03	0.13	0.39	15	4		0.6	1.35	630.2	3.7
6	13	1353	2	12.08	4.84	1.35	0.59	3.26	0.23	0.11	0.41	0.30	6	2		0.6	1.35	630.2	3.7
6	13	1353	3	14.73	4.06	1.03	0.49	3.46	0.35	0.07	0.29	0.25	11	1		0.6	1.35	630.2	3.7
6	14	917	6	6.82	1.91	0.24	0.15	5.01	0.30	0.04	0.05	0.79	34	4	1	0.5	0.67	609.4	2.4
6	14	917	7	3.14	0.93	0.41	0.22	3.35	0.39	0.14	0.13	1.26	23	3(3)	1	0.5	0.67	609.4	2.4
6	14	926	1	7.35	7.44	0.28	0.17	4.79	0.42	0.05	0.06	0.96	32	4	1.3	0.5	0.69	608.3	2.5
6	14	926	2	2.95	0.78	0.33	0.17	3.03	0.25	0.12	0.11	1.10	24	3	1	0.5	0.69	608.3	2.5
6	14	926	3	6.54	1.88	0.44	0.25	3.27	0.23	0.07	0.14	0.54	26	4	1	0.5	0.69	608.3	2.5
6	14	926	4	9.07	2.65	0.36	0.19	4.60	0.32	0.04	0.08	0.54	12	5	3	0.5	0.69	608.3	2.5
6	14	926	5	11.52	6.87	0.48	0.36	5.44	0.18	0.04	0.09	0.63	7	5	3	0.5	0.69	608.3	2.5
6	14	1036	6	10.84	5.39	0.28	0.13	4.89	0.21	0.03	0.06	0.55	21	4	1	0.5	0.85	599.9	3.0
6	14	1036	7	3.89	1.17	0.45	0.19	2.70	0.25	0.11	0.17	0.78	18	2	1	0.5	0.85	599.9	3.0
6	14	1044	1	11.05	4.96	0.40	0.22	4.66	0.24	0.04	0.09	0.49	21	4	2.3	0.5	0.86	599.0	3.1
6	14	1044	2	3.96	1.09	0.59	0.29	2.74	0.25	0.14	0.21	0.74	17	3	1	0.5	0.86	599.0	3.1
6	14	1044	3	9.70	3.60	0.65	0.37	3.05	0.36	0.07	0.21	0.35	19	3	1	0.5	0.86	599.0	3.1
6	14	1044	4	17.00	4.22	0.73	0.25	4.57	0.24	0.05	0.16	0.28	6	4		0.5	0.86	599.0	3.1
6	14	1044	5	11.00	4.89	0.43	0.29	4.65	0.37	0.04	0.09	0.51	8	4		0.5	0.86	599.0	3.1
6	14	1522	1	17.51	6.41	0.75	0.30	5.13	0.35	0.04	0.15	0.33	13	5		0.5	1.48	540.4	3.6
6	14	1522	2	6.66	2.76	0.80	0.44	3.54	0.20	0.12	0.22	0.61	11	4	3	0.5	1.48	540.4	3.6
6	14	1522	3	8.40	3.89	0.44	0.28	3.71	0.20	0.05	0.12	0.53	20	4	3	0.5	1.48	540.4	3.6
6	14	1522	4	18.89	4.23	0.72	0.24	5.07	0.07	0.04	0.14	0.28	5	5	3	0.5	1.48	540.4	3.6
6	14	1522	5	31.58	1.52	1.09	0.21	5.16	0.32	0.04	0.21	0.16	3	5	3	0.5	1.48	540.4	3.6
6	14	1534	7	5.14	0.80	0.70	0.27	3.74	0.12	0.13	0.19	0.74	14	5		0.5	1.65	533.6	3.6
6	14	1639	1	11.44	6.58	0.23	0.24	6.16	0.35	0.02	0.04	0.69	20	5	3	0.5	1.70	531.7	3.6

APPENDIX 2.4: BEDFORM DATA

6	14	1639	2	5.89	2.67	0.50	0.34	4.41	0.14	0.08	0.11	0.98	13	5	3	0.5	1.70	531.7	3.6
6	14	1639	3	14.22	5.39	0.51	0.35	4.71	0.29	0.03	0.11	0.39	11	5	3	0.5	1.70	531.7	3.6
6	14	1639	4	11.37	4.12	0.59	0.39	5.32	0.28	0.05	0.11	0.52	8	5	3	0.5	1.70	531.7	3.6
6	14	1639	5	13.14	6.64	0.44	0.24	5.97	0.34	0.03	0.07	0.59	7	5	3	0.5	1.70	531.7	3.6
6	17	1020	7	2.74	0.67	0.28	0.11	3.34	0.24	0.11	0.08	1.32	25	4		0.8	0.55	517.6	1.6
6	17	1426	1	14.10	4.61	0.79	0.29	4.44	0.21	0.06	0.18	0.35	16	4	2	0.8	1.10	494.1	3.0
6	17	1426	2	3.83	1.03	0.56	0.21	2.47	0.18	0.16	0.23	0.72	17	2(3)	2	0.8	1.10	494.1	3.0
6	17	1426	3	9.21	3.99	0.56	0.26	2.60	0.22	0.06	0.22	0.34	19	2(3)	1	0.8	1.10	494.1	3.0
6	17	1426	4	10.94	2.75	0.63	0.21	4.39	0.15	0.06	0.14	0.43	10	2		0.8	1.10	494.1	3.0
6	17	1426	5	31.37	7.11	0.90	0.37	4.03	0.41	0.03	0.22	0.13	6	2		0.8	1.10	494.1	3.0
6	17	1439	6	14.21	5.03	0.67	0.35	4.72	0.27	0.05	0.14	0.38	16	4		0.8	1.13	493.0	3.0
6	17	1439	7	2.99	0.69	0.55	0.19	2.60	0.12	0.19	0.21	0.92	23	2(3)	3	0.8	1.13	493.0	3.0
6	17	1555	1	17.60	5.18	0.98	0.34	4.59	0.22	0.06	0.22	0.29	12	5		0.8	1.31	486.4	3.0
6	17	1555	2	4.04	0.90	0.55	0.20	2.74	0.13	0.14	0.20	0.72	16	3(2)		0.8	1.31	486.4	3.0
6	17	1555	3	11.76	3.32	0.88	0.53	2.92	0.22	0.08	0.30	0.27	14	3(2)		0.8	1.31	486.4	3.0
6	17	1555	4	11.41	2.27	0.59	0.22	4.39	0.22	0.05	0.13	0.40	8	4		0.8	1.31	486.4	3.0
6	17	1555	5	18.55	6.98	1.01	0.34	5.63	0.24	0.06	0.18	0.44	4	4		0.8	1.31	486.4	3.0
6	17	1621	6	9.28	5.04	0.26	0.22	4.84	0.34	0.03	0.05	0.66	25	5	1.4	0.8	1.37	485.3	3.0
6	17	1621	7	2.92	0.66	0.47	0.24	2.88	0.20	0.16	0.16	1.04	24	4(2)		0.8	1.37	485.3	3.0
6	19	1120	1	9.90	4.90	0.36	0.17	5.13	0.23	0.02	0.07	0.35	10	4	3	1.2	0.49	577.9	1.2
6	19	1120	2	2.62	0.90	0.30	0.11	3.38	0.09	0.12	0.09	1.54	27	4		1.2	0.49	577.9	1.2
6	19	1120	3	3.85	0.98	0.27	0.12	3.53	0.20	0.07	0.08	0.98	42	3		1.2	0.49	577.9	1.2
6	19	1120	4	22.35	6.90	0.60	0.21	5.88	0.20	0.03	0.10	0.30	5	5	3	1.2	0.49	577.9	1.2
6	19	1120	5	7.59	4.61	0.33	0.15	5.82	0.13	0.05	0.06	1.08	10	5	3	1.2	0.49	577.9	1.2
6	19	1134	6	8.29	2.89	0.15	0.13	5.31	0.26	0.02	0.03	0.72	28	4	1.4	1.2	0.52	576.2	1.3
6	19	1308	6	6.30	2.97	0.24	0.18	5.01	0.28	0.04	0.05	0.92	31	4	1	1.2	0.75	565.2	1.8
6	19	1538	1	14.05	3.07	0.63	0.28	4.60	0.21	0.04	0.14	0.34	14	5		1.2	1.12	552.3	2.4
6	19	1538	2	3.24	0.89	0.45	0.17	2.67	0.14	0.14	0.17	0.88	21	3		1.2	1.12	552.3	2.4
6	19	1538	3	7.39	2.39	0.62	0.32	2.80	0.25	0.08	0.22	0.41	20	3	2	1.2	1.12	552.3	2.4
6	19	1538	4	10.70	2.75	0.67	0.30	5.16	0.19	0.07	0.13	0.52	9	5		1.2	1.12	552.3	2.4
6	19	1538	5	32.87	8.15	0.94	0.25	4.98	0.26	0.03	0.19	0.16	6	5		1.2	1.12	552.3	2.4
6	19	1551	6	9.07	3.29	0.30	0.20	4.90	0.24	0.03	0.06	0.61	22	5	1	1.2	1.15	551.4	2.4
6	19	1551	7	3.58	0.75	0.51	0.25	2.72	0.17	0.15	0.19	0.79	19	3	1	1.2	1.15	551.4	2.4
6	19	1712	1	12.31	3.25	0.54	0.27	4.50	0.56	0.05	0.12	0.41	17	4		1.2	1.35	549.3	2.4
6	19	1712	2	3.28	1.09	0.38	0.16	2.98	0.16	0.12	0.12	1.01	20	5		1.2	1.35	549.3	2.4
6	19	1712	3	8.40	2.82	0.61	0.25	3.17	0.29	0.07	0.19	0.42	21	4		1.2	1.35	549.3	2.4
6	19	1712	4	9.11	3.11	0.43	0.25	4.88	0.28	0.05	0.09	0.59	9	5		1.2	1.35	549.3	2.4
6	19	1712	5	11.29	3.25	0.79	0.49	5.50	0.18	0.07	0.14	0.54	8	5		1.2	1.35	549.3	2.4
6	19	1733	6	12.28	5.11	0.41	0.33	5.14	0.30	0.03	0.08	0.47	18	4	1	1.2	1.40	548.9	2.4
6	20	1134	1	12.85	3.20	0.31	0.13	5.24	0.25	0.01	0.06	0.23	8	4	3	1.6	0.41	549.7	0.7

APPENDIX 2.4: BEDFORM DATA

6	20	1134	2	2.01	0.62	0.25	0.12	3.52	0.09	0.13	0.07	1.97	34	4		1.6	0.41	549.7	0.7
6	20	1134	3	3.94	1.87	0.28	0.11	3.63	0.17	0.08	0.08	1.10	41	4	3	1.6	0.41	549.7	0.7
6	20	1134	4	14.57	3.21	0.49	0.12	6.41	0.25	0.03	0.08	0.47	7	5	3	1.6	0.41	549.7	0.7
6	20	1134	5	12.22	2.54	0.43	0.17	5.56	0.20	0.03	0.08	0.48	7	5	3	1.6	0.41	549.7	0.7
6	20	1148	6	8.18	5.85	0.21	0.22	5.45	0.24	0.03	0.04	0.99	27	4	1,4	1.6	0.44	548.7	0.8
6	20	1148	7	1.92	0.53	0.21	0.11	3.56	0.11	0.12	0.06	2.02	35	4		1.6	0.44	548.7	0.8
6	20	1359	1	5.84	1.61	0.28	0.13	4.66	0.25	0.05	0.06	0.87	38	5	2,3	1.6	0.78	541.5	1.4
6	20	1359	2	2.66	0.65	0.35	0.17	2.80	0.11	0.13	0.13	1.12	27	4		1.6	0.78	541.5	1.4
6	20	1359	3	4.98	1.36	0.41	0.14	2.87	0.13	0.08	0.14	0.66	32	4	2	1.6	0.78	541.5	1.4
6	20	1359	4	6.92	3.91	0.28	0.12	4.78	0.18	0.04	0.06	0.85	14	5	3	1.6	0.78	541.5	1.4
6	20	1359	5	7.06	2.71	0.35	0.18	5.27	0.19	0.05	0.07	0.87	12	5	3	1.6	0.78	541.5	1.4
6	20	1413	6	6.40	1.65	0.21	0.11	4.88	0.30	0.03	0.04	0.81	35	5	1	1.6	0.82	541.0	1.5
6	20	1413	7	2.47	0.60	0.26	0.13	2.91	0.16	0.10	0.09	1.26	28	4		1.6	0.82	541.0	1.5
6	20	1553	1	8.60	2.55	0.44	0.26	4.47	0.28	0.05	0.10	0.63	25	5	2	1.6	1.07	538.1	1.8
6	20	1553	2	2.29	0.78	0.33	0.18	2.75	0.12	0.14	0.12	1.42	30	4		1.6	1.07	538.1	1.8
6	20	1553	3	5.44	1.63	0.43	0.15	2.79	0.16	0.08	0.15	0.58	32	4		1.6	1.07	538.1	1.8
6	20	1553	4	6.28	2.35	0.34	0.14	5.26	0.19	0.06	0.06	0.95	14	5		1.6	1.07	538.1	1.8
6	20	1553	5	6.37	2.32	0.45	0.22	5.01	0.41	0.08	0.09	0.91	14	5		1.6	1.07	538.1	1.8
6	20	1612	6	8.80	3.58	0.28	0.20	5.09	0.18	0.03	0.05	0.66	20	5	1,4	1.6	1.12	537.9	1.8
6	20	1803	1	8.70	2.91	0.44	0.17	4.73	0.35	0.05	0.09	0.60	24	5		1.6	1.41	543.2	1.8
6	20	1803	2	2.48	0.57	0.32	0.25	3.26	0.15	0.13	0.10	1.37	29	5		1.6	1.41	543.2	1.8
6	20	1803	3	4.64	1.96	0.29	0.16	3.31	0.11	0.06	0.09	0.81	36	5		1.6	1.41	543.2	1.8
6	20	1803	4	7.92	2.04	0.31	0.15	5.64	0.16	0.04	0.06	0.76	13	5		1.6	1.41	543.2	1.8
6	20	1803	5	8.14	1.56	0.43	0.19	5.92	0.18	0.05	0.07	0.75	11	5		1.6	1.41	543.2	1.8
6	20	1815	7	2.50	0.82	0.28	0.11	3.27	0.59	0.12	0.12	1.45	27	5		1.6	1.44	545.2	1.8
6	21	1120	1	5.48	2.27	0.24	0.15	5.35	0.50	0.05	0.05	1.17	38	4		1.9	0.23	637.2	0.3
6	21	1120	2	2.73	0.73	0.32	0.11	3.78	0.11	0.12	0.09	1.52	25	5		1.9	0.23	637.2	0.3
6	21	1120	3	4.61	1.49	0.41	0.23	3.86	0.19	0.10	0.11	0.95	36	5		1.9	0.23	637.2	0.3
6	21	1120	4	5.69	2.10	0.24	0.12	6.17	0.24	0.05	0.04	1.20	17	6		1.9	0.23	637.2	0.3
6	21	1120	5	4.93	2.07	0.29	0.13	6.55	0.31	0.06	0.04	1.62	18	6		1.9	0.23	637.2	0.3
6	21	1135	6	5.22	3.25	0.15	0.14	5.79	0.28	0.03	0.03	1.38	38	4	1,4	1.9	0.27	636.3	0.4
6	21	1135	7	2.40	0.54	0.32	0.12	3.70	0.12	0.14	0.09	1.64	29	5		1.9	0.27	636.3	0.4
6	21	1225	1	4.87	2.35	0.26	0.17	4.86	0.60	0.05	0.06	1.26	46	5		1.9	0.41	633.2	0.6
6	21	1225	2	2.14	0.62	0.29	0.15	3.50	0.09	0.14	0.08	1.80	33	4		1.9	0.41	633.2	0.6
6	21	1225	3	6.11	2.26	0.48	0.22	3.64	0.17	0.08	0.13	0.71	27	4		1.9	0.41	633.2	0.6
6	21	1225	4	5.02	2.29	0.24	0.16	6.14	0.21	0.05	0.04	1.45	20	5	3	1.9	0.41	633.2	0.6
6	21	1225	5	7.45	6.35	0.32	0.16	6.33	0.31	0.06	0.05	1.31	12	5	3	1.9	0.41	633.2	0.6
6	21	1241	6	5.15	1.40	0.18	0.09	5.78	0.29	0.04	0.03	1.22	24	5	1,4	1.9	0.45	632.2	0.6
6	21	1241	7	2.82	0.71	0.42	0.18	3.55	0.22	0.15	0.12	1.34	24	4		1.9	0.45	632.2	0.6
6	21	1431	1	6.82	2.87	0.37	0.12	5.00	0.27	0.06	0.07	0.95	30	4		1.9	0.76	627.3	1.1

APPENDIX 2.4: BEDFORM DATA

6	21	1431	2	2.59	0.57	0.35	0.13	3.12	0.13	0.14	0.11	1.26	27	4		1.9	0.76	627.3	1.1
6	21	1431	3	5.85	3.28	0.49	0.30	3.15	0.23	0.09	0.15	0.71	30	4		1.9	0.76	627.3	1.1
6	21	1431	4	6.55	2.15	0.33	0.15	5.26	0.21	0.05	0.06	0.90	15	5		1.9	0.76	627.3	1.1
6	21	1431	5	6.30	2.04	0.32	0.12	5.78	0.12	0.05	0.06	1.02	13	5		1.9	0.76	627.3	1.1
6	21	1559	1	7.29	1.54	0.39	0.18	4.62	0.41	0.05	0.08	0.63	26	4		1.9	1.00	624.3	1.4
6	21	1559	2	2.92	0.83	0.39	0.20	2.92	0.11	0.13	0.13	1.11	24	4		1.9	1.00	624.3	1.4
6	21	1559	3	7.58	2.36	0.59	0.31	3.02	0.20	0.08	0.19	0.47	21	4	2	1.9	1.00	624.3	1.4
6	21	1559	4	7.13	2.19	0.38	0.18	5.22	0.12	0.06	0.07	0.80	14	5		1.9	1.00	624.3	1.4
6	21	1559	5	5.98	1.33	0.32	0.16	5.68	0.14	0.05	0.06	0.99	14	5		1.9	1.00	624.3	1.4
6	21	1612	7	3.36	0.76	0.41	0.23	2.98	0.18	0.12	0.14	0.93	21	5		1.9	1.03	624.9	1.4
6	21	1705	1	7.96	1.76	0.45	0.18	4.92	0.33	0.06	0.09	0.65	27	5		1.9	1.18	628.3	1.4
6	21	1705	2	2.72	0.77	0.42	0.19	3.09	0.12	0.16	0.14	1.25	25	5		1.9	1.18	628.3	1.4
6	21	1705	3	6.60	2.66	0.48	0.26	3.11	0.16	0.07	0.15	0.54	25	5		1.9	1.18	628.3	1.4
6	21	1705	4	7.61	2.12	0.46	0.21	5.05	0.10	0.06	0.09	0.71	13	5		1.9	1.18	628.3	1.4
6	21	1705	5	8.40	1.26	0.51	0.20	5.36	0.20	0.06	0.10	0.65	10	5		1.9	1.18	628.3	1.4
6	21	1720	6	8.29	2.49	0.28	0.17	5.23	0.28	0.03	0.05	0.68	28	5	1.4	1.9	1.22	631.1	1.4
6	21	1720	7	3.33	1.02	0.54	0.21	3.20	0.21	0.17	0.17	1.02	21	5		1.9	1.22	631.1	1.4
6	22	557	1	6.87	2.48	0.25	0.14	5.39	0.43	0.04	0.05	0.89	33	4		2.3	0.96	759.0	1.9
6	22	557	2	3.33	0.60	0.42	0.25	3.49	0.18	0.13	0.12	1.09	21	2(3)		2.3	0.96	759.0	1.9
6	22	557	3	6.84	2.86	0.50	0.27	3.53	0.30	0.07	0.14	0.60	25	2(3)		2.3	0.96	759.0	1.9
6	22	557	4	7.47	1.85	0.33	0.17	5.34	0.52	0.05	0.06	0.75	14	5		2.3	0.96	759.0	1.9
6	22	557	5	4.59	1.15	0.18	0.13	6.63	0.40	0.04	0.03	1.54	18	5		2.3	0.96	759.0	1.9
6	22	610	6	9.67	3.16	0.25	0.12	5.63	0.28	0.03	0.04	0.64	24	4	1	2.3	0.99	757.2	2.0
6	22	610	7	2.52	0.64	0.37	0.15	3.43	0.13	0.16	0.11	1.46	28	2(3)		2.3	0.99	757.2	2.0
6	22	729	1	6.96	2.46	0.23	0.14	5.77	0.35	0.03	0.04	0.90	33	5		2.3	1.18	744.8	2.0
6	22	729	2	3.78	1.23	0.52	0.27	3.56	0.19	0.14	0.15	1.04	18	2	2	2.3	1.18	744.8	2.0
6	22	729	3	10.94	2.91	0.78	0.27	3.70	0.35	0.07	0.21	0.36	16	2		2.3	1.18	744.8	2.0
6	22	729	4	7.45	1.88	0.38	0.15	5.94	0.31	0.06	0.07	0.86	13	5		2.3	1.18	744.8	2.0
6	22	729	5	7.33	1.96	0.37	0.18	6.15	0.09	0.05	0.06	0.92	12	5		2.3	1.18	744.8	2.0
6	22	744	6	7.73	1.76	0.22	0.14	5.73	0.31	0.03	0.04	0.79	30	5	1	2.3	1.21	741.9	2.0
6	22	744	7	2.37	0.52	0.41	0.12	3.57	0.16	0.18	0.11	1.60	29	3		2.3	1.21	741.9	2.0
6	22	852	1	6.74	2.05	0.24	0.15	5.76	0.32	0.04	0.04	0.95	27	5		2.3	1.37	729.0	2.0
6	22	852	2	4.24	0.99	0.59	0.29	3.81	0.18	0.14	0.16	0.97	16	2		2.3	1.37	729.0	2.0
6	22	852	3	10.63	2.65	0.77	0.29	3.84	0.20	0.07	0.20	0.38	16	2		2.3	1.37	729.0	2.0
6	22	852	4	7.85	1.61	0.43	0.15	5.87	0.42	0.06	0.07	0.78	13	5		2.3	1.37	729.0	2.0
6	22	852	5	7.33	1.94	0.44	0.20	6.19	0.13	0.06	0.07	0.91	12	5		2.3	1.37	729.0	2.0
6	22	906	6	7.93	1.80	0.19	0.15	5.85	0.31	0.02	0.03	0.78	24	5	1.3	2.3	1.41	726.7	2.0
6	22	906	7	2.43	0.44	0.48	0.21	3.81	0.16	0.20	0.12	1.64	28	2		2.3	1.41	726.7	2.0
6	22	957	1	8.00	2.07	0.34	0.14	5.84	0.30	0.04	0.06	0.79	29	4		2.3	1.53	719.7	2.0
6	22	957	2	3.77	0.97	0.44	0.24	3.89	0.13	0.12	0.11	1.11	19	4		2.3	1.53	719.7	2.0

APPENDIX 2.4: BEDFORM DATA

6	22	957	3	9.88	3.29	0.66	0.34	4.00	0.27	0.06	0.17	0.49	16	4		2.3	1.53	719.7	2.0
6	22	957	4	7.95	1.68	0.39	0.18	6.05	0.11	0.05	0.06	0.81	13	5		2.3	1.53	719.7	2.0
6	22	957	5	7.27	1.99	0.31	0.17	6.42	0.22	0.04	0.05	0.93	12	5		2.3	1.53	719.7	2.0
6	22	1013	6	7.94	2.37	0.24	0.11	5.90	0.32	0.03	0.04	0.82	24	4		2.3	1.59	717.2	2.0
6	22	1124	1	7.85	1.85	0.27	0.12	5.60	0.41	0.03	0.05	0.73	25	5		2.3	1.74	704.5	2.0
6	22	1124	2	3.68	1.08	0.53	0.16	3.92	0.13	0.15	0.14	1.16	19	4		2.3	1.74	704.5	2.0
6	22	1124	3	9.51	4.86	0.51	0.25	4.12	0.36	0.06	0.13	0.58	18	4	3	2.3	1.74	704.5	2.0
6	22	1124	4	6.98	3.01	0.24	0.12	5.82	0.34	0.04	0.04	1.05	15	5	3	2.3	1.74	704.5	2.0
6	22	1124	5	5.44	1.77	0.20	0.13	6.77	0.22	0.04	0.03	1.38	15	5	3	2.3	1.74	704.5	2.0
6	22	1139	6	12.21	9.67	0.26	0.22	5.77	0.18	0.03	0.04	0.59	19	5	4	2.3	1.77	701.3	2.0
6	22	1139	7	2.26	0.42	0.45	0.17	3.94	0.16	0.20	0.12	1.81	31	4		2.3	1.77	701.3	2.0
6	22	1234	1	8.04	3.11	0.29	0.13	5.72	0.35	0.04	0.05	0.80	29	5	3	2.3	1.90	690.5	2.0
6	22	1234	2	3.68	0.88	0.48	0.23	3.82	0.14	0.13	0.13	1.11	19	4		2.3	1.90	690.5	2.0
6	22	1234	3	9.16	4.62	0.45	0.27	3.80	0.22	0.05	0.12	0.54	19	4	3	2.3	1.90	690.5	2.0
6	22	1234	4	7.39	2.14	0.23	0.11	6.07	0.10	0.03	0.04	0.88	14	5		2.3	1.90	690.5	2.0
6	22	1234	5	7.23	2.49	0.29	0.13	6.44	0.18	0.04	0.04	1.02	12	5		2.3	1.90	690.5	2.0
6	22	1247	6	12.94	8.66	0.51	0.43	5.66	0.55	0.04	0.09	0.60	18	5	4	2.3	1.93	688.0	2.0
6	22	1247	7	2.69	0.65	0.41	0.23	3.77	0.18	0.16	0.11	1.49	26	4		2.3	1.93	688.0	2.0
6	23	606	2	2.93	0.87	0.42	0.16	2.90	0.23	0.15	0.15	1.06	23	2		2.2	0.88	693.9	1.9
6	23	606	4	8.98	1.90	0.40	0.16	5.87	0.15	0.05	0.07	0.69	11	4		2.2	0.88	693.9	1.9
6	23	606	5	12.10	3.40	0.52	0.26	5.69	0.07	0.04	0.09	0.53	7	4		2.2	0.88	693.9	1.9
6	23	1115	6	11.12	3.67	0.37	0.28	5.21	0.68	0.03	0.06	0.45	18	5	1,4	2.2	1.58	642.8	2.2
6	23	1115	7	3.18	1.14	0.52	0.27	3.90	0.19	0.17	0.13	1.34	22	4		2.2	1.58	642.8	2.2
6	23	1225	1	8.48	3.51	0.34	0.23	5.86	0.49	0.04	0.06	0.82	22	5	5	2.2	1.74	632.8	2.2
6	23	1225	2	4.38	1.65	0.46	0.15	4.00	0.18	0.12	0.11	1.05	16	5	3	2.2	1.74	632.8	2.2
6	23	1225	3	12.14	4.44	0.66	0.29	4.23	0.33	0.06	0.16	0.42	14	5	3	2.2	1.74	632.8	2.2
6	23	1225	4	8.04	2.55	0.27	0.12	6.62	0.20	0.04	0.04	0.91	13	6	3	2.2	1.74	632.8	2.2
6	23	1225	5	8.71	3.35	0.25	0.11	6.73	0.34	0.03	0.04	0.90	10	6	3	2.2	1.74	632.8	2.2
6	23	1241	6	9.15	3.58	0.37	0.23	5.87	0.41	0.04	0.07	0.78	25	5	1,4	2.2	1.78	629.7	2.2
6	23	1241	7	2.87	0.70	0.43	0.15	3.93	0.15	0.15	0.11	1.45	24	5		2.2	1.78	629.7	2.2
6	24	1028	1	9.71	3.63	0.39	0.25	5.59	0.40	0.04	0.07	0.70	20	5		1.9	1.36	645.7	2.4
6	24	1028	2	4.82	2.16	0.59	0.22	3.48	0.21	0.14	0.17	0.93	15	2		1.9	1.36	645.7	2.4
6	24	1028	3	11.86	4.36	0.69	0.30	3.70	0.36	0.06	0.19	0.35	14	3		1.9	1.36	645.7	2.4
6	24	1028	4	12.11	2.39	0.77	0.36	6.04	0.40	0.06	0.13	0.53	8	5		1.9	1.36	645.7	2.4
6	24	1028	5	20.33	7.21	1.20	0.33	6.06	0.18	0.07	0.20	0.35	5	5		1.9	1.36	645.7	2.4
6	24	1040	6	9.47	4.92	0.31	0.25	4.59	0.89	0.03	0.06	0.48	21	5	1	1.9	1.38	643.8	2.4
6	24	1040	7	3.44	0.92	0.75	0.34	3.58	0.21	0.22	0.21	1.10	20	3		1.9	1.38	643.8	2.4
6	24	1251	1	12.44	4.92	0.42	0.28	5.84	0.48	0.04	0.07	0.56	18	5	3	1.9	1.67	619.9	2.4
6	24	1251	2	3.98	1.86	0.34	0.16	3.91	0.19	0.09	0.09	1.17	18	4	3	1.9	1.67	619.9	2.4
6	24	1251	3	12.14	5.58	0.56	0.31	4.17	0.21	0.05	0.13	0.47	14	4	3	1.9	1.67	619.9	2.4

APPENDIX 2.4: BEDFORM DATA

6	24	1251	4	12.04	3.84	0.40	0.15	6.89	0.24	0.04	0.06	0.65	9	5	3	1.9	1.67	619.9	2.4
6	24	1251	5	9.05	3.61	0.41	0.34	7.21	0.22	0.05	0.06	0.98	10	5	3	1.9	1.67	619.9	2.4
6	24	1305	6	14.32	6.07	0.45	0.30	5.61	0.44	0.03	0.08	0.46	15	5	1	1.9	1.70	617.2	2.4
6	24	1305	7	3.50	0.89	0.44	0.26	4.04	0.14	0.12	0.11	1.24	20	4		1.9	1.70	617.2	2.4
6	25	923	1	14.45	7.30	0.41	0.28	4.95	0.64	0.03	0.08	0.43	15	4		1.5	1.12	652.2	2.8
6	25	923	2	6.50	1.63	0.83	0.40	3.13	0.18	0.13	0.23	0.51	11	2	1	1.5	1.12	652.2	2.8
6	25	923	3	12.69	4.63	0.76	0.34	3.08	0.38	0.06	0.25	0.27	13	2	1	1.5	1.12	652.2	2.8
6	25	923	4	35.78	7.85	0.66	0.21	4.78	0.15	0.02	0.14	0.14	6	5		1.5	1.12	652.2	2.8
6	25	923	5	21.73	8.05	0.99	0.19	5.20	0.45	0.05	0.19	0.28	4	5		1.5	1.12	652.2	2.8
6	25	935	6	11.60	5.10	0.46	0.31	5.03	0.33	0.04	0.09	0.51	20	4	1,4	1.5	1.15	650.1	2.8
6	25	935	7	5.38	1.57	0.74	0.30	3.24	0.23	0.14	0.23	0.65	13	2	1	1.5	1.15	650.1	2.8
6	25	1036	1	7.20	4.11	0.22	0.22	5.17	0.69	0.03	0.05	0.91	32	5		1.5	1.28	641.1	2.8
6	25	1036	2	5.35	1.96	0.66	0.33	3.26	0.20	0.12	0.20	0.69	13	1	1	1.5	1.28	641.1	2.8
6	25	1036	3	12.10	3.48	0.86	0.35	3.41	0.24	0.07	0.25	0.31	14	1	1	1.5	1.28	641.1	2.8
6	25	1050	7	6.08	1.86	0.87	0.50	3.54	0.31	0.13	0.24	0.63	11	2	2	1.5	1.31	639.1	2.8
6	25	1228	6	12.21	9.05	0.48	0.47	5.67	0.63	0.04	0.09	0.69	19	5	4	1.5	1.52	621.8	2.8
6	25	1228	7	5.57	1.77	0.60	0.28	3.87	0.21	0.11	0.15	0.77	12	4		1.5	1.52	621.8	2.8
6	25	1316	1	9.38	4.86	0.30	0.23	5.92	0.55	0.03	0.05	0.83	24	5	3	1.5	1.63	612.9	2.8
6	25	1316	2	6.29	1.65	0.52	0.21	3.95	0.10	0.08	0.13	0.69	11	5	3	1.5	1.63	612.9	2.8
6	25	1316	3	13.03	5.43	0.63	0.31	4.12	0.33	0.05	0.15	0.40	3	5	3	1.5	1.63	612.9	2.8
6	25	1316	4	20.40	2.55	0.78	0.16	5.94	0.19	0.04	0.13	0.30	5	5	3	1.5	1.63	612.9	2.8
6	25	1316	5	11.82	4.74	0.45	0.33	5.81	0.21	0.03	0.08	0.59	7	5	3	1.5	1.63	612.9	2.8
6	25	1328	6	7.70	3.05	0.28	0.20	5.73	0.61	0.04	0.05	0.86	30	5	4	1.5	1.65	610.9	2.8
6	25	1328	7	5.00	2.21	0.34	0.22	4.19	0.15	0.07	0.08	0.99	14	5	3	1.5	1.65	610.9	2.8
6	27	644	1	7.35	3.52	0.42	0.61	5.00	0.50	0.06	0.08	0.82	31	5	3	0.8	0.61	721.8	2.1
6	27	644	2	3.21	0.95	0.40	0.15	3.41	0.14	0.13	0.12	1.18	22	3	2	0.8	0.61	721.8	2.1
6	27	644	3	7.75	2.53	0.35	0.13	3.54	0.37	0.05	0.10	0.49	21	3	1	0.8	0.61	721.8	2.1
6	27	644	4	10.61	7.28	0.39	0.27	4.82	0.21	0.04	0.08	0.57	9	5		0.8	0.61	721.8	2.1
6	27	644	5	6.68	3.44	0.18	0.16	5.81	0.32	0.03	0.03	1.10	11	5		0.8	0.61	721.8	2.1
6	27	657	6	9.86	4.18	0.28	0.18	5.16	0.33	0.03	0.05	0.61	23	5	1	0.8	0.64	719.2	2.2
6	27	657	7	3.33	0.53	0.32	0.13	3.52	0.25	0.09	0.09	1.08	21	4		0.8	0.64	719.2	2.2
6	27	745	1	9.63	4.55	0.25	0.17	5.00	0.49	0.03	0.05	0.62	24	5		0.8	0.74	711.1	2.5
6	27	745	2	4.38	1.12	0.54	0.34	3.16	0.12	0.12	0.17	0.78	16	2	1	0.8	0.74	711.1	2.5
6	27	745	3	10.19	3.40	0.61	0.23	3.55	0.46	0.06	0.18	0.41	17	2	1	0.8	0.74	711.1	2.5
6	27	745	4	19.83	##	0.45	0.19	4.86	0.14	0.03	0.09	0.31	6	5		0.8	0.74	711.1	2.5
6	27	745	5	15.68	3.57	0.77	0.48	4.77	0.07	0.05	0.16	0.32	5	5		0.8	0.74	711.1	2.5
6	27	756	6	10.55	5.74	0.38	0.17	5.14	0.33	0.04	0.07	0.58	22	5	1	0.8	0.76	709.3	2.6
6	27	756	7	4.19	1.30	0.50	0.37	3.20	0.13	0.11	0.15	0.83	16	1(3)	1,4	0.8	0.76	709.3	2.6
6	27	858	1	13.23	6.29	0.50	0.30	4.77	0.48	0.05	0.10	0.41	17	4		0.8	0.89	698.7	3.0
6	27	858	2	5.42	2.11	0.71	0.30	3.12	0.17	0.15	0.22	0.66	12	1	1	0.8	0.89	698.7	3.0

APPENDIX 2.4: BEDFORM DATA

6	27	858	3	14.85	5.88	0.91	0.38	3.28	0.47	0.06	0.27	0.26	12	1	1	0.8	0.89	698.7	3.0
6	27	858	4	17.68	9.23	0.58	0.13	4.19	0.26	0.04	0.14	0.31	6	5		0.8	0.89	698.7	3.0
6	27	858	5	17.21	3.77	0.54	0.13	4.90	0.25	0.03	0.11	0.30	4	5		0.8	0.89	698.7	3.0
6	27	909	6	12.89	5.68	0.47	0.18	4.77	0.37	0.04	0.10	0.42	18	4	1.4	0.8	0.91	696.9	3.1
6	27	909	7	5.38	1.58	0.65	0.23	2.91	0.20	0.13	0.22	0.59	13	1	1	0.8	0.91	696.9	3.1
6	27	1110	1	16.23	6.36	0.57	0.39	4.63	0.56	0.04	0.12	0.33	14	4		0.8	1.17	676.9	3.4
6	27	1110	2	5.42	1.69	0.62	0.27	2.87	0.17	0.12	0.22	0.59	13	1	1	0.8	1.17	676.9	3.4
6	27	1110	3	18.55	4.18	1.03	0.47	3.21	0.46	0.06	0.31	0.18	9	1	1	0.8	1.17	676.9	3.4
6	27	1110	4	31.77	7.66	1.46	0.40	4.10	0.10	0.05	0.36	0.14	4	4		0.8	1.17	676.9	3.4
6	27	1110	5	12.29	4.56	0.21	0.06	3.99	0.08	0.02	0.05	0.37	5	5		0.8	1.17	676.9	3.4
6	27	1121	6	22.21	##	0.73	0.55	5.53	0.75	0.04	0.15	0.37	8	4	1.4	0.8	1.21	674.0	3.4
6	27	1121	7	6.36	1.80	0.76	0.40	3.10	0.22	0.12	0.24	0.53	11	1	1	0.8	1.21	674.0	3.4
6	27	1251	1	14.83	7.83	0.62	0.48	4.77	0.51	0.04	0.13	0.47	15	5		0.8	1.38	660.7	3.4
6	27	1251	2	5.48	2.02	0.81	0.41	3.07	0.19	0.15	0.26	0.65	13	1	1.3	0.8	1.38	660.7	3.4
6	27	1251	3	19.76	7.18	0.92	0.40	3.53	0.30	0.05	0.26	0.21	8	2	3	0.8	1.38	660.7	3.4
6	27	1251	4	24.66	8.05	1.26	0.29	4.77	0.28	0.06	0.26	0.23	4	5	1.3	0.8	1.38	660.7	3.4
6	27	1251	5	44.00	4.55	1.51	0.47	4.60	0.43	0.03	0.32	0.10	2	5	3	0.8	1.38	660.7	3.4
6	27	1304	6	15.96	8.08	0.54	0.35	4.38	1.13	0.04	0.13	0.34	12	5	1.4	0.8	1.41	658.7	3.4
6	27	1304	7	7.91	1.74	0.91	0.38	3.33	0.23	0.11	0.27	0.44	9	1	1	0.8	1.41	658.7	3.4
6	27	1408	1	14.87	5.66	0.48	0.31	5.51	0.48	0.03	0.09	0.45	16	5	3	0.8	1.54	649.7	3.4
6	27	1408	2	6.91	1.25	0.67	0.31	3.78	0.19	0.09	0.18	0.57	10	5	3	0.8	1.54	649.7	3.4
6	27	1408	3	12.38	4.94	0.53	0.30	4.07	0.35	0.05	0.13	0.40	14	5	3	0.8	1.54	649.7	3.4
6	27	1408	4	18.59	4.84	0.78	0.49	5.03	0.08	0.04	0.15	0.30	5	5	3	0.8	1.54	649.7	3.4
6	27	1408	5	22.45	6.41	0.94	0.72	4.97	0.28	0.04	0.19	0.24	4	5	3	0.8	1.54	649.7	3.4
6	27	1418	6	19.33	##	0.57	0.51	5.60	0.30	0.03	0.10	0.44	12	5	1.4	0.8	1.56	648.3	3.4
6	27	1418	7	7.25	1.38	0.77	0.30	3.98	0.14	0.10	0.19	0.57	10	5	2	0.8	1.56	648.3	3.4
6	28	742	1	10.55	7.61	0.39	0.25	4.87	0.55	0.04	0.08	0.65	22	5		0.5	0.64	685.1	2.4
6	28	742	2	2.96	1.23	0.47	0.24	3.22	0.19	0.16	0.15	1.26	24	3		0.5	0.64	685.1	2.4
6	28	742	3	7.61	2.05	0.50	0.28	3.62	0.31	0.06	0.14	0.51	22	4		0.5	0.64	685.1	2.4
6	28	742	4	18.54	6.32	0.64	0.22	5.12	0.17	0.04	0.13	0.32	5	4		0.5	0.64	685.1	2.4
6	28	742	5	13.15	8.72	0.57	0.37	5.26	0.14	0.05	0.11	0.62	6	4		0.5	0.64	685.1	2.4
6	28	1312	6	21.09	##	0.68	0.57	4.47	1.00	0.03	0.22	0.31	11	5	1.4	0.5	1.33	624.6	3.7
6	28	1312	7	9.37	2.27	0.96	0.32	3.10	0.14	0.11	0.31	0.35	8	1(3)	2	0.5	1.33	624.6	3.7
6	28	1419	1	16.68	6.17	0.70	0.42	5.10	0.60	0.04	0.14	0.36	14	5	3	0.5	1.47	616.1	3.7
6	28	1419	2	7.51	3.00	0.72	0.49	3.49	0.20	0.09	0.20	0.56	9	4	3	0.5	1.47	616.1	3.7
6	28	1419	3	8.84	5.38	0.62	0.47	3.74	0.50	0.08	0.16	0.61	19	3	3	0.5	1.47	616.1	3.7
6	28	1419	4	19.65	8.14	0.81	0.33	5.54	0.36	0.04	0.15	0.33	6	4	3	0.5	1.47	616.1	3.7
6	28	1419	5	12.48	8.72	0.78	0.53	5.59	0.41	0.08	0.14	0.69	6	4	3	0.5	1.47	616.1	3.7
6	28	1429	6	15.59	5.91	0.52	0.35	5.29	0.37	0.03	0.10	0.42	14	5	1.3	0.5	1.49	615.1	3.7
6	28	1429	7	7.56	2.47	0.76	0.43	3.79	0.12	0.10	0.20	0.57	9	4	3	0.5	1.49	615.1	3.7

APPENDIX 2.4: BEDFORM DATA

6	29	957	1	10.48	3.97	0.28	0.24	5.03	0.50	0.03	0.06	0.55	21	4	1	0.2	0.82	756.3	3.4
6	29	957	2	4.64	3.21	0.46	0.26	2.70	0.15	0.11	0.17	0.75	15	1(3)	1.5	0.2	0.82	756.3	3.4
6	29	957	3	19.87	6.18	1.08	0.45	3.60	0.44	0.06	0.31	0.20	9	1(3)	1	0.2	0.82	756.3	3.4
6	29	957	4	14.53	4.60	0.53	0.28	4.00	0.28	0.03	0.13	0.30	6	4	2	0.2	0.82	756.3	3.4
6	29	957	5	18.17	5.48	0.42	0.24	4.86	0.13	0.02	0.09	0.31	4	4	2	0.2	0.82	756.3	3.4
6	30	734	1	10.83	6.23	0.26	0.16	5.64	0.37	0.02	0.05	0.66	14	5	3	0.1	0.40	729.9	1.7
6	30	734	2	2.57	0.54	0.27	0.13	3.94	0.17	0.11	0.07	1.59	27	5		0.1	0.40	729.9	1.7
6	30	734	3	5.09	2.16	0.28	0.13	4.71	0.52	0.06	0.06	1.14	33	4	3	0.1	0.40	729.9	1.7
6	30	734	4	25.50	9.04	0.58	0.27	6.48	0.24	0.02	0.09	0.29	4	5	3	0.1	0.40	729.9	1.7
6	30	734	5	35.47	0.68	1.14	0.60	6.70	0.10	0.03	0.17	0.19	2	5	3	0.1	0.40	729.9	1.7
6	30	745	6	7.48	5.05	0.18	0.11	5.84	0.48	0.03	0.03	0.95	31	5	1.4	0.1	0.43	726.6	1.8
6	30	745	7	2.98	1.17	0.34	0.18	3.98	0.22	0.12	0.08	1.54	23	5	2	0.1	0.43	726.6	1.8
6	30	952	1	10.09	4.20	0.37	0.26	4.87	0.62	0.04	0.08	0.58	23	5	1	0.1	0.71	691.1	3.0
6	30	952	2	4.62	1.26	0.65	0.30	2.84	0.28	0.14	0.23	0.68	16	2	1	0.1	0.71	691.1	3.0
6	30	952	3	10.29	2.07	0.53	0.25	3.50	0.27	0.05	0.15	0.35	16	2	1	0.1	0.71	691.1	3.0
6	30	952	4	15.34	4.99	0.60	0.26	4.14	0.17	0.04	0.15	0.30	7	4		0.1	0.71	691.1	3.0
6	30	952	5	18.67	2.79	0.52	0.42	5.11	0.29	0.03	0.10	0.28	4	5		0.1	0.71	691.1	3.0
6	30	1005	6	10.23	3.45	0.41	0.25	4.75	0.49	0.04	0.09	0.50	23	5	1.4	0.1	0.74	687.6	3.1
6	30	1005	7	5.78	1.40	0.65	0.30	2.73	0.26	0.11	0.24	0.50	12	2	1	0.1	0.74	687.6	3.1
6	30	1330	1	16.72	5.52	0.69	0.46	4.80	0.57	0.04	0.15	0.31	14	4	1	0.1	1.19	639.1	4.2
6	30	1330	2	10.53	2.74	1.16	0.52	2.61	0.52	0.11	0.43	0.25	7	1(3)	1	0.1	1.19	639.1	4.2
6	30	1330	3	18.59	7.19	0.72	0.31	3.68	0.46	0.04	0.20	0.24	9	1(3)	1	0.1	1.19	639.1	4.2
6	30	1330	4	28.80	7.68	1.35	0.30	4.03	0.39	0.05	0.33	0.15	4	1	1	0.1	1.19	639.1	4.2
6	30	1330	5	19.80	5.51	0.49	0.44	4.34	0.29	0.02	0.11	0.24	4	2	1	0.1	1.19	639.1	4.2
6	30	1437	1	18.71	9.31	0.66	0.43	4.95	0.59	0.04	0.14	0.33	13	4	1	0.1	1.33	621.8	4.2
6	30	1437	2	10.04	3.12	1.12	0.46	2.94	0.38	0.12	0.37	0.35	8	1(3)	1	0.1	1.33	621.8	4.2
6	30	1437	3	17.78	##	0.75	0.31	3.99	0.62	0.05	0.20	0.36	9	1(3)	1	0.1	1.33	621.8	4.2
6	30	1437	4	43.75	##	1.45	0.39	5.14	0.30	0.03	0.28	0.13	3	2	1	0.1	1.33	621.8	4.2
6	30	1437	5	64.34	0.00	1.75	0.00	5.46	0.00	0.03	0.32	0.08	1	3	1	0.1	1.33	621.8	4.2
7	10	1408	1	5.25	2.33	0.16	0.13	5.72	0.35	0.03	0.03	1.48	44	5		1.0	1.61	458.1	3.4
7	10	1408	2	3.86	0.81	0.34	0.16	3.61	0.14	0.09	0.10	0.98	18	5		1.0	1.61	458.1	3.4
7	10	1408	3	8.14	2.58	0.41	0.19	4.19	0.30	0.05	0.10	0.58	21	5		1.0	1.61	458.1	3.4
7	10	1408	4	8.25	2.73	0.34	0.23	5.55	0.17	0.04	0.06	0.78	13	6		1.0	1.61	458.1	3.4
7	10	1408	5	6.54	1.40	0.27	0.13	5.29	0.11	0.04	0.05	0.85	12	6		1.0	1.61	458.1	3.4
7	10	1420	6	8.93	2.38	0.29	0.16	5.28	0.51	0.03	0.05	0.63	25	5		1.0	1.63	458.4	3.4
7	10	1420	7	4.38	1.12	0.29	0.09	3.81	0.18	0.07	0.08	0.94	16	5		1.0	1.63	458.4	3.4
7	12	546	1	9.33	3.04	0.24	0.15	5.35	0.50	0.02	0.05	0.65	25	6		0.7	0.35	485.0	1.2
7	12	546	2	3.99	1.12	0.19	0.08	3.72	0.13	0.05	0.05	1.01	16	5	3	0.7	0.35	485.0	1.2
7	12	546	3	6.74	4.46	0.24	0.19	4.24	0.29	0.04	0.05	0.99	26	5	3	0.7	0.35	485.0	1.2
7	12	546	4	6.95	1.67	0.24	0.15	5.17	0.13	0.03	0.05	0.80	14	6	3	0.7	0.35	485.0	1.2

APPENDIX 2.4: BEDFORM DATA

7	12	546	5	6.22	2.01	0.22	0.13	5.45	0.21	0.03	0.04	0.96	14	6	3	0.7	0.35	485.0	1.2
7	12	559	6	11.60	4.12	0.35	0.19	5.09	0.41	0.03	0.07	0.53	20	6		0.7	0.37	484.9	1.3
7	12	559	7	3.50	0.65	0.18	0.08	3.67	0.17	0.05	0.05	1.11	20	5		0.7	0.37	484.9	1.3
7	12	1256	1	8.84	3.15	0.52	0.31	3.77	0.34	0.06	0.14	0.49	27	5		0.7	1.27	449.3	3.4
7	12	1256	2	3.79	0.72	0.51	0.19	2.19	0.14	0.13	0.23	0.60	19	2(3)		0.7	1.27	449.3	3.4
7	12	1256	3	8.38	3.67	0.62	0.35	2.64	0.28	0.07	0.23	0.36	20	3(3)		0.7	1.27	449.3	3.4
7	12	1256	4	10.99	2.35	0.51	0.26	4.19	0.14	0.05	0.02	0.40	9	5		0.7	1.27	449.3	3.4
7	12	1256	5	10.39	2.73	0.78	0.35	4.32	0.31	0.07	0.18	0.44	8	5		0.7	1.27	449.3	3.4
7	13	1156	6	7.91	2.92	0.38	0.20	4.56	0.41	0.05	0.09	0.63	25	5	1	0.7	1.06	441.1	3.3
7	13	1156	7	3.50	1.32	0.37	0.21	2.05	0.21	0.11	0.18	0.71	20	3		0.7	1.06	441.1	3.3
7	13	1356	1	8.76	2.18	0.44	0.18	4.33	0.25	0.05	0.10	0.52	26	5		0.7	1.32	434.9	3.3
7	13	1356	2	4.14	1.32	0.53	0.24	2.34	0.25	0.13	0.22	0.61	17	4		0.7	1.32	434.9	3.3
7	13	1356	3	8.82	2.03	0.58	0.21	2.91	0.25	0.07	0.20	0.34	19	5		0.7	1.32	434.9	3.3
7	14	625	1	7.32	2.52	0.22	0.15	5.75	0.37	0.03	0.04	0.85	27	5		0.7	0.22	470.9	0.7
7	14	625	2	4.76	2.31	0.16	0.06	4.04	0.11	0.04	0.04	1.01	14	5	3	0.7	0.22	470.9	0.7
7	14	625	3	7.86	2.31	0.28	0.19	4.49	0.35	0.03	0.06	0.63	22	5	3	0.7	0.22	470.9	0.7
7	14	625	4	11.03	3.31	0.43	0.19	6.85	0.14	0.04	0.06	0.70	10	5		0.7	0.22	470.9	0.7
7	14	625	5	11.12	2.53	0.65	0.25	6.91	0.14	0.06	0.09	0.65	8	5		0.7	0.22	470.9	0.7
7	14	638	6	8.81	2.40	0.22	0.08	5.77	0.46	0.03	0.04	0.71	24	5		0.7	0.25	469.5	0.8
7	14	638	7	5.27	0.96	0.25	0.09	4.09	0.23	0.05	0.06	0.80	13	5		0.7	0.25	469.5	0.8
7	15	741	1	6.93	2.38	0.22	0.15	5.47	0.48	0.03	0.04	0.90	30	5		0.8	0.29	401.7	0.9
7	15	741	2	4.30	0.68	0.27	0.17	3.72	0.13	0.06	0.07	0.88	17	5		0.8	0.29	401.7	0.9
7	15	741	3	8.43	2.82	0.30	0.16	4.34	0.26	0.04	0.07	0.58	19	5		0.8	0.29	401.7	0.9
7	15	741	4	9.61	1.92	0.44	0.16	6.84	0.17	0.04	0.06	0.75	11	5		0.8	0.29	401.7	0.9
7	15	741	5	7.19	3.33	0.44	0.33	6.47	0.13	0.05	0.07	1.27	12	6		0.8	0.29	401.7	0.9
7	15	756	6	7.55	2.76	0.22	0.10	5.62	0.63	0.03	0.04	0.86	30	5		0.8	0.33	401.1	1.0
7	15	756	7	5.17	1.73	0.23	0.08	3.73	0.22	0.05	0.06	0.79	12	5		0.8	0.33	401.1	1.0
7	15	847	1	9.64	6.13	0.27	0.19	4.86	0.36	0.03	0.06	0.64	25	5		0.8	0.45	396.9	1.4
7	15	847	2	4.23	1.12	0.27	0.15	3.13	0.11	0.06	0.09	0.80	15	5		0.8	0.45	396.9	1.4
7	15	847	3	9.04	3.05	0.29	0.16	3.81	0.23	0.03	0.08	0.48	17	4		0.8	0.45	396.9	1.4
7	15	847	4	9.58	3.30	0.49	0.27	5.54	0.17	0.05	0.09	0.67	11	5		0.8	0.45	396.9	1.4
7	15	847	5	10.60	1.40	0.65	0.21	6.02	0.22	0.06	0.11	0.58	8	6		0.8	0.45	396.9	1.4
7	15	902	6	8.83	4.03	0.27	0.17	5.09	0.29	0.03	0.05	0.69	23	5		0.8	0.48	395.7	1.5
7	15	902	7	2.99	1.13	0.16	0.07	3.18	0.26	0.06	0.05	1.26	22	5		0.8	0.48	395.7	1.5
7	15	1003	6	8.60	2.30	0.26	0.09	4.63	0.23	0.03	0.06	0.59	26	5		0.8	0.62	392.3	1.9
7	15	1003	7	3.48	1.15	0.29	0.13	2.56	0.16	0.09	0.11	0.83	19	4		0.8	0.62	392.3	1.9
7	15	1251	1	8.40	2.71	0.51	0.26	3.64	0.37	0.06	0.14	0.49	28	5		0.8	1.01	378.9	3.1
7	15	1251	2	2.75	0.96	0.42	0.27	1.83	0.18	0.15	0.23	0.75	25	2(3)	2	0.8	1.01	378.9	3.1
7	15	1251	3	6.39	2.13	0.41	0.22	2.28	0.30	0.06	0.18	0.39	27	2(3)		0.8	1.01	378.9	3.1
7	15	1251	4	7.68	2.31	0.40	0.19	4.14	0.15	0.05	0.10	0.59	13	4		0.8	1.01	378.9	3.1

APPENDIX 2.4: BEDFORM DATA

7	15	1251	5	9.47	2.72	0.55	0.29	4.12	0.24	0.06	0.13	0.48	9	4	2	0.8	1.01	378.9	3.1
7	15	1304	6	7.19	2.69	0.35	0.20	4.15	0.25	0.05	0.09	0.67	32	5	2	0.8	1.04	377.8	3.1
7	15	1304	7	4.18	1.27	0.44	0.16	1.99	0.17	0.11	0.22	0.55	16	3(3)		0.8	1.04	377.8	3.1
7	16	701	1	8.38	2.39	0.21	0.11	6.08	0.31	0.03	0.03	0.79	25	5		0.9	0.10	407.6	0.3
7	16	701	2	3.89	2.14	0.18	0.09	4.05	0.23	0.05	0.04	1.40	18	5	3	0.9	0.10	407.6	0.3
7	16	701	3	8.79	3.86	0.24	0.17	4.87	0.31	0.03	0.05	0.79	17	5	3	0.9	0.10	407.6	0.3
7	16	701	4	5.39	2.44	0.16	0.10	7.60	0.12	0.03	0.02	1.80	18	6	3	0.9	0.10	407.6	0.3
7	16	701	5	8.00	2.84	0.30	0.19	5.51	0.14	0.04	0.05	0.81	11	6	3	0.9	0.10	407.6	0.3
7	16	714	6	7.88	2.40	0.23	0.13	5.92	0.39	0.03	0.04	0.88	26	5		0.9	0.13	407.1	0.4
7	16	714	7	4.57	1.42	0.18	0.05	4.10	0.22	0.04	0.04	0.98	15	5		0.9	0.13	407.1	0.4
7	16	808	1	7.88	2.99	0.22	0.15	5.47	0.62	0.03	0.04	0.79	29	5		0.9	0.26	405.0	0.7
7	16	808	2	5.66	2.46	0.22	0.11	3.77	0.18	0.04	0.06	0.77	10	5	3	0.9	0.26	405.0	0.7
7	16	808	3	9.18	4.45	0.25	0.14	4.35	0.26	0.03	0.06	0.58	18	5	3	0.9	0.26	405.0	0.7
7	16	808	4	8.69	2.29	0.32	0.20	6.86	0.12	0.04	0.05	0.86	12	5		0.9	0.26	405.0	0.7
7	16	808	5	8.36	2.21	0.28	0.13	6.79	0.07	0.03	0.04	0.89	10	5		0.9	0.26	405.0	0.7
7	16	822	6	9.36	3.99	0.24	0.10	5.79	0.28	0.03	0.04	0.74	24	5		0.9	0.29	404.3	0.8
7	16	822	7	3.46	1.32	0.15	0.07	3.78	0.23	0.05	0.04	1.39	20	5		0.9	0.29	404.3	0.8
7	16	909	1	8.82	3.36	0.24	0.13	4.84	0.46	0.03	0.05	0.62	26	5		0.9	0.40	401.8	1.2
7	16	909	2	1.44	0.78	0.10	0.06	3.28	0.18	0.08	0.03	2.90	48	4	3	0.9	0.40	401.8	1.2
7	16	909	3	4.47	3.37	0.13	0.07	3.65	0.17	0.03	0.03	1.18	37	5	3	0.9	0.40	401.8	1.2
7	16	909	4	8.56	3.21	0.34	0.18	6.00	0.13	0.04	0.06	0.81	11	5		0.9	0.40	401.8	1.2
7	16	909	5	9.97	3.31	0.51	0.26	6.29	0.15	0.05	0.08	0.70	9	5		0.9	0.40	401.8	1.2
7	16	927	6	8.59	3.42	0.20	0.10	5.31	0.22	0.02	0.04	0.69	26	5		0.9	0.45	400.9	1.3
7	16	927	7	2.97	1.30	0.15	0.07	3.18	0.21	0.05	0.05	1.39	23	4		0.9	0.45	400.9	1.3
7	16	1327	1	6.69	3.38	0.31	0.24	3.82	0.40	0.04	0.09	0.82	34	4		0.9	1.02	392.6	2.9
7	16	1327	2	2.59	0.60	0.35	0.12	1.89	0.20	0.14	0.19	0.77	28	2(2)	2	0.9	1.02	392.6	2.9
7	16	1327	3	7.14	2.27	0.39	0.24	2.36	0.22	0.05	0.16	0.37	23	3(2)	2	0.9	1.02	392.6	2.9
7	16	1327	4	7.29	2.22	0.35	0.20	3.79	0.14	0.05	0.09	0.58	14	4		0.9	1.02	392.6	2.9
7	16	1327	5	9.49	2.28	0.57	0.19	4.20	0.20	0.06	0.14	0.47	9	4		0.9	1.02	392.6	2.9
7	17	844	6	7.25	1.84	0.15	0.11	5.85	0.19	0.02	0.03	0.88	32	6		1.2	0.24	490.3	0.6
7	17	940	1	10.00	3.51	0.21	0.15	5.24	0.40	0.02	0.04	0.58	22	5		1.2	0.38	485.6	1.0
7	17	940	2	1.79	0.62	0.16	0.08	3.30	0.18	0.09	0.05	2.08	39	4		1.2	0.38	485.6	1.0
7	17	940	3	2.44	0.85	0.12	0.07	3.41	0.58	0.04	0.03	1.40	63	4		1.2	0.38	485.6	1.0
7	17	940	4	9.10	1.58	0.38	0.16	6.25	0.08	0.04	0.06	0.71	10	5		1.2	0.38	485.6	1.0
7	17	940	5	9.49	2.53	0.49	0.18	5.99	0.17	0.05	0.08	0.68	9	5		1.2	0.38	485.6	1.0
7	17	1126	1	4.75	2.34	0.15	0.09	4.45	0.19	0.03	0.03	1.13	43	5		1.2	0.64	474.1	1.7
7	17	1126	2	2.40	0.60	0.23	0.10	2.50	0.17	0.10	0.09	1.12	30	4		1.2	0.64	474.1	1.7
7	17	1126	3	3.95	1.09	0.21	0.09	3.08	0.28	0.05	0.07	0.84	43	4		1.2	0.64	474.1	1.7
7	17	1126	4	6.82	2.94	0.21	0.08	4.62	0.20	0.03	0.05	0.85	15	5		1.2	0.64	474.1	1.7
7	17	1126	5	7.70	2.32	0.26	0.13	4.46	0.15	0.03	0.06	0.63	12	5		1.2	0.64	474.1	1.7

APPENDIX 2.4: BEDFORM DATA

7	17	1143	6	5.16	1.89	0.20	0.08	4.69	0.28	0.04	1.02	45	5		1.2	0.68	472.0	1.8	
7	17	1143	7	2.53	0.71	0.24	0.12	2.53	0.22	0.10	1.09	28	4		1.2	0.68	472.0	1.8	
7	17	1237	1	5.25	1.95	0.24	0.16	4.03	0.42	0.05	0.06	0.89	44	5		1.2	0.82	466.1	2.1
7	17	1237	2	2.45	0.67	0.28	0.14	2.08	0.17	0.11	0.14	0.91	28	4	2	1.2	0.82	466.1	2.1
7	17	1237	3	4.46	1.38	0.25	0.13	2.58	0.19	0.06	0.10	0.63	37	4		1.2	0.82	466.1	2.1
7	17	1237	4	8.10	1.80	0.26	0.12	4.41	0.27	0.03	0.06	0.57	12	5		1.2	0.82	466.1	2.1
7	17	1237	5	4.69	1.23	0.23	0.11	5.03	0.15	0.05	0.05	1.16	19	5		1.2	0.82	466.1	2.1
7	17	1249	6	6.57	4.52	0.24	0.13	4.32	0.33	0.05	0.06	0.83	34	5		1.2	0.85	464.9	2.2
7	17	1249	7	2.33	0.64	0.26	0.13	2.22	0.18	0.11	1.02	30	4		1.2	0.85	464.9	2.2	
7	17	1440	6	7.12	2.59	0.31	0.19	4.54	0.43	0.04	0.07	0.72	32	5	1	1.2	1.13	453.5	2.6
7	17	1440	7	3.11	0.72	0.37	0.21	2.20	0.16	0.12	0.17	0.75	22	2		1.2	1.13	453.5	2.6
7	17	1533	1	6.73	2.63	0.35	0.19	4.26	0.23	0.05	0.08	0.74	33	5		1.2	1.26	449.3	2.6
7	17	1533	2	4.71	2.28	0.43	0.20	2.22	0.17	0.10	0.20	0.63	23	4		1.2	1.26	449.3	2.6
7	17	1533	3	7.89	1.87	0.45	0.18	2.78	0.19	0.06	0.16	0.37	20	4		1.2	1.26	449.3	2.6
7	17	1533	4	10.66	2.26	0.42	0.29	4.35	0.13	0.04	0.10	0.43	10	5		1.2	1.26	449.3	2.6
7	17	1533	5	7.89	1.86	0.55	0.21	4.32	0.10	0.07	0.13	0.58	11	5	2	1.2	1.26	449.3	2.6
7	17	1635	1	7.70	3.17	0.28	0.18	4.52	0.31	0.04	0.06	0.69	30	5		1.2	1.41	446.2	2.6
7	17	1635	2	3.21	1.05	0.35	0.16	2.65	0.20	0.11	0.13	0.93	23	5		1.2	1.41	446.2	2.6
7	17	1635	3	6.33	2.19	0.40	0.21	3.20	0.25	0.06	0.12	0.56	26	5		1.2	1.41	446.2	2.6
7	17	1635	4	7.50	2.01	0.34	0.15	4.35	0.19	0.05	0.08	0.63	14	6		1.2	1.41	446.2	2.6
7	17	1635	5	10.72	2.65	0.48	0.20	5.34	0.12	0.05	0.09	0.53	8	6		1.2	1.41	446.2	2.6
7	17	1650	6	7.19	6.34	0.16	0.19	5.19	0.21	0.02	0.03	0.99	28	5	4	1.2	1.45	445.7	2.6
7	17	1650	7	2.77	0.72	0.34	0.16	2.87	0.19	0.12	1.10	26	5		1.2	1.45	445.7	2.6	
7	18	1019	1	1.96	1.23	0.07	0.06	3.56	1.63	0.03	0.01	1.43	82	5		1.4	0.37	478.4	0.9
7	18	1019	2	1.95	0.49	0.19	0.08	3.37	0.18	0.10	0.06	1.84	35	5		1.4	0.37	478.4	0.9
7	18	1019	3	3.48	1.06	0.16	0.09	3.88	0.21	0.05	0.04	1.25	48	5		1.4	0.37	478.4	0.9
7	18	1019	4	9.84	2.33	0.32	0.19	5.68	0.10	0.03	0.06	0.62	10	5		1.4	0.37	478.4	0.9
7	18	1019	5	11.00	3.21	0.35	0.09	5.90	0.24	0.03	0.06	0.60	8	5		1.4	0.37	478.4	0.9
7	18	1034	6	4.86	1.82	0.20	0.14	5.47	0.24	0.01	0.04	0.61	15	5		1.4	0.41	476.5	0.9
7	18	1034	7	2.69	0.99	0.18	0.07	3.30	0.16	0.07	0.05	1.37	26	5	3	1.4	0.41	476.5	0.9
7	18	1445	6	4.90	1.71	0.21	0.27	4.65	0.30	0.04	0.04	1.07	45	5		1.4	1.06	449.6	2.3
7	18	1445	7	3.18	1.19	0.33	0.17	2.24	0.14	0.10	0.15	0.83	22	4		1.4	1.06	449.6	2.3
7	19	957	6	4.30	1.83	0.12	0.10	5.77	0.26	0.03	0.02	1.55	52	6		1.8	0.19	501.1	0.4
7	19	957	7	2.59	0.91	0.22	0.09	3.80	0.19	0.09	0.06	1.71	27	5		1.8	0.19	501.1	0.4
7	19	1054	6	4.72	1.37	0.12	0.06	5.60	0.18	0.03	0.02	1.34	41	6		1.8	0.35	494.0	0.6
7	19	1054	7	2.47	0.95	0.21	0.10	3.50	0.19	0.09	0.06	1.67	28	4		1.8	0.35	494.0	0.6
7	19	1200	6	4.54	1.38	0.12	0.07	5.21	0.28	0.03	0.02	1.25	43	5		1.8	0.53	488.0	0.9
7	19	1200	7	2.14	0.67	0.26	0.11	3.14	0.16	0.12	0.08	1.59	32	4		1.8	0.53	488.0	0.9
7	19	1540	7	2.72	1.01	0.33	0.15	2.56	0.13	0.13	0.13	1.09	26	4		1.8	1.12	475.1	1.8
7	19	1634	1	4.66	1.51	0.20	0.09	4.85	0.21	0.04	0.04	1.14	44	5		1.8	1.27	475.0	1.8

APPENDIX 2.4: BEDFORM DATA

7	19	1634	3	5.36	1.49	0.35	0.16	3.10	0.29	0.06	0.11	0.63	32	5		1.8	1.27	475.0	1.8
7	19	1650	6	5.47	1.76	0.15	0.09	5.23	0.29	0.03	0.03	1.04	38	5	1,4	1.8	1.31	475.1	1.8
7	19	1650	7	3.26	0.81	0.35	0.08	2.83	0.10	0.12	0.12	0.93	21	5		1.8	1.31	475.1	1.8
7	20	946	1	4.02	1.67	0.11	0.09	5.71	0.34	0.03	0.02	1.58	57	5		2.1	0.02	529.8	0.0
7	20	946	2	2.58	0.72	0.24	0.09	3.80	0.17	0.10	0.06	1.58	28	4		2.1	0.02	529.8	0.0
7	20	946	3	6.11	2.02	0.27	0.11	4.37	0.22	0.04	0.06	0.79	27	5		2.1	0.02	529.8	0.0
7	20	946	4	6.10	2.03	0.18	0.09	5.99	0.11	0.03	0.03	1.10	16	6		2.1	0.02	529.8	0.0
7	20	946	5	6.87	1.75	0.24	0.11	6.17	0.08	0.03	0.04	0.96	14	6		2.1	0.02	529.8	0.0
7	20	1002	6	4.89	1.86	0.09	0.05	6.21	0.14	0.02	0.01	1.43	16	5	1,4	2.1	0.06	528.1	0.1
7	20	1002	7	3.01	1.05	0.27	0.12	3.83	0.20	0.10	0.07	1.49	23	4		2.1	0.06	528.1	0.1
7	20	1047	1	2.27	0.86	0.07	0.05	4.90	1.01	0.03	0.01	1.96	67	5		2.1	0.19	523.3	0.3
7	20	1047	2	2.70	0.86	0.30	0.10	3.66	0.19	0.12	0.08	1.49	25	4		2.1	0.19	523.3	0.3
7	20	1047	3	5.21	1.92	0.27	0.12	4.28	0.22	0.05	0.06	0.96	33	4		2.1	0.19	523.3	0.3
7	20	1047	4	5.37	1.74	0.16	0.09	5.55	0.21	0.03	0.03	1.16	19	6		2.1	0.19	523.3	0.3
7	20	1047	5	5.08	1.13	0.15	0.06	5.62	0.15	0.03	0.03	1.17	17	6		2.1	0.19	523.3	0.3
7	20	1102	6	3.77	1.30	0.10	0.06	5.74	0.27	0.03	0.02	1.66	53	5		2.1	0.24	521.7	0.3
7	20	1102	7	2.93	0.93	0.24	0.13	3.49	0.65	0.09	0.08	1.30	23	5		2.1	0.24	521.7	0.3
7	20	1156	6	4.19	1.51	0.09	0.07	5.73	0.20	0.02	0.02	1.53	47	5	1	2.1	0.39	516.0	0.5
7	20	1156	7	2.76	0.69	0.31	0.14	3.42	0.18	0.11	0.09	1.32	24	5		2.1	0.39	516.0	0.5
7	27	1000	1	10.09	5.71	0.47	0.35	3.95	0.46	0.04	0.13	0.56	23	5		0.5	0.97	410.3	3.6
7	27	1000	2	3.49	0.94	0.41	0.13	1.81	0.12	0.12	0.23	0.56	20	2(3)	1	0.5	0.97	410.3	3.6
7	27	1000	3	11.39	3.93	0.53	0.32	2.33	0.23	0.05	0.22	0.23	16	2(3)	2	0.5	0.97	410.3	3.6
7	27	1000	4	9.81	4.66	0.57	0.34	4.40	0.14	0.06	0.13	0.58	10	5		0.5	0.97	410.3	3.6
7	27	1000	5	13.27	4.39	0.75	0.25	4.13	0.12	0.06	0.18	0.36	7	5		0.5	0.97	410.3	3.6
7	27	1102	1	12.31	5.49	0.57	0.23	3.76	0.39	0.05	0.15	0.37	18	5		0.5	1.10	403.9	3.7
7	27	1102	2	3.06	0.77	0.40	0.17	1.78	0.12	0.14	0.23	0.62	23	1(1)	2	0.5	1.10	403.9	3.7
7	27	1102	3	10.54	4.30	0.56	0.25	2.21	0.26	0.06	0.25	0.24	17	1(1)		0.5	1.10	403.9	3.7
7	27	1102	4	12.09	3.09	0.58	0.37	3.97	0.24	0.05	0.15	0.36	8	3		0.5	1.10	403.9	3.7
7	27	1102	5	11.69	4.21	0.74	0.42	3.69	0.22	0.06	0.20	0.36	7	3		0.5	1.10	403.9	3.7
7	28	859	6	10.55	4.79	0.29	0.21	4.27	0.34	0.03	0.07	0.58	22	5		0.3	0.74	417.2	2.9
7	28	859	7	3.50	1.24	0.24	0.10	2.04	0.16	0.07	0.12	0.68	20	3(3)		0.3	0.74	417.2	2.9
7	28	944	1	13.65	6.04	0.47	0.33	3.86	0.58	0.03	0.12	0.35	17	5	4	0.3	0.83	413.2	3.3
7	28	944	2	3.07	0.90	0.32	0.11	1.71	0.10	0.11	0.19	0.61	23	2(1)	2	0.3	0.83	413.2	3.3
7	28	944	3	9.01	4.04	0.42	0.20	2.24	0.29	0.05	0.19	0.28	19	2(1)	1	0.3	0.83	413.2	3.3
7	28	944	4	9.46	3.14	0.38	0.28	3.26	0.24	0.04	0.12	0.38	11	3		0.3	0.83	413.2	3.3
7	28	944	5	14.02	7.23	0.69	0.28	3.31	0.23	0.05	0.16	0.27	6	3		0.3	0.83	413.2	3.3
7	29	728	1	16.42	4.99	0.47	0.26	4.72	0.53	0.03	0.10	0.32	14	5	4	0.2	0.40	458.3	1.7
7	29	728	2	3.50	1.37	0.16	0.11	3.37	0.16	0.06	0.05	1.31	20	5	3	0.2	0.40	458.3	1.7
7	29	728	3	7.42	4.35	0.17	0.13	3.78	0.21	0.02	0.04	0.86	23	5	3	0.2	0.40	458.3	1.7
7	29	728	4	18.19	2.66	0.69	0.40	6.05	0.17	0.04	0.11	0.34	6	5		0.2	0.40	458.3	1.7

APPENDIX 2.4: BEDFORM DATA

7	29	728	5	15.50	7.26	0.53	0.39	5.77	0.14	0.04	0.09	0.47	6	5		0.2	0.40	458.3	1.7
7	29	919	1	13.65	8.27	0.52	0.28	3.65	0.38	0.04	0.14	0.45	17	5	5	0.2	0.66	446.0	2.7
7	29	919	2	2.33	0.85	0.21	0.12	2.28	0.22	0.09	0.10	1.08	30	4		0.2	0.66	446.0	2.7
7	29	919	3	7.21	2.95	0.32	0.15	2.59	0.18	0.05	0.12	0.41	23	4		0.2	0.66	446.0	2.7
7	29	919	4	15.87	4.85	0.47	0.28	4.68	0.16	0.04	0.10	0.34	7	5	3	0.2	0.66	446.0	2.7
7	29	919	5	7.73	3.02	0.25	0.15	4.25	0.17	0.03	0.06	0.62	11	5		0.2	0.66	446.0	2.7
7	29	1137	1	13.65	7.61	0.65	0.36	3.75	0.25	0.05	0.17	0.35	17	3		0.2	0.97	428.6	4.0
7	29	1137	2	3.75	1.06	0.40	0.16	1.84	0.16	0.11	0.21	0.53	19	1(3)	1	0.2	0.97	428.6	4.0
7	29	1137	3	9.73	2.45	0.53	0.21	2.26	0.21	0.06	0.24	0.25	18	1(3)	1	0.2	0.97	428.6	4.0
7	29	1137	4	12.95	4.53	0.52	0.33	3.91	0.30	0.04	0.13	0.34	7	4		0.2	0.97	428.6	4.0
7	29	1137	5	13.89	4.79	0.71	0.31	3.46	0.24	0.05	0.20	0.28	7	4		0.2	0.97	428.6	4.0
7	29	1150	6	11.15	3.22	0.38	0.23	4.37	0.29	0.03	0.09	0.45	21	3	4	0.2	1.00	427.1	4.1
7	29	1150	7	4.14	1.38	0.38	0.13	1.97	0.20	0.10	0.20	0.55	17	1(1)		0.2	1.00	427.1	4.1
7	29	1420	1	12.95	3.97	0.69	0.34	3.65	0.45	0.05	0.19	0.31	17	5		0.2	1.34	415.9	4.1
7	29	1420	2	3.93	0.79	0.41	0.14	1.96	0.14	0.11	0.20	0.52	18	3(1)		0.2	1.34	415.9	4.1
7	29	1420	3	10.63	3.68	0.67	0.23	2.47	0.22	0.07	0.27	0.26	16	3(1)	5	0.2	1.34	415.9	4.1
7	29	1420	4	17.85	2.16	0.91	0.40	4.29	0.33	0.05	0.21	0.25	6	5		0.2	1.34	415.9	4.1
7	29	1420	5	17.03	4.84	0.96	0.23	4.25	0.31	0.06	0.22	0.27	5	5		0.2	1.34	415.9	4.1
7	29	1432	6	10.88	5.37	0.38	0.25	4.55	0.25	0.04	0.08	0.52	21	5		0.2	1.37	415.1	4.1
7	29	1432	7	4.12	0.84	0.43	0.12	2.37	0.16	0.11	0.18	0.60	17	3		0.2	1.37	415.1	4.1
7	30	1025	1	10.09	4.97	0.34	0.20	3.95	0.31	0.03	0.09	0.49	23	5		0.4	0.69	459.1	2.7
7	30	1025	2	2.80	0.80	0.23	0.08	2.09	0.16	0.08	0.11	0.82	25	4		0.4	0.69	459.1	2.7
7	30	1025	3	6.39	3.96	0.29	0.12	2.68	0.27	0.05	0.11	0.55	26	4	5	0.4	0.69	459.1	2.7
7	30	1025	4	8.72	3.18	0.35	0.17	4.18	0.21	0.04	0.08	0.55	11	5		0.4	0.69	459.1	2.7
7	30	1025	5	10.00	3.53	0.47	0.26	4.27	0.17	0.05	0.11	0.50	7	5		0.4	0.69	459.1	2.7
7	30	1354	1	11.60	6.13	0.58	0.29	3.71	0.36	0.05	0.16	0.41	20	4		0.4	1.19	435.9	3.9
7	30	1354	2	3.60	0.69	0.44	0.17	1.85	0.13	0.13	0.24	0.53	19	1(1)		0.4	1.19	435.9	3.9
7	30	1354	3	11.81	4.45	0.51	0.24	2.33	0.30	0.05	0.22	0.22	15	1(1)	1	0.4	1.19	435.9	3.9
7	30	1354	4	17.00	3.69	0.86	0.22	3.75	0.26	0.05	0.23	0.23	6	2		0.4	1.19	435.9	3.9
7	30	1354	5	17.60	4.73	1.07	0.46	3.84	0.20	0.06	0.28	0.23	5	2		0.4	1.19	435.9	3.9
7	30	1406	6	11.05	4.52	0.52	0.37	4.36	0.29	0.05	0.12	0.45	21	4		0.4	1.21	435.0	3.9
7	30	1406	7	3.50	1.04	0.35	0.20	2.02	0.18	0.10	0.17	0.63	20	1		0.4	1.21	435.0	3.9
7	31	728	1	9.67	4.01	0.20	0.09	4.59	0.78	0.02	0.04	0.54	24	5		0.7	0.13	505.1	0.5
7	31	728	2	7.44	3.17	0.14	0.06	4.42	0.11	0.02	0.03	0.74	10	6	3	0.7	0.13	505.1	0.5
7	31	728	3	8.98	5.64	0.12	0.08	4.86	0.17	0.02	0.02	0.86	18	6	3	0.7	0.13	505.1	0.5
7	31	728	4	10.00	1.78	0.54	0.30	7.46	0.23	0.05	0.07	0.78	7	6		0.7	0.13	505.1	0.5
7	31	728	5	16.36	2.09	0.72	0.20	7.13	0.09	0.04	0.10	0.44	5	6	3	0.7	0.13	505.1	0.5
7	31	943	7	1.82	0.52	0.16	0.06	3.31	0.16	0.09	0.05	1.98	38	5		0.7	0.47	485.4	1.6
7	31	1136	1	5.80	2.25	0.23	0.12	4.03	0.21	0.04	0.06	0.80	40	4		0.7	0.75	470.3	2.6
7	31	1136	2	2.55	0.83	0.23	0.10	2.08	0.19	0.10	0.11	0.92	27	3		0.7	0.75	470.3	2.6

APPENDIX 2.4: BEDFORM DATA

7	31	1136	3	5.31	1.84	0.24	0.08	2.57	0.15	0.05	0.09	0.53	32	4			0.7	0.75	470.3	2.6
7	31	1136	4	6.80	3.02	0.19	0.14	3.89	0.13	0.03	0.05	0.66	15	4			0.7	0.75	470.3	2.6
7	31	1136	5	13.20	6.05	0.59	0.31	4.09	0.25	0.05	0.14	0.44	6	4			0.7	0.75	470.3	2.6
8	1	814	1	11.60	5.64	0.19	0.12	6.53	0.28	0.02	0.03	0.71	20	6	3	1.1	0.10	525.7	0.3	
8	1	814	2	4.01	1.26	0.25	0.13	4.39	0.16	0.06	0.06	1.20	17	5	3	1.1	0.10	525.7	0.3	
8	1	814	3	9.09	2.13	0.26	0.10	4.99	0.22	0.03	0.05	0.58	19	5	3	1.1	0.10	525.7	0.3	
8	1	814	4	13.74	5.27	0.49	0.31	7.23	0.17	0.03	0.07	0.61	8	6	3	1.1	0.10	525.7	0.3	
8	1	814	5	13.48	3.68	0.48	0.28	7.46	0.19	0.03	0.06	0.63	6	6	3	1.1	0.10	525.7	0.3	
8	1	828	6	8.84	4.39	0.16	0.08	6.15	0.12	0.02	0.03	0.89	23	6	3	1.1	0.14	523.9	0.4	
8	1	828	7	4.67	1.20	0.17	0.06	4.44	0.19	0.04	0.04	1.01	15	5		1.1	0.14	523.9	0.4	
8	1	924	1	8.00	3.70	0.14	0.08	5.57	0.35	0.02	0.03	0.87	29	6		1.1	0.28	516.5	0.8	
8	1	924	2	3.33	1.36	0.09	0.05	3.83	0.15	0.03	0.02	1.42	21	5		1.1	0.28	516.5	0.8	
8	1	924	3	6.33	4.66	0.15	0.13	4.62	0.35	0.02	0.03	1.35	27	5	5	1.1	0.28	516.5	0.8	
8	1	924	4	17.00	2.72	0.59	0.30	6.92	0.24	0.03	0.08	0.42	6	6		1.1	0.28	516.5	0.8	
8	1	924	5	19.50	3.20	0.88	0.25	6.65	0.17	0.04	0.13	0.35	4	6	3	1.1	0.28	516.5	0.8	
8	1	940	6	14.50	9.73	0.16	0.12	6.08	0.25	0.01	0.03	0.56	16	6	3,4	1.1	0.32	514.2	1.0	
8	1	940	7	2.54	0.72	0.15	0.07	3.74	0.16	0.06	0.04	1.58	24	5		1.1	0.32	514.2	1.0	
8	1	1051	7	2.04	0.67	0.19	0.09	3.23	0.15	0.10	0.06	1.75	33	5		1.1	0.51	504.3	1.5	
8	2	1154	7	2.92	0.86	0.22	0.10	3.22	0.15	0.08	0.07	1.21	24	5		1.6	0.53	482.0	1.3	
8	3	1023	1	7.73	2.13	0.17	0.17	6.02	0.31	0.02	0.03	0.84	30	5		1.8	0.10	466.1	0.2	
8	3	1023	2	4.12	0.86	0.20	0.09	4.00	0.17	0.05	0.05	1.00	17	5		1.8	0.10	466.1	0.2	
8	3	1023	3	7.74	2.01	0.21	0.09	4.60	0.18	0.03	0.05	0.64	21	5		1.8	0.10	466.1	0.2	
8	3	1023	4	7.29	2.19	0.17	0.12	7.27	0.24	0.02	0.02	1.12	14	6		1.8	0.10	466.1	0.2	
8	3	1023	5	6.29	2.30	0.20	0.09	7.10	0.09	0.03	0.03	1.28	14	6		1.8	0.10	466.1	0.2	
8	3	1037	6	6.23	2.17	0.14	0.13	6.16	0.32	0.02	0.02	1.11	37	5	4	1.8	0.14	463.9	0.2	
8	3	1037	7	3.56	0.52	0.20	0.07	4.09	0.16	0.06	0.05	1.18	19	5		1.8	0.14	463.9	0.2	
8	3	1123	1	6.96	1.87	0.17	0.07	5.82	0.24	0.03	0.03	0.92	30	5		1.8	0.27	456.3	0.4	
8	3	1123	2	4.16	0.77	0.21	0.08	3.81	0.16	0.05	0.05	0.95	16	5		1.8	0.27	456.3	0.4	
8	3	1123	3	8.95	2.45	0.18	0.08	4.32	0.27	0.02	0.04	0.52	19	5		1.8	0.27	456.3	0.4	
8	3	1123	4	7.29	1.67	0.25	0.13	6.55	0.15	0.04	0.04	0.95	14	5		1.8	0.27	456.3	0.4	
8	3	1123	5	9.78	3.05	0.35	0.10	6.87	0.06	0.04	0.05	0.77	9	5		1.8	0.27	456.3	0.4	
8	3	1136	6	7.38	2.28	0.17	0.10	5.83	0.29	0.03	0.03	0.87	29	5	4	1.8	0.31	453.8	0.5	
8	3	1136	7	3.68	0.79	0.14	0.07	3.84	0.14	0.04	0.04	1.08	19	5		1.8	0.31	453.8	0.5	
8	3	1503	1	4.73	1.83	0.18	0.15	4.55	0.32	0.04	0.04	1.10	49	5	3	1.8	0.92	431.4	1.5	
8	3	1503	2	2.09	0.69	0.19	0.10	2.47	0.10	0.09	0.08	1.33	34	5		1.8	0.92	431.4	1.5	
8	3	1503	3	4.05	1.18	0.19	0.09	2.87	0.16	0.05	0.07	0.77	42	5		1.8	0.92	431.4	1.5	
8	3	1503	4	6.38	1.69	0.19	0.08	4.71	0.14	0.03	0.04	0.79	16	5		1.8	0.92	431.4	1.5	
8	3	1503	5	8.80	3.08	0.24	0.17	5.25	0.21	0.03	0.05	0.68	10	5	3	1.8	0.92	431.4	1.5	
8	3	1520	6	6.01	1.71	0.13	0.06	4.78	0.22	0.02	0.03	0.84	40	5		1.8	0.97	431.4	1.6	
8	3	1520	7	3.33	1.05	0.22	0.08	2.54	0.08	0.07	0.09	0.83	21	5		1.8	0.97	431.4	1.6	

APPENDIX 2.4: BEDFORM DATA

8	3	1605	1	4.83	1.53	0.16	0.10	4.58	0.26	0.03	0.04	1.04	48	5	4	1.8	1.10	431.4	1.6
8	3	1605	3	4.36	1.27	0.20	0.12	3.00	0.19	0.05	0.07	0.75	39	5		1.8	1.10	431.4	1.6
8	3	1620	6	4.18	1.20	0.14	0.07	4.74	0.25	0.04	0.03	1.26	48	5	4	1.8	1.15	431.5	1.6
8	7	726	1	4.99	1.45	0.14	0.17	4.71	0.27	0.03	0.03	1.05	43	4		1.2	0.93	556.4	2.9
8	7	726	2	3.93	1.53	0.46	0.18	2.25	0.18	0.12	0.20	0.64	18	3(2)	2	1.2	0.93	556.4	2.9
8	7	726	3	10.22	5.52	0.53	0.24	2.79	0.24	0.06	0.19	0.34	16	3(2)		1.2	0.93	556.4	2.9
8	7	726	4	7.85	1.97	0.28	0.16	4.31	0.24	0.04	0.07	0.60	13	4		1.2	0.93	556.4	2.9
8	7	726	5	11.00	4.44	0.40	0.18	4.61	0.10	0.04	0.09	0.52	8	4		1.2	0.93	556.4	2.9
8	7	739	6	8.29	5.03	0.18	0.11	4.98	0.39	0.03	0.04	0.73	28	4	4	1.2	0.96	555.1	3.0
8	7	739	7	4.67	1.76	0.38	0.14	2.36	0.13	0.09	0.16	0.58	15	3(2)	1	1.2	0.96	555.1	3.0
8	7	824	1	5.71	1.40	0.23	0.11	4.67	0.24	0.04	0.05	0.86	40	5		1.2	1.05	550.6	3.1
8	7	824	2	3.59	0.81	0.44	0.17	2.28	0.11	0.13	0.19	0.68	20	4		1.2	1.05	550.6	3.1
8	7	824	3	8.89	2.61	0.56	0.16	2.80	0.19	0.07	0.20	0.34	19	4		1.2	1.05	550.6	3.1
8	7	824	4	13.69	3.43	0.67	0.36	4.74	0.32	0.05	0.14	0.37	8	5		1.2	1.05	550.6	3.1
8	7	824	5	8.51	3.83	0.52	0.30	4.78	0.08	0.06	0.11	0.73	7	5		1.2	1.05	550.6	3.1
8	7	833	1	6.00	1.75	0.24	0.16	4.62	0.96	0.04	0.06	0.83	35	4		1.2	1.07	542.5	3.1
8	7	833	2	4.09	1.10	0.54	0.27	2.44	0.24	0.13	0.22	0.64	17	2(3)		1.2	1.07	542.5	3.1
8	7	833	3	10.04	3.06	0.53	0.20	2.95	0.23	0.06	0.18	0.32	17	3(3)		1.2	1.07	542.5	3.1
8	7	944	7	4.53	1.10	0.57	0.20	2.59	0.09	0.13	0.22	0.61	15	2		1.2	1.22	541.0	3.1
8	7	1130	1	6.63	2.15	0.16	0.11	5.36	0.21	0.03	0.03	0.90	35	5		1.2	1.44	524.2	3.1
8	7	1130	2	3.64	0.89	0.45	0.18	2.97	0.13	0.12	0.15	0.87	18	3		1.2	1.44	524.2	3.1
8	7	1130	3	8.36	2.21	0.47	0.22	3.38	0.24	0.06	0.14	0.44	20	3		1.2	1.44	524.2	3.1
8	8	1019	1	5.97	2.63	0.26	0.13	4.39	0.29	0.05	0.06	0.83	41	5		1.2	1.19	425.8	2.9
8	8	1019	2	3.33	0.76	0.39	0.16	2.08	0.22	0.12	0.19	0.65	21	3(3)		1.2	1.19	425.8	2.9
8	8	1019	3	8.50	1.93	0.56	0.22	2.73	0.20	0.07	0.21	0.34	20	3(3)		1.2	1.19	425.8	2.9
8	8	1019	4	12.75	5.65	0.66	0.32	4.33	0.34	0.05	0.15	0.42	8	5		1.2	1.19	425.8	2.9
8	8	1019	5	8.80	4.89	0.34	0.19	3.87	0.15	0.04	0.09	0.56	10	5		1.2	1.19	425.8	2.9
8	8	1144	2	3.30	0.97	0.39	0.15	2.53	0.18	0.13	0.15	0.82	20	3		1.2	1.36	413.1	2.9
8	8	1249	1	6.06	1.43	0.22	0.10	5.23	0.22	0.04	0.04	0.91	38	5		1.2	1.50	405.2	2.9
8	8	1249	2	3.52	1.05	0.32	0.16	3.06	0.22	0.09	0.10	0.96	20	5		1.2	1.50	405.2	2.9
8	8	1249	3	7.66	2.20	0.36	0.18	3.60	0.18	0.05	0.10	0.52	22	5		1.2	1.50	405.2	2.9
8	8	1302	7	3.33	0.79	0.25	0.10	3.22	0.16	0.07	0.08	1.03	21	5		1.2	1.53	403.7	2.9
8	8	1352	1	7.25	2.19	0.14	0.06	5.95	0.28	0.02	0.02	0.88	32	5	3	1.2	1.63	398.6	2.9
8	8	1352	2	3.11	1.26	0.18	0.09	3.56	0.19	0.06	0.05	1.28	23	5		1.2	1.63	398.6	2.9
8	8	1352	3	9.36	1.67	0.27	0.12	4.03	0.16	0.03	0.07	0.45	16	5		1.2	1.63	398.6	2.9
8	8	1352	4	14.57	5.15	0.79	0.16	6.02	0.32	0.06	0.13	0.45	7	5		1.2	1.63	398.6	2.9
8	8	1352	5	12.57	4.22	0.55	0.31	6.38	0.12	0.05	0.09	0.58	7	5		1.2	1.63	398.6	2.9
8	8	1404	6	7.28	2.04	0.20	0.10	5.54	0.42	0.03	0.04	0.81	33	5		1.2	1.65	397.6	2.9
8	8	1404	7	3.33	0.54	0.19	0.09	3.75	0.15	0.06	0.05	1.15	21	5		1.2	1.65	397.6	2.9
8	10	855	1	5.97	3.16	0.24	0.16	3.71	0.45	0.04	0.07	0.87	38	4		1.0	0.68	294.4	2.0

APPENDIX 2.4: BEDFORM DATA

8	10	855	2	3.09	1.66	0.21	0.10	1.68	0.13	0.07	0.12	0.70	23	4		1.0	0.68	294.4	2.0
8	10	855	3	4.55	2.47	0.15	0.08	2.09	0.24	0.04	0.07	0.58	37	4		1.0	0.68	294.4	2.0
8	10	855	4	6.61	3.50	0.25	0.23	4.56	0.15	0.04	0.05	0.83	16	5		1.0	0.68	294.4	2.0
8	10	855	5	8.00	2.43	0.34	0.22	4.48	0.12	0.04	0.08	0.61	11	5		1.0	0.68	294.4	2.0
8	10	1005	1	5.89	2.88	0.30	0.18	3.53	0.38	0.05	0.09	0.72	39	4		1.0	0.94	289.2	2.7
8	10	1005	2	2.23	0.87	0.25	0.11	1.55	0.19	0.12	0.16	0.79	31	3		1.0	0.94	289.2	2.7
8	10	1005	3	4.41	1.71	0.25	0.11	2.02	0.22	0.06	0.12	0.54	39	3		1.0	0.94	289.2	2.7
8	10	1005	4	6.21	1.84	0.31	0.18	4.37	0.20	0.05	0.07	0.76	16	5		1.0	0.94	289.2	2.7
8	10	1005	5	8.40	3.20	0.45	0.14	4.19	0.21	0.06	0.11	0.57	11	5		1.0	0.94	289.2	2.7
8	10	1119	1	7.07	2.58	0.33	0.18	3.43	0.35	0.05	0.10	0.58	28	5		1.0	1.11	285.4	2.9
8	10	1119	2	2.30	0.79	0.27	0.15	1.58	0.15	0.12	0.09	1.50	30	2(3)		1.0	1.11	285.4	2.9
8	10	1119	3	5.12	1.67	0.27	0.12	1.94	0.21	0.05	0.14	0.42	33	3(3)		1.0	1.11	285.4	2.9
8	10	1119	4	6.85	2.48	0.30	0.20	3.54	0.22	0.04	0.08	0.57	14	4		1.0	1.11	285.4	2.9
8	10	1119	5	7.49	3.99	0.37	0.22	3.95	0.20	0.05	0.09	0.68	12	4		1.0	1.11	285.4	2.9
8	10	1138	6	6.11	2.37	0.26	0.16	3.85	0.27	0.04	0.07	0.73	38	5		1.0	1.15	284.7	2.9
8	10	1138	7	2.89	0.96	0.31	0.12	1.65	0.12	0.12	0.19	0.64	24	2(1)		1.0	1.15	284.7	2.9
8	11	1310	1	7.61	2.15	0.36	0.22	3.90	0.30	0.04	0.09	0.56	30	5		1.0	1.26	358.1	2.9
8	11	1310	2	3.60	1.02	0.35	0.12	1.90	0.16	0.10	0.18	0.57	19	5	2	1.0	1.26	358.1	2.9
8	11	1310	3	6.07	1.71	0.35	0.16	2.23	0.19	0.06	0.16	0.39	28	5		1.0	1.26	358.1	2.9
8	11	1310	4	10.37	1.81	0.48	0.31	4.41	0.17	0.05	0.11	0.44	10	5		1.0	1.26	358.1	2.9
8	11	1310	5	9.94	3.08	0.67	0.32	4.58	0.22	0.07	0.15	0.54	9	5		1.0	1.26	358.1	2.9
8	11	1325	6	7.48	2.28	0.35	0.17	4.16	0.34	0.05	0.09	0.64	31	5		1.0	1.30	357.5	2.9
8	11	1325	7	3.18	0.67	0.26	0.13	2.04	0.16	0.09	0.13	0.67	22	5		1.0	1.30	357.5	2.9
8	22	1320	7	3.09	0.69	0.30	0.10	3.90	0.61	0.10	0.08	1.31	23	5		1.3	1.82	296.6	2.8
8	22	1405	1	8.29	2.80	0.25	0.15	5.73	0.42	0.03	0.05	0.80	28	5		1.3	1.92	290.5	2.8
8	22	1405	2	3.11	0.78	0.27	0.12	3.97	0.11	0.09	0.07	1.35	22	5		1.3	1.92	290.5	2.8
8	22	1405	3	6.58	1.92	0.27	0.10	4.27	0.18	0.04	0.06	0.71	26	5		1.3	1.92	290.5	2.8
8	22	1405	4	7.51	2.23	0.23	0.14	7.11	0.12	0.03	0.03	1.03	13	6		1.3	1.92	290.5	2.8
8	22	1405	5	10.35	1.76	0.50	0.25	7.01	0.09	0.05	0.07	0.70	9	6		1.3	1.92	290.5	2.8
8	22	1418	6	8.32	2.69	0.23	0.12	5.71	0.43	0.03	0.04	0.77	27	5		1.3	1.94	289.2	2.8
8	22	1418	7	3.50	0.75	0.29	0.12	4.08	0.10	0.08	0.07	1.22	20	5		1.3	1.94	289.2	2.8
8	23	1119	6	6.48	2.59	0.26	0.14	4.33	0.34	0.04	0.06	0.79	35	6		1.1	0.78	259.2	2.3
8	23	1119	7	3.33	0.78	0.27	0.10	2.53	0.11	0.08	0.11	0.80	21	5		1.1	0.78	259.2	2.3
8	25	650	1	5.11	3.29	0.20	0.14	3.01	1.04	0.04	0.06	0.59	29	4		0.7	0.61	281.2	2.0
8	25	650	2	3.40	1.03	0.25	0.09	2.05	0.09	0.08	0.12	0.60	20	4		0.7	0.61	281.2	2.0
8	25	650	3	5.48	2.55	0.20	0.09	1.99	0.56	0.03	0.08	0.36	27	5		0.7	0.61	281.2	2.0
8	25	650	4	9.82	3.73	0.45	0.24	4.39	0.16	0.05	0.10	0.45	11	5		0.7	0.61	281.2	2.0
8	25	650	5	10.21	2.64	0.41	0.21	4.56	0.14	0.04	0.09	0.45	8	5		0.7	0.61	281.2	2.0
8	25	705	6	8.18	2.61	0.30	0.18	3.25	0.44	0.04	0.09	0.40	24	4		0.7	0.64	281.0	2.1
8	25	705	7	3.60	1.05	0.27	0.10	2.00	0.11	0.08	0.14	0.56	19	5		0.7	0.64	281.0	2.1

REFERENCES

- Allen, J.R.L. (1969). "On the geometry of current ripples in relation to stability of fluid flow". *Geografiska Annaler*, **51A (1-2)**: p.61-96.
- Allen, J.R.L. (1973a). "Phase differences between bed configuration and flow in natural environments, and their geologic relevance". *Sedimentology*, **20**: p.323-329.
- Allen, J.R.L. (1973b). "Features of cross-stratified units due to random and other changes in bed forms". *Sedimentology*, **20**: p.189-202.
- Allen, J.R.L. (1976a). "Computational models for dune time-lag: general ideas, difficulties, and early results". *Sedimentary Geology*, **15**: p.1-53.
- Allen, J.R.L. (1976b). "Computational models for dune time-lag: population structures and the effects of discharge pattern and coefficient of change". *Sedimentary Geology*, **16**: p.99-130.
- Allen, J.R.L. (1976c). "Computational models for dune time lag: an alternative boundary condition". *Sedimentary Geology*, **16**: p.255-279.
- Allen, J.R.L. (1977). "Bedforms and unsteady processes: some concepts of classification and response illustrated by common one-way types". *Earth Surface Processes and Landforms*, **1**: p.361-374.
- Allen, J.R.L. (1983). "River bedforms: progress and problems" in: Collinson, J.D. and J. Lewin(eds.) Modern and Ancient Fluvial Systems . Special Publication Number 6 International Association of Sedimentologists. Blackwell Scientific, Oxford. p.19-33.
- Allen, J.R.L. (1984). Sedimentary structures. Their character and physical basis. Elsevier Publishing, New York.
- Allen, J.R.L. (1986). Physical Sedimentology. George Allen and Unwin Publishers, London.
- Allen, J.R.L. (1987). "Streamwise erosional structures in muddy sediments, Southwestern U.K.". *Geografiska Annaler*, **69A (1)**: p.35-46.
- Allen, J.R.L. and P.F. Friend. (1976a). "Relaxation time of dunes in decelerating aqueous flows". *Journal of the Geological Society of London*, **132**: p.17-26.

- Allen, J.R.L. and P.F. Friend. (1976b). "Changes in intertidal dunes during two spring-neap cycles, Lifeboat Station Bank, Wells-next-the-sea, Norfolk(England)". *Sedimentology*, **23**: p.329-346.
- Anwar, H.O. (1981). "A study of the turbulent structure in a tidal flow". *Estuarine, Coastal and Shelf Science*, **13**: p.373-387.
- Anwar, H.O. (1983). "Turbulence measurements in stratified and well-mixed estuarine flows". *Estuarine, Coastal and Shelf Science*, **17**: p.243-260.
- Bendat, J.S. and A.G. Piersol. (1969). Random data: analysis and measurement procedures. Wiley Interscience, New York.
- Best, J. (1992). "On the entrainment of sediment and initiation of bed defects: insights from recent developments within turbulent boundary layer research". *Sedimentology*, **39**: p.797-811.
- Best, J. and S. Bennett. (1993). "The structure of turbulent flow over dunes and the origins of dune-related macroturbulence". Conference Proceedings of the 5th International Conference on Fluvial Sedimentology. University of Queensland, Brisbane, Australia.
- Boersma, J.R. and J. H. J. Terwindt. (1981). "Neap-Spring tide sequences of intertidal shoal deposits in a mesotidal estuary". *Sedimentology*, **28**: p.151-170.
- Boothroyd, J.C. and D. K. Hubbard. (1975). "Genesis of bedforms in mesotidal estuaries" in: Cronin, L.E. (ed.), Estuarine Research: Volume 2 Geology and Engineering. Academic Press, p.217-234.
- Bowden, K.F. (1962). "Measurements of turbulence near the sea bed in a tidal current". *Journal of Geophysical Research*, **67**: p.3181-3186.
- Bowden, K.F. and S.R. Ferguson. (1980). "Variations with height of the turbulence in a tidally-induced bottom boundary layer" in: Nihoul, J.C.J. (ed.), Marine Turbulence. Elsevier Science Publishers, Amsterdam. p.259-286.
- Bowden, K.F. and M.R. Howe. (1963). "Observations of turbulence in a tidal current". *Journal of Fluid Mechanics*, **17**: p.271-284.
- Bridge, J.S. and J. L. Best. (1988). "Flow, sediment transport and bedform dynamics over the transition from dunes to upper-stage plane beds: implications for the formation of planar laminae". *Sedimentology*, **35**: p.753-763.

- Brownlie, W.R. (1983). "Flow depth in sand-bed channels". *Journal of Hydraulic Engineering, American Society of Civil Engineers*, **109** (7): p.959-990.
- Buckley, J.R. (1976). *The circulation and its forcing in a fjord, Howe Sound, B.C.* Unpublished Ph.D. thesis, University of British Columbia.
- Chang, F.F.M. (1970). "Ripple concentration and friction factor". *Journal of Hydraulics American Society of Civil Engineers*, **96**: p.417-430.
- Chang, H.H. (1988). *Fluvial Processes in River Engineering*. J. Wiley and Sons, New York.
- Chattergee, S. and A. S. Hadi. (1988). *Sensitivity analysis in linear regression*. Wiley, New York.
- Chattergee, S. and B. Price. (1991). *Regression Analysis by Example (2nd Edition)*. John Wiley and Sons, New York.
- Coleman, J.M. (1969). "Brahmaputra River: Channel processes and sedimentation". *Sedimentary Geology*, **3**: p.129-239.
- Collinson, J.D. (1970). "Bedforms of the Tana River, Norway". *Geografiska Annaler*, **52A** (1): p.31-56.
- Costello, W.R. (1974). "Development of bed configurations in coarse sands". Report 74-1, Department of Earth and Planetary Science, Massachusetts Institute of Technology. 120pp.
- Dalrymple, R.W., R.J. Knight and J.J. Lambiase. (1978). "Bedforms and their hydraulic stability relationships in a tidal environment, Bay of Fundy, Canada". *Nature*, **275**: p.100-104.
- Davies, A.G. (1977). "A mathematical model of sediment in suspension in a uniform reversing tidal flow". *Journal of Geophysics of the Royal Astronomical Society*, **51**: p.503-529.
- Davies, T.R. and A.J. Sutherland. (1980). "Resistance to flow past deformable boundaries". *Earth Surface Processes and Landforms*, **5**: p.175-179.
- Davis, R.A.D. and B.W. Flemming. (1991). "Time-Series study of mesoscale tidal bedforms, Martens Plate, Wadden Sea, Germany" in: Smith, D.G., G.E. Ranson, B.A. Zaitlin, and R.A. Rahmani (eds.), *Canadian Society of Petroleum Geologists Memoir Number 16*. p.275-283.

Dement'ev, V.V. (1962). "Investigations of pulsation of velocities of flow of mountain streams and of its effect on the accuracy of discharge measurements". Soviet Hydrology: Selected Papers, **1**: p.588-623.

Dinehart, R.L. (1992). "Gravel-bed deposition and erosion by bedform migration observed ultrasonically during storm flow, North Fork Toutle River, Washington". Journal of Hydrology, **136**: p.51-71.

Drake, T.G., R.L. Shreeve, W.E. Dietrich, P.J. Whiting and L.B. Leopold. (1988). "Bedload transport of fine gravel observed by motion-picture photography". Journal of Fluid Mechanics, **192**: p.193-217.

Dyer, K.R. (1986). Coastal and Estuarine Sediment Dynamics. John Wiley and Sons, New York.

Ebdon, D. (1985). Statistics in Geography (2nd edition). Blackwell Publishing, Oxford.

Einstein, H.A. and N.L. Barbarossa. (1952). "River channel roughness". Transactions of the American Society of Civil Engineers, **117**: p.1121-1146.

Engel, P. (1981). "Length of flow separation over dunes". Journal of Hydraulic Engineering, **107 (HY10)**: p.1133-1143.

Engel, P. and Y. L. Lau. (1980). "Friction factor for a two dimensional dune roughness". Journal of Hydraulic Research, **18**: p.213-225.

Engelund, F. (1966). "Hydraulic resistance of alluvial streams". Journal of Hydraulics, Division of American Society of Civil Engineers, **92 (HY2)**: p.315-326.

Engelund, F. and J. Fredsoe. (1982). "Sediment ripples and dunes". Annual Review of Fluid Mechanics, **14**: p.13-37.

Falco, R.E. (1977). "Coherent motions in the outer region of turbulent boundary layers". The Physics of Fluids, **20 (10, 2)**: p.124-132.

Fielding, C.R. (1993). "A review of recent research in fluvial sedimentology". Sedimentary Geology, **85**: p.3-14.

Flack, V.F. and P.C. Chang. (1987). "Frequency of selecting noise variables in subset regression analysis: a simulation study". The American Statistician, **41 (1)**: p.84-86.

Forrester, W.D. (1983). Canadian Tidal Manual. Department of Fisheries and Oceans, Ottawa.

Fredsoe, J. (1982). "Shape and dimensions of stationary dunes in rivers". *Journal of Hydraulics, Division of the American Society of Civil Engineers*, **108**: p.932-947.

Fukuoka, S. and Y. Fukushima. (1980). "Characteristics of ascending currents and boils induced by large-scale eddies". 3rd International Symposium on Stochastic Hydraulics. Tokyo, Japan. p.D5(1)- D5(11).

Gabel, S.L. (1993). "Geometry and kinematics of dunes during steady and unsteady flows in the Calamus River, Nebraska, USA". *Sedimentology*, **40**: p.237-269.

Gelfenbaum, G. (1983). "Suspended-sediment response to semidiurnal and fortnightly tidal variations in a mesotidal estuary: Columbia River, USA". *Marine Geology*, **52**: p.39-57.

Glen, N.C. (1979). "Tidal Measurement" in: Dyer, K.R., Estuarine hydrography and sedimentation. Cambridge Press. p.21-40.

Gordon, C.M. (1975a). "Period between bursts at high Reynolds number". *The Physics of Fluids*, **18 (2)**: p.141-143.

Gordon, C.M. (1975b). "Sediment entrainment and suspension in a turbulent tidal flow". *Marine Geology*, **18**: p.M57-M64.

Gordon, C.M. and C.F. Dohne. (1973). "Some observations of turbulent flow in a tidal estuary". *Journal of Geophysical Research*, **78 (12)**: p.1971-1978.

Grass, A.J. (1971). "Structural features of turbulent flow over smooth and rough boundaries". *Journal of Fluid Mechanics*, **50 (2)**: p.233-255.

Green, C.D. (1975). "A study of hydraulics and bedforms at the mouth of the Tay estuary, Scotland" in: Cronin, L.E.(ed.), Estuarine Research: Vol. 2 Geology and Engineering. Academic Press, New York. p.323-344.

Gulliver, J.S. and M.J. Halverson. (1987). "Measurements of large streamwise vortices in an open-channel flow". *Water Resources Research*, **23 (1)**: p.115-123.

Harms, J.C. (1969). "Hydraulic significance of some sand ripples". *Geological Society of America Bulletin*, **80**: p.363-396.

Hassan, M.A., M.A. Church and A.P. Schick. (1991). "Distance of movement of coarse particles in gravel bed streams". *Water Resources Research*, **27 (4)**: p.503-511.

Hickin, E.J. (1978). "Mean flow structure in meanders of the Squamish River, B.C.". Canadian Journal of Earth Sciences, **15**: p.1833-1849.

Hickin, E.J. (1989). "Contemporary Squamish River sediment flux to Howe Sound, British Columbia". Canadian Journal of Earth Sciences, **26**: p.1953-1963.

Hine, A.C. (1975). "Bedform distribution and migration patterns on tidal deltas in the Chatham harbor estuary, Cape Cod, Mass." in: Cronin, L.E. (ed.), Estuarine Research: Vol. 2 Geology and Engineering. Academic Press, New York. p.235-255.

Hoos, L.M. and C.L. Vold. (1975). The Squamish River estuary: status of environmental knowledge to 1974. Special Estuary Series, 2, Environment Canada.

Howarth, D.A. and J.C. Rogers. (1992). "Problems associated with smoothing and filtering of geophysical time-series data". Physical Geography, **13** (1): p.81-99.

Hubbell, D.W., J.L. Glenn and H.H. Stevens Jr. (1971). "Studies of sediment transport in the Columbia River estuary". Proceedings of the Technical Conference on Estuaries of the Pacific Northwest, Circular #42. Engineering Experiment Station, Oregon St. Univ., Corvallis.

Ikeda, S. (1980). "Suspended sediment on sand ripples". 3rd International Symposium on Stochastic Hydraulics. Tokyo, Japan. p.D4(1)-D4(10).

Ikeda, S. and T. Asaeda. (1983). "Sediment suspension with rippled bed". Journal of Hydraulics, Division of the American Society of Civil Engineers, **109** (3): p.409-423.

Iseya, F. and H. Ikeda. (1987). "Pulsations in bedload transport rates induced by a longitudinal sediment sorting: a flume study using sand and gravel mixtures". Geografiska Annaler, **69A** (1): p.15-27.

Itakura, T. and T. Kishi. (1980). "Open channel flow with suspended sediments on sand waves". 3rd International Symposium on Stochastic Hydraulics. Tokyo, Japan. p.B1(3)-B1(10).

Jackson, R.G. (1975). "Velocity-bedform-texture patterns of meander bends in the lower Wabash River of Illinois and Indiana". Geological Society of America Bulletin, **86**: p.1511-1522.

Jackson, R.G. (1976). "Sedimentological and fluid-dynamic implications of the turbulent bursting phenomenon in geophysical flows". Journal of Fluid Mechanics, **77** (3): p.531-561.

Jackson, R.G. (1977). "Mechanisms and hydrodynamic factors of sediment transport in alluvial streams" in: Davidson-Arnott, R. and W. Nickling (eds.) Proceedings of 5th Guelph Symposium on Geomorphology. GEO Abstracts Publishers, Norwich. p.9-44.

Jimenez, J. (1983). "A spanwise structure in the plane shear layer". *Journal of Fluid Mechanics*, **132**: p.319-336.

Jones, T.A. (1979). "Fitting straight lines when both variables are subject to error". *Mathematical Geology*, **11 (1)**: p.1-25.

Kachel, N.B. and R.W. Sternberg. (1971). "Transport of bedload as ripples during an ebb current". *Marine Geology*, **10**: p.229-244.

Kalinske, A.A. (1939). "Relation of the statistical theory of turbulence to hydraulics". *Transactions of the American Society of Civil Engineers*, **104**: p.1547-1600.

Karahan, M.E. and A.W. Peterson. (1980). "Visualization of separation over sand waves". *Journal of Hydraulics, Division of the American Society of Civil Engineers*, **106 (HY8)**: p.1345-1352.

Kinori, B.Z. and J. Mevorach. (1984). Manual of Surface Drainage Engineering: Volume 2-Stream Flow Engineering and Flood Protection. Developments in Civil Engineering. Elsevier Publishing, New York.

Kiya, M. and K. Sasaki. (1983). "Structure of a turbulent separation bubble". *Journal of Fluid Mechanics*, **137**: p.83-113.

Kleinbaum, D.G., L.L. Kupper and K.E. Muller. (1988). Applied Regression Analysis and Other Multivariable Methods. PWS-Kent, Boston.

Kline, S.J., W.C. Reynolds, F.A. Schraub and P.W. Runstadler. (1967). "The structure of turbulent boundary layers". *Journal of Fluid Mechanics*, **30 (4)**: p.741-773.

Knight, R.J. (1977). Sediments, bedforms, and hydraulics in a macrotidal environment, Cobequid Bay, (Bay of Fundy), Nova Scotia. Unpublished Ph.D. thesis, McMaster University, Dept. of Geology.

Korchokha, Y.M. (1968). "Investigation of the dune movement of sediments on the Polomet' River". *Soviet Hydrology: Selected Papers*, **(6)**: p.541-559.

- Kostaschuk, R.A. and L.A. Atwood. (1989). "River discharge and tidal controls on salt-wedge position and implications for channel shoaling: Fraser River, B.C.". *Canadian Journal of Civil Engineering*, **17**: p.452-459.
- Kostaschuk, R.A. and M.A. Church. (1993). "Macroturbulence generated by dunes: Fraser River, Canada" in: Fielding, C.R.(ed.), Current Research in Fluvial Sedimentology. *Sedimentary Geology*, **85**: p.25-37.
- Kostaschuk, R.A., M.A. Church and J.L. Luternauer. (1989b). "Bedforms, bed material, and bedload transport in a salt-wedge estuary: Fraser River, British Columbia". *Canadian Journal of Earth Sciences*, **26**: p.1440-1452.
- Kostaschuk, R.A., M.A. Church and J.L. Luternauer. (1991). "Acoustic images of turbulent flow structures in Fraser River estuary, British Columbia". *Current Research, Part E, Geological Survey of Canada*, p.83-90.
- Kostaschuk, R.A., M.A. Church and J.L. Luternauer. (1992). "Sediment transport over salt-wedge intrusions: Fraser River estuary, Canada". *Sedimentology*, **39**: p.305-317.
- Kostaschuk, R.A., J.L. Luternauer and M. A. Church. (1989a). "Suspended sediment hysteresis in a salt-wedge estuary: Fraser River, Canada". *Marine Geology*, **87**: p.273-285.
- Lane, E.W. (1944). "A new method of sediment transportation". *Transactions of the American Geophysical Union*, **25**: p.900.
- Lapointe, M.F. (1989). Sediment suspension by turbulent bursting over advancing river dunes. Unpublished Ph.D. thesis, University of British Columbia, Department of Geography.
- Lapointe, M.F. (1992). "Burst-like sediment suspension events in a sand bed river". *Earth Surface Processes and Landforms*, **17**: p.253-270.
- Laufer, J. and M.A. Badri Narayanan. (1971). "Mean period of the turbulent production mechanism in a boundary layer". *The Physics of Fluids*, **14**: p.182-183.
- Leeder, M.R. (1983). "On the interactions between turbulent flow, sediment transport and bedform mechanics in channelized flows" in: Collinson, J.D. and J. Lewin (eds.), Modern and Ancient Fluvial Systems. Special Publication Number 6 International Association of Sedimentologists. Blackwell Scientific, Oxford. p.5-18.
- Leopold, L.B. and T. Maddock. (1953). "The hydraulic geometry of stream channels and some physiographic implications". *United States Geological Survey Professional Paper*, 252. 55pp.

Levi, E. (1983a). "Oscillatory model for wall-bounded turbulence". *Journal of Engineering Mechanics*, **109** (3): p.728-740.

Levi, E. (1983b). "A Universal Strouhal Law". *Journal of Engineering Mechanics*, **109** (3): p.718-727.

Levi, E. (1984). "Closure on Murty and El-Sabh's paper". *Journal of Engineering Mechanics*, **110** (5): p.841-845.

Levings, C.D. (1980). "Consequences of training walls and jetties for aquatic habitats at two B.C. estuaries". *Coastal Engineering*, **4**: p.111-136.

Lyapun, and Chebotarev. (1976). "Deformations and stability of river channels". *Meteorologiya i Gidrologiya*, **1**: p.55-64.

Mantel, N. (1970). "Why stepwise procedures in variable selection". *Technometrics*, **12**: p.621-625.

Mark, D.M. and M.A. Church. (1977). "On the misuse of regression analysis in earth science". *Mathematical Geology*, **9** (1): p.63-75.

Marquardt, D.W. and R.D. Snee. (1975). "Ridge regression in practice". *The American Statistician*, **29**: p.3-19.

Matthes, G.H. (1947). "Macroturbulence in natural stream flow". *Transactions of the American Geophysical Union*, **28** (2): p.255-265.

McCuen, R.H., R.B. Leahy and P.A. Johnson. (1990). "Problems with logarithmic transformations in regression". *Journal of Hydraulic Engineering*, **116** (3): p.414-428.

McDowell, D.M. and B.A. O'Connor. (1977). Hydraulic Behaviour of Estuaries. John Wiley and Sons, New York.

McLean, S.R. and J.D. Smith. (1979). "Turbulence measurements in the boundary layer over a sand wave field". *Journal of Geophysical Research*, **84** (C12): p.7791-7808.

McNeil, K.A., F.J. Kelly and J.T. McNeil. (1974). Testing Research Hypotheses Using Multiple Linear Regression. Southern Illinois University Press, Carbondale and Edwardsville.

- McQuivey, R.S. (1973a). "Principles and measuring techniques of turbulence characteristics in open-channel flows". Geological Survey Professional Paper 802-A. U.S. Government Printing Office, Washington. 44pp.
- McQuivey, R.S. (1973b). "Summary of turbulence data from rivers, conveyance channels, and laboratory flumes". Geological Survey Professional Paper 802-B. U.S. Government Printing Office, Washington. 62pp.
- McTigue, D.F. (1981). "Mixture theory for suspended sediment transport". Journal of Hydraulics, Division of the American Society of Civil Engineers, **107 (HY6)**: p.659-673.
- Mendoza, C. (1987). "Comment on 'Convective transport within stable river sediments' by Savant et. al.". Water Resources Research, **24 (7)**: p.1206-1207.
- Morisawa, M. (1985). Rivers: Form and Process. Longman Publishing, New York.
- Morris, H.M. (1955). "Flow in rough conduits". Transactions of the American Society of Civil Engineers, **120 (HY2)**: p.373-398.
- Müller, A. (1982). "Secondary Flow Vortices: A structure in turbulent open channel flow" in: Zaric, Z.P. (ed.), Structure and Turbulence in Heat and Mass Transfer. Hemisphere Publishing, Washington. p.451-460.
- Naden, P. (1987). "Modelling gravel-bed topography from sediment transport". Earth Surface Processes and Landforms, **12**: p.353-367.
- Nakagawa, H. and I. Nezu. (1977). "Prediction of the contributions to the Reynolds stress from the bursting events in open channel flows". Journal of Fluid Mechanics, **80**: p.99-128.
- Nakagawa, H. and I. Nezu. (1981). "Structure of space-time correlations of bursting phenomena in an open-channel flow". Journal of Fluid Mechanics, **104**: p.1-43.
- Nasner, H. (1974). "Über das Verhalten von Transportkörpern im Tiedegebiet". Mitt. Franziusus-Inst., **40**: p.1-149.
- Nasner, H. (1978). "Time-lag of dunes for unsteady flow conditions". Proceedings of 16th Coastal Engineering Conference, Hamburg. p.1801-1817.
- Nowell, A.R.M. and M.A. Church. (1979). "Turbulent flow in a depth-limited boundary layer". Journal of Geophysical Research, **84 (C8)**: p.4816-4824.

- Nychas, S.G., H.C. Hershey and R.S. Brodkey. (1973). "A visual study of turbulent shear flow". *Journal of Fluid Mechanics*, **61** (3): p.513-540.
- Offen, G.R. and S.J. Kline. (1975). "A proposed model of the bursting process in turbulent boundary layers". *Journal of Fluid Mechanics*, **70** (2): p.209-228.
- Ota, T., Y. Asano and J. Okawa. (1981). "Reattachment length and transition of the separated flow over blunt, flat plates". *Bulletin of the Japanese Society of Mechanical Engineers*, **24**: p.941-947.
- Pizzuto, J.E. (1984). "An evaluation of methods for calculating the concentration of suspended bed material in rivers". *Water Resources Research*, **20** (10): p.1381-1389.
- Pope, P.T. and J.T. Webster. (1972). "The use of an F-statistic in stepwise regression procedures". *Technometrics*, **14**: p.327-340.
- Postma, H. (1967). "Sediment transport and sedimentation in the estuarine environment" in: Lauff, G.H. (ed.), *Estuaries*. American Association for the Advancement of Science, Washington. p.158-179.
- Praturi, A.K. and R.S. Brodkey. (1978). "A stereoscopic visual study of coherent structures in turbulent shear flow". *Journal of Fluid Mechanics*, **89**: p.251-272.
- Pretious, E.S. and T. Blench. (1951). "Final report on special observations on bed movement in lower Fraser River at Ladner Reach during the 1950 freshet". National Research Council of Canada. 12pp.
- Rao, K.N., R. Narasimha and M.A. Badri Narayanan. (1971). "The 'bursting' phenomenon in a turbulent boundary layer". *Journal of Fluid Mechanics*, **48** (2): p.339-352.
- Raudkivi, A.J. (1963). "Study of sediment ripple formation". *Journal of Hydraulics, Division of the American Society of Civil Engineers*, **89** (HY6): p.15-33.
- Raudkivi, A.J. (1966). "Bed forms in alluvial channels". *Journal of Fluid Mechanics*, **26** (3): p.507-514.
- Rencher, A.C. and F.C. Pun. (1980). "Inflation of R Sqr. in best subset regression". *Technometrics*, **22** (1): p.49-53.
- Richards, K. (1988). "Fluvial Geomorphology". *Progress in Physical Geography*, **12**: p.435-456.

- Robert, A. and K.S. Richards. (1988). "On the modelling of sand bedforms using the semivariogram". *Earth Surface Processes and Landforms*, **13**: p.459-473.
- Rood, K.M. (1980). Large scale flow features in some gravel bed rivers. Unpublished M.Sc. thesis, Simon Fraser University, Department. of Geography.
- Rood, K.M. and E.J. Hickin. (1989). "Suspended-sediment concentration and calibre in relation to surface-flow structure in Squamish River estuary, southwestern British Columbia". *Canadian Journal of Earth Sciences*, **26**: p.2172-2176.
- Rouse, H. (1937). "Modern conceptions of the mechanics of fluid turbulence". *Transactions of the American Society of Civil Engineers*, **19**: p.43-60.
- Savini, J. and G.L. Bodhaine. (1971). "Analysis of current-meter data at Columbia River gaging stations, Washington and Oregon". United States Geological Survey Water-Supply Paper, 1869-F.
- Schmitt, N., B.W. Coyle and J. Rauschenberger. (1977). "A Monte Carlo evaluation of three formula estimates of cross-validated multiple correlation". *Psychological Bulletin*, **84**: p.751-753.
- Simons, D.B. and E.V. Richardson. (1966). "Resistance to flow in alluvial channels". United States Geological Society Professional Paper 422J.
- Simons, D.B., E.V. Richardson and C.F. Nordin Jr. (1965). "Sedimentary structures generated by flow in alluvial channels". in: Middleton, G.V., Primary sedimentary structures and their hydrodynamic interpretation. Society of Economic Paleontologists and Mineralogists, Special Publication Number 12, p.34-52.
- Simons, D.B. and E.V. Richardson. (1966). "Forms of bed roughness in alluvial channels". *Journal of Hydraulics, Division of the American Society of Civil Engineers*, **92 (HY3)**: p.51-64.
- Smith, J.D. (1970). "Stability of sand beds subjected to a shear flow of a low Froude number". *Journal of Geophysical Research*, **75**: p.5928-5940.
- Smith, K.V.H. (1968). "Alluvial channel resistance related to bed form". *Proceedings of the American Society of Civil Engineers*, **94 (HY1)**: p.59-69.
- Smythe, S.R. (1987). Population differentiation in *Carex Lyngbyei* from three Puget trough wetlands. Unpublished M.Sc. thesis, Simon Fraser University, Department of Geography.

Snee, R.D. (1983). "Discussion: Developments in linear regression methodology: 1959-1982 by R.R. Hocking". *Technometrics*, **25** (3): p.230-237.

Sokal, R.R. and F.J. Rohlf (1981). Biometry (2nd ed.). W.H. Freeman and Company, New York.

Soulsby, R.L. (1980). "Selecting record length and digitization rate for near-bed turbulence measurements". *Journal of Physical Oceanography*, **10**: p.208-219.

Southard, J.B. (1975). "Depositional environment as interpreted from primary sedimentary structures and stratification sequences, Short Course 2". Society of Economic Paleontologists and Mineralogists, Tulsa.

Sumer, B.M. and R. Deigaard. (1981). "Particle motions near the bottom in turbulent flow in an open channel. Part 2". *Journal of Fluid Mechanics*, **109**: p.311-337.

Tamai, N., T. Asaeda and H. Ikeda. (1986). "Study on generation of periodical large surface eddies in a composite channel flow". *Water Resources Research*, **22** (7): p.1129-1138.

Terwindt, J.H.J., and M.J.N. Brouwer. (1986). "The behaviour of intertidal sandwaves during neap-spring tide cycles and the relevance for paleoflow reconstructions". *Sedimentology*, **33**: p.1-31.

Thompson, A. (1986). "Secondary flows and the pool-riffle unit: a case study of the processes of meander development". *Earth Surface Processes and Landforms*, **11**: p.631-641.

Thorn, M.F.C. (1975). "Deep tidal flow over a fine sand bed". *Proceedings of the 16th Congress of the International Association of Hydraulic Research*. Sao Paulo, Brazil. p.217-223.

Thorne, P.D., J.J. Williams and A.D. Heathershaw. (1989). "In situ acoustic measurements of marine gravel threshold and transport". *Sedimentology*, **36**: p.61-74.

Tiffany, J.B. (1950). "Turbulence in the Mississippi River". *Proceedings of 4th Conference on Hydraulics*, University of Iowa. p.237-264.

Till, R. (1973). "The use of linear regression in geomorphology". *Area*, **5** (4): p.303-308.

Van Rijn, L.C. (1990). Principles of Fluid Flow and Surface Waves in Rivers, Estuaries, Seas and Oceans. University of Utrecht, Utrecht.

- Vanoni, V.A. and L.S. Hwang. (1968). "Relation between bed forms and friction in streams". Proceedings of the American Society of Civil Engineers, **94 (HY6)**: p.1524-1527.
- Weisberg, S. (1983). "Some principles for regression diagnostics and influence analysis". Technometrics, **25 (3)**: p.240-244.
- West, J.R. and K.O.K. Oduyemi. (1989). "Turbulence measurements of suspended solids concentration in estuaries". Journal of Hydraulic Engineering, **115 (4)**: p.457-474.
- Wiberg, P.L. and J.D. Smith. (1989). "Model for calculating bed load transport of sediment". Journal of Hydraulic Engineering, **115 (4)**: p.101-123.
- Wijbenga, J.H.A. and G.J. Klaassen. (1983). "Changes in bedform dimensions under unsteady flow conditions in a straight flume" in: Collinson, J.D. and J. Lewin, Modern and Ancient Fluvial Systems. Special Publication Number 6, International Association of Sedimentologists. Blackwell Scientific, Oxford. p.35-48.
- Wilkinson, L. (1979). "Tests of significance in stepwise regression". Psychological Bulletin, **86 (1)**: p.168-174.
- Williams, J.J., P.D. Thorne and A.D. Heathershaw. (1989). "Measurements of turbulence in the benthic boundary layer over a gravel bed". Sedimentology, **36**: p.959-971.
- Wright, F.F. (1976). Estuarine Oceanography. CEGS Publication No.18. McGraw-Hill, New York.
- Yalin, M.S. (1977). Mechanics of Sediment Transport. Pergamon Press, Oxford.
- Younger, M.S. (1979). Handbook for Linear Regression. Duxbury Press, North Scituate, Mass.
- Znamenskaya, N.S. (1963). "Experimental study of the dune movement of sediment". Trudy GGI, **108**: p.89-114.
- Zrymiak, P. and Y.J. Durette. (1979). "An investigation of the morphological processes occurring in the Squamish River estuary". Proceedings of 4th National Hydrotechnical Conference, Environment Canada.